DEVELOPMENT AND APPLICATION OF LACUSTRINE ALKENONE PALEOTHERMOMETRY IN SOUTHWESTERN GREENLAND

BY

WILLIAM JOSEPH D'ANDREA

B.S., BINGHAMTON UNIVERSITY, 2001

B.A., BINGHAMTON UNIVERSITY, 2001

Sc.M., BROWN UNIVERSITY, 2005

A DISSERTATION SUBMITTED IN PARTIAL FULFILLMENT OF THE REQUIREMENTS FOR THE DEGREE OF DOCTOR OF PHILOSOPHY IN THE DEPARTMENT OF GEOLOGICAL SCIENCES AT BROWN UNIVERSITY

PROVIDENCE, RHODE ISLAND

MAY 2009

This dissertation by William D'Andrea is accepted in its present form by the Department of Geological Sciences as satisfying the dissertation requirements of the degree of Doctor of Philosophy.

Date 9/12/08

Yongsong Huang, Brown University

Recommended to the Graduate Council

Date 9/12/08

Timothy D. Herbert, Brown University

Date 9/12/2008

James M. Russell, Brown University

Date 9/12/2008

Alberto E. Saal, Brown University

Date 9/12/2008

Delia Oppo, WHOI

Approved by the Graduate School and Research

Date ____________

Dr. Sheila Bonde
Dean of the Graduate School

CURRICULUM VITAE

WILLIAM J. D'ANDREA

2005-2008 Brown University (Providence, RI)
Ph.D. Candidate, Geological Sciences. Yongsong Huang, advisor.
Defense date September 12, 2008.

2003-2005 Brown University
Master of Science, Geological Sciences. Yongsong Huang, advisor.

2001-2003 University of Nebraska - Lincoln (Lincoln, NE).
Master of Science student, Geosciences. Sherilyn C. Fritz, advisor.

1996-2001 Binghamton University (Binghamton, NY).
Bachelor of Science, Geology.
Bachelor of Arts, **Environmental Studies**.

RESEARCH EXPERIENCE:

2003-present *Ph.D. candidate*. Dept. of Geological Sciences, Brown University.

- Generated Holocene paleoclimate reconstructions from SW Greenland using multiple organic geochemical and stable isotope methods
- Organized, led eight field research trips in Kangerlussuaq, Greenland
- Investigated biomarkers using GC-FID, GC-MS, GC-IRMS
- Developed new techniques for hydrogen isotope measurement of individual alkenones
- Performed PCR and developed clone libraries from fossil DNA in lake sediment
- Conducted vegetation sampling to determine climate controls on leaf wax hydrogen isotopes
- Collected and performed hydrogen isotope analysis on sediments from a 30 lake transect in the southwestern US

2001-2003 *M.S. candidate*. Dept. of Geosciences, University of Nebraska-Lincoln.

2000 *NSF Fellow*. Limnological Research Center, University of Minnesota.

TEACHING EXPERIENCE:

2007 *Teaching Assistant*. Brown University, SPARK Program, Meteorology.
2006 *Teaching Assistant*. Brown University, GE022 Physical Geology.
2004 *Teaching Assistant*. Brown University, GE137 Environmental Geochemistry.
2001-2002 *Teaching Assistant*. University of Nebraska, GEO101 Physical Geology.

INFORMAL TEACHING AND OUTREACH:

2008	*Ice Stories Correspondent - NSF*. Exploratorium, San Francisco, CA.
2007-2008	*Guest Lecturer*. Brown University. GE22 Physical Geology.
2007-2008	*Reviewer*. The Holocene, Journal of Paleolimnology.
2007	*Field Trip Co-Leader*. Brown University undergrad field trip, Grand Canyon.
2006-2007	*Guest Lecturer (four classes)*. Brown University, GE137 Environmental Geochemistry.
2005-2007	*Science Outreach Teacher*. Vartan Gregorian Elementary School, Providence, RI.
2004-2007	*Senior Thesis Supervisor*. Brown University, Andrew Michelson, Mena Ramos, Fatma Khatib, Sarah Wattley, Sarah Ladd, Devina Swarup, Mark McGuire.

FELLOWSHIPS AND AWARDS:

2008	IPY Next Generation of Polar Researchers Symposium, National Science Foundation.
2007	Dissertation Fellowship. Brown University, Dept. of Geological Sciences.
2007	Student Travel Award, Northeastern GSA. Geological Society of America.
2006	Rose Provasoli Scholarship. Bigelow Laboratory for Ocean Sciences.
2006	Croasdale Fellowship. Phycological Society of America.
2003	Best Student Paper, Nebraska Academy of Sciences. Nebraska Geological Society.

PUBLICATIONS:

Hou, J., **D'Andrea, W.J**., Huang, Y. (2008) Can sedimentary leaf waxes record D/H ratios of continental precipitation? Field, model and experimental assessments. *Geochimica et Cosmochimicha Acta* 72, 3503-3517.

D'Andrea, W.J., Liu, Z.H., Alexandre, M.D., Wattley, S., Herbert, T.D., Huang, Y., 2007. An efficient method for isolating individual long-chain alkenones for compound-specific hydrogen isotope analysis, *Analytical Chemistry,* 79, 3430-3435.

Hou, J., **D'Andrea, W.J.**, MacDonald, D., Huang, Y., 2007. Evidence for water use efficiency as an important factor in determining the δD values of tree leaf waxes, *Organic Geochemistry*, 38, 1251-1255.

Hou, J., **D'Andrea, W.J.**, MacDonald, D., Huang, Y., 2007. Hydrogen Isotopic variability in leaf waxes among terrestrial and aquatic plants around Blood Pond, Massachusetts (USA), *Organic Geochemistry*, 38, 977-984.

D'Andrea, W.J., Lage, M., Hughes-Martiny, J.B., Laatsch, A.D., Amaral-Zettler, L.A., Sogin, M.L., Huang, Y., 2006. Alkenone producers inferred from well-preserved 18S rDNA in Greenland lake sediments, *Journal of Geophysical Research – Biogeoscience,* doi:10.1029/2005JG000121.

D'Andrea, W.J., Huang, Y., 2005. Long-chain alkenones in Greenland lake sediments: low $\delta^{13}C$ values and exceptional abundance, *Organic Geochemistry*, 36, 1234-1241.

SELECTED ABSTRACTS:

Alkenone-based temperature reconstruction from lakes of southwestern Greenland: insights from a haptophyte bloom and a new isotopic approach. **D'Andrea, W.J.**, Huang, Y., Fritz, S., Anderson, N.J., American Geophysical Union, December, 2007.

Uncovering the mysteries of lacustrine haptophytes using fossil DNA. INVITED. **D'Andrea,W.J.**, Theroux, S., Huang, Y., American Geophysical Union, December 2007.

High-resolution alkenone-based temperature reconstructions from southwestern Greenland. **D'Andrea, W.J.**, Huang, Y., Fritz, S., Anderson, N.J., Geological Society of America – Northeastern Section Meeting, March 2007.

Factors controlling hydrogen isotope ratios of sedimentary leaf waxes: implications for interpreting δD records of paleoclimate. Hou, J., **D'Andrea, W.J.**, Toney, J., Huang, Y., American Geophysical Union, December 2006.

Alkenone and isotopic records of Holocene climatic and environmental change from laminated West Greenland lakes. **D'Andrea, W.J.**, Huang, Y., American Geophysical Meeting, December 2004.

INVITED TALKS:

2008 IPY Next Generation of Polar Researchers Symposium, National Science Foundation, Colorado Springs, CO.

2008 University of Minnesota, Dept. of Geology and Geophysics, Minneapolis, MN.

2007 SUNY New Paltz, Geology Dept., New Paltz, NY.

2006 Boston University, Dept. of Earth Sciences, Boston, MA.

Dedicated to my grandparents
William and Lydia D'Andrea
Joseph and Elli Eisele

ACKNOWLEDGMENTS

A dissertation is a funny thing. Credit goes to a single person (in this case, me) even though a great many people contribute intellectually, financially and emotionally to its completion. And while the merit of a dissertation lies in its contribution to the greater scientific knowledge, it also represents the contributions of a great number of people to the development of an individual (also in this case, me) as a scientist, researcher and educator. This dissertation and I have become what we are at this moment thanks to the dedication, input, and support of a great many people.

Yongsong Huang, my major advisor and mentor during the course of my dissertation work has been an enormous inspiration and endless source of insight. I am particularly grateful to Yongsong for teaching me the importance of lateral thinking in scientific research. Yongsong, I can only hope to become half the strategist that you are.

Thanks to Tim Herbert for his guidance and role-modeling. Tim is a born communicator and one of the sharpest minds I've ever met. I admire his ability to see through the noise and clutter surrounding a topic and arrive immediately at the heart of it. This skill may come from extracting signals from noisy geological data or from learning to function efficiently in his office, but either way it serves him well as a theoretician and thinker, and it is a skill I have tried to develop after observing Tim.

I owe many thanks to Jim Russell, who is one of these people who seem to know the answer to any question you have (and therefore a great person to have down the hall with his door wide open). Thanks for the valuable input and for readily lending me coring equipment to take to Greenland, most of which was returned and some of which was returned unharmed.

Thanks to Alberto Saal for agreeing to serve on my committee. I've appreciated your practical advice and hallway pep talks, and the "fundamental" questions you've hit me with usually sent me scampering for a textbook. Thanks also go to Jeff Donnelly for serving as a member of my preliminary advisory committee and for always being ready to lend advice, knowledge, or coring equipment. I have learned a lot from Jeff in the classroom and in the field.

I want to thank Jan Tullis and Karen Fisher for reigniting my interest in undergraduate teaching. These two teach a Geo 101 class that can convert business students into geology majors…no small feat. Thanks Jan, also, for all your help and advice in my professional development as an aspiring academic.

Thanks to Thomson Webb III for our many discussions and for introducing me to synoptic climatology. I was lucky to get a piece of Tom as he's been slowly weaning himself away from the department and into his Emeritusness. I am grateful to have had the opportunity to get a glimpse of Earth's Climate System through his eyes.

Sheri Fritz, my master's advisor at the University of Nebraska-Lincoln, introduced me to Greenland and the lakes that would become my major research focus over the ensuing seven years. You have been an instrumental and motivational force in my development as a researcher and a scientist. Thanks for never giving up on me and for the constant encouragement and support.

Thanks to N. John Anderson for being such a warm and hospitable collaborator on the oligosaline lakes of Søndre Strøm. Sharing territory is not something that comes easily to researchers, but John loves Greenland so much that he constantly welcomes others to the wonderful sites he has been working on for over a decade now. Even though my field objectives were often specific, John's sense of wonder is contagious and kept me thinking about many aspects of Greenland (ecological, botanical and limnological) beyond hunting for haptophyte algae. Thanks for the many great meals and the company in the field and thanks for saying, knowing full-well it wasn't true, that you needed me to "save your career" whenever you sensed my frustration mounting.

Marcelo Alexandre taught me how to work in an organic geochemistry lab. Marcelo is the rarest of individuals; endlessly patient, tremendously insightful, as kind and gentle as they come, fun to be around and as far as I can tell, completely unflappable. Thanks for the constant help in the lab and for teaching me to slow down, rather than speed up, when time is of the essence. I'm not looking forward to being in a lab that doesn't have you behind its curtains.

Annette Coleman has been a trooper, teaching a geologist to grow algae. Thanks for putting up with me and for welcoming me into your phycology lairs. I also owe thanks to the following people for their time and scientific input: Melissa Lage, Jennifer Hughes-Martiny formerly of Brown EEB, Linda Amaral-Zettler and Mitch Sogin at the Marine Bio Lab, and Bob Anderson, Julie Sexton, Michael Sirecki and Nicole Poulton at the Bigelow Lab for Ocean Science.

The ESH graduate students are top notch and I've enjoyed learning with them and from them. Thanks to Juzhi Hou, my five year office mate, for our many days spent scribbling at the chalkboard and to Laura Cleaveland for helping me to keep perspective. Thanks to Jonathan Nichols for being the best field assistant anyone could ask for, and for knowing how to do *everything*, and to Kira Lawrence and Zhonghui Liu for being such tough acts to follow as graduate students. Thanks also to Caitlin Chazen, Jess

Tierney, Emily Pohlman, Susie Theroux and Jamie Toney and to Paige Newby and Dana MacDonald for many stimulating discussions and smiling faces.

Sincere thanks to Joe Orchardo, Dave Murray and Warren Prell for letting us borrow field equipment that we should have owned ourselves. Additional thanks to Joe for his patient lessons that served to demystify mass spectrometry for me (a little).

I was fortunate to get the opportunity to work with some bright and highly motivated undergraduate students during the course of this dissertation, and some of their sweat is in these pages, as well. Thanks to Mark (Kane) McGuire, Devina Swarup, Sarah Wattley, Nemiah Ladd, Fatma Khatib, Mena Ramos and Scott Lowenstein. I'd also like to thank the administrative staff, Ruth Crane, Caroline Sherman, Pauline Fennelly, Nancy Fjeldheim and Lisa Sheehan, in the Geological Sciences Department at Brown for their constant assistance and cheery nature. And thanks to Bill Collins for all the crisis management.

The logistical support folks in Kangerlussuaq are top notch. Thanks to Ed Stockard (photographer and Arctic penguin rancher, extraordinaire), Robin Abbott, Earl Vaughn and Sparky Begnaud for facilitating many years of smooth Arctic fieldwork. Thanks to the 109th Air Wing for always getting me to and from Greenland without the need to put that horrible O_2 bag over my head.

Heartfelt thanks and love to my parents, Bill and Carole D'Andrea, for instilling in me a love of learning and for encouraging my interest in research and in pursuing a Ph.D. My grandparents Joe and Elli Eisele, and Bill and Lydia D'Andrea put great value on education and took initiative early on to ensure that their grandchildren would be able to go to college. All my love goes to my Oma, Elli Eisele, who has had the responsibility

of providing the affection and insight of four grandparents over the past 25 years. You pulled it off, Oma. Thanks for all that you have given over the years. A day doesn't go by that an *Oma-ism* doesn't pop in my head.

Anyone who thinks they need some perspective in life should have kids. Calvin and Miles (5 and 3 years old, respectively, as I write this), without trying, reorganized my values and reprioritized my life, certainly for the better. It's hard to get too riled over life's details when there are two monkeys at home so full of love and wonder. I love you two more than you will ever know (until you have children, I suppose) and I thank you for being Calvin and Miles. And leaving the best (and most deserving of my praise and appreciation) for last, all the love that's fit to print and my endless thanks go to Alicyn, my love. I know that you are sometimes impressed by me (usually when no one else is watching), but I am forever in awe of you.

TABLE OF CONTENTS

LIST OF TABLES

LIST OF FIGURES

INTRODUCTION

WILLIAM J. D'ANDREA

BROWN UNIVERSITY, *Department of Geological Sciences*

Whatever the role anthropogenic greenhouse gas forcing plays in future climate change scenarios[1], it will be superimposed upon and interact with the natural variability of Earth's Climate System. Therefore, in order to anticipate future climate changes and their associated human impact we must document and understand the forcing and feedback mechanisms that have driven past climate variability. Instrumental records of temperature and precipitation extend back two or three centuries. These data have proven valuable for documenting the recent anthropogenic forcing of global temperatures[1], but also for uncovering and examining numerous modes of natural variability within Earth's climate system (including El Niño/Southern Oscillation, the Pacific Decadal Oscillation, the North Atlantic Oscillation and Northern Annular Mode, the Atlantic Multidecadal Oscillation, the Southern Annular Mode, and the Indian Ocean Dipole). Instrumental records are sufficiently long to detect subdecadal to multidecadal variability in the climate system, but are too short to adequately investigate centennial-scale modes of climate variability, which are also relevant over human timescales.

Reconstructing Past Climate Variability

To investigate centennial-scale climate variability we must exploit geological archives that serve as natural recorders of climate change. Part of the challenge of this is developing tools and techniques that allow geologic data to serve as surrogates or *proxies* for actual temperature or precipitation data. Paleoclimatologists are continually seeking quantitative climate proxies that can provide the most reliable climate reconstructions possible. They are also usually interested in identifying geologic archives that provide high sampling resolution, allowing them to evaluate the climate changes represented by their proxies at the smallest time slices possible, enabling them to examine the timing, the nature and ultimately the causes of past climate changes over the smallest possible time steps.

When considering decadal to centennial-scale climate variability (i.e., climate changes that occur over human timescales), the most useful natural archives of climate information are lake sediments, tree rings, speleothems, marine sediments (in areas where accumulation rates allow high resolution sampling) and ice cores. All of these archives have their benefits and their drawbacks, and all of them have provided paleoclimate data that have improved our present understanding of Holocene climate variability (cf. Mayewski *et al.*[2]). Lake sediments however, stand out from the other archives in that they combine the following attributes: 1) Lake sediments have generally high sedimentation rates, often offering decadal-scale (or better) sampling. 2) Numerous climate proxies (some quantitative, some qualitative) can be combined from a lake sediment record to maximize paleoclimatic interpretation. 3) It is relatively inexpensive to retrieve lake sediment cores, and 4) lakes are just about everywhere, so lacustrine sediment records are not geographically limited.

Alkenone Thermometry

This thesis describes the development and application of long-chain alkenones as a paleothermometer in lakes of Southern West Greenland. Long-chain alkenones are lipids produced by certain haptophyte algae and exhibit unsaturation patterns that are excellent sensors of temperature change[3]. The unsaturation index U^{K}_{37} (which simplifies to $U^{K'}_{37}$ in the absence of the tetra-unsaturated alkenone) has been shown to vary linearly with algal growth temperature in culture studies[4] and core-top studies[5] (although the temperature calibration function varies among different haptophytes[3]) and the temperature proxy has been used effectively in marine settings to reconstruct past sea surface temperatures[6]. The indices are defined as follows[4]:

$$U_{37}^{K} = \frac{[37:2]-[37:4]}{[37:2]+[37:3]+[37:4]} \quad \text{Eqn. 1}$$

$$U_{37}^{K'} = \frac{[37:2]}{[37:2]+[37:3]} \quad \text{Eqn. 2}$$

where, 37:2 represents the alkenone having 37 carbon atoms and 2 double-bonds; 37:3 has 37 carbons and 3 double bonds; and, 37:4 has 37 carbon atoms and 4 double bonds.

Alkenone thermometry is ideal for paleoclimate reconstruction because samples can be processed quickly and it is inexpensive and offers *quantitative* reconstructions of past water temperatures. Extending this approach to lakes would be of tremendous benefit to the study of terrestrial paleoclimate, allowing development of spatial networks of terrestrial temperature reconstructions to examine spatial and temporal patterns of natural variability of Earth's Climate System. In recent years, there have been numerous reports of lacustrine alkenones and their temperature dependence from various geographic settings including England, Germany, Austria, Spain, Turkey, China, USA, Peru and Antarctica[7,8], underscoring the potential of this proxy for terrestrial paleoclimate research.

Dissertation Outline

This dissertation investigates the stable isotopic and organic geochemical aspects of alkenones from brackish Greenlandic lakes and develops their use as a paleothermometer.

Chapter 1 reports the discovery of lacustrine alkenones in the brackish lakes near the head of the Søndre Strømfjord, outside Kangerlussuaq, Greenland. The alkenone distribution of the lacustrine alkenones is described and compared with alkenones reported from other lakes and marine settings. The $\delta^{13}C$ values of the alkenones are examined alongside the $\delta^{13}C$ values of other specific, algal-derived compounds found in the lake sediments. The work reported in Chapter 1 supports the conclusions that 1) the Greenland alkenones are most similar to those from lakes in Germany and Austria[8], suggesting a common producer organism, and 2) to achieve such low $\delta^{13}C$ values alkenone producers must either fractionate CO_2 to a greater extent than other algae or access a ^{13}C-depleted carbon source.

Chapter 2 reports the application of environmental genomic techniques intended to identify the alkenone-producing haptophyte algae in the Greenland lakes. Haptophyte-specific ribosomal DNA (rDNA) sequences obtained from lake sediment and water samples, and amplified using the polymerase chain reaction (PCR), were compared with rDNA sequences of known haptophytes, allowing comparative phylogenetic mapping. The major conclusions of this chapter are that the Greenland alkenone producers represent a new taxon of haptophyte algae, and that all Greenlandic lakes of the study contain the same haptophytes, indicating that the same alkenone-temperature calibration can be applied to the sediment records of all the lakes. Lastly, successful amplification of 1,000 year old “fossil” DNA from a sediment core indicates 1) the lake sediments act to preserve DNA, 2) the identity of the haptophytes has not changed over the past 1,000 years, and 3) the modern temperature calibration is applicable over this time period.

Chapter 3 reports a new liquid chromatographic procedure for separating alkenones having the same carbon number but different degrees of unsaturation for the purpose of compound-specific hydrogen isotopic analysis. This chapter reports the first δD measurements on separated alkenones and provides the first documentation that δD values of alkenones differ according to their degree of unsaturation. δD values of alkenones are potentially useful for determining past δD values of ocean water and lake water, which can be used as a proxy for ocean salinity and effective precipitation. Chapter 3 concludes that it is preferable to make δD measurements on specific alkenones rather than unseparated "pooled" alkenones, due to possible temperature-related effects on pooled δD values and because measurements on individual alkenones provide improved precision and accuracy.

Chapter 4 presents a 6,000 year temperature reconstruction for Kangerlussuaq, Greenland, based on alkenones from sediment cores of two lakes in the region. The excellent match in the timing and amplitude of inferred lake water changes from the two records confirms that lacustrine alkenones, at least in these sites, record regional climate forcing rather than lake-specific processes. Temperature in the Kangerlussuaq region appears to have been forced by changes in meridional overturning circulation (MOC) and the extent of the North Polar Vortex on millennial timescales, while being controlled by variability in the NAO and the position of the Baffin Trough over centennial timescales. The timing of major changes in Paleo-Eskimo, Norse and Inuit occupation of Southern West Greenland coincide with episodes of abrupt temperature change revealed by the alkenone record, and indicate that climatic and environmental changes played a fundamental role in the patterns of human migration in Greenland over the past 4,500 years.

References

1 IPCC, in *Climate Change 2007: The Physical Science Basis. Contribution of Working Group I to the Fourth Assessment Report of the Intergovernmental Panel on Climate Change*, edited by S. Solomon et al. (Cambridge University Press, Cambridge, UK and New York, NY, USA, 2007).

2 Mayewski, P. A. et al., Holocene climate variability. *Quaternary Research* **62** (3), 243 (2004).

3 Brassell, S.C., in *Organic Geochemistry*, edited by M.H. Engel, S.A. Macko (Plenum Press, New York, 1993), pp. 699.

4 Brassell, S.C., G. Eglinton, I.T. Marlowe, U. Pflaumann and M. Sarnthein, Molecular stratigraphy: A new tool for climatic assessment. *Nature* **320**, 129 (1986).

5 Prahl, F.G., and S.G. Wakeham, Calibration of unsaturation patterns in long-chain ketone compositions for paleotemperature assessment. *Nature* **330**, 367 (1987).

6 Herbert, T.D., in *Treatise on Geochemistry: The Oceans and Marine Geochemistry*, edited by H. Elderfield (Elsevier, Oxford, 2004), pp. 391.

7 Cranwell, P.A., Long-chain unsaturated ketones in recent lacustrine sediments. *Geochimica et Cosmochimica Acta* **49**, 1545 (1985); Li, J., R.P. Philip, F. Pu, and J. Allen, Long-chain alkenones in Qinghai Lake sediments. *Geochimica et Cosmochimica Acta* **60** (2), 235 (1996); Sheng, G.Y., K.Q. Cai, X.X. Yang, J.L. Lu, G.D. Jia, P.A. Peng, and J.M. Fu, Long-chain alkenones in Hotong Qagan Nur Lake sediments and its paleoclimatic implications. *Chinese Science Bulletin* **44**, 259 (1999); Sun, Q., G. Chu, S. Li, C. Lu, M. Zheng, Long-chain alkenones in sulfate lakes and its paleoclimatic implications. *Chinese Science Bulletin* **49**, 2082 (2004); Sun, Q. et al., Calibration of alkenone unsaturation index with growth temperature for a lacustrine species, Chrysotila lamellosa (Haptophyceae). *Organic Geochemistry* **38** (8), 1226 (2007); Theil, V., A. Jenisch, G. Landmann, A. Reimer, and W. Michaelis, Unusual distributions of long-chain alkenones and tetrahymanol from the highly alkaline Lake Van, Turkey. *Geochimica et Cosmochimica Acta* **61** (10), 2053 (1997); Theissen, K.M., D.A. Zinniker, J.M. Moldowan, R.B. Dunbar, H.D. Rowe, Pronounced occurrence of long-chain alkenones and dinosterol in a 25,000-year lipid molecular fossil record from Lake Titicaca, South America. *Geochimica et Cosmochimica Acta* **69** (3), 623 (2005); Volkman, J.K., D.I. Allen, P.L. Stevenson, and H.R. Burton, Bacterial and algal hydrocarbons in sediments from a saline Antarctic lake, Ace Lake. *Organic Geochemistry* **10**, 671 (1986); Wang, R., and M. Zheng, Occurence and environmental significance of long-chain alkenones in Tibetan Zabuye Salt Lake, S.W. China. *International Journal of Salt Lake Research* **6**, 281 (1998); Pearson, E.J., S. Juggins, and P. Farrimond, Distribution and significance of long-chain alkenones as salinity and temperature indicators in Spanish saline lake sediments. *Geochimica et Cosmochimica Acta* **72**, 4035 (2008).

8 Zink, K.G., D. Leythaeuser, M. Melkonian, and L. Schwark, Temperature dependency of long-chain alkenone distributions in Recent to fossil limnic sediments in lake waters. *Geochimica et Cosmochimica Acta* **65** (2), 253 (2001).

CHAPTER 2

LONG-CHAIN ALKENONES IN GREENLAND LAKE SEDIMENTS: LOW $\delta^{13}C$ VALUES AND EXCEPTIONAL ABUNDANCE

WILLIAM J. D'ANDREA[1]

YONGSONG HUANG[1]

[1]BROWN UNIVERSITY, *Department of Geological Sciences*

Published in:

Organic Geochemistry, 36: 1234-1241, doi:10.1016/j.orggeochem.2005.05.001, 2006

Abstract

Long-chain alkenones (LCAs) are a key class of biomarkers for certain members of the algal class Prymnesiophyceae (i.e., prymnesiophytes). These compounds are ubiquitous in ocean sediments where they are extensively used for paleotemperature reconstruction, but are rare in lake sediments. Here we report the discovery of LCAs (C_{37}-C_{39}) throughout a sediment core from one lake and in surface sediments of five lakes located in west Greenland. LCA concentrations in the surface sediments are one to two orders of magnitude higher than those reported from other lacustrine surface sediments around the world. The presence of C_{38} methyl ketones distinguishes Greenland LCA distributions from those found in other saline lakes in cold regimes. LCAs are present in five lakes with elevated salinity, but absent from five freshwater lakes in the study region. Using the published temperature calibration for lake sediments, alkenone unsaturation indices (U^{K}_{37} and $U^{K'}_{37}$) in the surface sediments of the Greenland lakes appear to record late spring/early summer temperature when algal blooms occur, supporting the use of lacustrine alkenones as a paleotemperature proxy. The LCAs have exceptionally low $\delta^{13}C$ values ranging from -40 to -42 ‰, and are depleted by 3 to 10 ‰ relative to short-chain fatty acids and sterols within the same samples. These $\delta^{13}C$ values are the lowest ever reported for alkenones in a natural setting and have important implications for tracing the alkenone producers in lakes.

1. Introduction

Long-chain alkenones (C_{37}-C_{39}) are ubiquitous in ocean sediments throughout the world and are important biomarkers for reconstruction of past sea surface temperatures (Brassell et al., 1986; Brassell, 1993; Marlowe et al., 1984; Prahl and Wakeham, 1987; Volkman et al., 1995). Alkenones, often dominated by tetraunsaturated forms, have been found in lacustrine sediments from at least 17 lakes around the world, located in England (Cranwell, 1985), Antarctica (Volkman et al., 1988), China (Li et al., 1996; Sheng et al., 1999; Wang and Zheng, 1998), Turkey (Theil et al., 1997), Norway (Innes et al., 1998), Gemany, Russia, U.S.A. (Zink et al., 2001) and South America (Theissen et al., 2005). Recent advances highlight the potential of lacustrine, biomarker-based paleothermometry (Powers et al., 2004; Zink et al., 2001). For example, Zink et al. (2001) showed that there exists a consistent relationship between environmental temperature and distributions of alkenone unsaturation in lake sediment.

Paleoclimate studies carried out on ice cores from the Greenland Ice Sheet reveal climatic variations reflecting large scale, hemispheric climate processes (Alley et al., 1997; Dahl-Jensen, 1998). However, regional climate variability at low altitude around the perimeter of the Greenland ice sheet is more sensitive to oceanic-atmospheric changes such as the North Atlantic Oscillation (Box, 2002; Hurrell, 1995), but is poorly constrained (Anderson and Leng, 2004). Lake sediments offer unique archives for understanding Holocene climate history and regional variations at low elevations in west Greenland, especially if alkenone paleothermometry can be applied to disentangle temperature from precipitation effects in paleolimnological proxy records. This work represents the first organic geochemical study in west Greenland lakes.

2. Samples and analytical methods

2.1. Study sites and samples

The Søndre Strømfjord region (Fig. 1) between the western edge of the Greenland ice sheet and the Davis Strait hosts ~20,000 lakes, most of which are dilute and oligotrophic. However, there are a small number of oligosaline lakes at the head of the Søndre Strømfjord with salinity of approximately 2-4 psu. The lack of hydrologic outflow from the lakes, coupled with locally negative effective precipitation (precipitation minus evaporation) has resulted in evaporative concentration of salts. These lakes are ~170m above sea level and ~110m above the regional marine limit, precluding seawater entrapment during isostatic uplift as a possible source of salinity. The dominant salts are $NaCO_3$, $NaHCO_3$ and $MgHCO_3$, which are delivered to the lakes by eolian transport from nearby sand sheets and by input from erosion within the lake catchments (Anderson et al., 2001). The lakes are calcium-depleted relative to fresh lakes of the region due to $CaCO_3$ precipitation. The oligosaline lakes of this study range in depth from ~12 to 33m. The photosynthetic zone of the shallowest lake SS6 (12m) may reach the water-sediment interface, while in the deeper lakes (BrayaSø, 22m; HundeSø, 33m; LimnæaSø, 28m; and Lake E, 20m) photosynthesis occurs to a depth of ~12m. Climate near the head of Søndre Strømfjord exhibits mean summer temperature of 9.3 ˚C and mean winter temperature of -18 ˚C (for the period 1961-1990; Box, 2002), and receives less than 150mm yr^{-1} of precipitation. Permafrost is continuous in the region and vegetation comprises dwarf-shrub tundra with *Betula nana* (dwarf birch), *Salix glauca* (glaucous willow), *Vaccinium* spp., *Empetrum nigrum* (crowberry) and various herbs and grasses.

Surface sediment samples (0-1 cm depth from sediment-water interface) from BrayaSø, HundeSø and LimnæaSø were retrieved with a gravity corer from the deepest part of each lake. Lake E, SS49 and SS86 sediments were retrieved with a Russian peat corer and were provided by N. John Anderson and Sheri Fritz. SS6 short-core samples and surface samples from freshwater lakes SS32, SS50, SS66 were retrieved with a gravity corer and were provided by N. John Anderson.

2.2. Experimental methods

Samples were freeze-dried and homogenized by mortar and pestle. They were extracted with dichloromethane (DCM) using an Accelerated Solvent Extractor ASE200 (Dionex). Extracts were separated into acid and neutral fractions using Supelco Supelclean™ LC-NH_2 solid phase extraction (SPE) tubes (Huang et al., 2004). The neutral fraction was further separated into aliphatic (hexane elution), ketone (DCM), and alcohol (ethyl acetate:hexane 1:3) fractions using a flash silica gel column. The acid fractions were methylated with 5% anhydrous HCl in methanol at 60 ˚C for 12 hours. The alcohol fractions were derivatized using pyridine: N, N-bis(trimethylsilyl)-

trifluoroacetamide (BSTFA) (1:4). Compounds were analyzed on GC-FID for quantification, GC-MS for identification and GC-IRMS for isotopic analyses (Huang et al., 2004). $^{13}C/^{12}C$ ratios were measured using an HP 6840^{+} GC-pyrolysis system interfaced to a Finnigan Delta^{+} XL stable isotope mass spectrometer. For fatty acids and sterols, the reported carbon isotope ratios were corrected for the carbon added during methylation and silylation, respectively (e.g., Huang et al., 2004). Organic compounds were identified by comparison of mass spectral data with previously reported standards and GC retention times (de Leeuw et al., 1980; Marlowe et al., 1984). Alkenone concentrations were determined from GC-FID analyses of the ketone fractions based on peak responses relative to *n*-C_{36} as the internal standard for SS6, or as the external standard for the other lakes.

3. Results and discussion

3.1. Occurrence and abundance of long-chain alkenones

We found C_{37}-C_{39} long-chain alkenones (LCAs) in surface sediments from all five oligosaline lakes investigated (HundeSø, BrayaSø, LimnæaSø, SS6, and Lake E) (Fig. 2) and in 14 sediment horizons throughout the upper 30cm of SS6 sediment (representing the past ~1100 years; Anderson and Leng, 2004). The alkenone concentrations are the highest reported from lacustrine surface sediments (Table 1). The C_{37} compounds comprise $C_{37:4}$ methyl ketone ($C_{37:4}$Me), $C_{37:3}$Me, and $C_{37:2}$Me; the C_{38} compounds include $C_{38:4}$ ethyl ketone ($C_{38:4}$Et), $C_{38:3}$Et, $C_{38:2}$Et, as well as $C_{38:4}$Me, $C_{38:3}$Me and

$C_{38:2}$Me; and the C_{39} compounds contain $C_{39:4}$Et, $C_{39:3}$Et, and $C_{39:2}$Et. In all samples, alkenones of the same carbon number are dominated by the more unsaturated forms (i.e., tetraenoic > trienoic > dienoic).

The dominance of the tetraunsaturated isomers in west Greenland lake sediments is common for lacustrine alkenones (Cranwell, 1985; Theil et al., 1997; Wang and Zheng, 1998; Schouten et al., 2001; Zink et al., 2001). However, the alkenone distributions in the west Greenland lakes contain C_{38} methyl ketones which are absent from other alkenone-containing, saline lakes in cold regimes (Volkman et al., 1988; Li et al., 1996; Theil et al., 1997; Wang and Zheng, 1998). The Greenland alkenone distributions appear more similar to those observed in marine sediments (e.g., Marlowe et al., 1984), and German (Zink et al., 2001) and English lake sediments (Cranwell, 1985). The similarity among the Greenland and German lake, and marine sediment alkenone distributions is enhanced by the absence of C_{40} compounds in these systems.

C_{38} methyl ketones have been found in cultured marine coccolithophorids belonging to *Emiliania huxleyi* and *Gephyrocapsa oceanica* (Conte et al., 1994; Brassell et al., 2004), but have not been definitively found in algal cultures of the family Isochrysidaceae (e.g., *Isochrysis galbana*; Conte et al., 1994). Partial 18S ribosomal DNA sequences recovered from sediments of Ace Lake, Antarctica suggest that the alkenones in this lake were produced by prymnesiophytes most closely related to *Isochrysis galbana* (Coolen et al., 2004). The presence of C_{38} methyl ketones in Greenland lake sediments but not in Ace Lake sediments may be due to the presence of different prymnesiophytes. We hypothesize that the Greenland prymnesiophytes are close relatives of *Emiliania huxleyi* and *Gephyrocapsa oceanica*, in contrast to the Ace Lake prymnesiophytes. Combined with literature reports of alkenone distributions in different environments (reviewed by Brassell et al., 2004), alkenone distributions in Greenland lake sediments and DNA evidence from Ace Lake (Coolen et al., 2004) suggest that C_{38} methyl ketones may be specific to the close relatives of *Emiliania huxleyi* and *Gephyrocapsa oceanica*. More work will be needed to test this hypothesis.

3.2. Temperature and salinity relationships

The U^{K}_{37} and $U^{K'}_{37}$ indices for alkenones in the surface sediment of five Greenland lakes are given in Table 1. Zink *et al.* (2001) developed an empirical relationship between alkenone unsaturation indices and summer average water temperature (T) using German lake sediment and water filtrates (Table 1). The similarity of alkenone distributions in Greenland and German lakes provides a basis for applying the German lake calibrations (U^{K}_{37} = 0.02T -0.121, r^2 = 0.89; $U^{K'}_{37}$ = 0.211T - 0.725, r^2 = 0.68) to Greenland lakes. Employing the calibrations, Greenland U^{K}_{37} data yield water temperature estimates ranging from ~2 to 5.5 ˚C, and $U^{K'}_{37}$ data yield water temperature estimates ranging from ~10 to 11.5 ˚C (Fig. 3). Measured surface water temperature from BrayaSø ranged from 0 ˚C in early June to ~17 ˚C in mid-July, 2000 (Anderson and Broderson, 2001), bracketing the temperatures calculated using the calibrations of Zink *et al.* (2001). The major algal bloom in the Greenland lakes takes place during this period, as sunlight increases and turn-over of lakes supplies nutrients to the photic zone. The U^{K}_{37} temperature calibration provides estimates similar to temperature immediately following ice melt (early June) while the higher $U^{K'}_{37}$ estimates resemble the measured temperatures a week or two later.

U^{K}_{37} (due to inclusion of $C_{37:4}$) may be influenced by environmental variables other than temperature. Previous workers reported strong correlation between water salinity and production of $C_{37:4}$ in the North Atlantic and Nordic Seas (r^2=0.699, Rosell-Melé et al., 2002; r^2=0.78, Sicre et al., 2002). However, application of these salinity calibrations to west Greenland lakes yields salinity estimates ranging from ~18 to 35 psu, an order of magnitude higher than the actual lake salinity (2-4 psu). It has been noted that the apparent salinity dependence in the North Atlantic and Nordic Seas may be an artifact of temperature dependence on $C_{37:4}$ production, given the co-varability of salinity and temperature in these waters (Sicre et al., 2002; Sikes and Sicre, 2002). Bendle and Rosell-Melé (2004) suggested that the complexity of water masses and differing relative contributions of different prymnesiophytes in the North Atlantic and Nordic Seas may be responsible for the difficulty met when applying U^{K}_{37} and $U^{K'}_{37}$ temperature calibrations in the region. Although the relationship is still not fully understood, evidence is mounting that salinity does not exert a significant control on $C_{37:4}$ production.

The *occurrence* of alkenones (and by inference, the presence of prymnesiophytes) in the Greenland lakes does appear to depend on salinity. Mean conductivity for the oligosaline lakes in this region is an order of magnitude higher than for freshwater lakes (2387 and 136 μScm^{-1}, respectively) (Anderson et al., 2001). While unusually high concentrations of alkenones are present in the surface sediment of the oligosaline lakes, surface sediments from five nearby freshwater lakes (SS32, SS49, SS50, SS66 and SS86) are devoid of alkenones. Absence of alkenones from the fresh lakes and their presence in lakes of slightly elevated salinity (~10% of seawater) implies a salinity threshold for the occurrence of alkenone-producing prymnesiophyte algae. Alkenones were not found in surface sediments of 36 freshwater lakes in North America (Huang et al., 2004). Indeed, reports of alkenone occurrence have been from marine capture basins (Volkman et al., 1988) or lakes in evaporative settings lacking outflow (Li et al., 1996; Theil et al., 1997; Wang and Zheng, 1998; Zink et al., 2001) with salinity ranging from ~6 to 21.6 psu. Furthermore, alkenones were found in Younger Dryas sediments from Lake Steisslingen, Germany (Zink et al., 2001) in concentrations almost as high as the Greenland lakes, but were absent or negligible elsewhere in the core. Dry conditions associated with the Younger Dryas may have increased lake salinity during this time (Zink et al., 2001), providing a habitat for alkenone-producing prymnesiophytes.

3.3. Alkenone carbon isotope ratios

Schouten *et al.* (2001) found that alkenones from Ace Lake, Antarctica had low $\delta^{13}C$ values (-31.7 to -36.1‰) (Table 2). They noted that ^{13}C-depleted alkenones could reflect: 1) low water temperature, and therefore high CO_2 concentrations and low cell growth rates, acting to maximize carbon isotope fractionation (Popp et al., 1998), and/or 2) recycling of CO_2 from decomposition of organic matter within the lake. The $\delta^{13}C$ values of alkenones in Greenland lake sediments are even lower than those from Ace Lake, ranging from -40.0 to

-41.7‰, with $C_{37:4}$ consistently more negative than $C_{37:3}$ (Table 2). However, the $\delta^{13}C$ offset between $C_{37:4}$ and $C_{37:3}$ in the Greenland samples (0.4 to 1‰) is significantly smaller than that observed in the Black Sea (2 to 4‰, Freeman and Wakeham, 1992). Furthermore, alkenone $\delta^{13}C$ values are ~3 to 10‰ lower than those of short chain alkanoic acids and sterols (primarily autochthonous lipids) within the same sediment samples. Depletion of ^{13}C in alkenones (by ~2 to 9‰) relative to sulfur-bound C_{27}-C_{29} steranes was also reported for Ace Lake sediment (Schouten et al., 2001). Based on results from culture studies (Laws et al., 2001) it is unlikely that sterols produced by prymnesiophytes are isotopically enriched relative to alkenones due to differences in biosynthetic isotopic fractionation. The $\delta^{13}C$ offset between alkenones and sterols suggests that the prymnesiophyte contribution to total sedimentary sterols is small relative to the full range of primary producers.

If atmospheric CO_2 ($\delta^{13}C_{atmosphere}$~ -8‰, yielding $\delta^{13}C_{CO2\ (aq)}$ ~ -9‰) is the sole carbon source for the alkenone producers in Greenland lakes, the observed $\delta^{13}C$ value of -41 ‰ for alkenones would require isotopic fractionation (ε_p) of ~27‰ by alkenone producers (assuming maximum isotopic depletion of 5.4‰ for alkenones relative to algal biomass; Laws et al., 2001). At high CO_2 (aq) and low growth rate, a maximum ε_p of 25‰ has been observed in culture experiments with *E. huxleyi* (Popp et al., 1998). $\delta^{13}C$ values as low as -43.7‰ have been observed for various sterols in suspended particulate organic matter in the Southern Ocean and were tentatively attributed to slow growth rates and high CO_2 concentrations resulting from low water temperature (Popp et al., 1999).

In addition to CO_2 concentration and growth rate, carbon isotope fractionation also increases with the surface area to volume ratio (i.e., decreasing cell size) of a cell and as cell geometry becomes less spherical (Popp et al., 1998). The low $\delta^{13}C$ values of alkenones relative to other aquatic compounds may also suggest that the prymnesiophytes in Greenland lakes are smaller in size than other primary producers in the lakes. Small cell size, in addition to high CO_2 (aq) and slow growth rate, offers an appealing explanation for the low $\delta^{13}C$ values of alkenones, as it may account for the difficulty encountered in previous attempts to isolate lacustrine alkenone-producers (Li et al., 1996; Theil et al., 1997; Zink et al., 2001).

An alternative explanation for the low $\delta^{13}C$ values of alkenones relative to fatty acids and sterols is that dissolved atmospheric CO_2 is not the only carbon source for photosynthetic organisms. Salinity stratification combined with a deep photic zone in the west Greenland lakes (Anderson et al., 2001) could create a habitat for autotrophic organisms directly above the chemocline, providing access to light for photosynthesis as well as recycled (^{13}C-depleted) $CO_{2,}$ such as that produced by methane oxidation. Alkenone-producing prymnesiophytes may live in a habitat with greater access to the recycled CO_2 than other algae, leading to $\delta^{13}C$ values of alkenones that are lower than sterols and short-chain alkanoic acids. However, $\delta^{13}C$ values of DIC in three of the Greenland lakes (HundeSø, BrayaSø and LimnæaSø) showed relative uniformity with water depth in May 1999, ranging from -1.1 to 0.8‰ (M. Leng, personal communication). If this homogenous DIC carbon isotope profile is representative of the entire algal growth season, then all submerged aquatic autotrophs in the lakes should utilize CO_2 having similar carbon isotope ratios. If this is the case, the $\delta^{13}C$ offset between alkenones and other autochthonous lipids is likely due to enhanced carbon isotope fractionation by alkenone-producing prymnesiophytes due to the combined effects of high CO_2(aq), low growth rate and small cell size as discussed above.

4. Conclusions

The identification of alkenones in the sediment of five oligosaline lakes extends the known geographic range of these compounds to west Greenland. The sedimentary alkenone concentrations are the highest ever reported, suggesting that the Greenland lakes offer a favorable habitat for certain prymnesiophyte species. U^{K}_{37} and $U^{K'}_{37}$ water temperature estimates for the Greenland lakes based on the calibrations of Zink *et al.* (2001) are in the range of measured lake water temperatures during the period of high aquatic productivity. Salinity calibrations from the North Atlantic and Nordic Seas based on the proportion of $C_{37:4}$ in alkenone distributions provide incorrect salinity estimates for the Greenland lakes. Contributions from various unmineralized (i.e., lacking coccoliths) alkenone-producers such as those in the west Greenland lakes, or varying relative contributions from one or more such organisms could help explain the complexity of alkenone-based temperature calibrations in the North Atlantic and Nordic Seas. The highly-negative $\delta^{13}C$ values for alkenones in west Greenland lakes represent the greatest isotopic depletion reported for alkenones from a natural setting. However, our data are insufficient to determine whether such low $\delta^{13}C$ values are due to enhanced carbon isotopic fractionation or utilization of ^{13}C-depleted carbon sources.

Acknowledgements

This work was supported by grants from the National Science Foundation (NSF0081478, 0318050, 0318123, 0402383), NASA (NAG5-10665, NNG04GJ34G) and American Chemical Society, Petroleum Research Fund (ACS-PRF#38878-AC2) to Y. Huang. We thank Simon Brassell and an anonymous reviewer for comments that helped improve the quality of this manuscript. We also thank N. John Anderson and Sheri Fritz for providing sediment samples (sample collection supported by ATM0081226 to Sheri Fritz), Melanie Leng for DIC $\delta^{13}C$ data, and Yi Wang for technical assistance.

References

Alley, R.B., Mayewski, P.A., Sowers, T., Stuiver, M., Taylor, K.C., Clark, P.U., 1997. Holocene climatic instability: A prominent, widespread event 8200 yr ago. Geology 25, 483-486.

Anderson, N.J., Harriman, R., Ryves, D.B., Patrick, S.T., 2001. Dominant Factors Controlling Variability in the Ionic Composition of West Greenland Lakes. Arctic, Antarctic, and Alpine Research 33, 418-425.

Anderson, N.J., Brodersen, K.P., 2001. Determining the date of ice-melt for low Arctic lakes along Søndre Strømfjord, southern West Greenland. Geology of Greenland Survey Bulletin 189, 54-58.

Anderson, N.J., Leng, M.J., 2004. Increased aridity during the early Holocene in West Greenland inferred from stable isotopes in laminated-lake sediments. Quaternary Science Reviews 23, 841-849.

Bendle, J., Rosell-Melé, A., 2004. Distributions of U^{K}_{37} and $U^{K}_{37'}$ in the surface waters and sediments of the Nordic Seas: Implications for paleoceanography. Geochemistry Geophysics Geosystems 5, doi:10.1029/2004GC000741.

Box, J.E., 2002. Survey of Greenland Instrumental Temperature Records: 1873-2001. International Journal of Climatology 22, 1829-1847.

Brassell, S.C., Dumitrescu, M., the ODP Leg 198 Shipboard Scientific Party, 2004. Recognition of alkenones in a lower Aptian porcellanite from the west-central Pacific.
Organic Geochemistry 35, 181-188.

Brassell, S.C., 1993. Applications of Biomarkers for Deliniating Marine Paleoclimatic Fluctuations during the Pleistocene. In: Engel, M.H., Macko, S.A. (Eds.), Organic Geochemistry. Plenum Press, New York, pp. 699-738.

Brassell, S.C., Eglinton, G., Marlowe, I.T., Pflaumann, U., Sarnthein, M., 1986. Molecular stratigraphy: A new tool for climatic assessment. Nature 320, 129-133.

Conte, M.H., Volkman, J.K., and Eglinton, G., 1994. Lipid biomarkers of the Haptophyta. In: Green, J.C., Leadbeater, B.S.C. (Eds.), The Haptophyte Algae. Clarendon Press, pp. 351-377.

Coolen, M.J.L., Muyzer, G., Rijpstra, W.I.C., Schouten, S., Volkman, J.K., Sinninghe Damste, J.S., 2004. Combined DNA and lipid analyses of sediments reveal changes in Holocene haptophyte and diatom populations in an Antarctic lake. Earth and Planetary Science Letters 223, 225-239.

Cranwell, P.A., 1985. Long-chain unsaturated ketones in recent lacustrine sediments. Geochimica et Cosmochimica Acta 49, 1545-1551.

Dahl-Jensen, D., Mosegaard, K., Gundestrup, N., Clow, G.D., Johnsen, S.J., Hansen, A.W., Balling, N., 1998. Past temperatures directly from the Greenland Ice Sheet. Science 282, 268-274.

de Leeuw, J.W., van der Meer, F.W., Rijpstra, W.I.C., Schenck, P.A., 1980. On the occurrence and structural identification of long chain unsaturated ketones and hydrocarbons in sediments. In: Douglas, A.C., Maxwell, J.R. (Eds.), Advances in Organic Geochemistry. Pergamon Press, pp. 211-217.

Freeman, K.H., Wakeham, S.G., 1991. Variations in the distributions and isotopic

compositions of alkenones in Black Sea particles and sediments. Organic Geochemistry 19, 277-285.
Huang, Y., Shuman, B., Wang, Y., Webb III, T., 2004. Hydrogen isotope ratios of individual lipids in lake sediments as novel tracers of climatic and environmental change: a surface sediment test. Journal of Paleolimnology 31, 363-375.
Hurrell, J.W., 1995. Decadal Trends in the North Atlantic Oscillation: Regional Temperatures and Precipitation. Science 269, 676-679.
Innes, H.E., Bishop, A.N., Fox, P.A., Head, I.M., Farrimond, P., 1998. Early diagenesis of bacteriohopanoids in Recent sediments of Lake Pollen, Norway. Organic Geochemistry 29, 1285-1295.
Laws, E.A., Popp, B.N., Bidigare, R.R., Riebesell, U., Burkhardt, S., Wakeham, S.G., 2001. Controls on the molecular distribution and carbon isotopic composition of alkenones in certain haptophyte algae. Geochemistry Geophysics Geosystems 2, doi:10.1029/2000GC000057.
Li, J., Philip, R.P., Pu, F., Allen, J., 1996. Long-chain alkenones in Qinghai Lake sediments. Geochimica et Cosmochimica Acta 60, 235-241.
Marlowe, I.T., Brassell, S.C., Eglinton, G., Green, J.C., 1984. Long chain unsaturated ketones and esters in living algae and marine sediments. Organic Geochemistry 6, 135-141.
Popp, B.N., Laws, E.A., Bidigare, R.R., Dore, J.E., Hanson, K.L., Wakeham, S.G., 1998. Effect of phytoplankton cell geometry on carbon isotopic fractionation. Geochimica et Cosmochimica Acta 62, 69-77.
Popp, B.N., Trull, T, Kenig, F., Wakeham, S.G., Rust, T.M., Tilbrook, B., Griffiths, F.B., Wright, S.W., Marchant, H.J., Bidigare, R.R., Laws, E.A. 1999. Controls on the carbon isotopic composition of Southern Ocean phytoplankton. Global Biogeochemical Cycles 13, 827-843.
Powers, L.A., Werne, J.P., Johnson, T.C., Hopmans, E.C., Sinninghe Damsté, J.S., Schouten, S., 2004. Crenarchaeotal membrane lipids in lake sediments. A new paleotemperature proxy for continental paleoclimate reconstruction? Geology 32, 613-616.
Prahl, F.G., Wakeham, S.G., 1987. Calibration of unsaturation patterns in long-chain ketone compositions for paleotemperature assessment. Nature 330, 367-369.
Rosell-Melé, A., Jansen, E., Weinelt, M., 2002. Appraisal of a molecular approach to infer variations in surface ocean freshwater inputs into the North Atlantic during the last glacial. Global and Planetary Change 34, 143-152.
Schouten, S., Rijpstra, W.I.C., Kok, M., Hopmans, E.C., Summons, R.E., Volkman, J.K., Sinninghe Damsté, J.S., 2001. Molecular organic tracers of biogeochemical processes in a saline meromictic lake (Ace Lake). Geochimica et Cosmochimica Acta 65, 1629-1640.
Sheng, G.Y., Cai, K.Q., Yang, X.X., Lu, J.L., Jia, G.D., Peng P.A., and Fu, J.M., 1999. Long-chain alkenones in Hotong Qagan Nur Lake sediments and its paleoclimatic implications. Chinese Science Bulletin 44, 259-263.
Sicre, M.-A., Bard, E., Ezat, U., Rostek, F., 2002. Alkenone distributions in the North Atlantic and Nordic sea surface waters. Geochemistry Geophysics Geosystems 3, doi:10.1029/2001GC000159.
Sikes, E.L., Sicre, M-A., 2002. Relationship of the tetra-unsaturated C_{37} alkenone to

salinity and temperature: Implications for paleoproxy applications. Geochemistry Geophysics Geosystems 3, doi:10.1029/2002GC000345.

Theil, V., Jenisch, A., Landmann, G., Reimer, A., Michaelis, W., 1997. Unusual distributions of long-chain alkenones and tetrahymanol from the highly alkaline Lake Van, Turkey. Geochimica et Cosmochimica Acta 61, 2053-2064.

Theissen, K.M., Zinniker, D.A., Moldowan, J.M., Dunbar, R.B., Rowe, H.D., 2005. Pronounced occurrence of long-chain alkenones and dinosterol in a 25,000-year lipid molecular fossil record from Lake Titicaca, South America. Geochimica et Cosmochimica Acta 69, 623-636.

Volkman, J.K., Burton, H.R., Everitt, D.A. Allen, D.I., 1988. Pigment and lipid compositions of algal and bacterial communities in Ace Lake, Vestfold Hills, Antarctica. Hydrobiologia 165, 41-57.

Volkman, J.K., Barrett, S.M., Blackburn, S.I., Sikes, E.L., 1995. Alkenones in *Gephyrocapsa oceanica*: Implications for studies of paleoclimate. Geochimica et Cosmochimica Acta 59, 513-520.

Wang, R., and Zheng, M., 1998. Occurence and environmental significance of long-chain alkenones in Tibetan Zabuye Salt Lake, S.W. China. International Journal of Salt Lake Research 6, 281-302.

Zink, K.G., Leythaeuser, D., Melkonian, M., Schwark, L., 2001. Temperature dependency of long-chain alkenone distributions in Recent to fossil limnic sediments in lake waters. Geochimica et Cosmochimica Acta 65, 253-265.

TABLE 1. LAKES WITH ALKENONES IN SURFACE SEDIMENT

Location	Lake	Alkenone concentration (μg/gTOC)	U^{K}_{37} [a]	$U^{K'}_{37}$ [a]
Greenland	SS6	11,100	-0.68	0.11
Greenland	BrayaSø	82,700	-0.61	0.085
Greenland	HundeSø	50,300	-0.66	0.072
Greenland	LimnæaSø	47,100	-0.61	0.089
Greenland	Lake E	5,900	-0.60	0.087
Germany	Lake Constance[b]	69	-0.18	0.28
Germany	Waldsee[b]	32	-0.25	0.33
Germany	Olzreuter See[b]	111	-0.25	0.33
Germany	Lake Steisslingen[b]	12	-0.27	0.38
Germany	Lake Stechlin[b]	143	-0.37	0.2
Germany	Brieter Luzin[b]	52	-0.39	0.2
Germany	Schmaler Luzin[b]	202	-0.29	0.3
Germany	Hausee[b]	205	-0.25	0.33
Germany	Tollensesee[b]	69	-0.38	0.25
Germany	Dagowsee[b]	n.a.	-0.08	0.38
Germany	Gr. Wummsee[b]	25	-0.33	0.21
U.S.A.	Brush Lake[b]	203	-0.57	0.18
Turkey	Lake Van[c]	4,911	-0.65	0.19
China	Qinghai Lake[d]	443	n.a.	0.20

n.a. = not available.

[a] U^{K}_{37} = (37:2-37:4)/(37:4+37:3+37:2); $U^{K'}_{37}$ = (37:2)/(37:3+37:2).

[b] Zink *et al*. (2001).

[c] Thiel *et al*. (1997).

[d] Li *et al*. (1996).

TABLE 2. $\delta^{13}C$ VALUES OF REPRESENTATIVE ORGANIC COMPOUNDS IN GREENLAND LAKES AND ACE LAKE, ANTARCTICA[a]

	Alkenones		Alkanoic Acids			Sterols	
Sediment sample	$C_{37:4}$	$C_{37:3}$	14	16	28	1[b]	2[b]
Greenland Lakes							
BrayaSø	-41.7	-41.0	-35.0	-32.5	-30.4	-36.7	-36.3
	(.08)	(.01)	(s.m.)	(s.m.)	(s.m.)	(.18)	(.01)
HundeSø	-41.0	-40.0	-35.1	-32.4	-29.4	-37.2	-36.6
	(.01)	(.01)	(.17)	(.13)	(1.3)	(.18)	(3.4)
LimnæaSø	-40.8	-40.4	-37.2	-34.0	-32.4	-34.6	-36.3
	(.08)	(.04)	(.59)	(.04)	(.34)	(.48)	(.26)
Lake E	-41.4	-41.0	n.d.	n.d.	n.d.	n.d.	n.d.
	(.42)	(.30)					

	Alkenones	Steroids		
	$C_{37:4} + C_{37:3}$	C_{27} sterane	C_{28} sterane	C_{29} sterane
Ace Lake, Antarctica[c]				
0-5cm	n.d.	-28.6	n.d.	-29.2
		(0.5)		(0.7)
6.6-8.3cm	-31.7	-28.2	-28.8	-28.3
	(0.3)	(0.2)	(0.2)	(0.1)
11.6-13.3cm	-34.6	-27.9	-29.2	-28.5
	(0.3)	(0.2)	(0.4)	(0.1)
16.6-18.3cm	-36.1	-30.3	-33.8	-30.6
	(0.4)	(0.3)	(0.1)	(0.1)
21.6-23.3cm	-34.9	-30.4	-30.7	-30.1
	(0.9)	(0.3)	(0.3)	(0.1)

s.m. = single measurement.
n.d. = not determined.
[a] Greenland lake samples are surface sediments while Ace Lake (Antarctica) samples are down-core. $\delta^{13}C$ values are reported as ‰ relative to VPDB. Numbers in parentheses are standard deviation from duplicated measurements.
[b] (1) 5α-cholest-22E-en-3β-ol; (2) 5β-cholestan-3β-ol.
[c] Schouten *et al.* (2001).

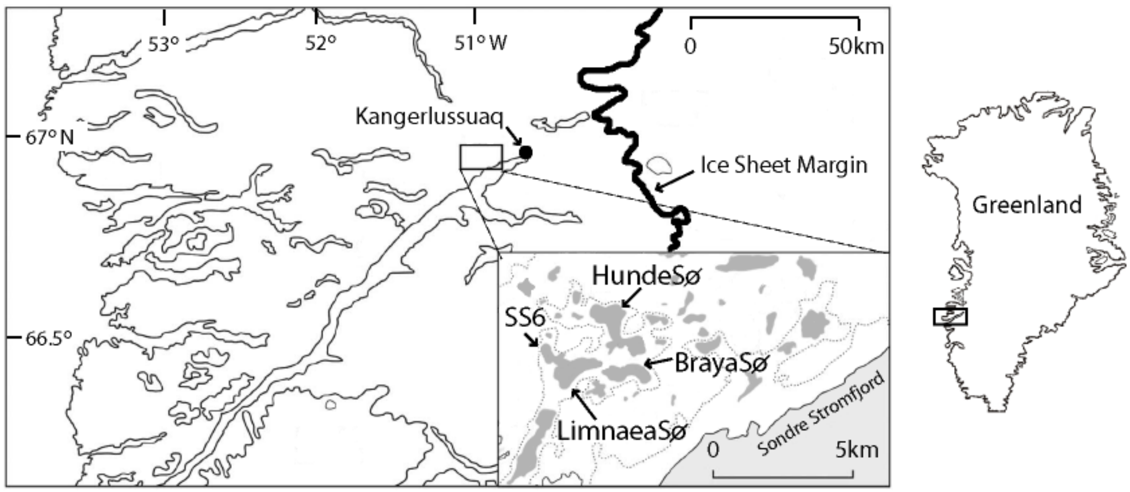

Figure 1. Study area at the head of Søndre Strømfjord, west Greenland. Labeled lakes contain high concentrations of alkenones in sediments. Lake E is located ~10km northwest of HundeSø.

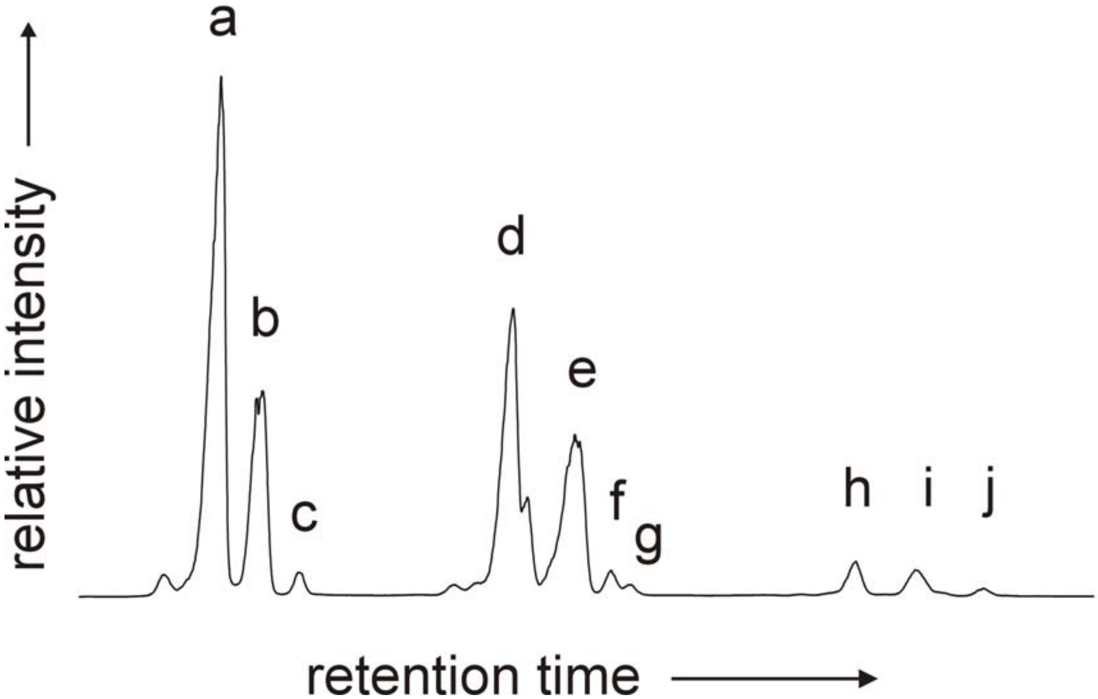

Figure 2. Partial gas chromatogram of the ketone fraction from SS6 lake sediment showing the characteristic distribution of long-chain alkenones found in west Greenland lake sediment. (a) $C_{37:4}$Me (b) $C_{37:3}$Me (c) $C_{37:2}$Me (d) $C_{38:4}$Et and $C_{38:4}$Me (e) $C_{38:3}$Et and $C_{38:3}$Me (f) $C_{38:2}$Et (g) $C_{38:2}$Me (h) $C_{39:4}$Et (i) $C_{39:3}$Et (j) $C_{39:2}$Et.

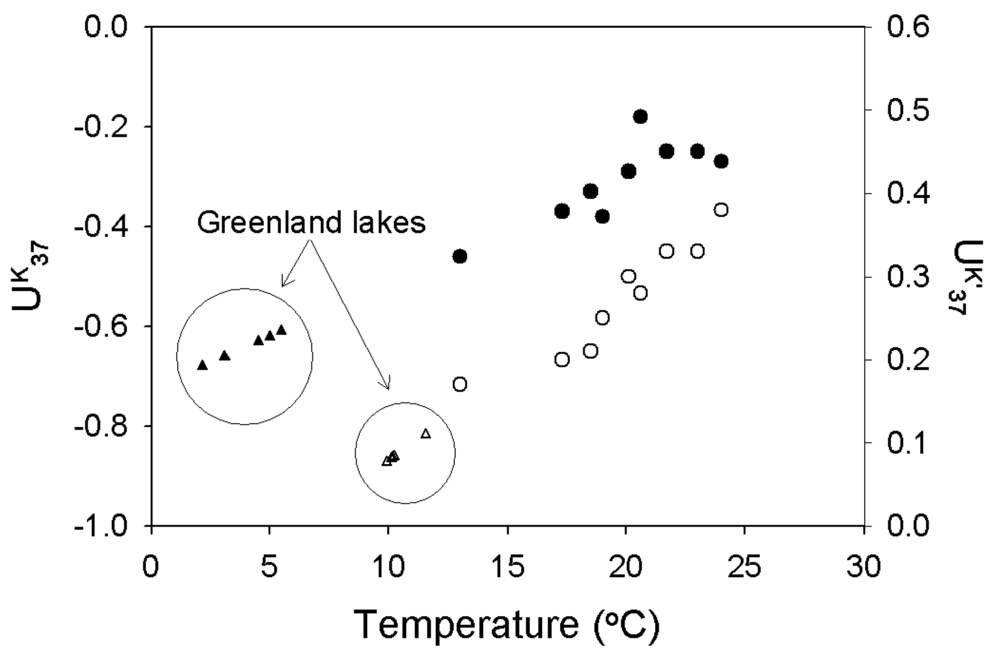

Figure 3. Estimated lake water temperatures from west Greenland lakes based on U^{K}_{37} (filled symbols) and $U^{K'}_{37}$ (empty symbols) temperature calibrations of Zink *et al*. (2001). German lake data are plotted as circles; Greenland lake data are plotted as triangles.

CHAPTER 2

ALKENONE PRODUCERS INFERRED FROM WELL-PRESERVED 18S rDNA IN GREENLAND LAKE SEDIMENTS

WILLIAM J. D'ANDREA[1]

YONGSONG HUANG[1]

MELISSA LAGE[2]

JENNIFER B.H. MARTINY[2]

ABBY D. LAATSCH[3]

LINDA A. AMARAL-ZETTLER[3]

MITCHELL L. SOGIN[3]

[1]BROWN UNIVERSITY, *Department of Geological Sciences*

[2]BROWN UNIVERSITY, Department of *Ecology and Evolutionary Biology*

[3]MARINE BIOLOGICAL LABORATORY, *Josephine Bay Paul Center*

Published in:

Journal of Geophysical Research 111, 03013, doi:10.1029/2005JG000121, 2006

Abstract

18S ribosomal DNA (rDNA) sequences of haptophyte algae were successfully amplified using the polymerase chain reaction (PCR) from water filtrate, surface sediments, and a late-Holocene sediment sample (~1000 years old) from a group of lakes in the Søndre Strømfjord region of west Greenland. The DNA of the algal primary producer is extremely well preserved in the laminated lake sediments which have been deposited in cold (1-2 ^{o}C), anoxic, and sulphidic bottom water. Phylogenetic analyses of the Greenland haptophyte rDNA sequences suggest that alkenones in the Greenland lake sediments are produced by haptophyte algae of the class Prymnesiophyceae. The 18S rDNA sequences from the Greenland samples cluster within a distinct phylotype, differing from both marine haptophytes and from those reported previously from Ace Lake, Antarctica. The similarity of haptophyte rDNA sequences among all samples in this study suggests a single alkenone-based temperature calibration may be applied to these lakes for at least the past 1000 years. These sedimentary archives hold great promise for high-resolution, alkenone-based paleotemperature reconstruction of southern west Greenland, a region sensitive to atmospheric-oceanic climate phenomena such as the North Atlantic Oscillation (NAO).

1. Introduction

1.1 Biomarkers and rDNA

Lipid biomarkers extracted from geological samples have been commonly used to study past environmental change due to their resistance to diagenesis and sensitivity to environmental parameters (e.g., Brassell, 1993; Meyers, 2003; Huang et al., 2004). However, most lipid biomarkers are characteristic of a general group of organisms (e.g., terrestrial plants, algae, bacteria, and in the case of long-chain alkenones, certain members of the algal division Haptophyta) rather than a single organism, limiting the effectiveness of lipids for inferring the identity of specific producer organisms and environmental history. Ribosomal DNA (rDNA) comprises genes coding for ribosomal RNA (rRNA), which is associated with ribosomal proteins. In contrast to lipid biomarkers, the gene coding for small-subunit rRNA (18S in eukaryotes, 16S in prokaryotes) has been effectively used for phylogenetic reconstruction, with taxonomic resolution to the species level (Sogin et al., 1986; Edvardsen et al., 2000). When such genes survive in the geologic record they can serve as exceptional biomarkers by offering species-level identification of producer organisms and reconstruction of the community structure of the ancient ecosystem (Banning et al., 2005; Coolen et al., 2004). The rapidly expanding catalogue of published nucleotide sequences of rRNA genes from specific organisms (e.g., GenBank and RDP-II, Benson et al., 2004; Cole et al., 2005) facilitates efficient identification of rDNA sequences obtained from environmental samples.

Unfortunately, DNA molecules are relatively unstable in geological systems, limiting the widespread use of rDNA as a biomarker. Consequently, preservation of meaningful DNA sequences in most geologic environments has typically not been expected beyond 10 kyr (Pääbo and Wilson, 1991). However, recent studies indicate excellent preservation of DNA in sediments of Ace Lake, Antarctica up to 10,000 years in age (Coolen et al., 2004), and in Siberian permafrost up to 400,000 years in age (Willerslev et al., 2003). These findings suggest that DNA may survive in certain depositional environments for a considerable length of time and, in such instances, can serve as an unrivaled biomarker for studying ancient biogeochemical systems.

1.2 Lacustrine alkenones in west Greenland

Previous work by D'Andrea and Huang (2005) has shown that sediment from oligosaline lakes (1-3 psu) of west Greenland contain exceptionally high abundances of long-chain alkenones. These important geochemical biomarkers are common in marine sediments and exhibit unsaturation patterns that are excellent sensors of temperature change (Brassell et al., 1986; Prahl and Wakeham, 1987; Brassell, 1993). Long-chain alkenones are specific to certain haptophyte algae (division Haptophyta, class Prymnesiophyceae; Edvardsen et al., 2000) and have been found in lake sediments from England (Cranwell, 1985), Antarctica (Volkman et al., 1988), China (Li et al., 1996; Wang and Zheng, 1998; Sheng et al., 1999), Turkey (Theil et al., 1997), Norway (Innes et al., 1998), Gemany, Russia, U.S.A. (Zink et al., 2001), and South America (Theissen et al., 2005). Despite the on-going discovery of lakes containing sedimentary alkenones, no one has been able to isolate and culture the lacustrine organisms responsible for producing these compounds.

The objectives of the present study are to (1) assess the preservation of DNA in sediments of the west Greenland lakes, (2) use 18S rDNA to test for the presence of haptophyte algae in the Greenland lakes, (3) identify haptophytes in the lakes by rDNA comparison with known haptophytes, and (4) determine the similarity of haptophyte species among the study lakes by rDNA comparison. We conclude that alkenones in the west Greenland lakes are produced by haptophytes of the class Prymnesiophyceae, and represent a new phylogenetic clade. The similarity of 18S rDNA among the haptophytes in all lakes of this study supports the application of a single alkenone-based temperature calibration to the respective sedimentary records. The west Greenland lakes appear to preserve DNA of primary producers exceptionally well, probably due to the bottom-water conditions associated with meromixis.

2. Site Description

The Søndre Strømfjord region (Fig. 1) is situated between the western edge of the Greenland ice sheet and the Davis Strait and houses ~20,000 lakes. Most are dilute and oligotrophic, but there are several lakes with elevated salinity (1-3 psu) which are best described as oligosaline. Extensive work describing the water chemistry of the lakes of the Søndre Strømfjord region has been done by Anderson *et al*. (2001). A summary of their findings concerning the major ion chemistry of the oligosaline and freshwater lakes is shown in Table 1b. The major difference in ionic composition between the oligosaline and freshwater lakes is the relative importance of calcium (Anderson et al., 2001). The amount of Ca with respect to other ions is greater in the freshwater lakes (Ca > Mg > Na > K) than in the oligosaline lakes (Na > Mg > K > Ca).

The oligosaline lakes are ~110m above the regional marine limit, ruling out seawater capture during isostatic uplift as a possible source of salinity. However, the major ion chemistry of the lakes implies that they have received ions through processes besides rainout. Nearby glacial outwash plains are a source of loess to the basins which likely delivers sodium to the lakes, while deflation of uplifted marine deposits adjacent to Søndre Strømfjord represents a source of chloride (Anderson et al., 2001).

While all of the study lakes (Hunde Sø, Braya Sø, Limnæa Sø, and SS6; Fig. 1) receive surface runoff during the spring melt, they are not connected by overland flow at any time of the year, with the exception of Limnæa Sø and SS6. These two basins have been physically connected to one another since 1998 (McGowan et al., 2003) when rising lake water levels breeched a sill that had previously separated the lakes. All of the oligosaline lakes are closed basins, having no hydrologic outflow except for evaporation. Groundwater flow in the region is limited by the presence of permafrost.

The enhanced salinity of the closed-basin lakes near the head of Søndre Strømfjord can be explained by the input of salts from local sources, and the negative effective precipitation of the region. The vicinity of the study lakes receives less than 150 mm of precipitation each year. Mean summer temperature is 9.3 ˚C and mean winter temperature is -18 ˚C (for the period 1961-1990; Box, 2002). Anderson *et al*. (1999) reported anoxic conditions in the hypolimnion of Braya Sø (Fig. 1), owing to stratification of the water column.

D'Andrea and Huang (2005) found exceptionally high concentrations of alkenones in sediments from four oligosaline lakes of the Søndre Strømfjord region (Braya Sø, Hunde Sø, Limnæa Sø and SS6; Fig. 1; Table 1a). The alkenone abundance suggests that the lakes provide a favorable habitat for certain alkenone-producing, haptophyte algae. However, the identity of such lacustrine haptophytes remains a mystery and despite numerous efforts, alkenone-producing haptophytes have not been observed from any alkenone-bearing lakes (Li et al., 1996; Theil et al, 1997; Zink et al., 2001).

3. Methods

3.1 Field work and sampling

Modern and late-Holocene sediment samples for DNA extraction were collected in August 2004 by Eckman dredge and gravity corer, respectively. The late-Holocene sample, collected from the deepest part of Braya Sø, is from a depth of 30cm below the sediment-water interface and is estimated to be ~1000 years old by comparison with a ^{14}C-dated, neighboring gravity core (Anderson and Leng, 2004). Sediment was extruded from the core barrel and a sub-sample for DNA extraction was removed from the center of the core to avoid potential contamination by younger sediments. Water filtrates were collected by filtration of 3L of lake water using 0.22μm Sterivex™ filters (Millipore). Water filtrates were immediately treated with pre-filtered (0.22μm) Puregene® lysis buffer (Gentra Systems, Inc.). Samples were kept cool and in the dark for ~12 hours before being frozen at -40˚C. Sediment samples for alkenone analysis were collected by gravity corer.

3.2 Alkenone extraction and identification

Details of alkenone extraction and analysis can be found in D'Andrea and Huang (2005). Briefly, samples were freeze-dried, homogenized, and extracted with dichloromethane (DCM). Compounds were analyzed by GC-FID for quantification, GC-MS for identification and GC-IRMS for isotopic analysis. Long-chain alkenones were identified by comparison of mass spectral data with previously reported standards and GC retention times (de Leeuw et al., 1980; Marlowe et al., 1984).

3.3 DNA extraction and amplification

DNA was extracted from sediment samples using a FastDNA® SPIN Kit for Soil (Qbiogene, Inc.) according to the manufacturer specifications. Double-stranded DNA from extracts was quantified with a Beckman Coulter DU® 530 spectrophotometer by measuring the amount of light (at 260nm, the wavelength of maximum absorption for DNA and RNA) absorbed by the extracted DNA. DNA was extracted from water filtrates using a Puregene Tissue Kit (Gentra Systems, Inc.). We used primers (Prym-429f: 5′-

GCG CGT AAA TTG CCC GAA -3′, and Prym-887r: 5′- GGA ATA CGA GTG CCC CTG AC -3′) to amplify partial 18S rDNA from haptophytes (Simon et al., 2000; Coolen et al., 2004). Polymerase chain reactions (PCR) were performed in a PTC-100™ thermocycler (MJ Research, Inc.). Reactions were performed as described by Coolen *et al*. (2004), and comprised initial denaturing for 4 min at 96˚C, followed by 35 cycles including denaturing (30 s at 94˚C), primer annealing (40 s at 55˚C), primer extension (40 s at 72˚C), and a final extension (10 min at 72˚C). DNA extracted from two different isolated strains of the haptophyte *Prymnesium parvum* was used for positive control during PCR amplification and a blank sample was used for negative control. PCR amplicons were purified using a QIAquick® PCR Purification Kit (QIAGEN, Inc.) and cloned with a TOPO-TA cloning kit for sequencing (Invitrogen). Sequences of cloned rDNA amplicons were determined with an Applied Biosystems 3730xl DNA analyzer at the Marine Biological Laboratory. 90 to 95 sequences of 426 nucleotides in length were obtained for each sample.

3.4 *PCR Contamination*

Steps were taken to avoid and detect possible contamination of the late-Holocene sediment sample with contemporary DNA, or cross-contamination among modern samples. All PCR reactions were conducted in a laboratory that does not routinely amplify 18S rDNA. Laboratory equipment was autoclaved or ethanol-washed prior to contact with a new sample and protective clothing was worn. All PCR steps, after DNA extraction, were conducted in a UV-sterilized bio-hood, and pipettes and pipette tips remained in this hood at all times. Additionally, all pipette tips were autoclaved prior to use. Negative controls were used throughout our experimentation to check for false positive results, and at no time yielded PCR products. Positive controls, in the form of haptophyte DNA from two strains of *Prymnesium parvum*, were also used throughout our experimentation. Because the positive control DNA is amplifiable with the primers we used, it served as a positive PCR amplification control while also providing a test for cross-contamination of samples. Sequences amplified from our positive control DNA could be easily distinguished from sequences amplified from extant DNA in our samples. DNA from the positive controls never appeared in any of the clone libraries, indicating the lack of cross-contamination among samples.

3.5 *Phylogenetic analyses*

We used BLAST 2.2.10 (McGinnis and Madden, 2004) to retrieve 18S rRNA gene sequences from GenBank that were most similar to our environmental clone sequences and included them in our phylogenetic analyses. Sequences were aligned in ARB using the FastAligner option to the PT server database which had been built with the latest database available from the ARB website (Ludwig et al., 2004). The alignments were then manually adjusted. Sequences from the environmental samples were selected for the phylogenetic analyses by first defining operational taxanomic units (OTUs) at the 98% level with the program DOTUR (Schloss and Handelsman, 2005). Representatives from each OTU were included in the analyses. The green algae *Pyramimonas olivaceae* and *Chlorella sp*. (GenBank accession numbers AB017122 and X72708) served as outgroups for the analyses. Our final dataset consisted of 67 taxa and 380 unambiguously aligned positions.

We used neighbor-joining analysis employing the Kimura 2-parameter algorithm (Kimura, 1980) as implemented in *MEGA* version 3.1 (Kumar et al., 2004) to infer phylogenetic trees. The confidence of branching in the neighbor-joining analysis was assessed using 500 bootstrap resamplings of the data sets.

We also subjected our dataset to a Bayesian analysis using MrBayes, Version 3.0b4 (Ronquist and Huelsenbeck, 2003), under the GTR model of substitution (Lanave et al., 1984; Rodriguez et al., 1990; Tavare, 1986) and considering invariants and a gamma-shaped distribution of the rates of substitution among sites. The chain length for our analysis was 5,000,000 generations with trees sampled every 100 generations using MCMC (Markoff Chain Monte Carlo) analysis. Chain parameters appeared to be stationary after several thousand sampled trees; the first 10,000 trees (10^6 generations) were discarded as burn-in for the tree topology and posterior probability. We ran two replicate analyses that yielded comparable tree topologies and posterior probability values.

4. Results

Haptophyte rDNA was successfully PCR-amplified from all sediment samples, including surface sediment from all four study lakes and a late-Holocene sediment sample (30cm core-depth, Braya Sø). Haptophyte rDNA was also amplified from water filtrate of one of the four lakes (Hunde Sø), but could not be amplified from water filtrates of the other lakes. Eight OTUs were identified among the Greenland sequences. Haptophyte rDNA in the west Greenland lakes does not belong to any haptophyte species previously catalogued in GenBank (Fig.2).

The total amount of extractable DNA in surface sediment of the study lakes ranges from 600 to 1200 µg/gTOC (total organic carbon) (Table 1a), while the 1000yr old sediment sample (30 cm depth) contains ~200 µg/gTOC of extractable DNA. These amounts are similar to the extractable DNA in sediment from Ace Lake, Antarctica (Coolen et al., 2004).

5. Discussion

5.1 *18S rDNA haptophyte identification*

The successful PCR amplification of haptophyte rDNA indicates the presence of haptophyte algae in the west Greenland lakes. Phylogenetic analysis revealed the 18S rDNA-inferred relationship between the Greenland lake haptophytes and those catalogued in GenBank (Fig. 2). The Greenland lake genotypes occupy a very strongly supported group (neighbor-joining bootstrap value of 93%; Bayesian posterior probability of 0.99) to the exclusion of all other haptophyte genotypes. Seven of the identified OTUs group within this “Greenland phylotype” and the OTUs do not indicate lake specificity. Approximately one percent of the environmental sequences (all from sediment of a single lake, Hunde Sø and representing the eighth OTU), did not occupy the Greenland phylotype, and instead grouped closely with *Isochrysis galbana* and certain haptophyte sequences from Ace Lake, Antarctica (Coolen et al., 2004) in the neighbor-joining analysis (bootstrap value of 84%). All Greenland haptophyte 18S rDNA sequences group with haptophyte sequences from the algal class Prymnesiophyceae (Fig. 2). The presence of prymnesiophyte rDNA in the lake sediment strongly implies that haptophyte algae are responsible for producing the alkenones found in Greenland lake sediments (D'Andrea and Huang, 2005). It remains to be seen whether haptophytes of the Greenland phylotype, or the *I. galbana*-like haptophytes, or both, produce alkenones. However, given the large concentrations of alkenones in sediments of all of the lakes of this study and the fact that sequences belonging to the Greenland phylotype were found in all lakes (while the *I. galbana*-like sequences were only amplified from Hunde Sø sediment) it seems likely that members of the Greenland phylotype are alkenone-producers. The similarity of the *I. galbana*-like sequences to that of a known alkenone-producer suggests these haptophytes also produce alkenones. Further work will be needed to test these hypotheses.

5.2 *Paleotemperature implications*

Phylogenetic analysis revealed that haptophytes in all of the lakes are very similar (Fig. 2). This was expected based on the similarity of alkenone distributions among the lakes (Fig. 3) and the unusual presence of C_{38} methyl ketones in all study lakes (D'Andrea and Huang, 2005). Genotypes from all four lakes (whether from surface sediment, late-Holocene sediment, or water filtrate) share a common phylotype, and show no finer-scale, lake-specific clustering that would suggest the presence of significantly different haptophytes among samples. The haptophytes appear to be the same within each lake, among the different lakes, and between ~1000 years ago and present. One exception to this general observation is found in the Hunde Sø surface sediment sample, where some of the rDNA sequences (5 out of 95) share a phylotype with *I. galbana* (as discussed above) rather than with the other Greenland sequences.

The presence of two distinct haptophyte phylotypes in Hunde Sø, as determined by 18S rDNA sequences, may have important implications for understanding environmental changes and the habitat preferences of specific haptophytes. It is possible that under certain environmental conditions the *I. galbana*-like species could represent the dominant alkenone producer, while under other environmental conditions members of the Greenland phylotype become dominant. Coolen *et al*. (2004) proposed that phylotype shifts were an important mechanism for down core changes in alkenone unsaturation ratios in Ace Lake, Antarctica. Varying proportions of the *I. galbana*-like phylotype relative to the Greenland phylotype throughout the Holocene could represent a temperature-independent mechanism for changes in the alkenone unsaturation index. If this is the case, it may be necessary to apply different alkenone-based temperature calibrations to such intervals when reconstructing lake water temperature. Additionally, haptophyte community changes throughout the Holocene could reflect various aspects of environmental change (e.g., salinity). Further investigation into the evolution of haptophyte communities in the west Greenland lakes using quantitative PCR methods on ancient DNA could offer both biological and paleoenvironmental insights.

Our inability to amplify haptophyte rDNA from water filtrates from three of the four lakes may indicate that the haptophyte algal bloom is not coincident with the sampling date. Ice-melt and lake turn-over occur between late May and mid-June (Anderson and Broderson, 2001) but water filtrates were collected in mid-August. Perhaps the haptophyte bloom occurs in these lakes soon after ice melt, when nutrients are supplied to the photic zone by water column mixing. Hunde Sø, the lake from which haptophyte DNA was successfully amplified from water filtrate, has the longest fetch and the most wind mixing. This may result in more nutrient upwelling than occurs in the other lakes, extending the haptophyte growth period in Hunde Sø later into the summer. Future field work and sampling during the spring thaw will be needed to test these hypotheses.

The similarity of haptophytes both spatially (among lakes) and temporally (between ~1000 yrs ago and present) in the west Greenland lakes suggests that a single alkenone-unsaturation temperature calibration can be applied to the different lake records. A culture-based, absolute temperature calibration has not yet been determined for lacustrine alkenones. However, using surface sediments from a series of German lakes, Zink *et al*. (2001) developed a lacustrine alkenone-based temperature calibration which, when applied to Greenland alkenones, provides good estimates of Greenland lake surface water temperature (D'Andrea and Huang, 2005). The German lake calibration should therefore be applied to the Greenland lake records until development of a culture-based calibration.

5.3 *DNA preservation in lake sediments*

Most ancient DNA studies have been carried out on fossil bone or tissue samples, and only a small number of studies have analyzed DNA extracted directly from sediments (Coolen and Overmann, 1998; Willerslev et al., 2003; Coolen et al., 2004). The effectiveness of DNA as a biomarker hinges on the preservation of the molecule (more specifically, the fragment of interest) in the sedimentary deposit. Unfortunately, DNA is fairly labile and degradation via macromolecular chain breakage occurs readily in the natural environment. Hydrolytic and oxidative attacks on the phosphodiester bonds represent the most common degradation pathways for DNA (Lindahl, 1993; Bada et al., 1999). Furthermore, crosslink formations can cause PCR amplification blockage of environmental DNA sequences, and oxidative and hydrolytic modification of nucleotide bases can lead to sequence errors (Willerslev and Cooper, 2005). Kinetic calculations place the upper limit for preservation of meaningful DNA sequences in most geologic environments on the order of 10 kyrs (Pääbo and Wilson, 1991). In cold environments this estimate increases to 100 kyrs, owing to slower reaction kinetics (Poinar et al., 1996; Smith et al., 2001), and under ideal conditions, 1 Myrs has been cited as the maximum duration for DNA preservation (Willerslev and Cooper, 2005).

Certain qualities of a depositional environment may be more important than the age of the deposit with regard to the preservation potential of DNA. Coolen *et al.* (2004) found that 10 kyr old sediments from Ace Lake, Antarctica contain well-preserved DNA of algal primary producers that inhabited the lake's photic zone, and attributed the preservation to anoxic and sulfidic conditions at the bottom of Ace Lake. Willerslev *et al*. (2003, 2004) found DNA reflecting a diversity of taxa in 400 kyr old permafrost and proposed that the exceptional preservation is due to the cold and anaerobic conditions associated with these deposits.

The Greenland lakes have many qualities that favor the preservation of DNA. Anoxic conditions in the hypolimnia of the Greenland lakes should act to limit oxidative degradation of DNA. Dissolved oxygen approaches 0 mg/L at a depth of ~6 m in Braya Sø (Anderson et al., 1999), which is 24 m deep. Thus, particulate matter derived from primary producers in this lake settles through a largely anoxic water column, limiting the oxidative degradation of primary producer DNA in the water column as well as on the lake bottom. The presence of H_2S in the hypolimnia of the Greenland lakes should also limit oxidation by inducing the precipitation of metal ions (e.g., Cu^{2+} precipitated as copper sulphide) which otherwise facilitate DNA oxidation (Eglinton and Logan, 1991). Perpetually cold temperatures at the bottom of the Greenland lakes (~1-2 ˚C) act to slow the kinetic reactions responsible for DNA degradation (Brodersen and Anderson, 2000; Willerslev et al., 2004). The presence of clays and other clastic material in the lake sediments enables the adsorption of DNA to mineral surfaces, shielding DNA from enzymatic degradation, while elevated concentrations of monovalent (Na^+; ~26,000 eq L^{-1}) and, especially, bivalent cations (Mg^{2+}; ~21,000 eq L^{-1}) in the oligosaline Greenland lakes (Anderson et al., 2001) likely facilitate the adsorption process (Romanowski et al., 1991). Along with excellent DNA preservation, the stratigraphic context provided by the

Greenland lake sediment allows detailed, chronologic reconstruction of phytoplankton, as well as zooplankton, and fish communities, and provides the opportunity to closely examine relationships between evolution and environmental processes over the past several thousand years.

6. Conclusions

18S rDNA analysis indicates that the large concentrations of alkenones previously identified in the study lakes of west Greenland are produced by haptophytes of the class Prymnesiophyceae. The haptophytes in these lakes occupy a new phylogenetic clade, distinct from those comprising the well-studied alkenone producers *Emiliania huxleyi*, *Gephyrocapsa oceanica*, and *Isochrysis galbana*. The overwhelming majority of west Greenland haptophyte 18S rDNA sequences (i.e., all but 5 of the ~540 sequences from this study) share a common phylotype, indicating the similarity of the alkenone producers in all four lakes studied. The presence of similar haptophytes implies that the same alkenone-based temperature calibration may be applied to all the lakes. 18S rDNA sequences from a late-Holocene sediment sample share a phylotype with the sequences from modern samples, suggesting that the same temperature calibration is valid for at least the past 1000 years of the sediment record.

DNA of the algal primary producer is well preserved in the sediment of the oligosaline lakes of the Søndre Strømfjord region. These lakes will provide a unique opportunity to investigate the evolution of haptophyte communities in concert with, and to the benefit of, alkenone paleothermometry. 18S rDNA stratigraphy (cf. Coolen et al., 2004) could reveal changes in haptophyte communities through time, elucidating the environmental preferences of different haptophytes and providing a test for the applicability of the modern alkenone-based temperature calibration for paleotemperature reconstruction. Additionally, the DNA of many other organisms should also be preserved in the sediments of the west Greenland lakes, recording the evolutionary history of other members of the lake ecosystem (e.g., other phytoplankton, zooplankton, macrophytes, fish), which will be of great value to the paleolimnologic reconstruction of these lakes.

Acknowledgements

This work was supported by grants from the National Science Foundation (NSF0081478, 0318050, 0318123, 0402383, 0520718), NASA (NAG5-10665, NNG04GJ34G) and the American Chemical Society, Petroleum Research Fund (ACS-PRF38878-AC2) to Y. Huang. We thank Paul Zimba for providing *Prymnesium parvum* cultures and N. John Anderson for the use of field equipment. We also thank Annette Coleman and two anonymous reviewers for comments that helped improve the quality of this manuscript.

References

Anderson, N.J., and K. Brodersen (2001), Determining the date of ice-melt for low Arctic lakes along Søndre Strømfjord, southern West Greenland, *Geology of Greenland Survey Bulletin*, *189*, 54-58.

Anderson, N.J., R. Harriman, D.B. Ryves, and S.T. Patrick (2001), Dominant Factors Controlling Variability in the Ionic Composition of West Greenland Lakes, *Arctic, Antarctic, and Alpine Research*, *33* (4), 418-425.

Anderson, N.J., Bennike, O., Christoffersen, K., Jeppesen, E., Markager, S., Miller, G and Renberg, I. (1999), Limnological and palaeolimnological studies of lakes in south-western Greenland, *Geology of Greenland Survey Bulletin*, *183*, 68-74.

Anderson, N.J., and Leng, M.J. (2004), Increased aridity during the early Holocene in West Greenland inferred from stable isotopes in laminated-lake sediments, *Quaternary Science Reviews*, *23*, 841-849.

Bada, J.L., X.S. Wang, H. Hamilton (1999), Preservation of key biomolecules in the fossil record: current knowledge and future challenges, *Philosophical Transactions of the Royal Society of London Series B*, *354*, 77-87.

Banning, N., F. Brock, J.C. Fry, R.J. Parkes, E.R.C. Hornibrook, A. Weightman (2005), Investigation of the methanogen population structure and activity in a brackish lake sediment, *Environmental Microbiology*, *7*, 947-960.

Benson, D.A., I. Karsch-Mizrachi, D.J. Lipman, J. Ostell, D.L. Wheeler (2004), GenBank: update, *Nucleic Acids Research*, *32*, D23-D26.

Box, J.E. (2002), Survey of Greenland Instrumental Temperature Records: 1873-2001, *International Journal of Climatology*, *22*, 1829-1847.

Brassell, S.C., Eglinton, G., Marlowe, I.T., Pflaumann, U. and Sarnthein, M. (1986), Molecular stratigraphy: A new tool for climatic assessment, *Nature*, *320*, 129-133.

Brassell, S.C. (1993), Applications of Biomarkers for Deliniating Marine Paleoclimatic Fluctuations during the Pleistocene, in *Organic Geochemistry*, edited by M.H. Engel, Macko, S.A., pp. 699-738, Plenum Press, New York, 1993.

Brodersen, K.P., N.J. Anderson (2000), Subfossil insect remains (Chironomidae) and lake-water temperature inference in the Sisimiut-Kangerlussuaq region, southern West Greenland, *Geology of Greenland Survey Bulletin*, *186*, 78-82.

Cole, J.R., B. Chai, R.J. Farris, Q. Wang, S.A. Kulam, D.M. McGarrell, G.M. Garrity, J.M. Tiedje (2005), The Ribosomal Database Project (RDP-II): sequences and tools for high-throughput rRNA analysis, *Nucleic Acids Research*, *33*, D294-D296, doi: 10.1093/nar/gki038.

Coolen, M.J.L., and J. Overmann (1998), Analysis of subfossil molecular remains of purple sulfur bacteria in a lake sediment, *Applied and Environmental Microbiology*, *64* (11), 4513-4521.

Coolen, M.J.L., Muyzer, G., Rijpstra, W.I.C., Schouten, S., Volkman, J.K., and Sinninghe Damste, J.S. (2004), Combined DNA and lipid analyses of sediments reveal changes in Holocene haptophyte and diatom populations in an Antarctic lake, *Earth and Planetary Science Letters*, *223*, 225-239.

Cranwell, P.A. (1985), Long-chain unsaturated ketones in recent lacustrine sediments, *Geochimica et Cosmochimica Acta*, *49*, 1545-1551.

D'Andrea, W.J., Y. Huang (2005), Long-chain alkenones in Greenland lake sediments: low δ^{13}C values and exceptional abundance, *Organic Geochemistry 36*, 1234-1241.

de Leeuw, J.W., F.W. van der Meer, W.I.C. Rijpstra, and P.A. Schenck (1980), On the occurrence and structural identification of long chain unsaturated ketones and hydrocarbons in sediments, in *Advances in Organic Geochemistry 1979*, edited by A.C. Douglas, and Maxwell, J.R.,Pergamon Press, pp. 211-217.

Edvardsen, B., W. Eikrem, J.C. Green, R.A. Andersen, S.Y.M-V. der Staay and L.K. Medlin (2000), Phylogenetic reconstructions of the Haptophyta inferred from 18S ribosomal DNA sequences and available morphological data, *Phlycologia*, *39* (1), 19-35.

Eglinton, G., G.A. Logan (1991), Molecular preservation, *Philosophical Transactions of the Royal Society of London Series B*, *333*, 315-328.

Huang, Y.S., B. Shuman, Y. Wang, and T. Webb III, (2004), Hydrogen isotope ratios of individual lipids in lake sediments as novel tracers of climatic and environmental change: a surface sediment test, *Journal of Paleolimnology*, *31* (3), 363-375.

Innes, H.E., A.N. Bishop, P.A. Fox, I.M. Head, and P. Farrimond (1998), Early diagenesis of bacteriohopanoids in Recent sediments of Lake Pollen, Norway, *Organic Geochemistry*, *29* (5-7), 1285-1295.

Kimura, M. (1980), A simple method for estimating evolutionary rate of base substitution through comparative studies of nucleotide sequences, *Journal of Molecular Evolution*, *16*, 111-120.

Kumar, S., K. Tamura, and M. Nei (2004) MEGA3: Integrated software for Molecular Evolutionary Genetics Analysis and sequence alignment, *Briefings in Bioinformatics 5*, 150-163.

Lanave, C., Preparata, G., Saccone, C. & Serio, G. (1984), A new method for calculating evolutionary substitution rates, *Journal of Molecular Evolution 20*, 86-93.

Li, J., R.P. Philip, F. Pu, and J. Allen (1996), Long-chain alkenones in Qinghai Lake sediments, *Geochimica et Cosmochimica Acta*, *60*, 235-241.

Lindahl, T. (1993), Instability and decay of the primary structure of DNA, *Nature*, *362*, 709-715.

Ludwig W., O. Strunk, R. Westram, L. Richter, H. Meier, Yadhukumar, A. Buchner, T. Lai, S. Steppi, G. Jobb, W. Förster, I. Brettske, S. Gerber, A.W. Ginhart, O. Gross, S. Grumann, S. Hermann, R. Jost, A. König, T. Liss, R. Lüßmann, M.May, B. Nonhoff, B. Reichel, R. Strehlow, A. Stamatakis, N. Stuckmann, A. Vilbig, M. Lenke, T. Ludwig, A. Bode and K.-H. Schleifer (2004), ARB: a software environment for sequence data, *Nucleic Acids Research, 32,* 1363-1371.

Marlowe, I.T., Brassell, S.C., Eglinton, G., and Green, J.C. (1984), Long chain unsaturated ketones and esters in living algae and marine sediments, *Organic Geochemistry*, *6*, 135-141.

McGinnis, S., T.I. Madden (2004), BLAST: at the core of a powerful and diverse set of sequence analysis tools, *Nucleic Acids Research*, *32*, W20-W25.

McGowan, S., Ryves, David B., and Anderson, N. John (2003), Holocene records of effective precipitation in West Greenland, *The Holocene*, *13* (2), 239-249.
Meyers, P.A. (2003), Applications of organic geochemistry to paleolimnological reconstructions: a summary of examples from the Laurentian Great Lakes, *Organic Geochemistry*, *34* (2), 261-289.
Pääbo S., A.C. Wilson (1991), Miocene DNA sequences - a dream come true?, *Current Biology*, *1*, 45-46.
Poinar, H.N., M. Hoss, J.L. Bada, and S. Paabo (1996), Amino acid racemization and the preservation of ancient DNA, *Science*, *272* (5263), 864-866.
Posada, D., K.A. Crandall (1998), Modeltest: testing the model of DNA substitution, *Bioinformatics 14*, 817-818.
Prahl, F.G., and S.G. Wakeham (1987), Calibration of unsaturation patterns in long-chain ketone compositions for paleotemperature assessment, *Nature*, *330*, 367-369.
Rodriguez, F., J. L. Oliver, A. Marin, J. R. Medina (1990), The general stochastic model of nucleotide substitution, *Journal of Theoretical Biology 14*, 485-501.
Romanowski, G., M.G. Lorenz, W. Wackernagel (1991), Adsorption of Plasmid DNA to Mineral Surfaces and Protection against DNase I, *Applied and Environmental Microbiology*, *57*, 1057-1061.
Ronquist, F., J. P. Huelsenbeck (2003), MRBAYES 3: Bayesian phylogenetic inference under mixed models, *Bioinformatics 19*, 1572-1574.
Schloss, P.D., and J. Handelsman (2005), Introducing DOTUR, a computer program for defining operational taxonomic units and estimating species richness, *Applied and Environmental Microbiology*, *71* (3), 1501-1506.
Sheng, G.Y., K.Q. Cai, X.X. Yang, J.L. Lu, G.D. Jia, P.A. Peng, and J.M. Fu (1999), Long-chain alkenones in Hotong Qagan Nur Lake sediments and its paleoclimatic implications, *Chinese Science Bulletin*, *44*, 259-263.
Simon, N., L. Campbell, E. Örnolfsdottir, R. Groben, L. Guillou, M. Lange, L.K. Medlin (2000), Oligonucleotide Probes for the Identification of Three Algal Groups by Dot Blot and Flourescent Whole-Cell Hybridization, *Journal of Eukaryotic Microbiology*, *47*, 76-84.
Smith, C.I., A.T. Chamberlain, M.S. Riley, A. Cooper, C.B. Stringer, M.J. Collins (2001), Not just old but old and cold?, *Nature*, *410*, 771-772.
Sogin, M.L., H.J. Elwood, J.H. Gunderson (1986), Evolutionary diversity of eukaryotic small-subunit rRNA genes, *Proceedings of the National Academy of Sciences, USA*, *83*, 1383-1387.
Tavare, S. (1986), Some probabilistic and statistical problems on the analysis of DNA sequences, *Lectures on Mathematics in the Life Sciences 17*, 57-86.
Theil, V., A. Jenisch, G. Landmann, A. Reimer, and W. Michaelis (1997), Unusual distributions of long-chain alkenones and tetrahymanol from the highly alkaline Lake Van, Turkey, *Geochimica et Cosmochimica Acta*, *61* (10), 2053-2064.
Theissen, K.M., D.A. Zinniker, J.M. Moldowan, R.B. Dunbar, H.D. Rowe (2005), Pronounced occurrence of long-chain alkenones and dinosterol in a 25,000-year lipid molecular fossil record from Lake Titicaca, South America, *Geochimica et Cosmochimica Acta*, *69* (3), 623-636.

Volkman, J.K., H.R. Burton, D.A. Everitt, D.I. Allen (1988), Pigment and lipid compositions of algal and bacterial communities in Ace Lake, Vestfold Hills, Antarctica, *Hydrobiologia*, *165*, 41-57.

Wang, R., and M. Zheng (1998), Occurence and environmental significance of long-chain alkenones in Tibetan Zabuye Salt Lake, S.W. China, *International Journal of Salt Lake Research*, *6*, 281-302.

Willerslev, E., A.J. Hansen, J. Binladen, T.B. Brand, M.T.P. Gilbert, B. Shapiro, M. Bunce, C. Wiuf, D.A. Gilichinsky, A. Cooper (2003), Diverse Plant and Animal Genetic Records from Holocene and Pleistocene Sediments, *Science*, *300*, 791-795.

Willerslev, E., A.J. Hansen, H.N. Poinar (2004), Isolation of nucleic acids and cultures from fossil ice and permafrost, *Trends in Ecology and Evolution*, *19*, 141-147.

Willerslev, E., A. Cooper (2005), Ancient DNA, *Proceedings of the Royal Society, Series B*, *272*, 3-16.

Zink, K.G., D. Leythaeuser, M. Melkonian, and L. Schwark (2001), Temperature dependency of long-chain alkenone distributions in Recent to fossil limnic sediments in lake waters, *Geochimica et Cosmochimica Acta*, *65*, 253.

TABLE 1A. PHYSICAL AND CHEMICAL PARAMETERS
OF LAKES FROM THIS STUDY

Lake	Max depth (m)	Area (m^2)	Salinity of epi-limion (ppt)	Salinity of hypo-limnion (ppt)	DNA concentration* (μg/g TOC)	Alkenone concentration*† (μg/g TOC)
BrayaSø	23	686,100	0.9	1.9	780	82,700
HundeSø	35	1,836,600	1.5	2.3	790	50,300
LimnæaSø	18	1,118,600	1.4	2.8	1,200	47,100
SS6	12	173,300	n.a.	n.a.	n.a.	11,100

TABLE 1B. CHEMICAL PARAMETERS OF SØNDRE STRØMFJORD LAKES

	pH	Alkalinity (eq L^{-1})	Cl (eq L^{-1})	SO_4 (eq L^{-1})	Ca (eq L^{-1})	K (eq L^{-1})	Mg (eq L^{-1})	Na (eq L^{-1})
Oligosaline Mean§	8.76	11302	10827	3344	1697	3075	12296	13206
Freshwater Mean§	7.36	783	242	60	517	82	399	263

n.a., not available
TOC, total organic carbon
*Concentration in surface sediment
†D'Andrea and Huang (2005)
§Mean water chemistry data from Anderson *et al*. (2001)

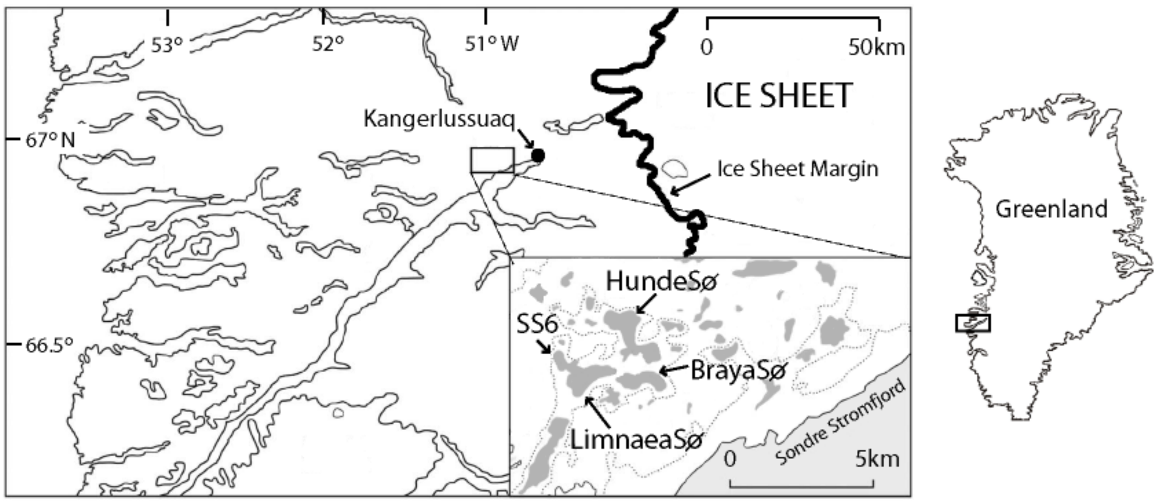

Figure 1. Site map showing study lakes in Kangerlussuaq, Greenland. Braya Sø, Hunde Sø, Limnæa Sø, and SS6 sediments all contain alkenones and 18S rDNA of haptophyte algae belonging to the class Prymnesiophyceae.

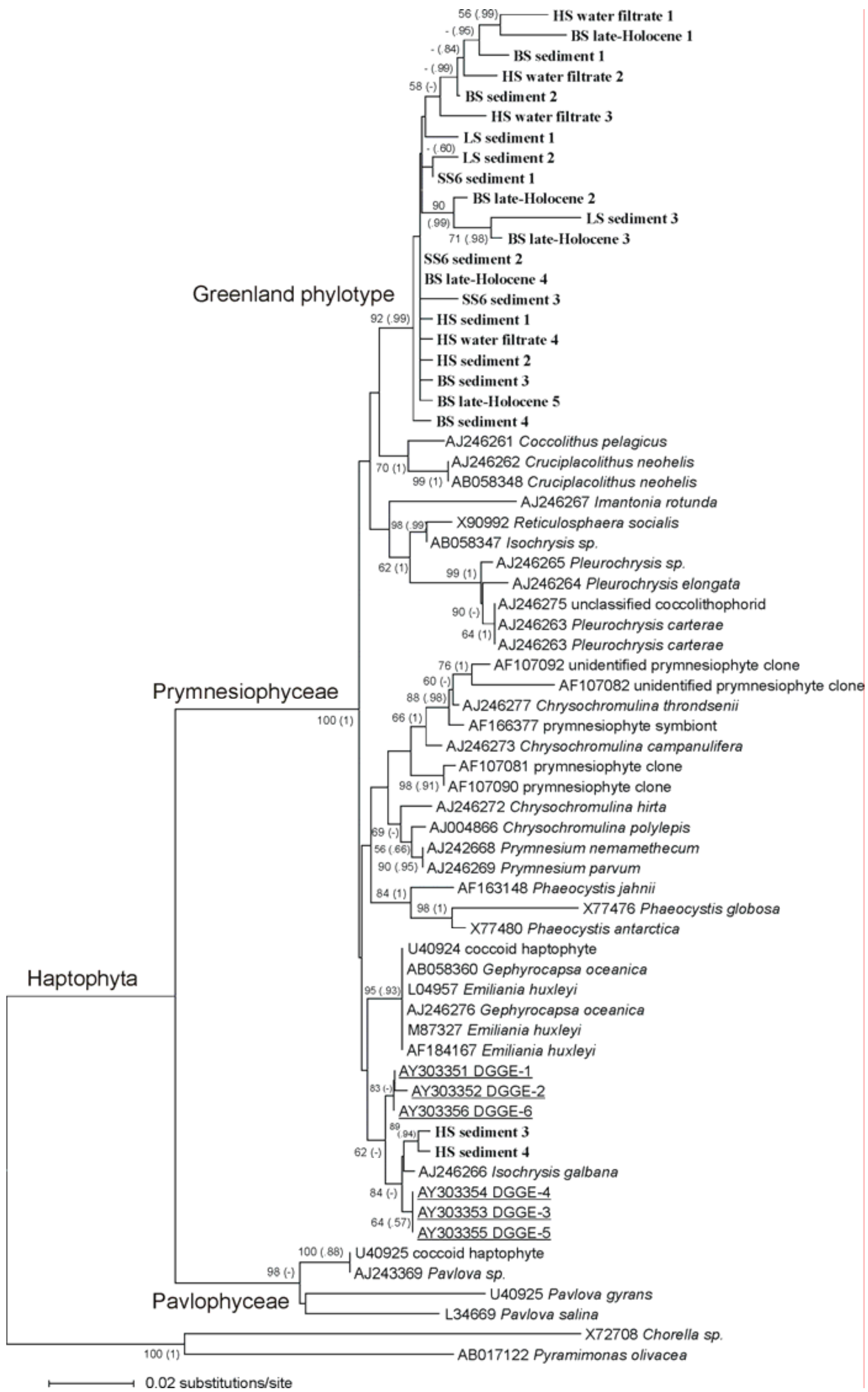

Figure 2. A consensus neighbor-joining phylogenetic tree depicting the 18S rDNA-inferred relationships between haptophytes in west Greenland lakes (bold; HS=Hunde Sø, BS=Braya Sø, LS=Limnæa Sø), in Ace Lake, Antarctica (underlined; Coolen et al., 2004) and haptophytes from GenBank (accession numbers are before genus names). Neighbor-joining bootstrap values greater than 50% are provided, followed by Bayesian posterior probabilities in parentheses. The evolutionary distance for the number of changes per site is represented by the scale bar.

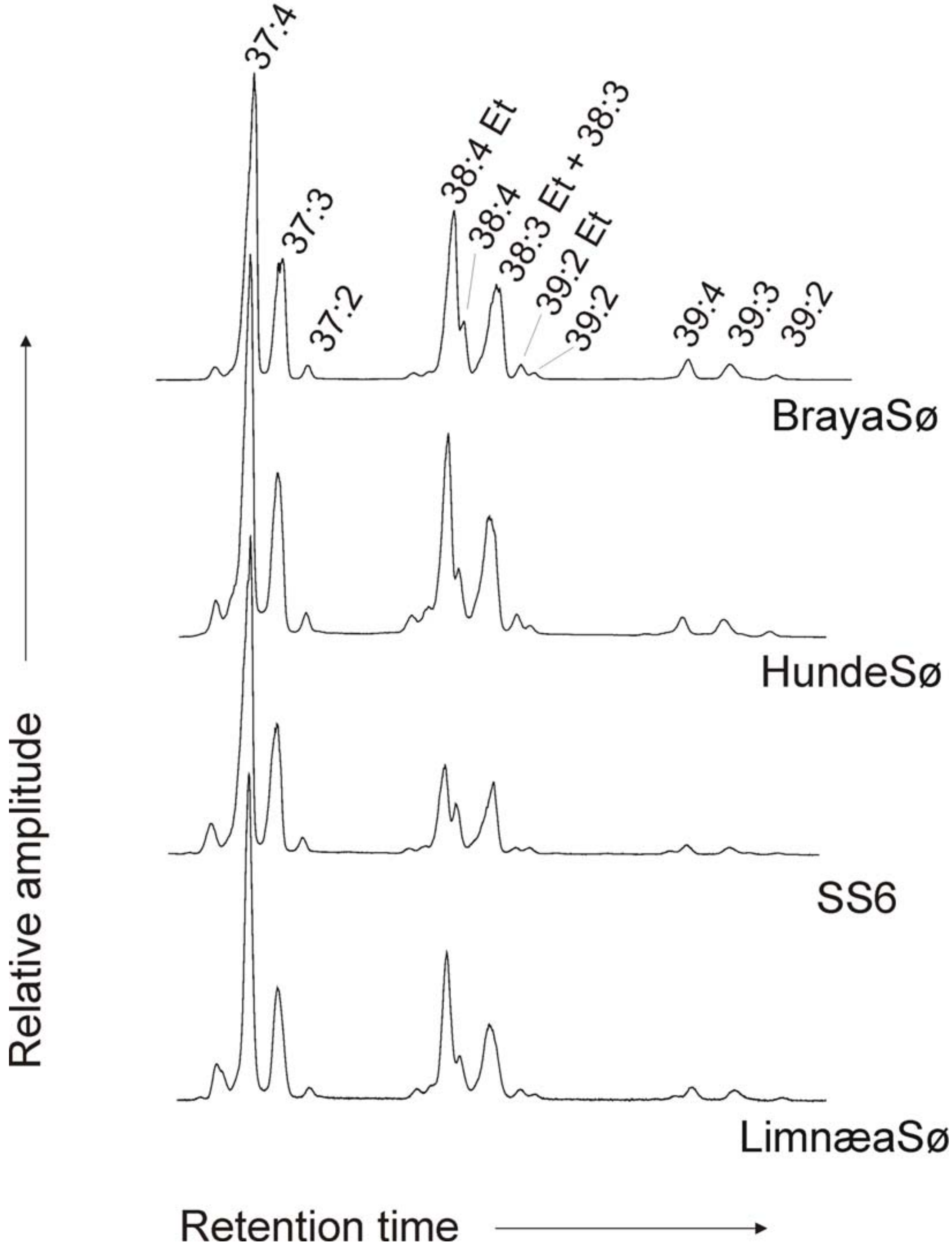

Figure 3. Gas chromatogram showing the similarity of alkenone distributions found in sediments of the four study lakes. The dominance of tetra-unsaturation is common for lacustrine alkenones, while the presence of C_{38} methyl ketones is unusual.

CHAPTER 3

AN EFFICIENT METHOD FOR ISOLATING INDIVIDUAL LONG-CHAIN ALKENONES FOR COMPOUND-SPECIFIC HYDROGEN ISOTOPE ANALYSIS

WILLIAM J. D'ANDREA

ZHONGHUI LIU

MARCELO Da ROSA ALEXANDRE

SARAH WATTLEY

TIMOTHY D. HERBERT

YONGSONG HUANG

BROWN UNIVERSITY, *Department of Geological Sciences*

Published in:
Analytical Chemistry 79: 3430-3435, doi:10.1021/ac062067w, 2007

ABSTRACT

Hydrogen isotope ratios (^{2}H/H or D/H) of long chain unsaturated ketones (alkenones) preserved in lake and marine sediments hold great promise for paleoclimate studies. However, compound-specific hydrogen isotope analysis of individual alkenones has not been possible due to chromatographic co-elution of alkenones with the same carbon chain length but different numbers of double bonds. Published studies have only reported the δD values of the mixture of co-eluting alkenones. We developed an efficient procedure to isolate individual alkenones based on double bond numbers using silica gel impregnated with silver nitrate. The chromatographic procedure is simple, inexpensive, and highly reproducible, offers 87-100% sample recovery and allows for the first time hydrogen-isotopic measurement on individual alkenones. δD values of specific di-, tri- and tetra-unsaturated C_{37} alkenones produced by an *Emiliania huxleyi* culture, as well as those isolated from Greenland lake sediments, differ consecutively by 43 to 65 ‰. These findings suggest that alkenones with different numbers of carbon-carbon double bonds express significantly different δD values and that co-elution of different alkenones may lead to erroneous source water δD reconstructions. Our alkenone isolation approach opens a new avenue for paleoclimate reconstructions using hydrogen isotope ratios of individual alkenones.

INTRODUCTION

Long-chain (C_{37}-C_{39}) unsaturated methyl and ethyl ketones (alkenones) are an important class of lipid compounds for paleoclimate reconstruction[1]. These compounds are only produced by certain members of the algal class Prymnesiophyceae (reviewed by Conte *et al.*[2]) and contain varying number of double bonds. The relative proportion of di-, tri-, and tetraunsaturated C_{37} alkenones (expressed as the U^{K}_{37} index) produced by the algae depends on the algal growth temperature[1, 3, 4], and this relationship has been widely exploited for reconstructing past sea surface temperatures from alkenones preserved in ocean sediment cores. Alkenones are also of distinctive value for reconstructing D/H ratios of their source water. Since these lipids are produced solely by aquatic algae, D/H ratios of alkenones should directly reflect that of the source water from which they were biosynthesized[5-9]. Short-chain *n*-alkanoic acids (e.g., palmitic acid) have been used for this purpose[6, 7, 10]; however, these compounds are produced by a whole host of aquatic and terrestrial organisms with potentially different water sources and isotope fractionation relative to source water, limiting the fidelity of the proxy in certain systems. Algal sterols are also potential candidates for source water D/H reconstruction[5], but again are not as biologically specific as alkenones.

The D/H ratio (like $^{18}O/^{16}O$) of ocean water is primarily a function of global ice volume, and can also reflect the amount of fresh water input in coastal areas and excessive evaporation from warm oceans (e.g., the Red Sea[11]). D/H of lake water is largely controlled by that of precipitation as well as the amount of precipitation relative to evaporation[12, 13]. Thus, the hydrogen isotopic compositions of ocean and lake waters are a direct consequence of climatic and environmental conditions[14, 15]. D/H reconstructions of ancient water bodies based on sedimentary alkenone D/H can thus offer valuable insight into past variability of oceanic and atmospheric systems.

Unfortunately, gas chromatographic (GC) techniques are unable to adequately resolve different alkenone compounds for compound-specific hydrogen isotopic measurement. Flame-ionization-detection (FID) is commonly used to quantify alkenone concentrations and to determine the $U_{37}^{K'}$ index and requires very small quantities for accurate measurements. Only ~1 ng of each alkenone compound needs to be injected onto the GC column for FID measurements; this amount is well below the capacity of typical GC columns. Each alkenone compound can therefore be fully resolved by GC-FID. However, isotope-ratio mass spectrometry (IRMS) requires relatively large amounts of analyte gas (e.g., CO_2 for $^{13}C/^{12}C$, H_2 for D/H) for isotope ratio measurements, and hydrogen isotope analyses require up to ten times the molar concentration of H than the C required for carbon isotope analyses[16]. The IRMS requirements call for the injection of up to 70 ng of each alkenone compound for $^{13}C/^{12}C$ measurement, and up to 400 ng of each desired alkenone for D/H measurement. These large quantities (particularly for D/H) exceed the capacity of typical GC columns and lead to chromatographic co-elution of alkenones with the same carbon chain length but different numbers of double bonds. Due to incomplete compound resolution, D/H ratios of alkenones have previously been determined by measuring the D/H ratio of the mixture of co-eluting alkenones of a given chain length [8, 9]. This approach is reasonable if the D/H ratios of the different alkenone compounds are identical. However, if there are significant differences among D/H ratios of the co-eluting alkenones, the weighted-average D/H will be influenced by the relative proportions of the co-eluting compounds, potentially obscuring attempts at source water D/H reconstruction.

Here, we report a silver nitrate-impregnated silica gel column chromatographic procedure for separating alkenones based on the number of double bonds. This procedure enables complete resolution of individual alkenone compounds for hydrogen isotope measurement by GC-IRMS. We also show that C_{37} alkenones with different degrees of unsaturation have very different D/H ratios; hence future studies may require measurements of individual alkenones for paleoclimate reconstructions.

EXPERIMENTAL SECTION

Chemicals and reagents. Silver nitrate-impregnated silica gel (10 wt%, 200+ mesh) was purchased from Sigma-Aldrich. HPLC grade dichloromethane and methanol were acquired from Burdick & Jackson, ethyl acetate was from Mallinckrodt and toluene was from J.T. Baker. *n*-Heptatriacontane was purchased from Aldrich, and Vienna Standard Mean Ocean Water (VSMOW) was purchased from the National Institute of Standards and Technology. Isotope reference materials (*n*-alkanes) were provided by Arndt Schimmelmann at Indiana University.

Sample and silver nitrate–silica gel column preparation. Sediment samples were freeze-dried and homogenized using a mortar and pestle. They were extracted with dichloromethane (DCM) using an Accelerated Solvent Extractor ASE200 (Dionex). 0.5-1.5 g of Greenland lake sediment[17] was used for extraction. Extracts were separated into acid and neutral fractions using Supelco Supelclean™ LC-NH_2 solid phase extraction (SPE) tubes[7]. The neutral fraction was further separated into aliphatic hydrocarbon (hexane elution), ketone (DCM), and alcohol (ethyl acetate:hexane [1:3, v/v]) fractions using a flash silica gel column. The alkenones (in the ketone fraction) were quantified by gas chromatography-flame ionization detection (GC-FID) with *n*-heptatriacontane as internal standard.

The bottle of silver nitrate-impregnated silica gel (Ag + Si gel) was wrapped in aluminum foil and stored in a drying oven at 50 ˚C to prevent photo-reduction of the silver nitrate. Flash columns were prepared immediately prior to use with 2.1 g of Ag + Si gel. Columns were tapped until compaction of the Ag + Si gel ceased and wrapped in aluminum foil for the duration of the procedure to avoid photo-reduction of the silver nitrate. The Ag + Si gel was rinsed with at least four bed volumes of DCM and was kept saturated with DCM. After the elution procedure (see below) samples were run on (GC-FID to assess the isolation of alkenones, and to verify the complete removal of *n*-heptatriacontane standard. *n*-Heptatriacontane was then re-added to each fraction as an internal standard to quantify alkenone recovery.

Eluent Scheme. Samples were loaded onto a DCM-wetted Ag + Si-gel column and eluted with the following solvents: 20 mL of DCM, 12 mL DCM:ethyl acetate (9:1, v/v), 12mL DCM:ethyl acetate (7:3, v/v), 14 mL DCM:ethyl acetate (1:1, v/v), 20 mL 100% ethyl acetate. Samples were collected in 2 mL increments to assess elution rates (Fig. 1).

Instrumentation. Concentrations of individual compounds were evaluated using a Hewlett Packard 6890 gas chromatograph (GC). A 30 m long, 0.25 mm × 0.25 μm HP-1MS capillary column was used for GC-FID. The temperature program for the GC oven was held at 60 ˚C for 1 minute, brought to 290 ˚C @ 30 ˚C min^{-1} and held for 1 minute, brought to 300 ˚C @ 5 ˚C min^{-1}, then brought to 315 ˚C @ 2 ˚C min^{-1} and held for 15 minutes. A Hewlett-Packard 6840+ GC-pyrolysis system interfaced to a Finnigan Delta+ XL stable isotope mass-spectrometer through a high-temperature pyrolysis reactor was used for hydrogen isotopic analysis[7]. Sessions (2006) provides an excellent review of isotope-ratio detection for gas chromatography, including gas chromatographythermochemolysis-isotope-ratio mass spectrometry (GC-TC-IRMS), which was employed here. The precision (1σ) of the triplicate analyses was generally <±2‰. Accuracy throughout the run was routinely checked by an injection of laboratory isotopic standards between every six injections and IRMS accuracy is periodically assessed using *n*-alkane isotope references from Indiana University. Alkenones were identified by comparison of mass spectral data with previously reported standards and GC retention times[18, 19].

Algal cultures. We obtained a culture of the alkenone-producing alga *Emiliania huxleyi* (CCMP 374) from the Provasoli-Guillard Center for the Culture of Marine Phytoplankton. Cultures were grown in f/2 medium[20] (using seawater from West Boothbay Harbor, Maine; δD ~ 0 %) at 20˚C and were harvested during log-phase of growth. 1L of medium was filtered onto pre-combusted Whatman GF/F glass fiber filters (porosity of 0.7μm). Filters were soaked once in methanol (MeOH) and twice in DCM:MeOH (1:1, v/v) to extract alkenones.

Terminology. We follow the standard delta notation (‰ VSMOW) for reporting hydrogen isotope values:

$$\delta D_{sample} = \frac{\left(R_{sample} - R_{std}\right)}{R_{std}} \times 1000‰ \qquad (1)$$

where R is the absolute D/H ratio of a sample or the internationally accepted reference standard (VSMOW).

The fractionation factor (α) between reactant and product is defined as

$$\alpha_{\text{product-reactant}} = \frac{R_{\text{product}}}{R_{\text{reactant}}} \tag{2}$$

Isotopic enrichment (ε) between reactant and product is defined as

$$\varepsilon_{\text{product-reactant}} = \left(\alpha_{\text{product-reactant}} - 1\right) \times 1000 \tag{3}$$

RESULTS AND DISCUSSION

Separation of individual alkenones

Alkenones can be effectively separated according to their degree of unsaturation using Ag + Si gel column chromatography (Fig. 1). Saturated compounds elute more quickly than unsaturated compounds due to the affinity of the silver nitrate for electrons on the double bonds. Our internal standard, *n*-Heptatriacontane, elutes with pure DCM and is completely separated from the alkenones. In the eluent scheme described above, diunsaturated alkenones ($C_{37:2}$, $C_{38:2}$, $C_{39:2}$) elute with DCM:ethyl acetate (9:1, v/v), triunsaturated alkenones ($C_{37:3}$, $C_{38:3}$, $C_{39:3}$) elute with DCM:ethyl acetate (7:3, v/v), and tetraunsaturated alkenones ($C_{37:4}$, $C_{38:4}$, $C_{39:4}$) elute with DCM:ethyl acetate (1:1, v/v). We tested various solvent elution schemes and found sequentially increasing solvent polarities afforded better isolation of target compounds than using a single solvent throughout. By collecting 12 mL of DCM:ethyl acetate (9:1, v/v) in one collection vial, 12mL of DCM:ethyl acetate (7:3, v/v) in another vial and 14 mL DCM:ethyl acetate (1:1, v/v) in a third vial, we routinely obtained fractions with cleanly separated C_{37} and C_{39} di-, tri-, and tetraunsaturated alkenones. C_{38} alkenones in marine and certain lacustrine sediments (including the Greenland lake sediments) comprise both methyl and ethyl ketones which apparently interfered with the complete Ag + Si-gel separation of $C_{38:4}$ and $C_{38:3}$ (Fig. 1). However, while $C_{38:4}$ is abundant in the Greenland lake sediment, it is not present in most marine sediments, making this isolation step unnecessary. By performing

GC-FID quantification before and after Ag + Si-gel column chromatography (with *n*-heptatriacontane as internal standard), alkenone recovery was determined to be 87-100%. We tested whether the incomplete recovery of alkenones from the Ag + Si-gel resulted in hydrogen isotope fractionation by eluting the same sample through a Ag + Si-gel column three times. The δD values of triunsaturated alkenones remained the same after each elution, indicating that the procedure does not result in hydrogen isotope fractionation.

Optimization of GC operation conditions

One major benefit of making δD measurements on isolated alkenones rather than the mixture of co-eluting alkenones is the improved accuracy associated with narrower peak baseline widths. Narrower peak width results in improved measurement accuracy through the incorporation of less background hydrogen into the measurement. We tested various GC operating conditions to optimize the peak shape of isolated alkenones. Seven different GC columns were tested (Table 1) allowing comparison of column length and film thickness, as well as a number of different temperature programs, inlet temperatures and carrier gas flow rates (Fig. 2). The optimization test results are reported in Fig. 2 as both width/height (W/H) ratios and theoretical plates (N) using the Gaussian 10% equation. All columns had chromatographic resolution (R) of the $C_{37:3}$ and $C_{38:3}$ peaks better than 1.5 (i.e., complete baseline separation), except for the 15 m HP-1MS column (Table 1).

The best peak shape (lowest W/H ratio) was achieved using the 30 m HP-1MS column, 315 ˚C inlet temperature, 1.2 mL/min flow rate, and the following temperature program: 40˚C for 1 min → 280˚C @ 15 ˚C min^{-1} → 315 ^oC @ 2 ˚C min^{-1} and hold for 20 min. Reducing the flow rate below 1.2 mL/min made negligible difference in W/H ratios.

GC-TC-IRMS traces of alkenone peaks prior to and following the Ag + Si-gel isolation are shown in Figure 3. Clearly, even with the best operating conditions, it was not possible to separate $C_{37:2}$, $C_{37:3}$ and $C_{37:4}$ by GC-TC-IRMS prior to Ag + Si-gel chromatography (upper panel, Fig. 3).

δD measurements of specific alkenones

δD measurements of Ag + Si gel-separated alkenones reveal that the individual C_{37} alkenones have different hydrogen isotopic compositions (Tables 2 and 3). Triunsaturated C_{37} alkenones ($C_{37:3}$) isolated from the *E. huxleyi* culture (CCMP 374) are deuterium-depleted relative to diunsaturated alkenones ($C_{37:2}$) isolated from the same culture with a fractionation factor ($\alpha_{C37:3\text{-}C37:2}$) of 0.94 (Table 2). Tetraunsaturated C_{37} alkenones ($C_{37:4}$) extracted from three Greenland lake sediment samples are deuterium-depleted relative to $C_{37:3}$ isolated from the same samples. Furthermore, the fractionation factor between $C_{37:3}$ and $C_{37:4}$ ($\alpha_{C37:4\text{-}C37:3}$) in all three samples is very similar (0.94, 0.95, and 0.94) suggesting that this value may represent the biosynthetic hydrogen-isotope fractionation that occurs as diunsaturated (and triunsaturated) alkenones bind to desaturase enzymes along the desaturation pathway toward triunsaturation (and tetraunsaturation).[21]

While the biosynthesis of alkenones is still poorly understood, two possibilities may be considered with respect to the fractionation of hydrogen isotopes during alkenone biosynthesis. The first possibility is that there is a fixed isotopic enrichment (ε) between source water δD and the *weighted-average* alkenone δD (i.e., $\varepsilon_{C37\text{-water}}$ is constant). If this is the case, then weighted-average alkenone δD measurements can be used to reconstruct source water δD, regardless of temperature-induced changes in the relative concentrations of $C_{37:4}$, $C_{37:3}$ and $C_{37:2}$. It would be advisable in this case, to isolate the different C_{37} alkenones for isotope measurement prior to calculating the weighted-average δD (rather than using the mixture of co-eluting alkenones) in order to achieve optimal analytical accuracy. The second possibility, with respect to biosynthetic fractionation, is that there is a fixed isotopic enrichment between source water δD and the δD of each *individual* alkenone (i.e., $\varepsilon_{C37:2\text{-water}}$, $\varepsilon_{C37:3\text{-water}}$, and $\varepsilon_{C37:4\text{-water}}$ are each constant, and distinct from one another). If this is the case, then source water δD reconstructions will require δD measurements on individual alkenones, as temperature-induced changes in the relative concentrations of $C_{37:4}$, $C_{37:3}$ and $C_{37:2}$ through time would obscure weighted-average alkenone δD measurements. Preliminary results from our culture experiments with *E. huxleyi* indicate constant $\varepsilon_{C37:3\text{-water}}$ at different growth temperatures, suggesting that the latter scenario is more likely the case.

To illustrate the potential confounding effect of temperature-induced U^{K}_{37} changes on weighted-average alkenone δD reconstructions, consider the following example. A sea surface temperature increase of 5 °C, from 12 °C during the Last Glacial Maximum (LGM) to 17 °C during the Holocene, at a hypothetical ocean location would result in a change in the $C_{37:2}$ to $C_{37:3}$ ratio from 0.78 to 1.53 (based on the $U^{K'}_{37}$ calibration[4]). If we consider the δD values measured for $C_{37:2}$ and $C_{37:3}$ (-188 and -233 ‰, respectively) from *E. huxleyi* cultures in this study, and assume that their respective δD values do not vary as a function of the $C_{37:2}$ to $C_{37:3}$ ratio (i.e., the second of the two possibilities outlined above), we would measure weighted-average δD values (combining $C_{37:2}$ and $C_{37:3}$) of -213 ‰ for the LGM and -206 % for the Holocene. This represents an apparent δD shift of +7 ‰ due solely to temperature-induced changes in relative concentrations of $C_{37:3}$ and $C_{37:2}$. The actual isotopic shift of ocean water δD due to ice volume changes between LGM and present is on the order of -7 ‰ (based on a $\delta^{18}O$ shift of -1.0 ‰[22, 23] due to ice volume changes, and an estimated relationship of $\delta D = 7 \cdot \delta^{18}O$ for ocean water[24]). Therefore, in this proposed scenario the temperature-induced change in $C_{37:2}$ to $C_{37:3}$ ratio causes an apparent ocean water δD shift that cancels the actual δD shift of ocean water between LGM and present. It should be noted that CCMP374 was collected from the North Atlantic Ocean (Gulf of Maine) and is not necessarily representative of all *E. huxleyi* strains present in the world's oceans. Nonetheless, based on our findings we strongly recommend the use of individual alkenone compounds for reconstructing past ocean δD values.

In addition to improving the accuracy of alkenone δD measurements though improved gas chromatographic resolution, as discussed above, measurement of individual alkenones also appears to improve the precision of replicate measurements. Englebrecht and Sachs (2005) reported a precision (1σ) of 2.9 ‰ for the replicate δD analysis of a single alkenone sample (n=34), with 1σ of weighted-average alkenone δD measurements from *E. huxleyi* cultures up to 6 ‰ (n=4). Schouten *et al*. (2006) reported 1σ of weighted-average alkenone δD measurements from *E. huxleyi* cultures up to 7 ‰. In this study, isolated alkenone δD measurements from *E. huxleyi* cultures had a precision of 1.7 ‰ and 0.6 ‰ for $C_{37:3}$ and $C_{37:2}$, respectively (Table 2).

Potential applications

One potential application for seawater δD reconstruction is for dating marine sediment records. Marine sediment cores are routinely correlated chronologically using $\delta^{18}O$ measurements from benthic foraminiferal calcite tests found throughout the cores[25-27] which reflect the changing $\delta^{18}O$ values of the world's oceans through time. This global $\delta^{18}O$ signal allows temporal correlation of geographically distinct cores. Sediment cores lacking foraminiferal tests, such as those from regions with poor carbonate preservation (e.g. large portions of the Southern Ocean, and certain upwelling regions with high organic content), cannot be aligned with global $\delta^{18}O$ records, limiting paleoceanographic and paleoclimatic reconstructions. Due to the fact that δD and $\delta^{18}O$ vary linearly in hydrologic systems[24,28], alkenone δD measurements could be useful for correlating sediment records to the global foraminiferal $\delta^{18}O$ time-series.

Alkenone δD values have been used to assess the degree of lateral transport at ocean sites (i.e. drift sites)[8]. In order to determine the provenance of alkenones in cores taken from such sites, alkenone δD can be used in conjunction with the temperature-dependent unsaturation ratios (U^{K}_{37})[8]. The use of isolated alkenones for δD measurement, rather than an integration of all C_{37} alkenones, may improve the effectiveness of this approach.

Alkenones continue to be discovered in lacustrine sediments worldwide[17, 29-37]. Alkenone-based δD reconstructions from these archives are valuable for reconstructing lake water isotopic variations. For example, Lake Qinghai, China offers the opportunity for long term (millions of years) alkenone-based climate reconstruction[38]. The alkenone-bearing lakes of the Søndre Strømfjord in southwestern Greenland[17] offer the possibility for paleohydrologic as well as temperature reconstructions from a region sensitive to the North Atlantic Oscillation[39, 40]. While sedimentary organic compounds such as sterols[5] and alkanoic acids[6, 7, 10] have been shown to record lake water δD, these compounds are produced by both aquatic and terrestrial sources, potentially complicating reconstructions. Alkenones derive solely from haptophyte algae and thus provide more robust lake water δD reconstructions. When present, accurate δD measurements of alkenones from lake sediments arguably offer the best opportunity for hydrogen isotope-based terrestrial paleoclimate reconstruction.

CONCLUSIONS

The silver nitrate-impregnated silica gel chromatographic procedure described here allows the isolation of individual alkenones for compound-specific hydrogen isotope analysis. Alkenone recovery using this procedure is ≥87% and there is no associated hydrogen-isotope fractionation.

δD values of di- and triunsaturated C_{37} alkenones isolated from a culture of *E. huxleyi* are very different, with $\alpha_{C37:3\text{-}C37:2}$ of 0.94. δD values of tri- and tetraunsaturated C_{37} alkenones isolated from Greenland lake sediments are also very different, with $\alpha_{C37:4\text{-}C37:3}$ of 0.94-0.95 in three distinct samples, suggesting that this value may represent the biosynthetic isotope fractionation that occurs as alkenones bind to enzymes along the desaturation pathway.

There are numerous applications for alkenone δD measurements to paleoclimate studies. We recommend measuring δD of isolated alkenones rather than from mixtures of co-eluting alkenones, as the latter may be significantly influenced the relative proportions of different C_{37} alkenones (i.e., water temperature) and the former can provide improved accuracy and analytical precision.

ACKNOWLEDGEMENTS

We are thankful to Arndt Schimmelmann, Alex Sessions and an anonymous reviewer for constructive comments which helped to improve the quality of this manuscript. This work was supported by grants from the National Science Foundation (NSF0318050, 0318123, 0402383, 0520718) and NASA (NAG5-10665, NNG04GJ34G) to Y. Huang. Support for Z. Liu was provided by a NSF S.G.E.R. Grant (OCE-0545525) to T. Herbert and Y. Huang.

REFERENCES

(1) Brassell, S. C. In *Organic Geochemistry*; Engel, M. H., Macko, S.A., Ed.; Plenum Press: New York, 1993, pp 699-738.
(2) Conte, M. H., Volkman, John K., and Eglinton, G. In *The Haptophyte Algae*; Green, J. C., and Leadbeater, B.S.C., Ed.; Oxford University: New York, 1994; Vol. The Systematics Association Special Volume, pp 351-377.
(3) Brassell, S. C., Eglinton, G., Marlowe, I.T., Pflaumann, U. and Sarnthein, M. *Nature* **1986**, *320*, 129-133.
(4) Prahl, F. G., and S.G. Wakeham *Nature* **1987**, *330*, 367-369.
(5) Sauer, P. E.; Eglinton, T. I.; Hayes, J. M.; Schimmelmann, A.; Sessions, A. L. *Geochimica et Cosmochimica Acta* **2001**, *65*, 213-222.
(6) Huang, Y. S.; Shuman, B.; Wang, Y.; Webb, T. *Geology* **2002**, *30*, 1103-1106.
(7) Huang, Y. S.; Shuman, B.; Wang, Y.; Webb, T. *Journal of Paleolimnology* **2004**, *31*, 363-375.
(8) Englebrecht, A. C.; Sachs, J. P. *Geochimica et Cosmochimica Acta* **2005**, *69*, 4253-4265.
(9) Schouten, S.; Ossebaar, J.; Schreiber, K.; Kienhuis, M. V. M.; Langer, G.; Benthien, A.; Bijma, J. *Biogeosciences* **2006**, *3*, 113-119.
(10) Hou, J. Z.; Huang, Y. S.; Wang, Y.; Shuman, B.; Oswald, W. W.; Faison, E.; Foster, D. R. *Geochemistry Geophysics Geosystems* **2006**, *7*.
(11) Craig, H. *Science* **1966**, *154*, 1544-1548.
(12) Dansgaard, W. *Tellus* **1964**, 436-468.
(13) Rozanski K., A. A. L., and Gonfiantini R. In *Climate Change in Continental Isotopic Records*; P. K. Swart, K. C. L., J. McKenzie, and S. Savin, Ed.; American Geophysical Union, 1993; Vol. Geophysical Monograph 78, pp 1-36.
(14) Gonfiantini, R. In *Handbook of Environmental Isotope Chemistry, Vol. 2, The Terrestrial Environment, B*; Fritz, P., Fontes, J.-Ch., Ed.; Elsevier: Amsterdam, 1986.
(15) Kelts, K., Talbot, M. In *Large Lakes: Ecological Structure and Function*; Tilzer, M. M., Serruya, C., Ed.; Springer-Verlag, 1990.
(16) Sessions, A. L. *Journal of Separation Science* **2006**, *29*, 1946-1961.
(17) D'Andrea, W. J., Huang, Y. *Organic Geochemistry* **2005**, *36*, 1234-1241.
(18) de Leeuw, J. W., F.W. van der Meer, W.I.C. Rijpstra, and P.A. Schenck In *Advances in Organic Geochemistry 1979*; Douglas, A. C., and Maxwell, J.R., Ed.; Pergamon Press, 1980, pp 211-217.
(19) Marlowe, I. T., Brassell, S.C., Eglinton, G., and Green, J.C. *Organic Geochemistry* **1984**, *6*, 135-141.
(20) Guillard, R. R. L. In *Culture of Marine Invertebrate Animals*; Smith, W. L., Chanley, M.H., Ed.; Plenum Press: New York, 1975.
(21) Rontani, J. F.; Prahl, F. G.; Volkman, J. K. *Journal of Phycology* **2006**, *42*, 800-813.
(22) Schrag, D. P., Hampt, G., Murray, D.W. *Science* **1996**, *272*, 1930-1932.
(23) Shackleton, N. J. *Science* **2000**, *289*, 1897-1902.

(24) Faure, G. *Principles of Isotope Geology*; John Wiley and Sons: New York, 1986.

(25) Imbrie, J., J. D. Hays, D. G. Martinson, A. McIntyre, A. C. Mix, J. J. Morley, N. G. Pisias, W. L. Prell, and N. J. Shackleton In *Milankovitch and Climate, Part 1*; Berger, A., Ed.; Springer: New York, 1984, pp 269–305.

(26) Shackleton, N. J.; Berger, A.; Peltier, W. R. *Transactions of the Royal Society of Edinburgh-Earth Sciences* **1990**, *81*, 251-261.

(27) Lisiecki, L. E.; Raymo, M. E. *Paleoceanography* **2005**, *20*, PA1003, doi:1010.1029/2004PA001071.

(28) Gat, J. R. *Annual Review of Earth and Planetary Sciences* **1996**, *24*, 225-262.

(29) Volkman, J. K., H.R. Burton, D.A. Everitt, D.I. Allen *Hydrobiologia* **1988**, *165*, 41-57.

(30) Cranwell, P. A. *Geochimica et Cosmochimica Acta* **1985**, *49*, 1545-1551.

(31) Li, J., R.P. Philip, F. Pu, and J. Allen *Geochimica et Cosmochimica Acta* **1996**, *60*, 235-241.

(32) Sheng, G. Y., K.Q. Cai, X.X. Yang, J.L. Lu, G.D. Jia, P.A. Peng, and J.M. Fu *Chinese Science Bulletin* **1999**, *44*, 259-263.

(33) Wang, R., and M. Zheng *International Journal of Salt Lake Research* **1998**, *6*, 281-302.

(34) Theil, V., A. Jenisch, G. Landmann, A. Reimer, and W. Michaelis *Geochimica et Cosmochimica Acta* **1997**, *61*, 2053-2064.

(35) Innes, H. E., A.N. Bishop, P.A. Fox, I.M. Head, and P. Farrimond *Organic Geochemistry* **1998**, *29*, 1285-1295.

(36) Zink, K. G., D. Leythaeuser, M. Melkonian, and L. Schwark *Geochimica et Cosmochimica Acta* **2001**, *65*, 253.

(37) Theissen, K. M., Zinniker, D.A., Moldowan, J.M., Dunbar, R.B., Rowe, H.D. *Geochimica et Cosmochimica Acta* **2005**, *69*, 623-636.

(38) Liu, Z.; Henderson, A. C. G.; Huang, Y. *Geophysical Research Letters* **2006**, *33*.

(39) Box, J. E. *International Journal of Climatology* **2002**, *22*, 1829-1847.

(40) Hurrell, J. W. *Science* **1995**, *269*, 676-679.

Table 1. Columns tested for gas chromatographic optimization

Column	Length (m)	Inner diameter (mm)	Film thickness (μm)	Width/Height (sec/mV)	Theoretical plates†	Resolution*
HP-1MS	60	0.32	0.50	0.040	91,000	6.8
HP-1MS	60	0.32	0.25	0.028	194,000	6.3
DB-1MS	60	0.32	0.10	0.026	105,000	4.3
HP-1MS	60	0.25	0.25	0.028	85,000	4.3
HP-1MS	30	0.25	0.25	0.019	73,000	1.7
HP-5MS	30	0.25	0.25	0.076	20,000	1.7
HP-1MS	15	0.25	0.25	0.058	17,000	1.3

†Theoretical plates (N) were calculated using the Gaussian 10% equation;
$N = 18.42(\text{retention time}/\text{peak width at 10\% peak height})^2$

*Chromatographic resolution between $C_{37:3}$ and $C_{38:3}$ is defined as $2[(t_{R2}-t_{R1})/(W_1+W_2)]$ where, t_R is retention time and W is peak width at baseline

Table 2. δD values of alkenones from *Emiliania huxleyi* (CCMP 374)

Sample ID	Alkenone measured	$\alpha_{C37:3\text{-}C37:2}$†	δD (‰ VSMOW)	1σ
E. huxleyi	$C_{37:2}$	{0.94}	-188.1	0.6
E. huxleyi	$C_{37:3}$		-232.8	1.7

†$\alpha_{C37:3\text{-}C37:2} = (\delta D_{C37:3} + 1000)/(\delta D_{C37:2} + 1000)$

Table 3. δD values of alkenones from Greenland lake sediment

Sample ID	Alkenone measured	$\alpha_{C37:4\text{-}C37:3}$†	δD (‰ VSMOW)	1σ
Limnæa Sø	$C_{37:3}$	{0.94}	-198.2	2.2
Limnæa Sø	$C_{37:4}$		-246.7	2.1
Lake E 80	$C_{37:3}$	{0.95}	-209.9	2.9
Lake E 80	$C_{37:4}$		-253.2	1.6
Lake E 80	$C_{37:2\text{-}4}$*		-244.6	0.1
Lake E 101	$C_{37:3}$	{0.94}	-217.1	0.6
Lake E 101	$C_{37:4}$		-266.0	0.6
Lake E 101	$C_{37:2\text{-}4}$*		-245.0	3.0

†$\alpha_{C37:4\text{-}C37:3} = (\delta D_{C37:4} + 1000)/(\delta D_{C37:3} + 1000)$

*δD of the mixture of co-eluting C_{37} alkenones (di-, tri-, and tetraunsaturated) measured prior to silver nitrate-silica gel separation.

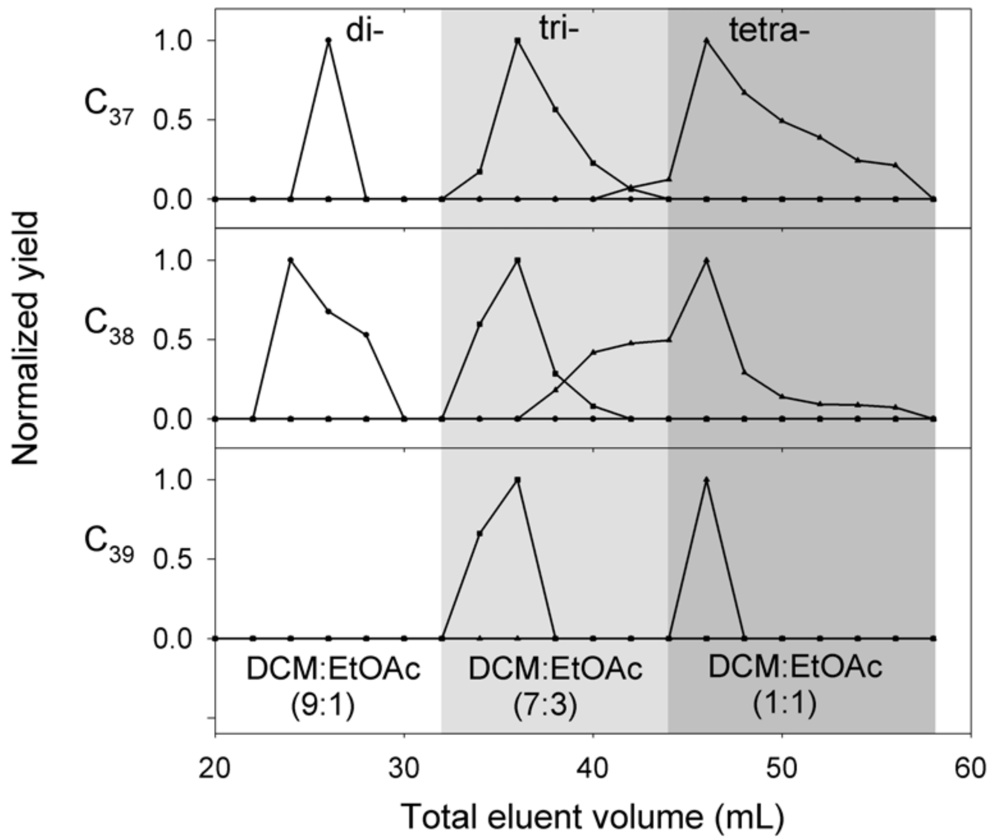

Figure 1. Normalized alkenone yield versus eluent volume for alkenone isolation by double bond number using silver nitrate-impregnated silica gel liquid chromatography. Top panel, C_{37} alkenones; middle panel, C_{38} alkenones; bottom panel, C_{39} alkenones. Shadings represent different solvents used as eluent. DCM = dichloromethane; EtOAc = ethyl acetate.

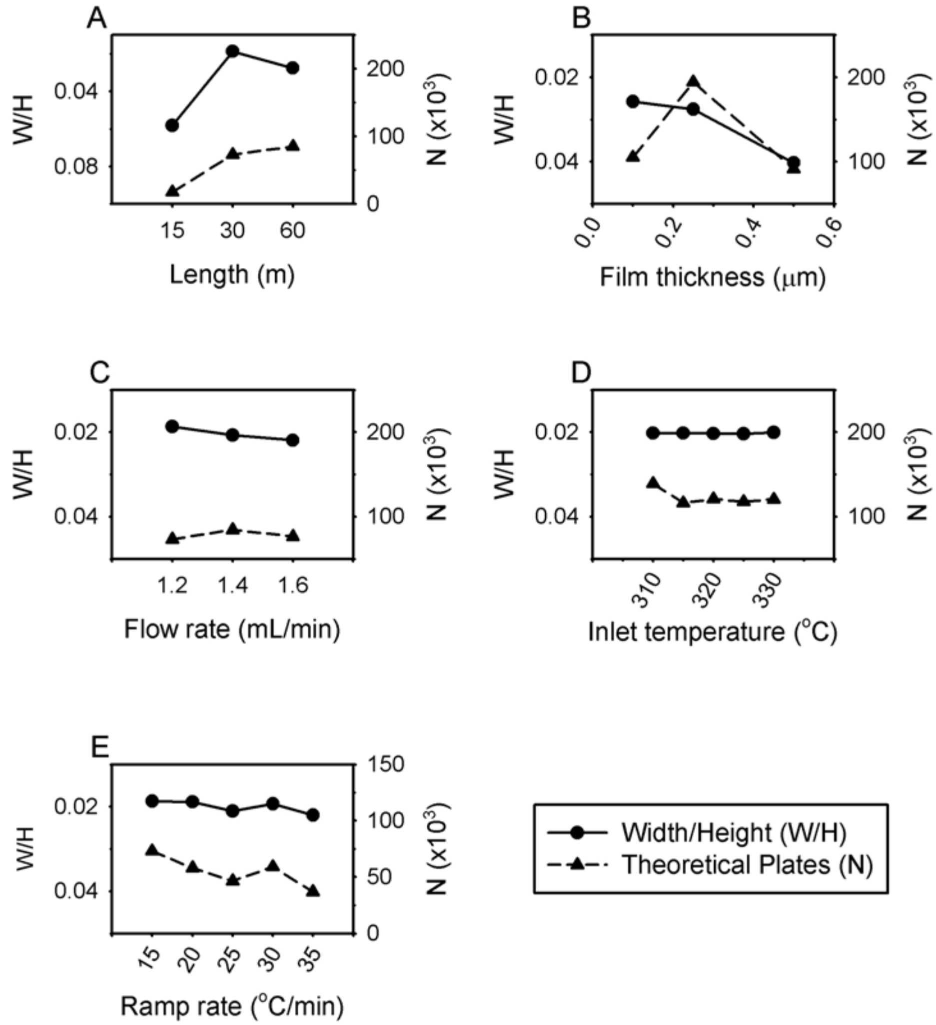

Figure 2. Optimization test results for shape (W/H = baseline width / maximum peak height [sec/mV]) and efficiency (N = theoretical plates at 10% peak height) of isolated $C_{37:3}$ alkenone peaks using GC-TC-IRMS. A. GC column length; B. Film thickness; C. Carrier gas flow rate; D. Inlet temperature; E. Rate at which temperature was increased from 280 to 315 ˚C. Note differences in y-axis scaling among panels.

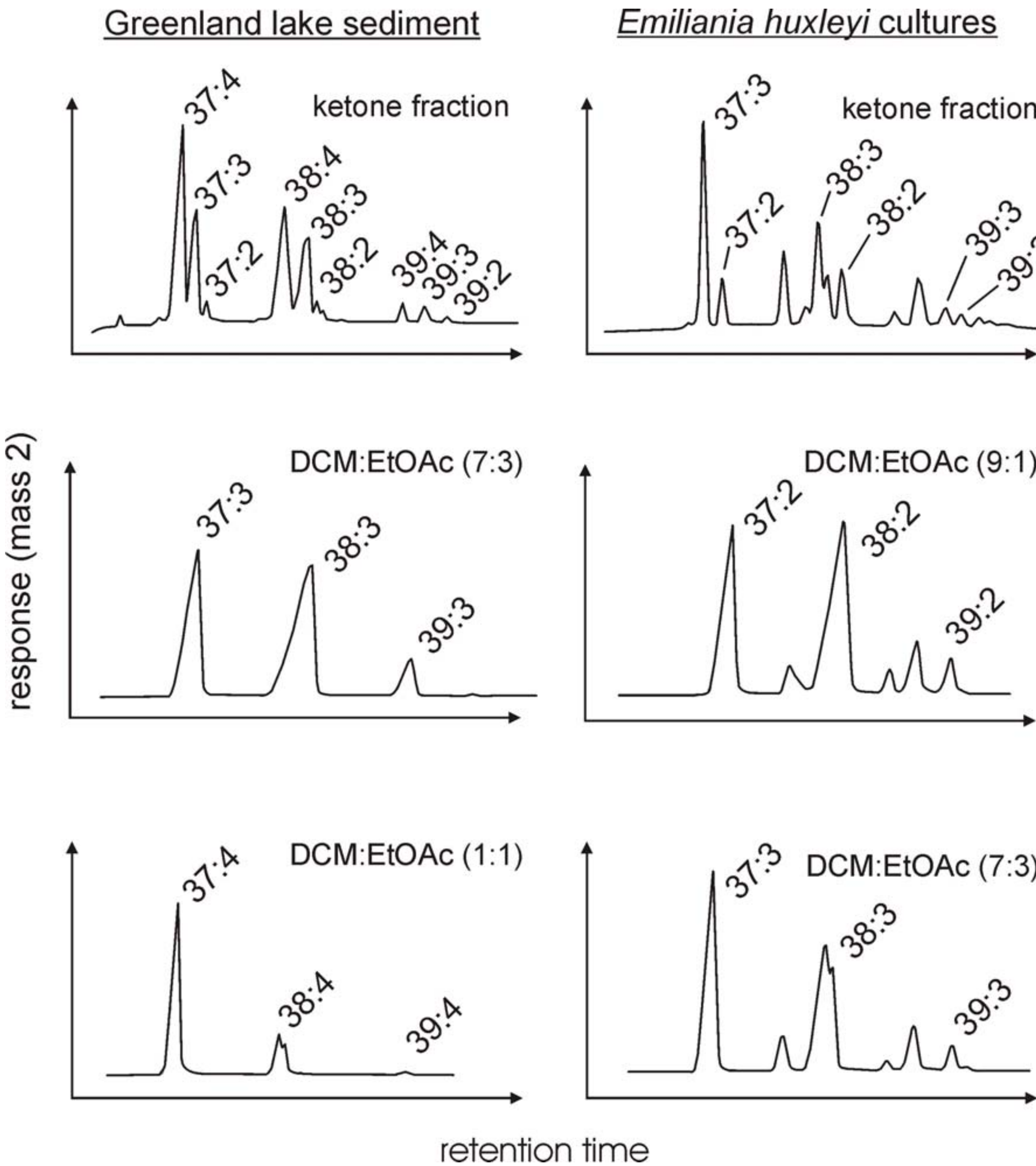

Figure 3. GC-TC-IRMS traces (mass 2) showing alkenones from Greenland lake sediment (left-hand panels) and *E. huxleyi* (right-hand panels). Upper panels show alkenones prior to separation by silver nitrate-impregnated silica gel liquid chromatography. The eluent used to isolate alkenones by double bond number is indicated on each plot (DCM = dichloromethane; EtOAc = ethyl acetate). See text for a discussion of the optimized GC-TC-IRMS conditions.

CHAPTER 4

6,000 YEARS OF TEMPERATURE VARIABILITY FROM LACUSTRINE ALKENONES IN SOUTHWESTERN GREENLAND

WILLIAM J. D'ANDREA[1]

YONGSONG HUANG[1]

SHERILYN C. FRITZ[2]

N. JOHN ANDERSON[3]

[1]BROWN UNIVERSITY, *Department of Geological Sciences*

[2]UNIVERSITY OF NEBRASKA-LINCOLN, *Department of Geosciences*

[3]UNIVERSITY OF LOUGHBOROUGH, *Department of Geography*

Millennial-scale Holocene climate variability in the North Atlantic has been documented from marine sediment cores and ice cores from the Greenland Ice Sheet[1-5]. However, to understand centennial-scale climate variability and the associated forcing and feedback mechanisms will require decadally to multi-decadally resolved quantitative climate reconstructions from throughout the North Atlantic Sector. Here we use the alkenone unsaturation index (U^{K}_{37})[6] to quantitatively reconstruct lake water temperature for the Kangerlussuaq region of Southern West Greenland at decadal timescales. We apply a temperature calibration based on new *in situ* measurements and previously published data[7] to convert U^{K}_{37} to degrees Celsius. Major reductions in Kangerlussuaq lake water temperature ca. 6-5 and 3-2.7 kyrs BP correspond to periods of decreased Meridional Overturning Circulation, expansion of the North Polar Vortex and advection of cold waters from north of Iceland into the North Atlantic Ocean[2,8,9]. Beginning ca. 4.2 kyrs BP the Kangerlussuaq record reveals centennial-scale temperature variability opposite in sign to Southwestern Ireland[10], suggesting centennial-scale variability in the dominant mode of the North Atlantic Oscillation (NAO) and the position of the Baffin Trough. The timing and severity of temperature changes depicted in the Kangerlussuaq record ca. 3.0-2.7, 2.0-1.8, and 0.85-0.55 kyrs BP support hypotheses[11,12] that climate and environmental change played a fundamental role in the final abandonment of settlements by the Paleo-Eskimo Saqqaq and Dorset cultures, and the Iron Age Norse culture.

The North Atlantic is a region where numerous water masses of different temperature and salinity interact, and where the formation of North Atlantic Deep Water (NADW), a major feature of the global oceanic conveyor[13], facilitates poleward transport of heat via the ocean. The climate of Southern West Greenland[14-16] is strongly influenced by the meridional position of the Baffin Trough, a low pressure feature and fixture of the general atmospheric circulation of the Northern Hemisphere[15,16]. The position of the Baffin Trough, which is associated with that of the Icelandic Low pressure system, is influenced by the mode of the North Atlantic Oscillation (NAO)[16], a redistribution of atmospheric mass between the Arctic (Icelandic Low) and subtropical North Atlantic (Azores High) that results in changes in the strength and trajectory of westerly air flow across the Atlantic Ocean, and which controls the distribution of heat and moisture from the eastern US to Siberia and from the Arctic to subtropical Atlantic over sub-decadal to multi-decadal timescales[17]. In the positive mode of the NAO, both the Icelandic Low and Azores High are intensified and shifted to the northeast, creating stronger mid-latitude westerly airflow that brings moist and humid conditions to Northern Europe, while the Baffin Trough is shifted eastward resulting in more cold, dry northerly airflow into Western Greenland[16]. In the negative mode of the NAO, reduced intensity and southwestern displacement of the Icelandic Low and Azores High pressure systems result in relaxation of the westerly airflow across the Atlantic and a westward displacement of the Baffin trough, which together result in cooler and drier conditions in Northern Europe and warmer and more humid conditions in Western Greenland. Interactions between complex ocean circulation patterns and decadal- to multidecadal scale NAO variability combine[18,19] to create a complicated and spatiotemporally diverse Holocene climate history for the North Atlantic. Here we present a 6 kyr temperature reconstruction from the ice free margin of Southern West Greenland that reveals the influence of meridional overturning circulation (MOC) changes and the onset of centennial-scale NAO-type variability after ca. 4.2 kyrs BP.

The data we present are lake water temperature reconstructions generated by measuring the alkenone unsaturation index (U^{K}_{37})[6] in sediment cores recovered from two lakes, Braya Sø and Lake E, at the head of the Søndre Strømfjord, near the town of Kangerlussuaq in Southern West Greenland (67°00' N, 50°42' W; Fig. 1; See Supplemental 1 for *Materials and Methods*). Alkenone thermometry is a well-established method for reconstructing sea surface temperatures from marine sediment cores[6,20,21], and temperature dependence has been demonstrated for lacustrine alkenones from Europe and China[7,22,23]. Alkenone producers in the Greenland lakes represent a newly discovered member of the algal class Haptophyta[24,25] and time-series sediment traps were used to determine that the haptophyte bloom and associated alkenone production occurs from mid-June to mid-July (see Supplemental 2) and therefore, that alkenone-based reconstructions in this region represent summer lake water temperature. We apply a temperature calibration to the Greenland lake records that combines an *in situ* calibration from Braya Sø with the published calibration of Zink *et al.* [7] (Supp. 2). The calibration ($T = 14.3\ [U^{K}_{37}] + 32.3$; $R^2 = 0.97$; $n = 26$) spans 3 - 24 °C and reveals that lake water temperature in the Kangerlussuaq region varied between 4 and 12°C over the past 6 kyrs BP (Fig. 2). The excellent agreement in the timing and amplitude of reconstructed temperature variability from Braya Sø and Lake E (Fig. 2), approximately 10 km apart, confirms that lacustrine alkenones from these lakes reflect regional climate rather than lake-specific processes and highlights the potential of lacustrine alkenone thermometry for paleoclimate studies. Accelerator mass spectrometry (AMS) ^{14}C dates of bulk sediment and terrestrial macrofossils were used to establish chronological control for the sediment cores (see Supplemental 3). After adjusting the records within their chronological uncertainty (2σ of calibrated ^{14}C ages), the records were resampled at 20 year intervals and stacked (arithmetic mean) to generate a master temperature curve (the "Kanger Stack"; Fig. 2) representing lake water temperature variability in the Kangerlussuaq region of Southern West Greenland over the past 6 kyrs.

Previous temperature inferences for West Greenland come from pollen analyses[26,27,28] and loss on ignition analysis from lake sediments[29] and indicate mid- to late Holocene peak warmth occurred between 4 and 3 kyr BP, followed by a deterioration of climate (onset of Neoglaciation) ca. 3 kyrs BP. This agrees well with reconstructions showing that the Baffin Bay region experienced Holocene Thermal Maximum (HTM) terminating ca. 3 kys BP[30,31]. The Kanger Stack shows lake temperatures in Kangerlussuaq increasing from ~4.5 °C at 5 kyrs BP to an HTM peak value of ~9.5 °C between 3.2 and 3 kyrs BP and sharply decreasing to 5 °C by 2.8 kyrs BP, supporting the millennial scale temperature patterns inferred from the other West Greenland records and from the GISP2 ice core[32,33] (Fig. 3). Over centennial timescales there are many similarities among these records, but many differences, as well, highlighting the spatial heterogeneity of temperature over centuries (particularly with respect to temperature at the GISP2 coring site, ~3 km above sea level at the summit of the Greenland Ice Sheet, and the

Kangerlussuaq area, at sea level) and underscores the fact that loss-on-ignition productivity records, while influenced by air temperature and duration of the ice-free season[29] are also impacted by other factors, such as lake ontogeny and the changing flux of aeolian deposition to the lake. Previous records have documented an especially cold interval in West Greenland centered at ca. 2 kyrs BP[27,29], at the same time that the greatest Neoglacial advance of the inland ice occurred near Kangerlussuaq[34]. The Kanger Stack depicts a dramatic cooling event (lake water temperatures ~4.5 °C) centered at 2 kyrs BP. The cold intervals at ca. 3 and 2 kyrs BP also correspond to intervals of increased aeolian activity in the Kangerlussuaq region (3.2-2.8 kyr BP and 2.2-1.8 kyr BP), indicating enhanced windiness and aridity[35]. Increased aridity between 6.5 – 4.5 kyrs BP followed by a period of increased moisture from 4.5 - 3.5 kyrs BP is indicated by diatom-inferred lake salinity and $\delta^{18}O$ of lacustrine carbonate[36,37]. Thus, periods of aridity and humidity in Kangerlussuq correspond, respectively, to intervals of relative cold and warmth in the Kanger Stack and suggest that the mode of NAO and/or position of the Baffin Trough have been important in determining Holocene climate in Kangerlussuaq, just as in the instrumental period[14]. The Kanger Stack clearly depicts severe cooling between 6 and 5 kyrs BP followed by warming to ca. 3kyrs BP and severe cooling to 2.8 kyrs BP. The record also indicates that after ca. 4.2 kyrs BP, temperature in the Kangerlussuaq began to vary on centennial timescales.

How do the past 6 kyrs of temperature variability in Kangerlussuaq fit within the context of larger patterns of climate change in the North Atlantic? Holocene reconstructions of the strength of NADW formation indicate major decreases in MOC between 6 and 5 kyrs

BP[8] and between 3 and 2.7 kyrs BP[2,8,9]. The periods of decreased NADW formation correspond to two of the most dramatic temperature decreases experienced in the Kangerlussuaq area (Fig. 4), suggesting that changes in MOC and poleward heat transport during the Holocene have dramatically impacted summer temperatures in Kangerlussuaq. The intervals of reduced NADW formation also coincide with periods increased “winter-like” conditions (expanded polar vortex) over Greenland between 6.1 – 5.0 kyrs BP and 3.1 – 2.4 kyrs BP[5] and to times of increased advection of cool, ice-bearing waters from north of Iceland into the North Atlantic[1], indicating that the cold temperatures experienced in Kangerlussuaq, centered at ca. 5.0 and 2.8 kyrs BP, were part of larger scale cooling events in the North Atlantic related to reduced MOC and expansion of the polar vortex. However, expansion of the polar vortex and increased ice rafting in the North Atlantic have also been documented for the past 600 years[5,38], a time when the Kanger Stack depicts variable lake water temperatures. It therefore seems that either the sensitivity of Kangerlussuaq summer temperatures to major North Atlantic reorganizations has changed throughout the Holocene, or the interval between 600 and 0 yrs BP was fundamentally different than the events ca. 6.1-5.0 and 3.1-2.4 kyrs BP; indeed, there is no evidence of decreased MOC between 600 yrs BP and present.

The nature of climate variability in the Kangerlussuaq region appears to change ca. 4.2 kyrs BP, at which time centennial-scale variability becomes apparent in the Kanger Stack. We propose that the centennial-scale temperature variability seen in the Kangerlussuaq temperature record reflects centennial-scale changes in the dominant mode of the NAO. Based on correlation over the instrumental record, we know that

Kangerlussuaq is the most sensitive site in all of Greenland to the NAO[14]. Comparison between the Kanger Stack and the $\delta^{18}O$ record from a speleothem (CC3) from Southwestern Ireland[10] reveals that after ca. 4.2 kyrs BP centennial-scale warm intervals in Kangerlussuaq correspond to centennial-scale intervals of lower $\delta^{18}O$ in the Irish speleothem (Fig. 5). Although the CC3 $\delta^{18}O$ record cannot be used quantitatively as a temperature record because the $\delta^{18}O$ changes reflect changes in air temperature as well as in the oceanic moisture source and storm track trajectories, McDerrmott *et al.* [10] specify that the latter changes act to accentuate temperature driven $\delta^{18}O$ changes and that therefore, the record is a qualitative record of temperature variability (with higher $\delta^{18}O$ values corresponding to warmer temperatures). The coherence between centennial-scale changes in the Kangerlussuaq temperature record and the Irish speleothem $\delta^{18}O$ strongly suggests changes in the dominant mode of the NAO as a common forcing mechanism. Centennial-scale temperature variability is unlikely to be driven by atmospheric processes alone, and instrumental records are too short to demonstrate centennial-scale variability in the NAO, but it has been proposed that the ocean modulates the NAO over multi-decadal and longer timescales[39,18]. Perhaps modulation of the NAO by the ocean is responsible for the centennial-scale variability described here.

The data presented here cannot determine what triggered the onset of NAO-type variability ca. 4.2 kyrs BP, but it has been proposed that the waning influence of shrinking northern ice sheets at this time caused a major reorganization of oceanographic conditions[31]. Furthermore, investigations of foraminiferal assemblages and $\delta^{18}O$ values from a sediment core in the Norwegian Sea suggest that at ca. 4 kyrs BP continuously strong mid-latitude westerlies crossing the North Atlantic relaxed, and Arctic water masses shifted westward allowing greater influence of Atlantic waters in the Norwegian Sea[4]. Perhaps this fundamental change in North Atlantic oceanic and atmospheric circulation ca. 4 kyrs BP favored the centennial-scale NAO-type variability seen thereafter. Whatever the reason for its onset, we propose that the centennial-scale variability in the Kangerlussuaq temperature and the CC3 temperature record reflect changes in the dominant mode of the NAO. Spectral analyses of the Kangerlussuaq temperature record and CC3 speleothem record (see Supplemental 4) for the period 4.2 kyrs BP to present indicate peaks in spectral power above the 99% confidence level at periods of 262 and 222 years, respectively.

NOA-type variability alone, however, cannot explain all of the centennial-scale changes seen in the Kangerlussuaq temperature record. From ca. 1000 to 850 yrs BP warming occurred in both Kangerlussuaq and southwest Ireland, while from 850 to 750 yrs BP both regions experienced cooling. It thus appears that the Thule people[41], ancestors of the modern Greenlandic Inuit, and the Norse[12] migrated to and settled in Greenland at a time (ca. 1015 yrs BP) when both Western Greenland and Northern Europe were experiencing mild temperatures. The Norse Western Settlement, in the Gothabsfjord district near Nuuk (Fig. 1), came to an abrupt end in the middle of the 14th century (ca. 650 yrs BP) likely due to cold temperatures, hostile interactions with Inuit neighbors and failure to adapt farming and living practices to a changing environment[12]. The Kanger Stack clearly shows that the period just before the demise of the Western Settlement was marked by a drastic cooling event (lake water temperature dropped ~4 °C in 80 years) and that temperatures remained low until the mid 15th century (ca. 570 yrs BP). This interval also corresponds to one of cooling in Southwestern Ireland as inferred from the CC3 $\delta^{18}O$ record, suggesting that while the cold snap may have played a critical role in the failure of the Western Settlement it was not initiated by centennial-scale variability in the NAO.

It has been proposed that the Paleo-Eskimo migration history of Greenland was also determined by climatic and environmental change[11,42]. The temperature reconstruction from Kangerlussuaq allows evaluation of the timing of human migration into and out of West Greenland in the context of Holocene temperature variability. The first wave of human occupation began with the Saqqaq culture who arrived in Greenland ca. 4.5 kyrs BP and quickly colonized the entire island[41,43]and who would have experienced the mid Holocene Thermal Maximum in West Greenland. Ca. 3.4 kyrs BP the Saqqaq population contracted toward Southern West Greenland[43]. Based on faunal material identified in archaeological sites, Meldgaard[11] speculated that a shift from subarctic to arctic conditions in the Disko Bugt region north of Kangerlussuaq (Fig. 1), ca. 3.5 kyrs BP, affected Saqqaq resources and led to their disappearance from Disko Bugt. Moros *et al.*[44] propose that reduced air temperatures inferred from diatom and lithological analysis of a sediment core from Disko Bugt support this interpretation. ~250 km south of Disko Bugt, the Saqqaq remained active in the coastal Sisimiut region (~100 km west of Kangerlussuaq; Fig. 1) until ca. 2.8 kyrs BP[41]. Perhaps the persistence of warm temperatures in Kangerlussuaq and Sisimiut until ca. 3 kyrs BP afforded the Saqqaq adequate access to marine and terrestrial resources. Furthermore, large caribou populations of the Sisimiut region would have provided a significant terrestrial food source as marine resources became more difficult to procure[43]. The Saqqaq departure from Sisimiut ca. 2.8 kyrs BP is coincident with severe cooling depicted in the Kanger Stack, and supports the idea that climate change led to their disappearance from Southern West Greenland. A shorter open water hunting season, coupled with colder summers that reduced populations of terrestrial game could have resulted in unsuitable living conditions for the Saqqaq people. It appears that the reduction in NADW formation and MOC, centered at 2.7 kyrs BP[8,2,9], coupled with the "winter-like" conditions associated with an expanded polar vortex[5] may have been responsible for the end of Saqqaq occupation of the Sisimiut region and Greenland altogether ca. 2.8 kyrs BP.

People of the Dorset culture occupied Greenland between 2.8 and 1.8 kyrs BP[43]. The Dorset were better-adapted to cold temperatures and sea-ice hunting than the Saqqaq, and while they hunted land mammals, their lack of bow and arrow suggests that terrestrial game did not constitute a large a part of their resource base [45]. The Dorset lifestyle was therefore well-adapted to the colder Neoglacial conditions they encountered in Southern West Greenland beginning after ca. 3 kyrs BP and depicted in the Kanger Stack and other records from this region[27,29]. The period of Dorset occupation was characterized by high amplitude centennial-scale temperature variability, seen in the Kanger Stack, but their continuous occupation indicates that these temperature fluctuations did not impact their resource base to the point of abandonment. The disappearance of the Dorset ca. 1.8 kyrs BP coincides with an extremely warm swing recorded in the Kanger Stack. Moros *et al.*[44] noted that in the Disko Bugt region the interval 2.0-1.8 kyrs BP was marked by warm sea surface temperatures and limited sea ice, and suggested that the climate shift at this time could have had unfavorable environmental repercussions for the Dorset way of life. Kangerlussuaq lake water warmed to nearly pre-Neoglacial temperatures ca. 1.8 kyrs BP, supporting the idea that warming in Southern West Greenland may have impacted the ecosystem to the extent that the Dorset people abandoned their settlements. This warm swing appears to have been an especially high amplitude feature of the centennial-scale temperature variability.

Once considered a period of stability, the Holocene is now viewed as one of variable and dynamic climate. As more high-resolution, quantitative climate reconstructions become available it becomes possible to evaluate spatial patterns of climate variability over centennial timescales. While our data cannot explain the mechanisms that have forced changes in MOC or the dominant mode of the NAO during the Holocene, they do offer a temporal temperature reconstruction from a new geographic location, allowing the past 6 kyrs of temperature variability in Kangerlussuaq to be considered in the context of North Atlantic climate variability. The major temperature decreases experienced in Kangerlussuaq between 6-5 kyrs BP and between 3.0-2.7 kyrs BP were in response to the reduction MOC and expansion of the north polar vortex that occurred at these times[8,2,9,5]. The temperature reductions in Southern West Greenland were probably due to reduced poleward transport of heat from the equator, but could also represent an eastward displacement of the Baffin Trough. After ca. 4.2 kyrs BP centennial-scale temperature variability with an NAO signature (West Greenland warm, Northern Europe cold) began and has persisted until present. Waning influence of shrinking northern ice sheets[31], relaxation of the westerlies and reorganization of water masses in the Greenland and

Norwegian Seas[4] likely allowed for ocean-modulated, centennial-scale variability in the dominant mode of the NAO after ca. 4.2 kyrs BP. The human migration history into Southern West Greenland includes that of the Paleo-Eskimo Saqqaq and Dorset cultures, the Norse (Vikings), and the Thule culture (ancestors of the modern Inuit population). Three of these cultures (all but the Thule) eventually abandoned their settlements, likely due to climate changes and associated changes to the structure of their resource base[11,12]. In the Kangerlussuaq region, a temperature decrease associated with reduced MOC ca. 2.8 kyrs BP marks the end of the Saqqaq occupation, a temperature increase ca. 1.8 kyrs BP (a high amplitude feature of the centennial-scale NAO-type variability) marks the end of Dorset occupation in Southern West Greenland, and lastly, cold temperatures between 800 and 500 yrs BP characterize the time of abandonment of the Western and Eastern Norse settlements in South Western and Southern Greenland, respectively.

Predicting future climate change scenarios is a major scientific challenge, particularly in the North Atlantic sector where air-sea interactions have complex and poorly understood feedbacks that influence global climate, and in the Arctic where rapid changes threaten traditional resources and food webs, while at the same time providing access to new resource development. If the NAO, and other coupled climate modes, have operated at centennial timescales during the Holocene, they must be thoroughly documented and described to explore the forcing and feedback mechanisms that cause them, and to provide better representation of such natural patterns of variability in future climate change scenarios. Dense networks of high-resolution quantitative paleoclimate reconstructions, such as alkenone-based temperature records from lakes, will be vital to understanding the past and future behavior of the climate system.

ACKNOWLEGEMENTS

Thanks to Jonathan Nichols, Kane McGuire, Scott Lowenstein and Jim Cotner for field assistance. Thanks to Devina Swarup, Marcelo Alexandre and Kane McGuire for laboratory assistance. Additional thanks to Juzhi Hou, Jaime Toney, Joe Orchardo, Dave Murray and Warren Prell. This work was supported by grants from the National Science Foundation (NSF0318050, 0318123, 0402383, 0520718) and NASA (NAG5-10665, NNG04GJ34G) to Y. Huang.

References

[1] Bond, G., A Pervasive Millenial-Scale Cycle in North Atlantic Holocene and Glacial Climates. *Science* **278**, 1257 (1997).

[2] Bianchi, G. G. and McCave, I. N., Holocene periodicity in North Atlantic climate and deep-ocean flow south of Iceland. *Nature* **397** (6719), 515 (1999).

[3] Calvo, E., Grimalt, J. O., and Jansen, E., High resolution U^{K}_{37} sea surface temperature reconstruction in the Norwegian Sea during the Holocene. *Quaternary Science Reviews* **21** (12-13), 1385 (2002).

[4] Risebrobakken, B. et al., A high-resolution study of Holocene paleoclimatic and paleoceanographic changes in the Nordic Seas. *Paleoceanography* **18** (1) (2003).

[5] O'Brien, S.R., Mayewski, P.A., Meeker, L.D., Meese, D.A., Twickler, M.S., and Whitlow, S.I, Complexity of Holocene climate as reconstructed from a Greenland ice core. *Science* **270**, 1962 (1995).

[6] Brassell, S.C., Eglinton, G., Marlowe, I.T., Pflaumann, U. and Sarnthein, M., Molecular stratigraphy: A new tool for climatic assessment. *Nature* **320**, 129 (1986).

[7] Zink, K.G., D. Leythaeuser, M. Melkonian, and L. Schwark, Temperature dependency of long-chain alkenone distributions in Recent to fossil limnic sediments in lake waters. *Geochimica et Cosmochimica Acta* **65** (2), 253 (2001).

[8] Oppo, D. W., McManus, J. F., and Cullen, J. L., Deepwater variability in the Holocene epoch (vol 422, pg 277, 2003). *Nature* **423** (6938), 400 (2003).

[9] Hall, I. R., Bianchi, G. G., and Evans, J. R., Centennial to millennial scale Holocene climate-deep water linkage in the North Atlantic. *Quaternary Science Reviews* **23** (14-15), 1529 (2004).

[10] McDermott, F., Mattey, D. P., and Hawkesworth, C., Centennial-scale holocene climate variability revealed by a high-resolution speleothem $\delta^{18}O$ record from SW Ireland. *Science* **294** (5545), 1328 (2001).

[11] Meldgaard, M., Ancient Harp Seal Hunters of Bisko Bay: Subsistence and Settlement at the Saqqaq Culture Site Qeqertasussuk (2400-1400 BC), West Greenland. *Meddelelser om Gronland, Man & Society* **30** (2004).

[12] Barlow, L. K. et al., Interdisciplinary investigations of the end of the Norse western settlement in Greenland. *Holocene* **7** (4), 489 (1997).

[13] Broecker, W. S., The Great Ocean Conveyor. *Oceanography* **4**, 79 (1991).

[14] Box, J.E., Survey of Greenland Instrumental Temperature Records: 1873-2001. *International Journal of Climatology* **22**, 1829 (2002).

[15] Williams, L.D., Bradley, R.S., in *Quaternary Environments: Eastern Canadian Arctic, Baffin Bay and Western Greenland*, edited by J.T. Andrews (Allen & Unwin, Boston, 1985).

[16] Barlow, L. K., Rogers, J. C., Serreze, M. C., and Barry, R. G., Aspects of climate variability in the North Atlantic sector: Discussion and relation to the Greenland Ice Sheet Project 2 high-resolution isotopic signal. *Journal of Geophysical Research-Oceans* **102** (C12), 26333 (1997).

[17] Hurrell, J.W., Decadal Trends in the North Atlantic Oscillation: Regional Temperatures and Precipitation. *Science* **269**, 676 (1995); Hurrell, J. W., Kushmir, Y., Ottersen, G., and Visbeck, M., The North Atlantic Oscillation:

Climatic Significance and Environmental Impact. **Geophysical Monograph 134**, 1 (2001); Hurrell, J. W. and VanLoon, H., Decadal variations in climate associated with the north Atlantic oscillation. *Climatic Change* **36** (3-4), 301 (1997).

18 Visbeck, M. et al., in *The North Atlantic Oscillation: Climate Significance and Environmental Impact*, edited by J. W. Hurrell, Y. Kushnir, G. Ottersen, and M. Visbeck (American Geophysical Union, Washington, DC, 2003).

19 Bellucci, A. and Richards, K. J., Effects of NAO variability on the North Atlantic ocean circulation. *Geophysical Research Letters* **33** (2) (2006).

20 Prahl, F.G., and Wakeham, S.G., Calibration of unsaturation patterns in long-chain ketone compositions for paleotemperature assessment. *Nature* **330**, 367 (1987).

21 Muller, P. J. et al., Calibration of the alkenone paleotemperature index UK'37 based on core-tops from the eastern South Atlantic and the global ocean (60 degrees N-60 degrees S). *Geochimica Et Cosmochimica Acta* **62** (10), 1757 (1998).

22 Chu, G. Q. et al., Long-chain alkenone distributions and temperature dependence in lacustrine surface sediments from China. *Geochimica Et Cosmochimica Acta* **69** (21), 4985 (2005).

23 Sun, Q., Chu, G., Li, S., Lu, C., Zheng, M., Long-chain alkenones in sulfate lakes and its paleoclimatic implications. *Chinese Science Bulletin* **49**, 2082 (2004).

24 D'Andrea, W.J. and Huang, Y., Long-chain alkenones in Greenland lake sediments: low $\delta^{13}C$ values and exceptional abundance. *Organic Geochemistry* **36**, 1234 (2005).

25 D'Andrea, W.J. et al., Alkenone producers inferred from well-preserved 18S rDNA in Greenland lake sediments. *Journal of Geophysical Research - Biogeoscience* doi:10.1029/2005JG000121, (2006).

26 Fredskild, B., The Holocene development of some low and high arctic Greenland lakes. *Hydrobiologia* **103**, 217 (1983).

27 Funder, S., and Fredskild, B., in *Quaternary geology of Canada and Greenland*, edited by R.J. Fulton (Geological Survey of Canada, 1989), Vol. 1, pp. Chapter 13.

28 Eisner, W.R., Tornqvist, T. E., Koster, E.A., Bennike, O., and van Leeuwen, J.F.N., Paleoecological Studies of a Holocene Lacustrine Record from the Kangerlussuaq (Sondre Stromfjord) Region of West Greenland. *Quaternary Research* **43**, 55 (1995).

29 Willemse, N.W., and Tornqvist, T.E., Holocene century-scale temperature variability from West Greenland lake records. *Geology* **27** (7), 580 (1999).

30 Kaufman, D. S. et al., Holocene thermal maximum in the western Arctic (0-180^{o} W) (vol 23, pg 529, 2003). *Quaternary Science Reviews* **23** (18-19), 2059 (2004).

31 Kaplan, M. R. and Wolfe, A. P., Spatial and temporal variability of Holocene temperature in the North Atlantic region. *Quaternary Research* **65** (2), 223 (2006).

32 Alley, R. B., The Younger Dryas cold interval as viewed from central Greenland. *Quaternary Science Reviews* **19** (1-5), 213 (2000).

[33] Cuffey, K. M. and Clow, G. D., Temperature, accumulation, and ice sheet elevation in central Greenland through the last deglacial transition. *Journal of Geophysical Research-Oceans* **102** (C12), 26383 (1997).

[34] Forman, S. L. et al., Little ice age and neoglacial landforms at the Inland Ice margin, Isunguata Sermia, Kangerlussuaq, west Greenland. *Boreas* **36** (4), 341 (2007).

[35] Willemse, N.W., Koster, E.A., Hoogakker, B., and van Tatenhove, F.G.M., A continuous record of Holocene eolian activity in West Greenland. *Quaternary Research* **59**, 322 (2003).

[36] McGowan, S., Ryves, D.B., and Anderson, N.J., Holocene records of effective precipitation in West Greenland. *The Holocene* **13** (2), 239 (2003).

[37] Anderson, N.J., and Leng, M.J., Increased aridity during the early Holocene in West Greenland inferred from stable isotopes in laminated-lake sediments. *Quaternary Science Reviews* **23**, 841 (2004).

[38] Bond, G., Persistent Solar Influence on North Atlantic Climate During the Holocene. *Science* **294**, 2130 (2001).

[39] Delworth, T. L., North Atlantic interannual variability in a coupled ocean-atmosphere model. *Journal of Climate* **9** (10), 2356 (1996).

[40] Seppa, H. and Birks, H.J.B, July mean temperature and annual precipitation trends during the Holocene in the Fennoscandian tree-line area: pollen-based climate reconstructions. *The Holocene* **11**, 527 (2001).

[41] Jensen, J.F., in *Contributions to the Study of the Dorset Palaeo-Eskimos*, edited by P.D. Sutherland (Canadian Museum of Civilization, 2005), Vol. Mercury Series, Archaeology Paper 167.

[42] McGhee, R., *Ancient People of the Arctic*. (UBC Press, 1996).

[43] Jensen, J.F., The Stone Age of Qeqertarsuup Tunua (Disko Bugt): A regional analysis of the Saqqaq and Dorset cultures of Central West Greenland. *Meddelelser om Gronland, Man & Society* **32** (2006).

[44] Moros, M., Jensen, K. G., and Kuijpers, A., Mid- to late-Holocene hydrological and climatic variability in Disko Bugt, central West Greenland. *Holocene* **16** (3), 357 (2006).

[45] Gad, F., *The History of Greenland*. (C. Hurst & Co., London, 1970).

[46] Huang, Y. S., Shuman, B., Wang, Y., and Webb, T., Hydrogen isotope ratios of individual lipids in lake sediments as novel tracers of climatic and environmental change: a surface sediment test. *J Paleolimnol* **31** (3), 363 (2004).

[47] de Leeuw, J.W., van der Meer, F.W., Rijpstra, W.I.C., and Schenck, P.A. in *Advances in Organic Geochemistry 1979*, edited by Douglas, A.C. and Maxwell, J.R. (Pergamon Press, 1980), pp. 211.

[48] Marlowe, I.T., Brassell, S.C., Eglinton, G., and Green, J.C., Long chain unsaturated ketones and esters in living algae and marine sediments. *Organic Geochemistry* **6**, 135 (1984).

[49] Sun, Q. et al., Calibration of alkenone unsaturation index with growth temperature for a lacustrine species, Chrysotila lamellosa (Haptophyceae). *Organic Geochemistry* **38** (8), 1226 (2007).

[50] Fairbanks, R. G. et al., Radiocarbon calibration curve spanning 0 to 50,000 years BP based on paired ^{230}Th/^{234}U/^{238}U and ^{14}C dates on pristine corals. *Quaternary Science Reviews* **24** (16-17), 1781 (2005).
[51] Olsson, I.U., in *Handbook of Holocene palaeoecology and palaeohydrology*, edited by B.E. Berglund (Wiley, Chichester, 1986), pp. 273.
[52] Schulz, M. and Mudelsee, M., REDFIT: estimating red-noise spectra directly from unevenly spaced paleoclimatic time series. *Computers & Geosciences* **28** (3), 421 (2002).

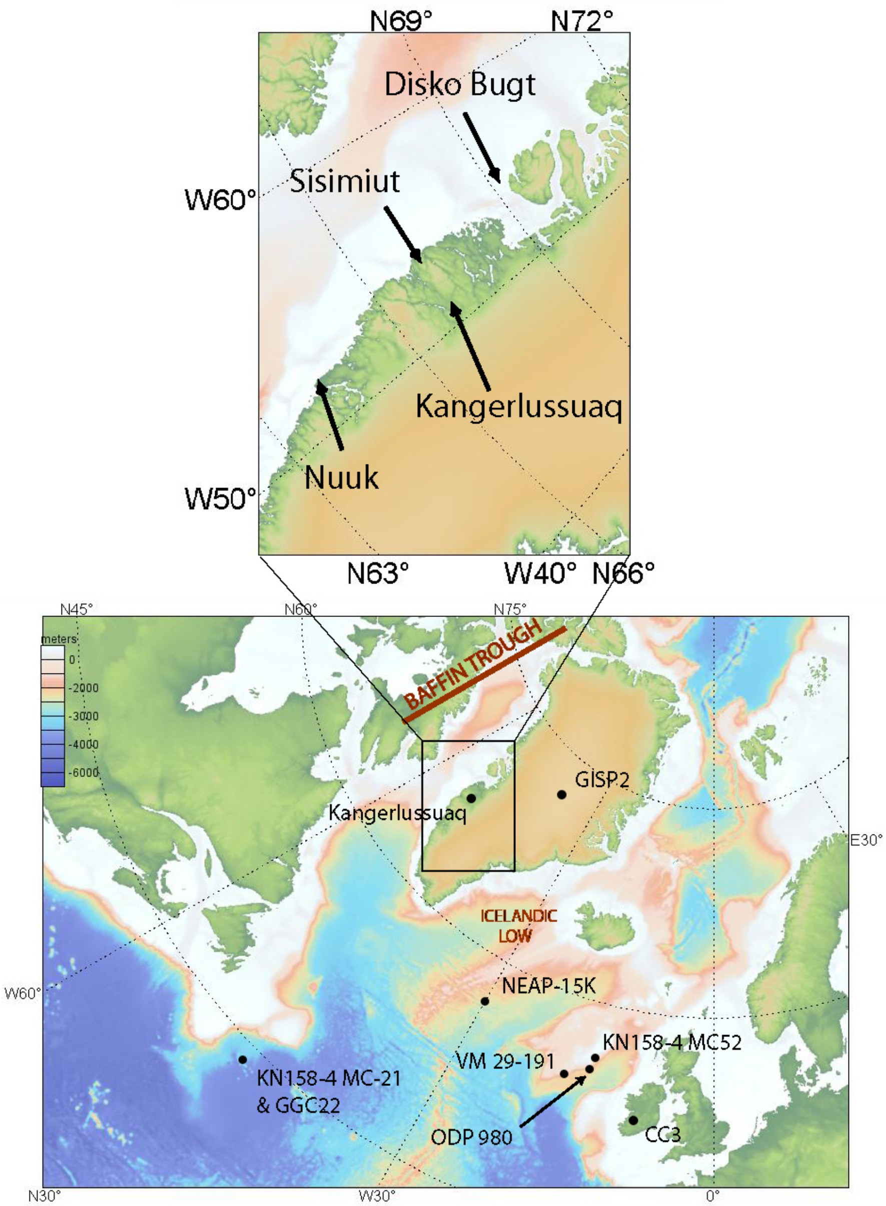

Figure 1. Map of sites from which data is presented that provide the North Atlantic context for evaluating the temperature variability over the past 6 kyrs BP in Kangerlussuaq, Greenland. *Kangerlussuaq*: Site of the lacustrine alkenone records reported in this study; *CC3*: Irish Speleothem discussed in text[10]; *GISP2*: Coring location for the GISP2 ice core at the summit of the Greenland Ice Sheet[32,33]. Marine sediment cores: *NEAP-15K*[2], *ODP 980*[8], *KN158-4 MC-21*, *KN158-4 GGC22*, *KN158-4 MC52*, *VM 29-191*[38]. Enlarged map shows Central and Southern West Greenland with sites of human occupation discussed in the text. Also shown are generalized locations for the axis of the Baffin Trough and the Icelandic Low, permanent features of the general atmospheric circulation that control the climate of Southern West Greenland. Color scale corresponds to ocean bathymetry.

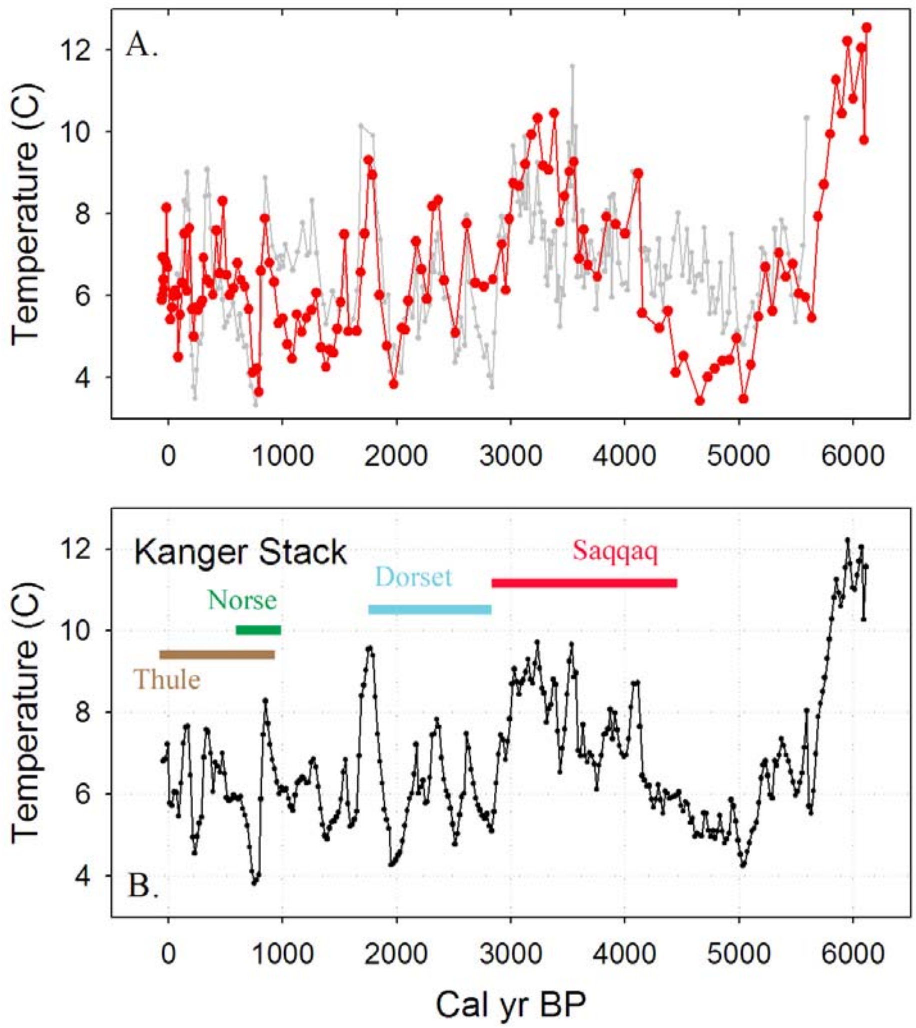

Figure 2. A. Alkenone-based lake water reconstruction for Lake E (grey) and Braya Sø (red). The curves have been visually aligned within the 2σ error of the calibrated ^{14}C dates. **B.** The *Kanger Stack* was developed by resampling and calculating the arithmetic mean of the individual temperature reconstructions from A. at 20 year intervals. Also shown are approximate timings of human occupations of Southern West Greenland[11,12,41] (see text for discussion).

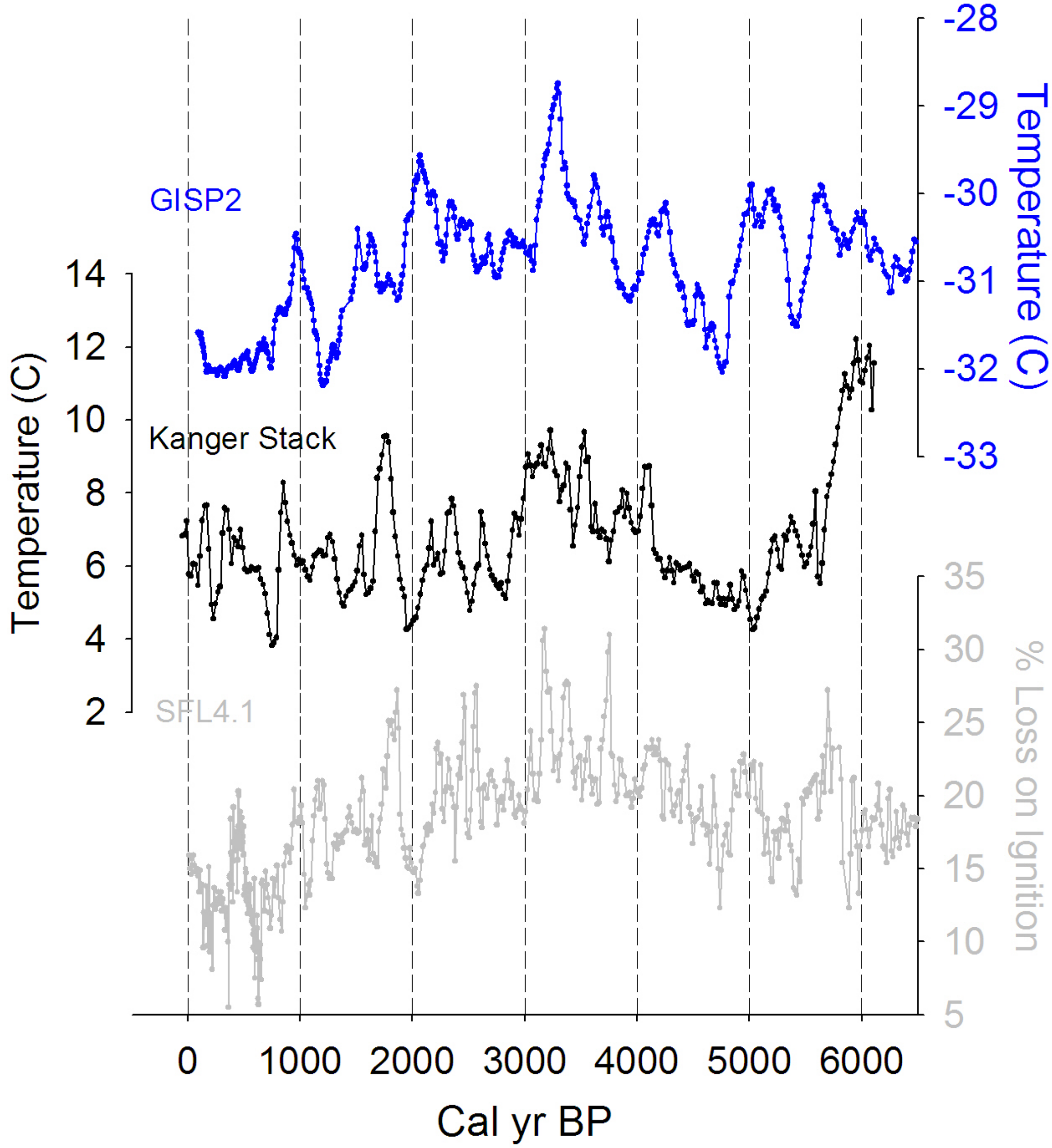

Figure 3. The Kangerlussuaq lake water temperature reconstruction (Kanger Stack; middle curve, black) shown with the GISP2[32,33] temperature reconstruction (top curve, blue) and the loss-on-ignition record from SFL4.1[29] (bottom curve, grey), a lake of Southern West Greenland. The millennial scale trends match, showing warming from ca. 5 kyrs BP to 3.2-3.0 kyrs BP, followed by cooling conditions (Neoglaciation). Some prominent centennial-scale agreement also exists among the records (e.g., warming at ca. 1.8 kyrs BP and between ca. 1100 and 850 yrs BP).

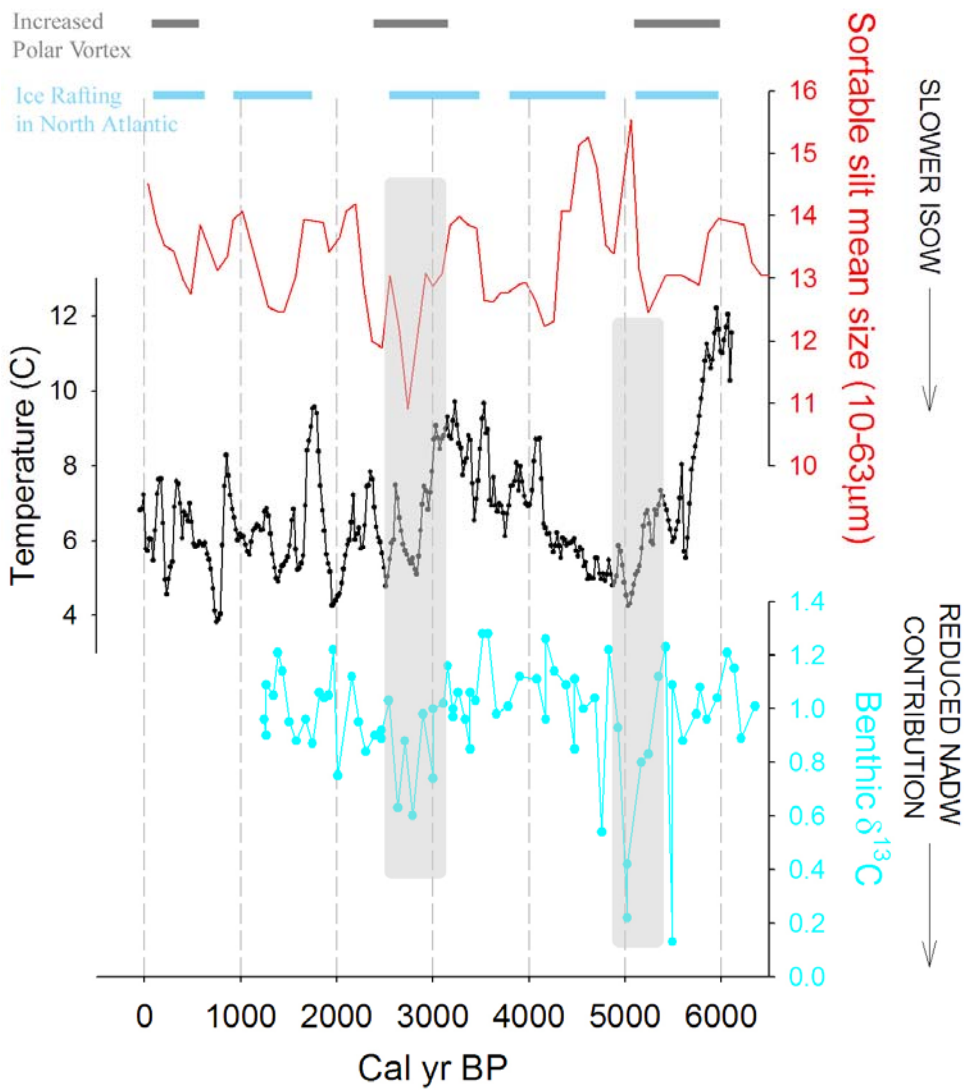

Figure 4. Comparison of the Kangerlussuaq temperature reconstruction (Kanger Stack; middle curve, black) with two indices of Meridional Overturning Circulation, the sortable silt mean size (10-63μm) from marine core NEAP-15K[2] and the $\delta^{13}C$ of benthic foraminifera from ODP Site 980[8]. Grey columns highlight intervals of major cooling in Kangerlussuaq that correspond to periods of inferred slowdown of NADW formation and MOC. Horizontal dark-grey bars indicate periods of increased winter-like conditions and expanded polar vortex over Greenland based on glaciochemical analyses from the GISP2 ice core[5]. Horizontal blue bars indicate intervals with increased advection of cold polar waters from north of Iceland into the North Atlantic based on four ice rafting records from the North Atlantic[38].

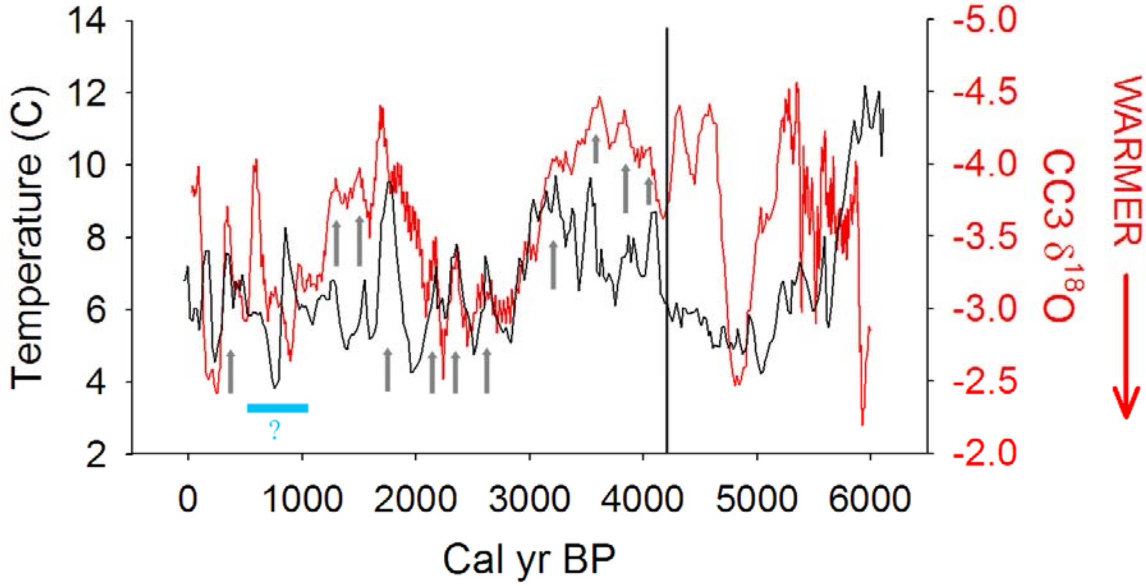

Figure 5. Time-series of alkenone-based Kangerlussuaq lake water reconstruction (Kanger Stack; black curve) and $\delta^{18}O$ record from a speleothem in Southwestern Ireland[10] (CC3; red curve), which reflects temperature (see text). Note the opposite temperature sense on the y-axes. Grey arrows indicate centennial-scale warm intervals in Kangerlussuaq that correspond to centennial-scale cold intervals in Southwestern Ireland, suggesting NAO-type climate variability beginning ca. 4.2 kyrs BP (vertical black line). Ca. 1000 to 550 yrs BP (blue bar and question mark), the interval during which the Norse occupied and later abandoned Southern West Greenland is characterized by a deviation from the centennial-scale NAO-type pattern, with the records indicating warming followed by cooling in both Kangerlussuaq and SW Ireland. Spectral analyses of these time-series reveal spectral power above the 99% confidence interval for periods 262 and 222 yrs (see Supplemental Information 4).

Supplemental Information 1

Materials and Methods

Sediment cores were sampled at 0.5 cm intervals. Samples were freeze-dried and homogenized by mortar and pestle. They were extracted with dichloromethane (DCM) using an Accelerated Solvent Extractor ASE200 (Dionex). Extracts were separated into acid and neutral fractions using Supelco Supelclean™ LC-NH_2 solid phase extraction (SPE) tubes[46].The neutral fraction was further separated into aliphatic (hexane elution), ketone (DCM), and alcohol (ethyl acetate:hexane 1:3) fractions using a flash silica gel column. Alkenones in the DCM fraction were quantified by gas-chromatography-flame-ionization-detection (GC-FID). U^{K}_{37} values were measured with a precision of ±0.01, corresponding to an analytical precision of ±0.4 °C. Alkenones from representative samples were identified by comparison of mass spectral data with previously reported standards and GC retention times[47,48].

Supplementary Information 2

Lacustrine Alkenone-Temperature Calibration

The timing of the Greenland haptophyte bloom was determined using time-series sediment traps. Traps were deployed in Braya Sø in April 2006, through the lake ice cover, and were collected in August 2006. The traps collected discrete samples of seston settling through the lake column, with each sample representing ten days during the sampling period. Results from the time-series sediment trap clearly reveal that alkenone productivity occurred between mid-June and mid-July, with peak alkenone flux to the lake bottom in late-June (Supp. 2; Fig. 1).

A robust temperature calibration for marine alkenones has been determined independently with laboratory culture experiments of *Emiliania huxlei* [20] and core-top studies [21]. While temperature dependence on the unsaturation ratios of lacustrine alkenones is evident from multiple geographic regions[22,23,49], a temperature calibration for lacustrine alkenones yet to be rigorously determined. Furthermore, alkenones from geographically disparate lakes may require independent calibrations. Zink *et al.*[7] provided the first calibration for lacustrine alkenones using alkenones in surface sediments and mean annual lake surface temperature from a series of lakes across Germany and Austria. Here, we report an *in situ* temperature calibration from the Southern West Greenland lake, Braya Sø. We measured U^{K}_{37} from material filtered from lake water taken at 0.5 m intervals throughout the water column. Regression of U^{K}_{37} values against water temperatures across the depth of maximum alkenone concentration (5-13 m) reveals a strong linear relationship (R^2 = 0.87; n=17; Supp. 2; Fig. 2A). The *in situ* detection of alkenone temperature dependence within the thermocline of a single lake and across a temperature range of only 3 ˚C provides strong evidence for temperature control over the unsaturation of lacustrine alkenones.

The *in situ* calibration from Braya Sø can only provide calibration between ~3.5 and 6.5 ˚C. To extend the calibration set to warmer temperatures we combined the *in situ* data from Braya Sø with published data from Zink *et al.*[7] (Supp. 2; Fig. 2B). D'Andrea and Huang[24] noted that the alkenone distributions (tetra-unsaturation dominance and presence of C38 methyl ketones) suggest the presence of a similar alkenone producer in the West Greenland and German/Austrian lakes. The calibrations provided by Sun *et al.*[23,49] for lacustrine alkenones lacking the C38 methyl ketones, which must derive from a different precursor haptophyte, are not used here.

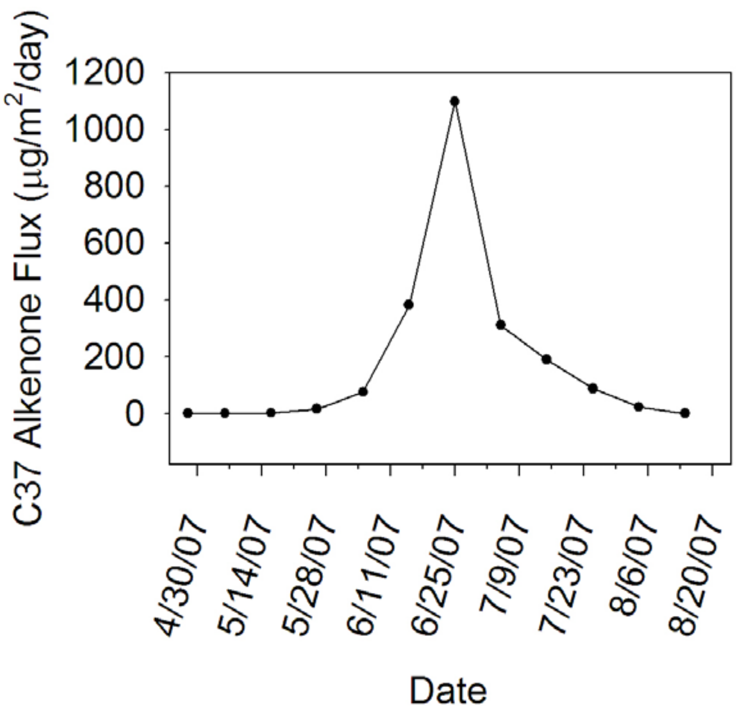

Supplemental 2; Figure 1. Flux of C37 alkenones to a time series sediment trap indicates that alkenone production occurs between mid June and mid July, with peak productivity in late June. The timing of the alkenone peak likely corresponds to the timing of the haptopohyte bloom in the shallow lake (23 m), and indicates that the alkenones in the Greenland lakes reflect water temperatures between mid June and mid July.

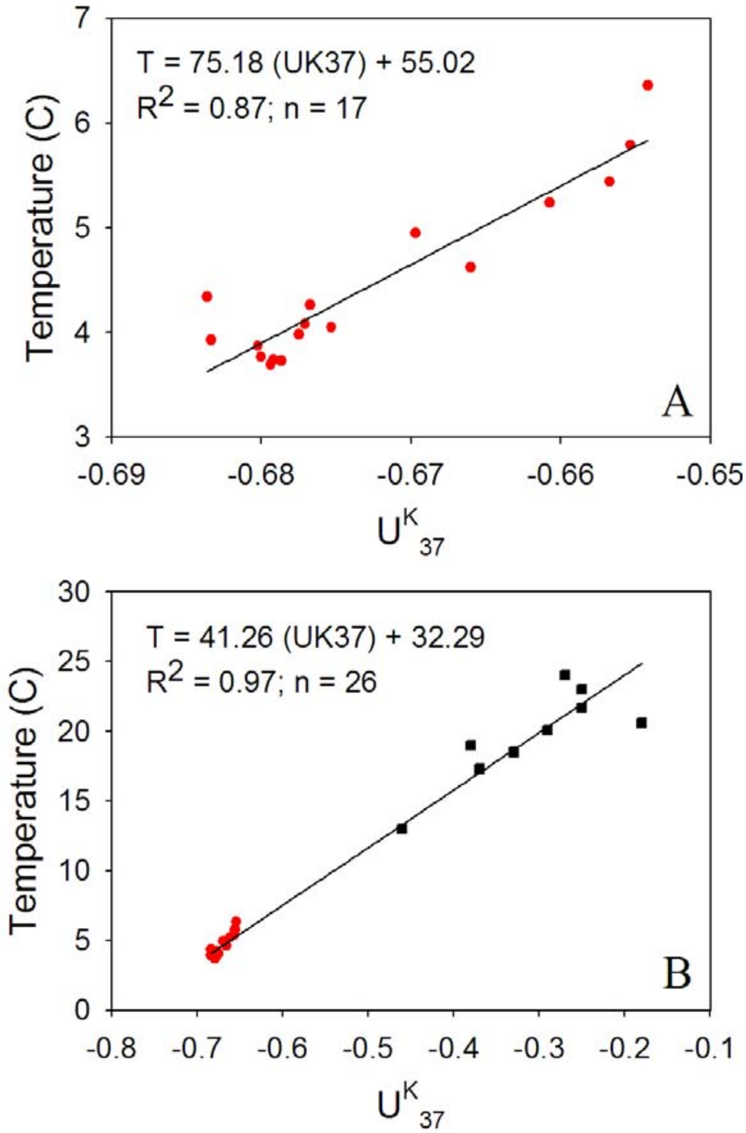

Supplemental 2; Figure 2. A) The i*n situ* alkenone-temperature calibration determined by sampling across the thermocline of Braya Sø. The excellent correlation between the alkenone unsaturation index (UK37) and lake water temperature across this small temperature range highlights the sensitivity of lacustrine alkenones to water temperature. **B)** The calibration used for the Greenland lake alkenone records was developed by combining the *in situ* calibration data (red circles) with the calibration data from Zink et al., 2001 (black squares).

Supplementary Information 3

Radiocarbon dating and chronology

Ten ^{14}C dates were used to establish chronological control for core BS01-01 from Braya Sø (Supp. 3; Fig. 1A). Radiocarbon dates were calibrated to years before present (BP; years before 1950 AD) using the Fairbanks0107 calibration curve[50]. Core BS01-01 was taken with a single drive piston corer, maintaining the sediment water interface and allowing the core top to be assigned a modern age of 2005 AD, the year prior to core recovery. Five of the radiocarbon dates were from core BS01-01 (AMS ^{14}C analysis performed at Woods Hole Oceanographic Institution) and five were from an overlapping core (AMS ^{14}C analysis performed at the University of Aarhus, DK) that was stratigraphically aligned to BS01-01 using loss-on-ignition and total organic carbon measurements (Supp. 3; Fig. 2). Three paired macrofossil and bulk sediment dates yielded a reservoir correction of 360 years, which was applied to the ^{14}C dates prior to calibration. The "reservoir effect" in these meromictic lakes is likely caused by 1) deposition of old carbon from the water column due to lack of complete lake overturn resulting in incomplete exchange of CO_2 with the atmosphere[51], and 2) deposition of ^{14}C-depleted organic matter from the lake catchments, due to the low rates of decomposition typical of Arctic environments[36]. Age reversals in the meromictic lakes of this region after ~1000 yrs BP have been previously noted[36,37] and two ^{14}C dates from this time period were excluded from the age model. Another erroneously old ^{14}C date at 2982 ± 61 yrs BP was excluded from the age model. A 4th order polynomial was fit to the ten remaining calibrated dates and the core top date to establish an age model.

Chronological control for the Lake E core (E-01; Supp. 3; Fig. 1B) was established using six AMS ^{14}C dates of bulk sediment (analysis was performed at the Arizona Accelerator Mass Spectrometry Lab). A seventh date that was erroneously old was excluded from the age model. Core E-01 was taken with a Russian Corer, which does not preserve the sediment water interface. To identify the depth of the core top, the % organic carbon record from core E-01 was compared to the % organic carbon record from an overlapping freeze-core (Supp. 3; Fig. 3). This allowed identification of the E-01 core top to a depth of 9 cm in the freeze-core. The top of the freeze-core represents the sediment water interface and was assigned an age of 2000 AD, the year the freeze-core was recovered. This approach allowed us to assign an age of 2000 AD to a theoretical -9 cm in the E-01 core, providing chronologic control for the top of the core. No macrofossils were isolated from the E-01 core, prohibiting the establishment of a carbon reservoir age for Lake E. Therefore, the reservoir age of 360 years determined in Braya Sø was applied to Lake E. A 4th order polynomial was fit to the six radiocarbon dates and the core top to establish the age model.

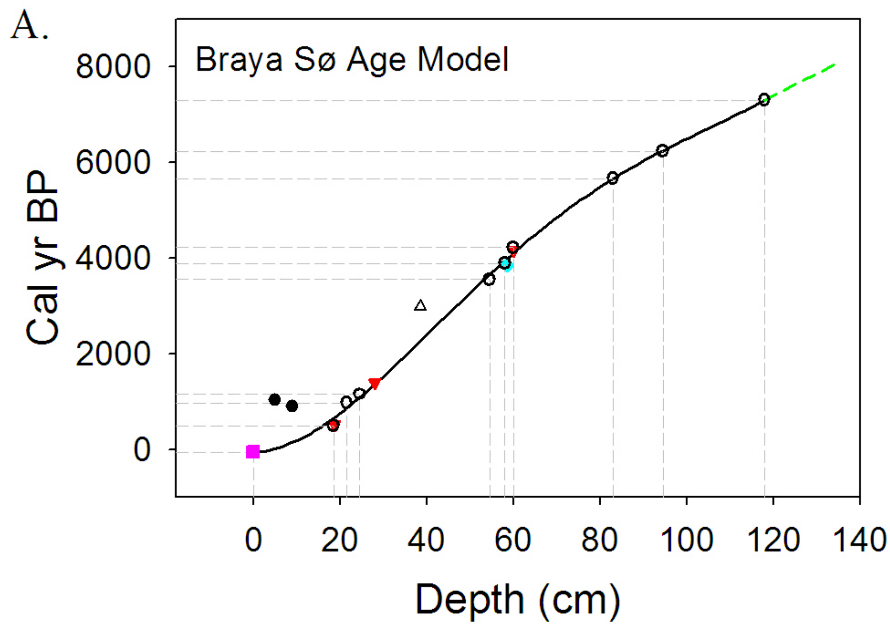

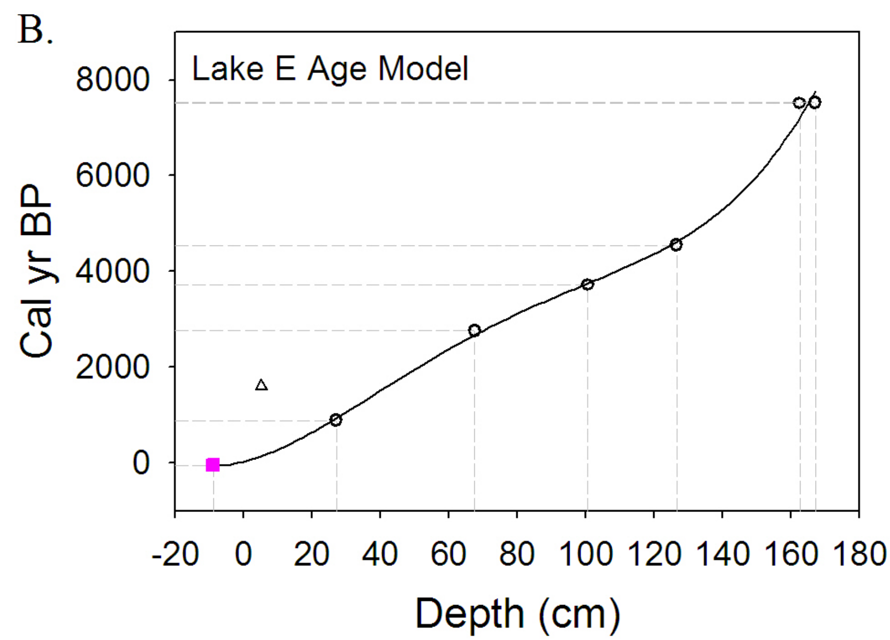

Supplemental 3; Figure 1. Age models for **A)** core BS01-01 from Braya Sø, and **B)** core E-01 from Lake E. Open circles are calibrated ^{14}C dates used in the age model. Pink squares are core tops, assigned a modern age and used in the age model. Open up-triangles are erroneously old ages that were excluded from the age model. Closed circles (in Braya Sø plot only) are erroneously old ages from a sedimentary interval previously shown to have age reversals, and were excluded from the age model. Red down-triangles and the blue diamond (Braya Sø only) are calibrated dates from terrestrial wood fragments and a gastropod shell, respectively.

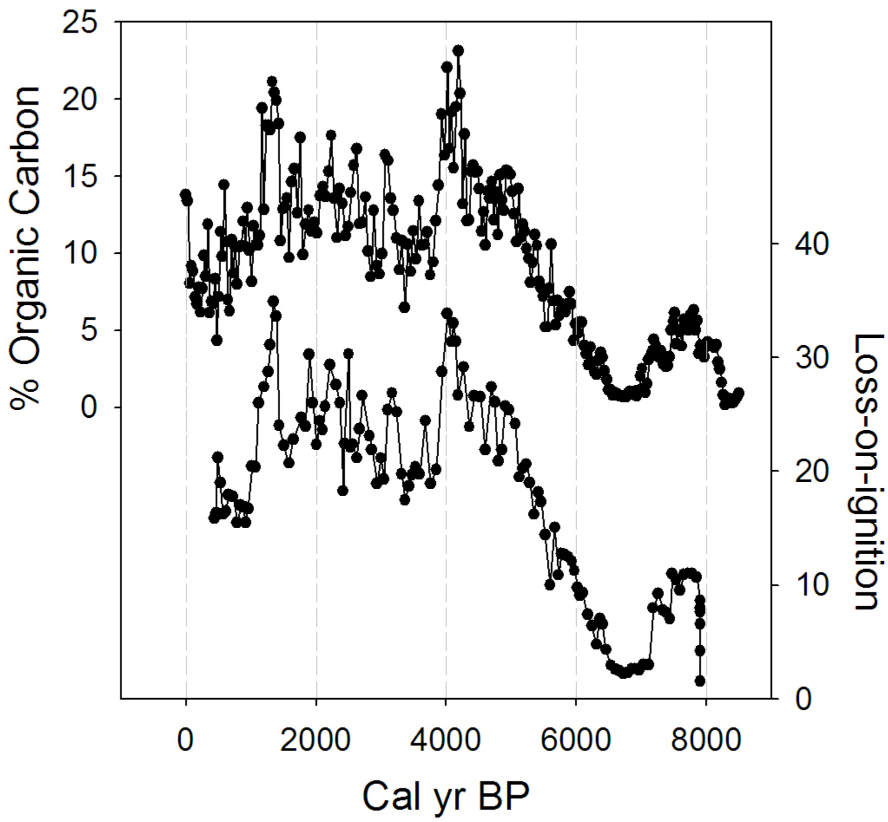

Supplemental 3; Figure 2. % Organic carbon from core BS01-01 (top curve) and loss-on-ignition for an overlapping core (bottom curve). These curves were used to stratigraphically align the overlapping cores, allowing five radiocarbon dates from the overlapping core to be transferred to core BS01-01.

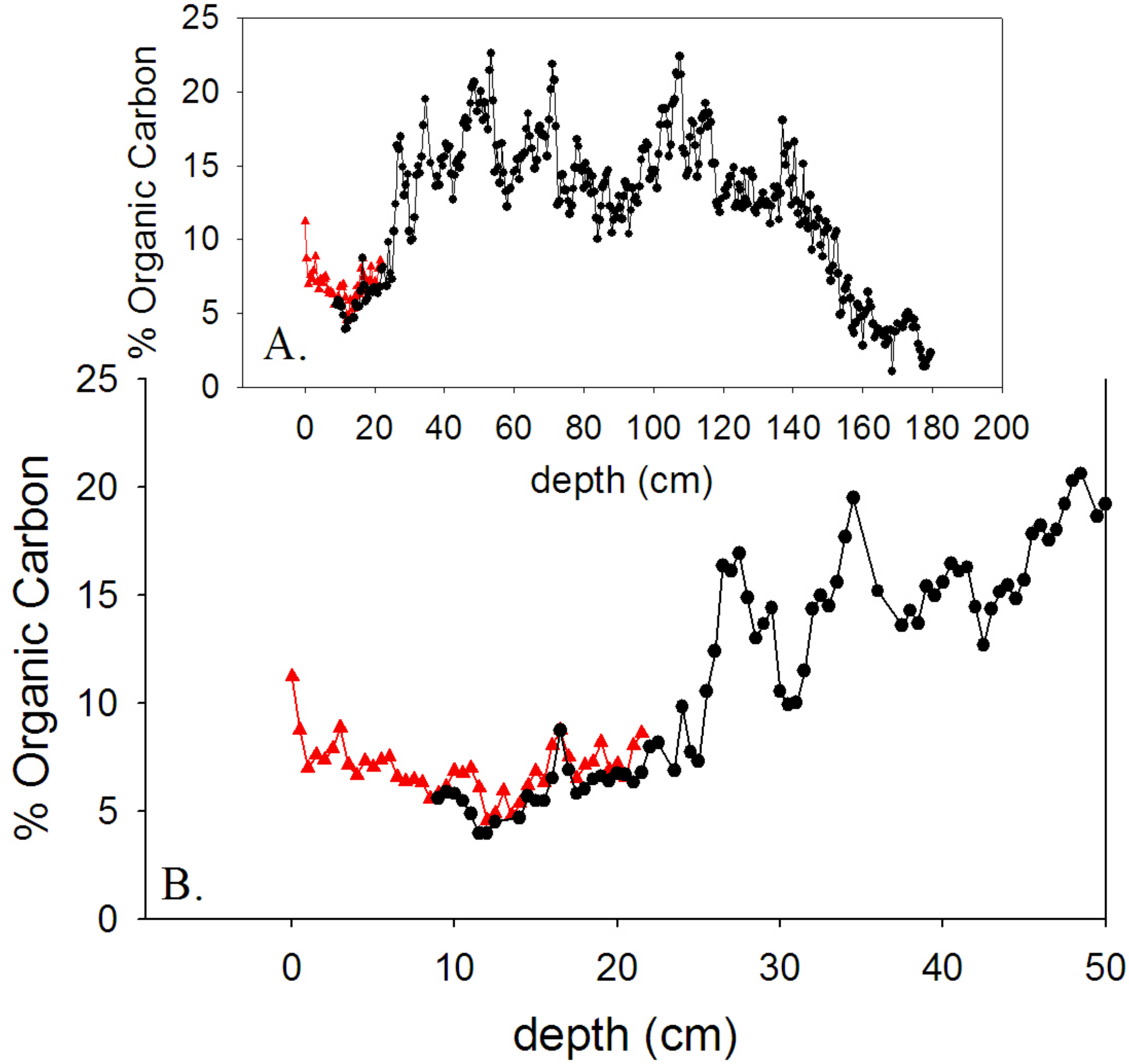

Supplemental 3; Figure 3. Black circles are % Organic carbon measurements from core E-01 (Russian core from Lake E). Red triangles are % Organic carbon from an overlapping freeze-core. **A)** The entire % Organic carbon record from E-01 aligned with the % Organic carbon records from the freeze core. **B)** The top 50 cm, highlighting the excellent match between the overlapping records used to assign a core top age to core E-01.

Supplemental 4

Spectral analysis

Spectral analysis was performed (using Redfit 3.8 [52]) on the Kangerlussuaq temperature reconstruction (Kanger Stack) and the CC3 $\delta^{18}O$ record[10] for the period 4.2 to 0 kyrs BP (Supp. 4; Fig. 1), the period for which there is apparent coupling of centennial-scale variability between the two records. Peaks in spectral power above the 99% confidence limit (Chi-square test[52]) were found for both time-series, centered at a frequency of 0.0038 cycles/yr (period 262 years) for the Kanger Stack and 0.0045 cycles/yr (period 222 years) for the CC3 $\delta^{18}O$ record. The slight mismatch of the precise centennial-scale periodicity in the two records could be due to errors in age models or could due to the influence of second-order controls (beyond NAO variability) on the $\delta^{18}O$ of CC3 or the temperature of Kangerlussuaq lakes.

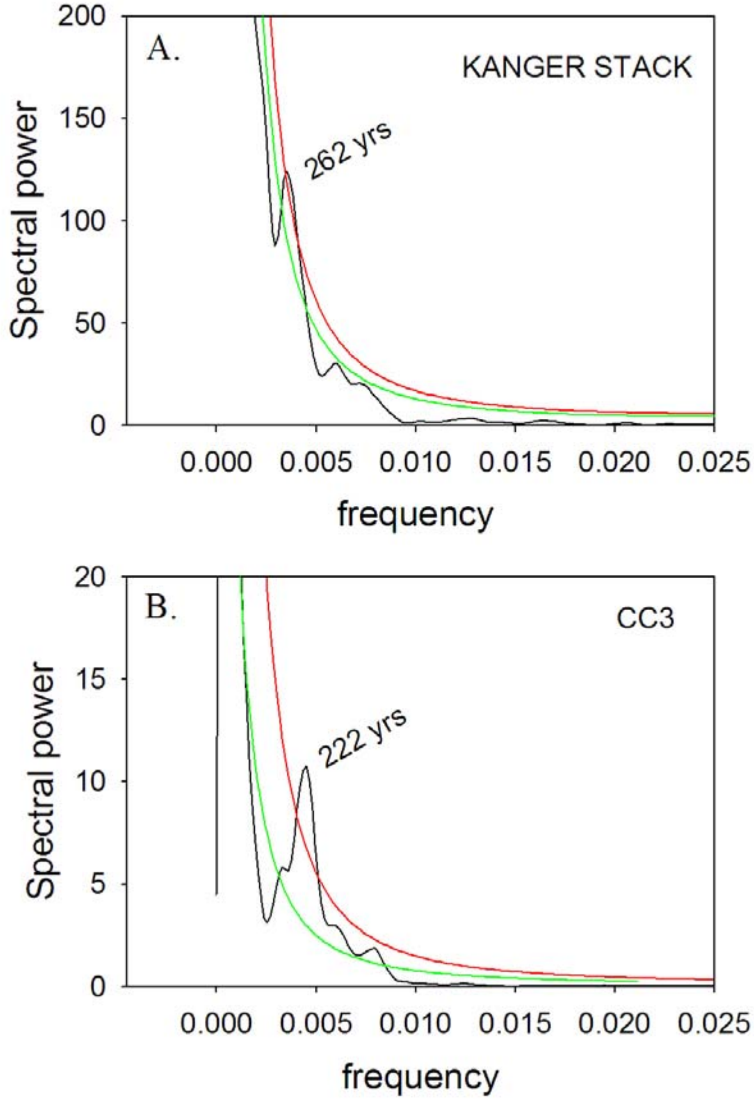

Supplemental 4. Figure 1. Spectral analysis of **A)** the Kangerlussuaq temperature record and **B)** the CC3 $\delta^{18}O$ record[10] for the time period 4.2 kyrs BP to present. Centennial-scale variability is evident in both records with spectral power above the 99% confidence interval (red line) centered at a frequency of 262 years for the Kangerlussuaq record and 222 years for the CC3 $\delta^{18}O$ record. 95% confidence interval (green line) is also shown.

APPENDICES

WILLIAM J. D'ANDREA

BROWN UNIVERSITY

APPENDIX A

RADIOCARBON DATA TABLE FOR LAKE E AND BRAYA SØ

LAKE E

Sample	Depth in core (cm)	Material	14C date	1 σ	Cal yr BP	1 σ
E1-05*	5	bulk sediment	2063	37	1602	51
E1-27	27	bulk sediment	1318	35	884	48
E1-67.5	67.5	bulk sediment	3015	40	2759	22
E2-55	100.5	bulk sediment	3820	52	3719	73
E3-57	126.5	bulk sediment	4423	57	4545	99
E3-92.5	162.5	bulk sediment	6986	75	7511	60
E3-97.5	167	bulk sediment	7004	50	7526	43

BRAYA SØ

Sample	Depth in core (cm)	Material	14C date	1 σ	Cal yr BP	1 σ
BS01-18.5	18.5	bulk sediment	780	25	493	18
BS01-21.5	21.5	bulk sediment	1430	30	967	27
AAR-4750	24.5	bulk sediment	1585	45	1154	65
BS01-38.5*	38.5	bulk sediment	3230	40	2982	61
AAR-4751	54.5	bulk sediment	3685	50	3552	64
BS01-58	58	bulk sediment	3950	30	3889	38
AAR-4752	60	bulk sediment	4185	55	4220	91
BS01-83	83	bulk sediment	5300	40	5657	41
AAR-4753	94.5	bulk sediment	5785	60	6232	61
AAR-4754	118	bulk sediment	6735	55	7301	58
BS01-macro1	18.75	wood fragment	465	140	510	
BS01-macro2	28	wood fragment	1500	140	1397	133
AAR-4755	60	wood fragment	3780	55	4150	85
BS01-shell1	58.5	gastropod shell	3920	35	3854	45

*Sample not used in age model

APPENDIX B

ALKENONE UNSATURATION DATA: ALIGNED CHRONOLOGIES FOR LAKE E AND BRAYA SØ AND KANGER STACK

Aligned chronology (cal yr BP)	Braya Sø UK37	Braya Sø Temperature (Celsius)	Lake E UK37	Lake E UK'37	Lake E Temperature (Celsius)	Kanger Stack Temp (Celsius)
-50	-0.617	6.8				6.8
-30	-0.616	6.8				6.8
-10	-0.607	7.2				7.2
10	-0.642	5.8				5.8
30	-0.644	5.7				5.7
50	-0.636	6.1				6.1
70	-0.636	6.0				6.0
90	-0.666	4.8	-0.634	0.062	6.1	5.5
110	-0.641	5.8	-0.620	0.067	6.7	6.3
130	-0.618	6.8	-0.595	0.069	7.7	7.2
150	-0.612	7.0	-0.583	0.070	8.2	7.6
170	-0.623	6.6	-0.570	0.071	8.8	7.7
190	-0.606	7.3	-0.646	0.065	5.7	6.5
210	-0.647	5.6	-0.678	0.063	4.3	4.9
230	-0.648	5.6	-0.696	0.055	3.6	4.6
250	-0.645	5.7	-0.679	0.059	4.3	5.0
270	-0.644	5.7	-0.665	0.058	4.9	5.3
290	-0.641	5.9	-0.661	0.059	5.0	5.4
310	-0.616	6.9	-0.615	0.076	6.9	6.9
330	-0.625	6.5	-0.572	0.081	8.7	7.6
350	-0.629	6.3	-0.572	0.079	8.7	7.5
370	-0.632	6.2	-0.594	0.076	7.8	7.0
390	-0.637	6.0	-0.635	0.069	6.1	6.1
410	-0.611	7.1	-0.626	0.067	6.4	6.8
430	-0.608	7.2	-0.633	0.067	6.2	6.7
450	-0.621	6.6	-0.627	0.064	6.4	6.5
470	-0.593	7.8	-0.633	0.068	6.1	7.0
490	-0.598	7.6	-0.652	0.069	5.4	6.5
510	-0.626	6.5	-0.653	0.068	5.3	5.9
530	-0.633	6.2	-0.649	0.065	5.5	5.8
550	-0.636	6.1	-0.645	0.064	5.7	5.9
570	-0.633	6.2	-0.643	0.064	5.8	6.0
590	-0.624	6.5	-0.654	0.062	5.3	5.9
610	-0.620	6.7	-0.660	0.062	5.0	5.9
630	-0.626	6.5	-0.651	0.066	5.4	5.9
650	-0.630	6.3	-0.663	0.063	5.0	5.6
670	-0.632	6.2	-0.668	0.063	4.8	5.5
690	-0.640	5.9	-0.672	0.064	4.6	5.2

Aligned chronology (cal yr BP)	Braya Sø UK37	Braya Sø Temperature (Celsius)	Lake E UK37	Lake E UK'37	Lake E Temperature (Celsius)	Kanger Stack Temp (Celsius)
710	-0.651	5.4	-0.686	0.062	4.0	4.7
730	-0.673	4.5	-0.693	0.059	3.7	4.1
750	-0.682	4.2	-0.698	0.058	3.5	3.8
770	-0.680	4.2	-0.696	0.061	3.6	3.9
790	-0.692	3.7	-0.677	0.067	4.4	4.0
810	-0.623	6.6	-0.657	0.066	5.2	5.9
830	-0.605	7.3	-0.599	0.078	7.6	7.5
850	-0.594	7.8	-0.569	0.080	8.8	8.3
870	-0.608	7.2	-0.583	0.078	8.2	7.7
890	-0.619	6.7	-0.596	0.077	7.7	7.2
910	-0.625	6.5	-0.608	0.077	7.2	6.8
930	-0.633	6.2	-0.612	0.082	7.1	6.6
950	-0.645	5.7	-0.615	0.086	6.9	6.3
970	-0.653	5.4	-0.620	0.078	6.7	6.0
990	-0.652	5.4	-0.614	0.079	6.9	6.2
1010	-0.653	5.3	-0.618	0.077	6.8	6.1
1030	-0.661	5.0	-0.608	0.079	7.2	6.1
1050	-0.667	4.8	-0.613	0.079	7.0	5.9
1070	-0.671	4.6	-0.617	0.078	6.8	5.7
1090	-0.671	4.6	-0.622	0.078	6.6	5.6
1110	-0.658	5.1	-0.617	0.077	6.8	6.0
1130	-0.649	5.5	-0.612	0.075	7.0	6.3
1150	-0.654	5.3	-0.604	0.077	7.4	6.3
1170	-0.659	5.1	-0.596	0.079	7.7	6.4
1190	-0.654	5.3	-0.601	0.077	7.5	6.4
1210	-0.650	5.5	-0.610	0.074	7.1	6.3
1230	-0.648	5.6	-0.612	0.070	7.0	6.3
1250	-0.646	5.6	-0.591	0.092	7.9	6.8
1270	-0.641	5.8	-0.591	0.093	7.9	6.9
1290	-0.636	6.0	-0.606	0.078	7.3	6.7
1310	-0.646	5.6	-0.618	0.073	6.8	6.2
1330	-0.662	5.0	-0.630	0.074	6.3	5.6
1350	-0.671	4.6	-0.639	0.077	5.9	5.3
1370	-0.676	4.4	-0.647	0.080	5.6	5.0
1390	-0.676	4.4	-0.651	0.080	5.4	4.9
1410	-0.670	4.6	-0.644	0.079	5.7	5.2
1430	-0.670	4.6	-0.638	0.079	6.0	5.3
1450	-0.669	4.7	-0.637	0.077	6.0	5.3

Aligned chronology (cal yr BP)	Braya Sø UK37	Braya Sø Temperature (Cesius)	Lake E UK37	Lake E UK'37	Lake E Temperature (Celsius)	Kanger Stack Temp (Celsius)
1470	-0.660	5.0	-0.641	0.075	5.8	5.4
1490	-0.651	5.4	-0.645	0.072	5.7	5.6
1510	-0.641	5.8	-0.639	0.075	5.9	5.9
1530	-0.618	6.8	-0.631	0.081	6.3	6.5
1570	-0.646	5.6	-0.639	0.086	5.9	5.8
1590	-0.658	5.1	-0.655	0.084	5.3	5.2
1610	-0.658	5.1	-0.652	0.081	5.4	5.3
1630	-0.658	5.1	-0.646	0.082	5.6	5.4
1650	-0.658	5.1	-0.636	0.087	6.0	5.6
1670	-0.640	5.9	-0.589	0.093	8.0	6.9
1690	-0.621	6.7	-0.537	0.099	10.1	8.4
1710	-0.607	7.2	-0.538	0.097	10.1	8.7
1730	-0.588	8.0	-0.539	0.095	10.1	9.0
1750	-0.563	9.1	-0.540	0.093	10.0	9.5
1770	-0.561	9.2	-0.541	0.092	10.0	9.6
1790	-0.567	8.9	-0.543	0.090	9.9	9.4
1810	-0.590	8.0	-0.569	0.083	8.8	8.4
1830	-0.613	7.0	-0.591	0.077	7.9	7.5
1850	-0.636	6.1	-0.600	0.074	7.6	6.8
1870	-0.646	5.6	-0.615	0.070	6.9	6.3
1890	-0.656	5.2	-0.637	0.066	6.0	5.6
1910	-0.666	4.8	-0.639	0.067	5.9	5.4
1930	-0.673	4.5	-0.642	0.069	5.8	5.2
1950	-0.680	4.2	-0.678	0.072	4.3	4.3
1970	-0.687	3.9	-0.669	0.072	4.7	4.3
1990	-0.682	4.1	-0.670	0.073	4.7	4.4
2010	-0.673	4.5	-0.674	0.075	4.5	4.5
2030	-0.663	4.9	-0.679	0.073	4.3	4.6
2050	-0.656	5.2	-0.673	0.075	4.5	4.9
2070	-0.657	5.2	-0.654	0.082	5.3	5.2
2090	-0.646	5.6	-0.647	0.090	5.6	5.6
2110	-0.635	6.1	-0.645	0.095	5.7	5.9
2130	-0.625	6.5	-0.648	0.082	5.5	6.0
2150	-0.615	6.9	-0.635	0.087	6.1	6.5
2170	-0.605	7.3	-0.610	0.105	7.1	7.2
2190	-0.612	7.1	-0.662	0.076	5.0	6.0
2210	-0.619	6.8	-0.647	0.082	5.6	6.2
2230	-0.626	6.5	-0.632	0.088	6.2	6.3

Aligned chronology (cal yr BP)	Braya Sø UK37	Braya Sø Temperature (Cesius)	Lake E UK37	Lake E UK'37	Lake E Temperature (Celsius)	Kanger Stack Temp (Celsius)
2250	-0.633	6.2	-0.652	0.069	5.4	5.8
2270	-0.636	6.0	-0.647	0.074	5.6	5.8
2290	-0.613	7.0	-0.642	0.080	5.8	6.4
2310	-0.590	7.9	-0.614	0.105	7.0	7.4
2330	-0.583	8.2	-0.620	0.088	6.7	7.5
2350	-0.581	8.3	-0.604	0.098	7.4	7.8
2370	-0.586	8.1	-0.608	0.085	7.2	7.6
2390	-0.603	7.4	-0.627	0.069	6.4	6.9
2410	-0.621	6.6	-0.635	0.071	6.1	6.4
2430	-0.632	6.2	-0.639	0.069	5.9	6.1
2450	-0.638	6.0	-0.638	0.066	6.0	6.0
2470	-0.645	5.7	-0.646	0.067	5.6	5.7
2490	-0.651	5.4	-0.659	0.069	5.1	5.3
2510	-0.657	5.2	-0.676	0.067	4.4	4.8
2530	-0.649	5.5	-0.672	0.073	4.6	5.0
2550	-0.636	6.0	-0.663	0.073	5.0	5.5
2570	-0.623	6.6	-0.654	0.064	5.3	5.9
2590	-0.610	7.1	-0.663	0.074	4.9	6.0
2610	-0.596	7.7	-0.606	0.090	7.3	7.5
2630	-0.602	7.5	-0.618	0.091	6.8	7.1
2650	-0.611	7.1	-0.634	0.086	6.1	6.6
2670	-0.620	6.7	-0.642	0.080	5.8	6.3
2690	-0.629	6.3	-0.650	0.077	5.5	5.9
2710	-0.630	6.3	-0.658	0.078	5.2	5.7
2730	-0.631	6.3	-0.662	0.078	5.0	5.6
2750	-0.631	6.2	-0.668	0.077	4.7	5.5
2770	-0.632	6.2	-0.672	0.077	4.5	5.4
2790	-0.630	6.3	-0.667	0.086	4.8	5.5
2810	-0.629	6.3	-0.682	0.072	4.1	5.2
2830	-0.628	6.4	-0.690	0.075	3.8	5.1
2850	-0.625	6.5	-0.669	0.075	4.7	5.6
2870	-0.620	6.7	-0.641	0.080	5.9	6.3
2890	-0.615	6.9	-0.613	0.087	7.0	7.0
2910	-0.610	7.2	-0.595	0.106	7.7	7.4
2930	-0.615	6.9	-0.595	0.114	7.7	7.3
2950	-0.631	6.2	-0.603	0.106	7.4	6.8
2970	-0.613	7.0	-0.599	0.108	7.6	7.3
2990	-0.589	8.0	-0.596	0.110	7.7	7.8

Aligned chronology (cal yr BP)	Braya Sø UK37	Braya Sø Temperature (Cesius)	Lake E UK37	Lake E UK'37	Lake E Temperature (Celsius)	Kanger Stack Temp (Celsius)
3010	-0.577	8.5	-0.567	0.119	8.9	8.7
3030	-0.570	8.7	-0.555	0.107	9.4	9.1
3050	-0.571	8.7	-0.570	0.093	8.8	8.8
3070	-0.572	8.7	-0.584	0.090	8.2	8.4
3090	-0.568	8.8	-0.575	0.089	8.6	8.7
3110	-0.563	9.0	-0.576	0.090	8.6	8.8
3130	-0.558	9.2	-0.571	0.091	8.7	9.0
3150	-0.552	9.5	-0.563	0.091	9.1	9.3
3170	-0.545	9.8	-0.593	0.090	7.8	8.8
3190	-0.540	10.0	-0.603	0.086	7.4	8.7
3210	-0.536	10.2	-0.583	0.095	8.2	9.2
3230	-0.533	10.3	-0.562	0.099	9.1	9.7
3250	-0.541	10.0	-0.584	0.083	8.2	9.1
3270	-0.553	9.5	-0.596	0.085	7.7	8.6
3290	-0.560	9.2	-0.594	0.095	7.8	8.5
3310	-0.562	9.1	-0.628	0.084	6.4	7.8
3330	-0.563	9.1	-0.610	0.094	7.1	8.1
3350	-0.550	9.6	-0.618	0.089	6.8	8.2
3370	-0.536	10.2	-0.601	0.100	7.5	8.8
3390	-0.541	10.0	-0.603	0.106	7.4	8.7
3410	-0.568	8.9	-0.632	0.082	6.2	7.5
3430	-0.594	7.8	-0.654	0.079	5.3	6.5
3450	-0.586	8.1	-0.634	0.105	6.1	7.1
3470	-0.578	8.4	-0.619	0.120	6.8	7.6
3490	-0.572	8.7	-0.584	0.116	8.2	8.4
3510	-0.565	9.0	-0.551	0.156	9.5	9.3
3530	-0.561	9.1	-0.535	0.176	10.2	9.7
3550	-0.559	9.2	-0.577	0.125	8.5	8.9
3570	-0.581	8.3	-0.550	0.186	9.6	9.0
3590	-0.608	7.2	-0.614	0.107	7.0	7.1
3610	-0.609	7.2	-0.620	0.090	6.7	6.9
3630	-0.600	7.5	-0.592	0.125	7.9	7.7
3650	-0.605	7.3	-0.623	0.083	6.6	6.9
3670	-0.616	6.9	-0.621	0.083	6.7	6.8
3690	-0.620	6.7	-0.606	0.098	7.3	7.0
3710	-0.622	6.6	-0.607	0.096	7.2	6.9
3730	-0.624	6.6	-0.615	0.088	6.9	6.7
3750	-0.625	6.5	-0.643	0.083	5.8	6.1

Aligned chronology (cal yr BP)	Braya Sø UK37	Braya Sø Temperature (Cesius)	Lake E UK37	Lake E UK'37	Lake E Temperature (Celsius)	Kanger Stack Temp (Celsius)
3770	-0.621	6.7	-0.619	0.099	6.7	6.7
3790	-0.612	7.0	-0.617	0.089	6.9	6.9
3810	-0.603	7.4	-0.600	0.114	7.5	7.5
3830	-0.594	7.8	-0.608	0.114	7.2	7.5
3850	-0.591	7.9	-0.606	0.099	7.3	7.6
3870	-0.592	7.9	-0.582	0.138	8.3	8.1
3890	-0.593	7.8	-0.616	0.126	6.9	7.3
3910	-0.594	7.8	-0.584	0.126	8.2	8.0
3930	-0.596	7.7	-0.602	0.081	7.4	7.6
3950	-0.597	7.7	-0.620	0.079	6.7	7.2
3970	-0.598	7.6	-0.628	0.083	6.4	7.0
3990	-0.599	7.5	-0.630	0.081	6.3	6.9
4010	-0.597	7.6	-0.631	0.078	6.3	7.0
4030	-0.591	7.9	-0.618	0.085	6.8	7.3
4050	-0.585	8.1	-0.587	0.084	8.1	8.1
4070	-0.579	8.4	-0.564	0.075	9.0	8.7
4090	-0.573	8.6	-0.570	0.074	8.8	8.7
4110	-0.567	8.9	-0.575	0.083	8.6	8.7
4130	-0.594	7.8	-0.600	0.083	7.5	7.7
4150	-0.641	5.8	-0.611	0.084	7.1	6.5
4170	-0.648	5.5	-0.609	0.072	7.2	6.3
4190	-0.649	5.5	-0.615	0.078	6.9	6.2
4210	-0.650	5.4	-0.613	0.076	7.0	6.2
4230	-0.652	5.4	-0.629	0.072	6.4	5.9
4250	-0.653	5.3	-0.637	0.070	6.0	5.7
4270	-0.654	5.3	-0.626	0.071	6.5	5.9
4290	-0.655	5.2	-0.608	0.082	7.2	6.2
4310	-0.655	5.3	-0.625	0.077	6.5	5.9
4330	-0.652	5.4	-0.644	0.079	5.7	5.5
4350	-0.649	5.5	-0.621	0.075	6.7	6.1
4370	-0.647	5.6	-0.627	0.085	6.4	6.0
4390	-0.654	5.3	-0.626	0.071	6.5	5.9
4410	-0.664	4.9	-0.614	0.073	7.0	5.9
4430	-0.674	4.5	-0.603	0.073	7.4	5.9
4450	-0.681	4.2	-0.594	0.070	7.8	6.0
4470	-0.679	4.3	-0.593	0.067	7.8	6.1
4490	-0.676	4.4	-0.612	0.065	7.0	5.7
4510	-0.674	4.5	-0.621	0.066	6.7	5.6

Aligned chronology (cal yr BP)	Braya Sø UK37	Braya Sø Temperature (Cesius)	Lake E UK37	Lake E UK'37	Lake E Temperature (Celsius)	Kanger Stack Temp (Celsius)
4530	-0.676	4.4	-0.608	0.073	7.2	5.8
4550	-0.680	4.3	-0.607	0.077	7.3	5.8
4570	-0.683	4.1	-0.625	0.076	6.5	5.3
4590	-0.687	3.9	-0.616	0.083	6.9	5.4
4610	-0.691	3.8	-0.634	0.082	6.1	5.0
4630	-0.694	3.6	-0.625	0.080	6.5	5.1
4650	-0.698	3.5	-0.625	0.092	6.5	5.0
4670	-0.696	3.6	-0.628	0.083	6.4	5.0
4690	-0.692	3.7	-0.605	0.114	7.3	5.5
4710	-0.687	3.9	-0.610	0.106	7.1	5.5
4730	-0.684	4.0	-0.633	0.097	6.2	5.1
4750	-0.683	4.1	-0.642	0.089	5.8	5.0
4770	-0.681	4.2	-0.636	0.078	6.0	5.1
4790	-0.680	4.2	-0.646	0.090	5.6	4.9
4810	-0.679	4.3	-0.639	0.078	5.9	5.1
4830	-0.677	4.3	-0.623	0.109	6.6	5.5
4850	-0.676	4.4	-0.643	0.095	5.8	5.1
4870	-0.676	4.4	-0.657	0.077	5.2	4.8
4890	-0.675	4.4	-0.652	0.079	5.4	4.9
4910	-0.675	4.4	-0.646	0.091	5.6	5.0
4930	-0.672	4.6	-0.609	0.090	7.2	5.9
4950	-0.668	4.7	-0.620	0.098	6.7	5.7
4970	-0.664	4.9	-0.643	0.094	5.8	5.3
4990	-0.669	4.7	-0.659	0.081	5.1	4.9
5010	-0.681	4.2	-0.664	0.081	4.9	4.5
5030	-0.693	3.7	-0.666	0.086	4.8	4.3
5050	-0.694	3.6	-0.661	0.088	5.0	4.3
5070	-0.688	3.9	-0.654	0.086	5.3	4.6
5090	-0.682	4.1	-0.650	0.088	5.5	4.8
5110	-0.675	4.4	-0.643	0.085	5.7	5.1
5130	-0.666	4.8	-0.649	0.079	5.5	5.2
5150	-0.657	5.2	-0.651	0.076	5.4	5.3
5170	-0.648	5.6	-0.637	0.081	6.0	5.8
5190	-0.639	5.9	-0.617	0.082	6.9	6.4
5210	-0.629	6.3	-0.610	0.083	7.1	6.7
5230	-0.620	6.7	-0.614	0.084	6.9	6.8
5250	-0.629	6.3	-0.623	0.085	6.6	6.4
5270	-0.637	6.0	-0.638	0.090	6.0	6.0

Aligned chronology (cal yr BP)	Braya Sø UK37	Braya Sø Temperature (Cesius)	Lake E UK37	Lake E UK'37	Lake E Temperature (Celsius)	Kanger Stack Temp (Celsius)
5290	-0.646	5.6	-0.633	0.094	6.2	5.9
5310	-0.635	6.1	-0.600	0.096	7.6	6.8
5330	-0.624	6.6	-0.617	0.094	6.8	6.7
5350	-0.612	7.0	-0.616	0.087	6.9	7.0
5370	-0.617	6.8	-0.592	0.073	7.8	7.3
5390	-0.621	6.7	-0.595	0.082	7.7	7.2
5410	-0.626	6.5	-0.602	0.083	7.5	7.0
5430	-0.623	6.6	-0.611	0.075	7.1	6.8
5450	-0.620	6.7	-0.627	0.075	6.4	6.5
5470	-0.619	6.8	-0.641	0.075	5.8	6.3
5490	-0.625	6.5	-0.651	0.073	5.4	6.0
5510	-0.631	6.2	-0.640	0.076	5.9	6.1
5530	-0.636	6.0	-0.625	0.079	6.5	6.3
5550	-0.637	6.0	-0.612	0.076	7.0	6.5
5570	-0.638	6.0	-0.581	0.083	8.3	7.1
5590	-0.640	5.9	-0.536	0.099	10.2	8.0
5610	-0.644	5.7				5.7
5630	-0.649	5.5				5.5
5650	-0.635	6.1				6.1
5670	-0.613	7.0				7.0
5690	-0.591	7.9				7.9
5710	-0.583	8.2				8.2
5730	-0.576	8.5				8.5
5750	-0.568	8.9				8.9
5770	-0.556	9.3				9.3
5790	-0.545	9.8				9.8
5810	-0.533	10.3				10.3
5830	-0.520	10.8				10.8
5850	-0.510	11.2				11.2
5870	-0.517	10.9				10.9
5890	-0.525	10.6				10.6
5910	-0.520	10.8				10.8
5930	-0.503	11.5				11.5
5950	-0.486	12.2				12.2
5970	-0.500	11.6				11.6
5990	-0.514	11.1				11.1
6010	-0.515	11.0				11.0
6030	-0.507	11.4				11.4

Aligned chronology (cal yr BP)	Braya Sø UK37	Braya Sø Temperature (Cesius)	Lake E UK37	Lake E UK'37	Lake E Temperature (Celsius)	Kanger Stack Temp (Celsius)
6050	-0.499	11.7				11.7
6070	-0.490	12.0				12.0
6090	-0.534	10.3				10.3
6110	-0.502	11.6				11.6

APPENDIX C

ALKENONE UNSATURATION DATA: LAKE E

Depth (cm)	Cal yr BP	UK37	UK'37	Temperature (Celsius)
2.0	68	-0.624	0.065	6.5
2.5	79	-0.644	0.071	5.7
3.0	90	-0.625	0.053	6.5
3.5	101	-0.625	0.066	6.5
5.0	138	-0.581	0.071	8.3
5.5	151	-0.584	0.07	8.2
6.0	164	-0.564	0.069	9.0
6.5	178	-0.586	0.078	8.1
7.0	191	-0.66	0.062	5.1
7.5	206	-0.673	0.067	4.5
8.0	220	-0.691	0.054	3.8
8.5	235	-0.698	0.056	3.5
9.0	250	-0.681	0.059	4.2
9.5	265	-0.664	0.059	4.9
10.0	281	-0.666	0.057	4.8
10.5	296	-0.66	0.06	5.1
11.0	313	-0.619	0.075	6.7
11.5	329	-0.578	0.083	8.4
12.0	345	-0.562	0.078	9.1
12.5	362	-0.578	0.079	8.5
13.0	379	-0.597	0.076	7.6
13.5	397	-0.635	0.069	6.1
14.0	414	-0.624	0.066	6.5
14.5	432	-0.633	0.069	6.2
15.0	450	-0.633	0.063	6.2
15.5	468	-0.622	0.065	6.6
16.0	487	-0.639	0.07	5.9
16.5	505	-0.656	0.069	5.2
17.0	524	-0.653	0.068	5.4
17.5	543	-0.649	0.065	5.5
18.5	581	-0.642	0.064	5.8
19.5	621	-0.663	0.061	4.9
20.0	640	-0.648	0.066	5.5
20.5	660	-0.661	0.064	5.0
21.0	681	-0.668	0.062	4.7

Depth (cm)	Cal yr BP	UK37	UK'37	Temperature (Celsius)
21.5	701	-0.667	0.064	4.8
22.0	721	-0.684	0.064	4.1
22.5	742	-0.691	0.059	3.8
23.5	783	-0.702	0.058	3.3
24.0	804	-0.679	0.069	4.3
24.5	825	-0.672	0.062	4.6
25.0	846	-0.607	0.077	7.3
25.5	868	-0.567	0.08	8.9
27.0	932	-0.608	0.076	7.2
28.0	975	-0.615	0.087	6.9
28.5	997	-0.621	0.078	6.6
29.0	1019	-0.613	0.079	7.0
29.5	1041	-0.62	0.077	6.7
30.0	1063	-0.607	0.079	7.2
31.5	1129	-0.622	0.078	6.6
32.5	1174	-0.611	0.075	7.1
33.5	1219	-0.594	0.079	7.8
34.5	1263	-0.613	0.073	7.0
35.0	1286	-0.612	0.069	7.1
35.5	1308	-0.581	0.103	8.3
36.5	1353	-0.612	0.072	7.0
37.5	1399	-0.636	0.075	6.0
38.0	1421	-0.642	0.08	5.8
38.5	1444	-0.654	0.08	5.3
39.5	1489	-0.635	0.079	6.1
40.5	1534	-0.646	0.071	5.6
41.5	1579	-0.621	0.087	6.7
42.0	1601	-0.655	0.085	5.3
42.5	1624	-0.651	0.079	5.4
43.0	1646	-0.634	0.088	6.1
43.5	1669	-0.537	0.099	10.1
45.5	1758	-0.542	0.09	9.9
46.5	1803	-0.588	0.078	8.0
47.5	1847	-0.604	0.072	7.4
48.5	1891	-0.641	0.065	5.8
49.5	1935	-0.637	0.069	6.0

Depth (cm)	Cal yr BP	UK37	UK'37	Temperature (Celsius)
50.0	1957	-0.682	0.072	4.1
51.0	2000	-0.667	0.072	4.8
51.5	2022	-0.673	0.075	4.5
52.0	2044	-0.682	0.072	4.1
52.5	2065	-0.651	0.083	5.4
53.0	2087	-0.644	0.097	5.7
53.5	2108	-0.65	0.077	5.5
54.0	2130	-0.609	0.106	7.2
54.5	2151	-0.662	0.076	5.0
55.5	2193	-0.632	0.088	6.2
56.0	2214	-0.652	0.069	5.4
57.0	2256	-0.643	0.079	5.8
57.5	2277	-0.613	0.107	7.0
58.0	2298	-0.623	0.085	6.6
58.5	2318	-0.605	0.1	7.3
59.0	2339	-0.6	0.094	7.5
59.5	2359	-0.624	0.069	6.5
60.5	2400	-0.639	0.071	5.9
61.5	2440	-0.638	0.065	6.0
62.5	2480	-0.661	0.07	5.0
63.0	2500	-0.677	0.067	4.4
63.5	2520	-0.672	0.072	4.5
64.0	2539	-0.669	0.079	4.7
64.5	2559	-0.65	0.06	5.5
65.5	2598	-0.666	0.078	4.8
66.0	2617	-0.59	0.093	8.0
66.5	2636	-0.629	0.09	6.3
67.5	2674	-0.645	0.077	5.7
68.0	2693	-0.656	0.078	5.2
68.5	2712	-0.661	0.078	5.0
69.5	2749	-0.673	0.076	4.5
70.0	2768	-0.667	0.086	4.8
70.5	2786	-0.684	0.071	4.0
71.0	2805	-0.691	0.076	3.8
71.5	2823	-0.659	0.075	5.1
72.5	2859	-0.602	0.09	7.5

Depth (cm)	Cal yr BP	UK37	UK'37	Temperature (Celsius)
73.0	2877	-0.59	0.118	7.9
73.5	2895	-0.603	0.106	7.4
74.5	2930	-0.595	0.11	7.7
75.0	2948	-0.549	0.125	9.6
75.5	2965	-0.558	0.098	9.2
76.5	3000	-0.582	0.088	8.3
77.0	3017	-0.59	0.096	8.0
77.5	3034	-0.569	0.086	8.8
78.0	3051	-0.583	0.091	8.3
78.5	3068	-0.543	0.088	9.9
79.0	3085	-0.585	0.092	8.1
79.5	3101	-0.56	0.091	9.2
80.5	3135	-0.605	0.09	7.3
81.0	3151	-0.603	0.086	7.4
81.5	3168	-0.589	0.094	8.0
82.5	3200	-0.558	0.1	9.3
83.0	3216	-0.583	0.082	8.2
83.5	3232	-0.588	0.088	8.0
84.0	3249	-0.603	0.083	7.4
84.5	3264	-0.593	0.096	7.8
85.0	3280	-0.626	0.089	6.5
85.5	3296	-0.631	0.075	6.3
86.0	3312	-0.604	0.099	7.4
86.5	3328	-0.621	0.086	6.7
87.0	3343	-0.606	0.099	7.3
87.5	3359	-0.599	0.1	7.6
88.0	3374	-0.599	0.109	7.6
88.5	3390	-0.64	0.077	5.9
89.0	3405	-0.626	0.086	6.5
89.5	3420	-0.655	0.078	5.3
90.0	3436	-0.633	0.113	6.2
90.5	3451	-0.637	0.088	6.0
91.0	3466	-0.607	0.141	7.3
91.5	3481	-0.582	0.114	8.3
92.0	3496	-0.546	0.167	9.7
92.5	3511	-0.572	0.115	8.7

Depth (cm)	Cal yr BP	UK37	UK'37	Temperature (Celsius)
93.0	3526	-0.501	0.233	11.6
93.5	3541	-0.593	0.102	7.8
94.0	3556	-0.537	0.202	10.1
94.5	3571	-0.626	0.087	6.5
95.0	3586	-0.599	0.131	7.6
95.5	3601	-0.626	0.078	6.5
96.0	3616	-0.587	0.131	8.1
96.5	3631	-0.632	0.076	6.2
97.0	3645	-0.612	0.092	7.0
97.5	3660	-0.624	0.08	6.6
98.0	3675	-0.606	0.098	7.3
98.5	3690	-0.605	0.098	7.3
99.5	3719	-0.616	0.087	6.9
100.0	3734	-0.645	0.082	5.7
100.5	3749	-0.624	0.091	6.5
101.0	3763	-0.612	0.11	7.0
101.5	3778	-0.618	0.082	6.8
102.0	3793	-0.598	0.117	7.6
102.5	3808	-0.622	0.084	6.6
103.0	3823	-0.587	0.157	8.1
103.5	3838	-0.613	0.078	7.0
104.0	3852	-0.579	0.141	8.4
104.5	3867	-0.638	0.076	6.0
105.0	3882	-0.577	0.214	8.5
105.5	3897	-0.587	0.084	8.1
106.5	3927	-0.618	0.078	6.8
107.5	3958	-0.63	0.084	6.3
108.5	3988	-0.63	0.077	6.3
109.0	4004	-0.634	0.08	6.1
109.5	4019	-0.6	0.09	7.5
110.5	4050	-0.564	0.075	9.0
111.5	4082	-0.574	0.073	8.6
112.0	4098	-0.575	0.092	8.6
112.5	4114	-0.61	0.08	7.1
113.0	4130	-0.611	0.085	7.1
113.5	4146	-0.609	0.072	7.2

Depth (cm)	Cal yr BP	UK37	UK'37	Temperature (Celsius)
114.0	4162	-0.616	0.078	6.9
114.5	4179	-0.61	0.077	7.1
115.5	4212	-0.636	0.07	6.1
116.0	4229	-0.637	0.07	6.0
116.5	4246	-0.62	0.071	6.7
117.0	4263	-0.604	0.086	7.4
117.5	4280	-0.63	0.075	6.3
118.0	4297	-0.646	0.08	5.6
118.5	4315	-0.62	0.075	6.7
119.0	4333	-0.627	0.085	6.4
119.5	4350	-0.626	0.071	6.5
120.5	4387	-0.604	0.074	7.4
121.5	4424	-0.588	0.068	8.0
122.5	4461	-0.625	0.064	6.5
123.5	4500	-0.598	0.078	7.6
124.0	4520	-0.629	0.074	6.3
124.5	4539	-0.612	0.083	7.1
125.0	4559	-0.635	0.082	6.1
125.5	4580	-0.625	0.08	6.5
126.0	4600	-0.625	0.093	6.5
126.5	4621	-0.628	0.081	6.4
127.0	4642	-0.597	0.125	7.7
127.5	4663	-0.617	0.095	6.8
128.0	4685	-0.648	0.098	5.6
128.5	4707	-0.633	0.074	6.2
129.0	4729	-0.647	0.091	5.6
129.5	4751	-0.639	0.077	5.9
130.0	4774	-0.618	0.118	6.8
130.5	4797	-0.659	0.079	5.1
131.0	4820	-0.654	0.075	5.3
131.5	4844	-0.647	0.091	5.6
132.0	4867	-0.601	0.09	7.5
132.5	4892	-0.633	0.103	6.2
133.0	4916	-0.658	0.081	5.1
133.5	4941	-0.665	0.081	4.9
134.0	4966	-0.666	0.089	4.8

Depth (cm)	Cal yr BP	UK37	UK'37	Temperature (Celsius)
134.5	4992	-0.655	0.086	5.2
135	5018	-0.65	0.088	5.5
135.5	5044	-0.641	0.084	5.8
136.0	5071	-0.656	0.074	5.2
136.5	5098	-0.637	0.081	6.0
137.0	5125	-0.609	0.083	7.2
137.5	5153	-0.612	0.084	7.0
138.0	5181	-0.625	0.085	6.5
138.5	5210	-0.647	0.093	5.6
139	5239	-0.598	0.096	7.6
139.5	5268	-0.627	0.093	6.4
140.0	5298	-0.592	0.073	7.9
140.5	5328	-0.597	0.087	7.6
141.0	5359	-0.612	0.075	7.0
141.5	5390	-0.637	0.075	6.0
142.0	5422	-0.653	0.073	5.4
142.5	5454	-0.627	0.08	6.4
143.0	5486	-0.607	0.074	7.2
143.5	5519	-0.532	0.1	10.3

APPENDIX D

ALKENONE UNSATURATION DATA: BRAYA SØ

Depth (cm)	Cal yr BP	UK37	UK '37	Temperature (Celsius)
0	-55	-0.64	0.055	5.9
0.5	-53	-0.637	0.059	6.0
1	-50	-0.614	0.063	6.9
1.5	-45	-0.627	0.051	6.4
2	-40	-0.633	0.061	6.2
2.5	-33	-0.616	0.061	6.9
3	-25	-0.617	0.072	6.8
3.5	-16	-0.585	0.07	8.1
4	-6	-0.62	0.061	6.7
5	16	-0.651	0.071	5.4
5.5	29	-0.644	0.051	5.7
6	43	-0.637	0.063	6.0
6.5	58	-0.634	0.09	6.1
7	74	-0.637	0.078	6.0
7.5	90	-0.673	0.049	4.5
8	108	-0.648	0.057	5.5
8.5	126	-0.629	0.073	6.3
9	146	-0.6	0.1	7.5
9.5	166	-0.634	0.07	6.1
10	187	-0.597	0.07	7.7
10.5	209	-0.645	0.067	5.7
10.75	220	-0.661	0.067	5.0
11	231	-0.644	0.073	5.7
11.5	255	-0.646	0.069	5.6
12	279	-0.642	0.058	5.8
12.25	291	-0.64	0.063	5.9
12.5	304	-0.615	0.063	6.9
13	329	-0.628	0.079	6.4
13.5	356	-0.63	0.057	6.3
14	383	-0.637	0.075	6.0
14.5	410	-0.599	0.106	7.6
15	439	-0.624	0.064	6.5
15.5	468	-0.581	0.085	8.3
16	497	-0.625	0.059	6.5
16.5	527	-0.637	0.062	6.0
17	558	-0.633	0.057	6.2
17.5	590	-0.618	0.059	6.8
18	622	-0.628	0.058	6.4
18.5	654	-0.632	0.067	6.2
19	687	-0.645	0.056	5.7

Depth (cm)	Cal yr BP	UK37	UK '37	Temperature (Celsius)
19.5	721	-0.683	0.054	4.1
20	755	-0.68	0.048	4.2
20.25	772	-0.694	0.047	3.6
20.5	790	-0.622	0.06	6.6
21	825	-0.591	0.063	7.9
21.5	860	-0.618	0.068	6.8
22	896	-0.629	0.067	6.3
22.5	933	-0.653	0.063	5.3
23	970	-0.651	0.064	5.4
23.5	1007	-0.666	0.049	4.8
24	1045	-0.674	0.057	4.5
24.5	1083	-0.648	0.068	5.5
25	1121	-0.659	0.075	5.1
25.5	1160	-0.65	0.075	5.5
26	1199	-0.646	0.07	5.7
26.5	1239	-0.635	0.091	6.1
27	1279	-0.668	0.072	4.7
27.5	1319	-0.679	0.072	4.3
28	1359	-0.669	0.073	4.7
28.5	1400	-0.671	0.073	4.6
29	1441	-0.657	0.074	5.2
29.5	1482	-0.641	0.076	5.8
30	1524	-0.601	0.087	7.5
30.5	1566	-0.658	0.074	5.1
31.5	1650	-0.658	0.081	5.1
32	1692	-0.623	0.08	6.6
32.5	1735	-0.6	0.085	7.5
33	1777	-0.557		9.3
33.5	1820	-0.566		9.0
34	1863	-0.637		6.0
34.5	1907	-0.667		4.8
35	1950	-0.689	0.065	3.8
36	2037	-0.656		5.2
36.5	2081	-0.657	0.069	5.2
37	2124	-0.64	0.076	5.9
38	2212	-0.605		7.3
38.5	2256	-0.622	0.084	6.6
39	2300	-0.639	0.075	5.9
39.5	2344	-0.584		8.2
40	2389	-0.58		8.3

Depth (cm)	Cal yr BP	UK37	UK '37	Temperature (Celsius)
40.5	2433	-0.628	0.086	6.4
41.5	2521	-0.659	0.068	5.1
42.5	2610	-0.594	0.08	7.8
43.5	2698	-0.629	0.076	6.3
44.5	2786	-0.632	0.072	6.2
45.5	2874	-0.627	0.07	6.4
46.5	2962	-0.607	0.09	7.3
47	3006	-0.634	0.106	6.1
47.5	3050	-0.591	0.08	7.9
48	3094	-0.57	0.115	8.8
48.5	3137	-0.572	0.088	8.7
49	3180	-0.559	0.088	9.2
49.5	3224	-0.542	0.081	9.9
50	3267	-0.532	0.1	10.3
50.5	3310	-0.56	0.107	9.2
51	3353	-0.563	0.113	9.1
51.5	3396	-0.529	0.107	10.5
52	3439	-0.594	0.085	7.8
52.5	3481	-0.578	0.115	8.4
53	3524	-0.564	0.077	9.0
53.5	3566	-0.558	0.083	9.3
54	3608	-0.615	0.083	6.9
54.5	3650	-0.598	0.083	7.6
55	3691	-0.619	0.075	6.8
56	3774	-0.626	0.081	6.5
57	3856	-0.59	0.084	7.9
58	3938	-0.595	0.083	7.7
59	4018	-0.6	0.07	7.5
60.5	4137	-0.565	0.067	9.0
61	4177	-0.647	0.07	5.6
63	4332	-0.656	0.064	5.2
64	4408	-0.646	0.064	5.6
65	4483	-0.682	0.057	4.1
66	4557	-0.673	0.059	4.5
68	4701	-0.699	0.054	3.4
69	4772	-0.685	0.06	4.0
70	4842	-0.68	0.057	4.2
71	4911	-0.676	0.06	4.4
72	4979	-0.675	0.061	4.4
73	5045	-0.662	0.063	5.0

Depth (cm)	Cal yr BP	UK37	UK '37	Temperature (Celsius)
74	5111	-0.698	0.053	3.5
75	5175	-0.678	0.054	4.3
76	5239	-0.65	0.06	5.5
77	5301	-0.62	0.064	6.7
78	5363	-0.646	0.06	5.6
79	5423	-0.612	0.069	7.0
80	5482	-0.626	0.07	6.5
81	5540	-0.618	0.078	6.8
82	5598	-0.636	0.083	6.1
83	5654	-0.638	0.063	6.0
84	5709	-0.65	0.074	5.5
85	5763	-0.59	0.078	7.9
86	5817	-0.571	0.085	8.7
87	5869	-0.541	0.086	10.0
88	5921	-0.509	0.083	11.3
89	5972	-0.529	0.094	10.4
90	6022	-0.486	0.129	12.2
91	6071	-0.52	0.147	10.8
92.5	6143	-0.49	0.106	12.1
93	6167	-0.545	0.063	9.8
93.5	6191	-0.478	0.106	12.5

APPENDIX E

BRAYA SØ WATER COLUMN PROFILE DATA

Braya Sø water column profile, 28 June 2007

depth (m)	Temp (ºC)	Dissolved O_2 (%)	Conductivity (mS/cm)	Salinity (ppt)	[C_{37} alkenone] (µg/L water)	U^K_{37}	U^K_{37}'
0	15.53	122	5.51	2.99		-0.715	
0.5			5.49	2.99	1.02	-0.656	0.064
1	15.33	124	5.47	2.98	2.42	-0.670	0.057
1.5	15.14	124	5.48	2.98	2.17	-0.645	0.070
2	14.77	125	5.49	2.99	2.94	-0.657	0.067
2.5	14.42	124	5.5	2.99	2.65	-0.663	0.056
3	13.6	125	5.54	3.01	1.51	-0.655	0.057
3.5	11.99	128	5.62	3.06	1.54	-0.643	0.082
4	10.64	127	5.73	3.12	4.08	-0.652	0.069
4.5	8.6	121	6.27	3.43	2.32	-0.644	0.078
5	6.36	107	6.95	3.8	3.92	-0.654	0.071
5.5	5.79	102	7.04	3.85	4.76	-0.655	0.068
6	5.44	100	7.08	3.87	8.42	-0.657	0.066
6.5	5.24	97	7.1	3.88	9.65	-0.661	0.064
7	4.95	93	7.16	3.91	12.33	-0.670	0.062
7.5	4.62	87	7.19	3.93	12.32	-0.666	0.069
8	4.34	80	7.22	3.94	13.62	-0.684	0.063
8.5	4.26	76	7.23	3.95	13.23	-0.677	0.064
9	4.08	65	7.25	3.96	12.30	-0.677	0.063
9.5	4.05	65	7.26	3.96	12.04	-0.675	0.066
10	3.98	61	7.26	3.96	14.27	-0.677	0.064
10.5	3.93	60	7.26	3.96	14.73	-0.683	0.057
11	3.87	58	7.28	3.97	17.13	-0.680	0.060
11.5	3.77	58	7.28	3.97	11.26	-0.680	0.058
12	3.74	49	7.29	3.97	12.41	-0.679	0.062
12.5	3.73	35	7.29	3.97	10.61	-0.679	0.060
13	3.69	12	7.31	3.98	8.72	-0.679	0.058
13.5	3.65	3	7.32	3.99	5.05	-0.672	0.059
14	3.66	2	7.33	4	1.35	-0.612	0.073
14.5			7.34	4	1.13	-0.615	0.087
16	3.66	2	7.36	4.01		-0.663	0.065
17	3.68	2	7.38	4.02			
18	3.7	2	7.38	4.03	1.21		
19	3.71	2	7.4	4.03		-0.628	0.066
20	3.72	2	7.39	4.04			
21	3.72	2	7.41	4.04	1.00		
22	3.73	2	7.44	4.06		-0.642	0.066

Alkenone δ^{13}C from Braya Sø water column filters (collected 28 June 2007)

depth (m)	$C_{37:4}$	stdev	$C_{37:3}$	stdev	$C_{38:4}$	stdev	$C_{38:3}$	stdev
0.5	-39.85	3.57	-39.95	3.17	-41.18		-49.79	
4.5	-41.73	0.43	-42.83	0.56	-42.04	0.01		
5.0	-41.84	0.03	-42.55	0.16	-39.79	0.70	-45.15	
5.5	-42.05	0.70	-40.97	1.71	-39.19	0.01	-41.01	0.50
7.0	-41.36	0.08	-39.31	3.60	-41.43	0.37	-41.54	0.10
8.0	-43.02	2.61	-39.71	2.02	-41.10	1.37	-41.73	0.27
9.0	-41.29	0.12	-42.30	0.37	-42.03	0.17	-39.75	2.98
10.0	-42.03	0.61						
11.0	-41.61	0.54						
13.5	-39.70	1.38						

APPENDIX F

n-ALKANOIC ACID δD DATA: LAKE E

Depth (cm)	ID	C14	σ	C16	σ	C18	σ	C20	σ	C22	σ	C24	σ	C26	σ	C28	σ
2.5	168	-240.1	6.0	-236.1	4.7	-225.6	1.4			-198.1	2.0	-209.0	1.3	-213.7	2.3	-201.4	3.7
15.5	25	-219.3	0.9	-210.4	3.5	-205.6	1.2	-168.4	1.4	-175.7	1.1	-197.0	1.5	-173.1	0.2	-164.9	0.9
17.0	28	-231.8	1.5	-217.6	0.5	-218.8	0.5	-187.7	7.0	-183.7	1.3	-199.1	1.2	-186.5	0.9	-197.5	1.7
18.5	30	-215.1	5.0	-212.7	0.3	-210.8	2.0	-193.3	1.8	-188.1	2.7	-207.8	0.4	-201.0	0.9	-217.0	0.7
20.0	32	-235.6	0.4	-213.3	5.3	-209.9	3.3	-182.4	4.1	-183.2	1.9	-200.5	1.7	-184.1	0.8	-196.7	1.8
21.0	34	-228.2	1.8	-207.9	1.4	-219.5	1.0	-171.8	4.5	-170.0	3.8	-197.7	2.5	-175.3	2.8	-173.7	2.4
22.0	36	-229.7	0.9	-212.1	3.6	-206.0	6.7	-168.9	0.6	-173.0	3.4	-200.3	4.1	-174.0	1.8	-182.7	1.0
24.0	169	-250.7	4.0	-224.7	2.7	-221.9	2.2	-204.9	10.2	-196.4	4.5	-214.8	1.4	-217.0	1.4	-214.0	2.7
28.0	170	-215.5	2.1	-215.4	0.4	-223.1	0.8	-190.9	5.8	-186.9	2.1	-204.2	0.7	-195.8	2.8	-194.6	1.6
29.5	44	-214.5	2.4	-208.8	1.0	-212.4	1.1	-202.2	2.1	-189.8	1.9	-197.8	0.2	-200.3	0.8	-197.7	2.2
33.5	48	-235.4	4.2	-221.0	1.1	-209.1	2.3	-215.9	4.0	-197.3	2.1	-217.4	2.1	-208.6	0.8	-204.5	2.9
35.5	172			-233.5	0.5	-221.5	3.4	-197.4	1.6	-192.3	1.6	-212.6	1.2	-212.7	1.6	-204.7	2.4
37.5	52	-262.7	2.1	-232.2	1.2	-217.2	4.0	-216.6	2.9	-202.3	2.1	-209.8	1.7	-210.9	0.4	-203.5	0.2
38.5	53	-269.9	0.8	-229.3	2.2	-217.4	2.6	-223.3	3.1	-215.0	1.3	-211.3	2.5	-213.7	1.9	-204.6	1.1
42.0	174	-247.8	2.1	-218.3	1.8	-218.4	0.7	-214.3	1.4	-205.6	2.1	-216.1	2.5	-212.3	2.5	-205.5	3.6
43.5	58	-203.2	2.0	-188.7	1.2	-205.3	5.9	-197.8	1.6	-196.6	0.6	-205.6	0.3	-201.1	2.3	-195.8	1.9
46.5	61	-189.6	1.8	-185.5	1.7	-201.4	0.6	-192.4	2.0	-194.1	2.3	-196.9	0.5	-188.3	0.5	-181.3	0.5
48.5	63	-217.8	2.2	-216.1	7.4	-204.8	1.9	-191.5	1.6	-203.6	0.7	-209.9	2.5	-188.5	0.6	-183.1	1.7
49.5	64	-261.5	2.0	-223.0	3.2	-215.9	2.8	-202.0	1.3	-208.1	1.1	-213.6	2.6	-184.4	0.8	-182.1	0.5
52.0	177			-233.4	2.9	-219.3	3.3	-229.1	0.1	-211.1	1.8	-223.6	0.2	-222.1	2.1	-213.1	2.4
53.0	178	-267.5	2.0	-225.3	3.4	-220.0	1.1	-206.4	2.8	-209.1	2.1	-215.3	2.9	-223.9	0.5	-211.9	2.0
54.0	179	-266.7	2.9	-226.5	0.9	-215.3	1.8	-191.2	3.2	-192.4	2.6	-210.3	1.2	-217.5	1.1	-217.1	2.0
54.5	180	-249.8	4.2	-216.3	0.3	-216.9	1.0	-195.6	1.6	-188.4	1.4	-210.8	0.5	-219.1	1.5	-215.0	1.1
57.5	181	-261.3	0.8	-220.7	1.4	-212.2	0.6	-178.6	1.6	-182.9	0.3	-200.9	1.8	-205.8	0.7	-211.5	0.6
59.0	182	-212.7	3.6	-225.9	1.4	-220.2	1.6	-174.5	1.0	-171.8	1.4	-203.2	2.2	-186.2	1.4	-179.5	1.0
63.0	183	-241.1	10.0	-233.6	2.4	-216.9	1.0	-172.2	4.7	-170.1	1.0	-189.9	2.0	-203.1	0.9	-208.6	1.8
64.0	184	-256.9	2.0	-228.7	2.1	-214.1	2.2	-177.9	2.8	-176.1	2.6	-201.4	0.6	-213.8	0.8	-216.0	0.9
66.0	185	-269.1	8.0	-219.8	0.5	-218.9	3.9	-189.0	3.6	-182.7	3.3	-205.0	1.6	-203.6	0.6	-209.7	1.3
68.0	186	-268.7	2.3	-217.0	0.6	-214.0	2.8	-176.4	3.1	-178.0	1.2	-196.4	0.4	-196.8	0.4	-193.6	3.7
70.0	187	-274.6	1.2	-231.8	2.2	-213.0	0.4	-187.4	2.0	-187.1	1.5	-207.8	1.9	-210.8	0.6	-199.1	1.1
71.0	188	-263.3	8.2	-225.9	2.2	-216.5	0.9	-200.5	1.2	-193.0	0.6	-209.9	1.6	-211.3	0.2	-208.3	0.7
73.0	189	-263.9	3.9	-239.0	1.4	-207.8	0.6	-174.8	0.4	-181.2	1.6	-206.2	0.2	-212.9	0.8	-211.7	3.0
74.0	190	-247.6	8.4	-225.5	1.5	-221.7	4.3	-179.2	4.4	-181.3	5.0	-207.2	2.1	-211.8	2.5	-208.3	2.6
75.0	191	-260.5	3.3	-235.8	2.3	-207.0	1.7	-207.6	1.6	-197.3	1.5	-206.0	0.7	-204.3	1.3	-204.3	2.4
77.0	192	-243.4	11.9	-223.2	3.1	-213.1	2.0	-194.3	2.1	-188.2	2.6	-195.4	2.2	-193.7	0.5	-192.5	2.4
78.0	193	-230.3	8.9	-213.7	1.1	-213.4	2.4	-201.2	3.4	-187.4	1.1	-200.0	1.1	-190.1	1.7	-190.7	2.6
79.0	194	-229.3	7.3	-229.3	4.1	-214.3	2.0	-192.7	3.3	-195.1	4.4	-213.1	1.6	-191.4	0.7	-185.0	2.1
79.5	195	-251.1	6.9	-230.7	1.4	-210.9	3.4	-210.3	3.3	-208.3	0.8	-213.7	1.5	-194.8	2.2	-192.2	0.1
80.5	196	-263.2	2.2	-237.1	1.4	-212.3	3.6	-210.0	2.0	-215.2	1.7	-211.9	1.8	-200.5	1.0	-200.4	2.5
81.5	198	-263.2	3.6	-236.0	2.8	-207.1	3.3	-198.4	2.4	-202.2	0.4	-210.6	1.1	-190.6	1.0	-187.6	1.4
82.5	200	-252.7	1.0	-234.6	3.6	-212.5	2.3	-198.5	1.9	-200.7	1.6	-208.2	1.0	-178.6	1.2	-175.0	1.3
83.0	201	-249.5	5.1	-227.9	0.8	-216.4	1.0	-201.4	4.9	-193.8	1.3	-204.5	0.3	-190.0	0.2	-180.7	0.9
84.0	204			-225.7	3.6	-209.1	2.7	-175.3	3.8	-176.1	1.6	-206.6	2.2	-178.7	1.0	-175.8	0.7
85.0	205	-248.8	6.4	-224.8	0.6	-205.4	0.5	-175.3	1.6	-179.6	1.6	-203.0	4.2	-201.7	2.9	-197.7	1.7
85.5	206			-224.2	3.6	-209.7	2.2	-175.6	4.0	-174.6	0.7	-198.8	2.4	-181.6	0.5	-183.8	2.3
86.5	207	-236.3	10.4	-222.2	1.6	-208.9	0.2	-169.5	1.1	-171.7	1.8	-199.3	0.7	-186.7	1.1	-183.7	0.9
87.5	208			-219.0	0.8	-210.4	2.0	-171.2	3.0	-173.3	1.6	-198.8	2.7	-191.2	1.9	-186.5	4.2
88.5	209			-217.3	4.8	-208.6	3.0	-173.5	2.9	-178.1	0.4	-198.8	0.5	-188.0	0.2	-190.9	1.8
89.5	210	-247.5	6.0	-212.1	8.9	-213.2	3.1	-182.9	1.3	-179.4	1.7	-199.6	2.1	-201.5	1.4	-187.8	2.0
90.5	211			-208.9	3.6	-208.4	5.0	-166.5	2.7	-170.1	1.8	-200.9	2.9	-194.6	2.0	-196.1	1.8

Depth (cm)	ID	C14	σ	C16	σ	C18	σ	C20	σ	C22	σ	C24	σ	C26	σ	C28	σ
91.5	212			-202.1	5.1	-195.3	2.1	-163.7	1.5	-164.7	1.7	-194.2	3.8	-181.0	0.4	-178.4	1.7
92.5	213	-244.7	14.9	-203.6	2.5	-196.4	2.0	-162.5	2.6	-165.6	1.9	-194.8	2.1	-196.9	1.7	-195.2	2.0
93.5	214	-233.9	14.8	-199.1	5.5	-209.2	1.9	-164.8	1.4	-164.8	1.8	-192.7	2.0	-187.9	1.2	-193.0	1.0
94.5	215	-251.5	6.9	-197.0	2.7	-202.9	1.0	-164.1	2.1	-167.1	0.8	-190.2	1.9	-201.6	3.0	-196.5	3.5
95.5	216	-239.7	10.4	-216.8	2.7	-213.4	2.0	-170.6	3.3	-173.2	2.2	-191.5	2.2	-207.5	5.1	-198.3	2.1
96.5	217	-247.9	2.9	-212.2	1.2	-219.0	0.2	-174.3	0.9	-176.5	0.7	-202.2	1.9	-191.8	0.9	-195.2	0.9
97.5	218	-247.2	1.6	-218.7	0.5	-214.3	4.0	-185.7	1.6	-183.5	3.2	-200.7	2.9	-205.3	1.0	-203.3	0.8
100.0	219			-205.4	3.7	-210.7	5.5	-176.1	2.5	-171.0	4.4	-192.1	3.4	-170.5	2.0	-166.5	1.0
100.5	112	-247.8	2.5			-200.0	3.5	-156.9	1.7	-157.6	0.8	-179.3	1.4	-158.4	0.9	-157.1	1.6
101.5	113					-190.5	1.1	-149.3	0.3	-150.0	0.5	-167.8	0.5	-160.7	0.8	-164.1	1.1
102.5	114	-240.1	0.4			-197.5	0.0	-153.0	1.3	-152.4	0.9	-171.9	1.7	-167.4	1.3	-175.0	1.3
103.5	115	-249.0	0.5			-196.6	1.5	-150.0	0.7	-155.6	0.4	-177.6	0.2	-193.3	2.5	-182.1	2.9
104.5	120	-253.5	1.9			-194.6	0.7	-153.6	0.9	-158.1	0.6	-180.3	1.5	-196.2	0.6	-196.8	1.4
105.5	121	-233.7	3.0			-163.6	2.4	-144.5	3.3	-151.1	1.7	-180.1	1.6	-188.0	2.3	-190.6	0.4
106.5	122	-250.7	0.7			-188.8	3.3	-150.5	1.9	-153.8	1.0	-171.3	1.5	-185.1	3.1	-206.8	0.6
107.5	123	-252.5	0.8			-194.6	1.1	-163.2	1.9	-163.7	1.4	-183.8	1.4	-197.2	2.5	-189.5	2.4
108.5	124	-266.0	0.6			-191.6	0.6	-155.4	1.2	-155.3	0.6	-186.5	0.9	-162.9	1.6	-172.3	0.6
109.5	125	-258.9	2.7			-197.2	0.6	-176.6	1.0	-175.6	0.9	-197.6	0.2	-175.1	0.7	-186.5	4.5
110.5	126	-254.5	2.2			-196.1	0.4	-177.4	0.8	-175.3	2.9	-201.0	0.9	-179.4	0.4	-185.6	1.8
111.5	127	-254.7	0.9			-194.6	0.4	-172.0	1.5	-170.3	0.5	-197.9	1.6	-171.6	0.8	-187.6	1.5
112.5	128	-241.7	12.0	-226.1	3.4	-207.3	1.7	-185.9	3.9	-193.1	0.6	-204.5	3.0	-173.2	0.7	-170.0	2.1
112.5	128	-251.5	2.0			-193.7	1.0	-161.1	0.4	-158.1	1.1	-189.8	1.5	-164.9	1.7	-169.8	1.4
113.5	129	-254.2	1.9			-199.3	0.1	-165.9	1.6	-163.5	0.6	-195.1	1.1	-166.0	0.4	-179.7	0.9
114.5	130	-243.0	2.9	-224.6	2.1	-214.5	1.1	-172.0	1.5	-180.0	1.0	-197.4	1.1	-163.2	0.7	-164.0	1.6
114.5	130	-246.0	2.9			-193.0	0.7	-155.1	1.0	-152.8	0.4	-184.3	2.9	-153.9	1.0	-166.5	1.4
115.5	131	-255.0	2.1			-200.6	1.2	-160.3	1.5	-155.6	0.7	-185.6	0.4	-157.8	0.6	-164.8	2.5
117.0	230	-252.7	4.7	-235.2	3.2	-209.8	4.4	-181.5	4.8	-185.5	1.1	-204.4	2.1	-175.8	1.3	-173.6	1.6
117.5	133	-251.3	3.5	-225.5	3.9	-209.4	1.5	-198.9	1.8	-191.4	1.0	-197.6	0.7	-163.8	1.6	-165.7	0.7
118.5	134	-257.3	0.6	-226.4	1.0	-218.3	4.4	-199.5	2.4	-195.4	1.6	-202.0	1.0	-177.8	1.0	-171.3	1.5
119.5	135	-254.8	5.7	-228.6	0.9	-217.6	2.4	-206.6	1.5	-208.9	0.8	-205.9	4.6	-182.3	1.3	-180.7	0.4
120.5	233	-240.0	0.1	-215.2	1.4	-213.3	1.0	-206.5	1.3	-203.8	1.0	-208.0	1.1	-187.8	2.2	-181.5	0.8
121.5	137	-254.5	2.3			-196.4	3.0	-167.6	0.6	-170.0	1.7	-195.5	0.6	-168.6	1.5	-176.8	3.7
121.5	137	-244.3	5.0	-222.2	0.8	-206.4	1.4	-204.9	2.4	-214.0	1.8	-208.7	1.8	-175.9	2.8	-173.8	1.4
121.5	137	-244.3	5.0	-222.2	0.8	-206.4	1.4	-204.8	2.3	-214.0	1.8	-208.7	1.8	-175.9	2.8	-173.8	1.4
122.5	138	-254.1	5.5	-217.9	3.6	-209.0	2.1	-180.0	0.4	-188.8	0.9	-202.9	0.5	-169.7	1.0	-171.0	1.2
123.5	139	-255.6	2.2	-215.8	2.0	-201.6	2.9	-201.5	1.6	-209.9	0.3	-203.5	2.7	-173.4	0.4	-173.3	0.9
124.5	140	-246.4	4.1	-207.7	3.8	-199.8	1.4	-183.4	1.7	-195.1	1.6	-200.9	1.8	-162.9	1.0	-161.5	1.0
125.5	141	-261.9	4.1	-215.0	4.4	-208.5	1.6	-191.0	3.4	-194.4	2.0	-205.5	4.5	-206.9	2.3	-196.9	2.2
126.5	142	-266.1	1.6	-226.0	1.5	-204.3	2.6	-177.3	1.8	-178.5	1.1	-202.5	1.2	-216.1	1.2	-202.6	0.8
128.5	144	-232.0	1.4	-231.3	0.8	-218.5	1.8	-206.2	3.2	-199.1	0.9	-200.0	2.2	-220.1	0.8	-207.0	0.6
130.5	146	-251.0	1.4	-221.4	1.1	-211.1	1.3	-185.3	3.8	-182.8	1.1	-198.6	1.4	-210.1	1.4	-202.1	1.7
132.0	148	-231.9	2.2	-229.2	1.7	-208.4	1.7	-192.8	4.1	-189.9	1.1	-197.6	2.2	-214.8	2.6	-205.9	1.7
133.5	245	-242.9	2.1	-228.5	1.4	-214.7	4.0	-188.9	4.1	-181.9	2.0	-197.4	0.3	-211.6	1.6	-197.8	4.0
135.5	247	-236.0	1.9	-231.2	2.4	-219.6	1.5	-229.6	3.0	-222.7	1.3	-201.9	1.8	-211.8	0.7	-203.7	3.1
137.0	153	-230.8	2.3	-242.3	0.8	-220.7	3.3	-219.0	6.2	-209.7	1.7	-210.7	1.0	-211.7	2.0	-202.1	1.9
138.5	250	-222.5	2.2	-245.1	0.4	-225.9	1.2	-240.7	1.3	-226.8	1.7	-209.8	0.9	-216.8	1.2	-207.1	1.4
140.5	252	-231.1	1.4	-242.7	1.5	-212.9	6.5	-227.9	1.2	-226.9	0.9	-209.8	2.6	-221.4	0.5	-212.7	2.6
141.5	116					-224.8	1.5	-242.5	1.3	-236.2	1.1	-210.2	2.2	-219.8	0.4	-204.9	1.5
144.0	160	-234.0	0.9	-241.2	1.3	-223.3	1.2	-236.0	1.4	-233.0	0.7	-215.4	3.7	-221.0	1.7	-212.6	2.6
146.0	162	-241.9	4.1	-239.6	3.1	-212.4	2.6	-223.6	1.3	-230.9	1.7	-210.5	3.4	-203.8	0.5	-204.0	4.5

Depth (cm)	**ID**	**C14**	**σ**	**C16**	**σ**	**C18**	**σ**	**C20**	**σ**	**C22**	**σ**	**C24**	**σ**	**C26**	**σ**	**C28**	**σ**
148.0	164	-244.4	4.1	-242.4	0.9	-219.3	1.7	-230.6	2.6	-238.7	2.4	-218.5	1.5	-221.2	2.3	-214.8	0.5
150.0	166	-252.3	1.4	-236.8	1.5	-210.6	1.3	-238.4	2.8	-245.9	2.6	-210.3	2.4	-211.0	0.8	-205.3	4.0
151.0	167	-269.5	5.7	-239.8	1.2	-206.3	1.4	-220.3	1.9	-219.0	7.8	-206.9	1.6	-200.8	1.8	-194.5	5.2

APPENDIX G

n-ALKANOIC ACID δD DATA: BRAYA SØ

Depth (cm)	ID	C14	σ	C16	σ	C18	σ	C20	σ	C22	σ	C24	σ	C26	σ	C28	σ
0.0	38	-288.0	1.0	-221.8	5.5	-230.6	3.5	-158.4	0.8	-181.3	1.9	-184.2	1.0	-198.6	0.2		
0.5	2	-301.1	0.2	-256.0	1.6	-212.4	38.1	-149.1	2.8	-148.0	1.8	-184.7	3.1	-169.6	3.8	-176.2	1.4
1.0	48	-293.8	0.3	-236.4	1.1	-247.0	0.3	-167.0	1.2	-160.7	8.0	-184.4	1.7	-183.7	3.1		5.1
1.5	43	-280.9	1.7	-206.7	2.5	-225.6	1.1	-165.6	2.6	-166.2	2.2	-186.1	0.8	-181.3	3.3	-185.5	4.8
2.5	18	-250.1	4.5	-211.3	2.3	-188.4	2.2	-172.0	9.0	-151.2	1.2	-164.5	0.4	-179.9	0.9	-176.5	4.7
3.0	4	-251.4	0.6	-222.7	1.3	-177.8	1.9	-198.5	1.6	-153.2	23.4	-176.9	1.8	-186.6	1.6	-199.1	0.9
3.5	35	-243.5	1.1	-175.7	2.7	-161.8	0.3	-192.9	5.8	-170.1	2.3	-178.2	0.3	-187.3	3.3	-185.6	1.0
4.0	40	-244.5	2.3	-218.1	2.3	-196.4	0.7	-193.0	4.7	-173.5	0.3	-188.3	1.1	-191.6	0.8	-178.9	2.2
5.0	5	-244.3	2.4	-213.3	0.7	-163.4	25.2	-158.9	4.5	-164.5	6.8	-193.3	2.9	-179.9	4.1	-187.7	0.2
6.0	49	-241.6	6.5	-224.2	1.9	-178.5	4.7	-179.4	3.5	-180.6	1.2	-194.6	2.6	-190.5	1.8	-186.3	3.3
6.5	50	-227.3	1.3	-216.2	1.5	-162.1	2.9	-169.3	6.5	-174.5	1.3	-186.1	1.3	-183.3	1.6	-187.8	0.5
7.5	19	-281.6	1.7	-221.5	2.4	-228.2	1.0	-159.1	1.3	-145.9	0.2	-167.9	1.5	-178.4	1.8	-191.0	2.8
8.0	29	-259.8	0.4	-218.3	1.4	-191.1	2.6	-172.8	3.7	-165.3	0.4	-188.1	0.8	-186.5	2.2	-184.8	0.7
8.5	24	-243.7	2.2	-194.2	1.1	-201.8	1.6	-192.0	4.4	-170.5	3.2	-184.7	2.8	-189.6	2.7	-193.6	0.2
9.0	52	-234.9	1.3	-196.6	15.7	-182.9	4.2	-189.5	12.3	-178.1	6.9	-188.8	1.7	-188.9	1.2	-186.9	4.0
10.0	28	-252.1	0.8	-209.9	14.7	-191.5	4.1	-198.7	0.8	-184.4	1.6	-193.4	1.9	-191.8	3.0	-190.3	1.2
10.8	3	-258.7	0.9	-220.2	2.1	-194.5	0.8	-184.7	0.4	-168.5	1.8	-185.2	0.9	-185.4	1.4	-183.0	2.0
11.5	45	-250.6	1.6	-219.3	1.2			-153.1	3.1	-163.3	0.8	-190.7	0.7	-185.8	1.2	-197.8	0.3
12.5	20	-285.3	2.3	-234.1	3.4	-182.6	0.7	-205.9	2.8	-179.8	1.8	-187.4	2.8	-193.2	0.8	-201.4	7.3
13.0	14	-239.2	2.5	-211.0	2.3	-184.7	3.4	-201.3	7.5	-173.2	0.4	-187.8	4.5	-196.4	3.8	-198.0	1.7
14.0	34	-235.0	4.3	-227.8	0.2	-193.5	2.6	-183.9	5.0	-177.5	1.6	-198.5	2.7	-181.1	1.4	-190.8	6.9
14.5	53	-199.4	9.3	-183.5	3.9	-169.4	9.8	-153.7	6.8	-166.0	3.8	-193.6	2.0	-181.5	3.2	-190.0	4.7
15.0	33	-238.7	1.3	-194.0	1.5	-180.2	0.7	-170.3	4.4	-166.1	4.6	-181.7	2.5	-177.5	2.1	-176.8	5.5
15.5	8	-251.1	0.8	-217.6	1.9	-181.5	1.4	-186.9	2.3	-174.8	1.6	-179.9	0.8	-179.1	0.2	-202.3	2.5
16.5	42	-233.6	3.4	-227.2	0.5	-160.9	2.2	-152.9	1.8	-165.4	2.0	-189.6	0.9	-169.4	0.8	-180.9	0.2
17.5	32	-250.4	0.8	-205.1	0.2	-179.8	5.5	-161.5	0.7	-160.4	4.4	-184.0	2.0	-165.7	2.8	-169.7	1.7
18.0	27	-248.9	3.6	-236.5	3.2	-179.7	3.9	-158.2	2.1	-162.3	1.4	-187.5	1.6	-167.0	0.5	-164.1	1.4
18.5	7	-251.3	2.9	-238.3	2.5	-183.3	4.3	-172.8	1.2	-178.3	1.0	-184.7	1.1	-163.1	1.1	-167.5	1.5
19.0	13	-252.9	3.2	-221.3	2.3	-181.7	4.6	-159.9	6.7	-158.4	1.1	-201.2	1.4	-158.7	2.4	-166.8	1.3
19.5	6	-307.7	1.7	-260.2	1.2	-247.3	1.8	-140.0	0.3	-140.4	0.6	-184.9	2.6	-162.7	1.8	-164.3	0.7
20.5	36	-274.2	3.8	-212.6	0.8	-203.1	7.0	-167.7	2.6	-165.1	2.6	-193.8	1.9	-175.5	0.9	-177.4	4.3
21.0	31	-251.4	3.0	-206.2	11.0	-182.6	4.1	-174.5	4.9	-181.6	1.1	-187.5	1.0	-181.4	1.5	-180.9	2.4
22.0	46	-232.3	1.0	-210.0	1.4	-185.3	2.1	-167.4	5.0	-170.5	2.2	-194.2	2.1	-183.2	1.3	-187.6	5.7
22.5	41	-213.4	2.9	-209.1	3.2	-127.3	17.0	-151.8	8.0	-164.7	2.6	-184.5	0.8	-176.6	0.7	-184.2	1.2
24.0	16	-270.7	1.8	-226.0	1.8	-178.3	1.3	-160.1	2.4	-166.7	0.6	-191.2	1.8	-164.3	0.7	-173.6	1.1
24.5	1	-262.8	2.5	-232.2	1.2	-185.9	3.2	-162.6	1.6	-167.1	1.6	-198.2	1.4	-174.9	0.5	-171.2	0.9
25.0	54	-258.8	2.2	-215.1	1.5	-208.2	4.7	-147.4	1.1	-155.6	0.5	-195.4	1.8	-179.4	0.4	-179.5	1.8
26.0	56	-251.9	2.4	-212.8	3.7	-186.4	4.5	-155.2	2.4	-154.6	2.2	-197.9	3.8	-164.2	1.0	-162.4	0.1
26.5	57	-206.7	7.5	-193.4	9.1	-170.1	6.5	-151.5	3.9	-164.2	4.6	-184.5	3.4	-163.1	1.8	-155.3	5.9
27.5	59	-279.9	1.9	-224.3	2.8	-185.2	0.1	-160.2	1.6	-168.4	1.2	-195.2	0.9	-188.7	2.8	-184.2	2.3
28.0	60	-284.3	0.8	-226.5	0.8	-236.1	1.0	-171.1	2.6	-180.6	1.4	-195.7	3.0	-199.5	0.8	-204.4	0.6
28.5	61	-282.8	1.7	-229.8	2.6	-228.3	6.3	-156.5	8.2	-160.8	0.8	-187.4	1.5	-176.2	1.8	-181.2	1.6
29.0	62	-293.5	2.6	-238.5	2.9	-174.1	0.9	-193.7	2.0	-197.4	1.5	-200.8	0.5	-201.9	1.7	-214.8	35.8
30.0	64	-248.7	1.0	-201.6	1.3	-166.6	4.4	-164.9	2.3	-170.9	3.8	-197.3	3.1	-171.7	2.3	-175.4	3.4
30.5	65	-275.9	0.9	-228.4	2.8	-175.7	5.1	-158.3	1.8	-156.3	1.0	-189.4	2.3	-178.1	0.3	-184.1	1.1
31.5	66	-293.4	0.7	-239.4	0.9	-167.5	1.0	-184.0	1.7	-179.1	1.7	-193.8	1.0	-168.5	0.8	-190.6	31.5
32.5	68	-283.4	1.8	-240.0	1.2	-224.2	2.4	-166.0	3.4	-161.1	4.2	-185.1	2.4	-166.7	1.4	-177.6	0.9
33.0	69	-242.1	2.1	-209.6	2.8	-194.1	2.2	-187.2	2.9	-177.1	0.8	-194.9	0.5	-185.4	1.5	-183.8	2.1
34.0	71	-225.8	3.0	-200.6	2.8	-191.6	5.6	-186.1	2.6	-176.0	2.0	-185.9	2.1	-176.6	2.5	-179.7	2.7
34.0	132	-258.9	1.7	-210.9	1.1	-223.2	7.2	-177.4	3.8	-160.6	2.6	-160.8	1.0	-166.9	2.2	-176.2	24.0
35.0	73	-261.4	0.6	-219.8	1.8	-174.2	6.6	-146.0	5.9	-148.4	3.3	-186.0	2.2	-164.1	0.4	-161.9	2.4

Depth (cm)	ID	C14	σ	C16	σ	C18	σ	C20	σ	C22	σ	C24	σ	C26	σ	C28	σ
35.0	133	-163.4	3.5	-248.8	0.3	-222.2	2.4	-195.1	1.2	-165.6	1.9	-159.5	3.0	-187.7	0.4	-162.2	1.9
36.0	134	-181.0	6.1	-253.2	3.3	-228.5	0.5	-201.6	4.1	-175.8	0.5	-170.3	0.2	-193.0	1.7	-171.1	0.9
36.5	155	-308.2	1.8	-247.5	2.4	-162.2	2.8	-193.2	14.1	-181.0	2.6	-192.2	0.5	-189.5	4.2	-189.2	3.8
37.0	75	-235.6	4.6	-201.6	1.3	-178.2	3.7	-168.2	5.6	-168.7	2.5	-187.0	2.2	-183.3	2.9	-173.0	0.6
38.0	136	-186.7	4.2	-252.3	2.7			-201.7	1.5	-171.8	1.3	-167.3	1.5	-196.1	2.0	-174.3	1.5
38.5	157	-232.7	6.0	-196.5	0.9	-189.5	1.9	-189.9	5.2	-176.5	0.3	-186.9	1.0	-174.7	2.5	-182.9	2.9
39.0	77	-221.4	5.2	-202.1	0.6	-192.9	1.4	-185.7	6.1	-173.5	1.4	-189.8	0.2	-167.4	0.5	-181.9	1.3
40.5	159	-220.8	6.6	-204.4	2.2	-184.1	6.2	-177.1	0.6	-167.8	4.8	-190.4	1.3	-178.7	2.6	-171.0	1.3
40.5	159	-218.0	5.6	-218.9	0.5	-166.9	3.5	-161.8	4.4	-166.7	1.6	-190.2	1.5	-174.6	1.6	-168.6	9.9
41.5	160	-263.5	0.5	-222.2	1.5	-181.7	1.7	-177.2	0.8	-177.5	1.6	-197.7	0.9	-159.4	2.2	-164.8	1.4
42.5	161	-249.0	2.6	-211.4	5.3	-195.8	1.9	-150.0	0.6	-156.0	1.6	-189.3	2.1	-162.3	1.9	-154.9	5.7
43.5	162	-285.7	1.2	-229.6	1.4	-175.5	2.2	-161.9	5.9	-161.8	1.5	-196.6	1.2	-162.1	0.6	-161.7	8.3
44.5	163	-222.4	8.6	-220.5	1.7	-194.2	6.6	-189.4	1.2	-176.4	0.3	-190.8	0.3	-179.5	0.8	-183.1	0.6
45.5	164	-229.2	2.9	-227.7	2.7	-199.7	1.2	-187.9	1.2	-175.9	1.9	-194.6	0.7	-175.6	1.2	-186.4	5.4
46.5	165	-228.0	6.3	-225.0	1.0	-182.3	2.8	-156.0	1.8	-161.1	2.5	-190.3	0.9	-161.9	2.0	-173.3	3.8
46.5	165	-221.5	4.8	-225.3	4.0	-172.2	1.6	-152.3	5.5	-161.0	3.1	-193.5	1.9	-164.8	1.7	-170.7	3.6
47.5	166	-256.4	1.2	-224.2	3.1	-176.0	5.8	-164.6	3.0	-165.4	2.2	-185.1	1.6	-158.9	0.9	-154.2	0.7
48.0	86	-261.9	2.9	-216.0	1.5	-186.1	2.2	-181.1	2.0	-190.5	4.0	-191.0	6.7	-151.7	1.6	-136.8	1.8
49.0	87	-251.1	1.9	-221.9	0.3	-181.0	4.4	-185.4	2.8	-195.4	0.5	-191.3	1.7	-156.4	1.8	-150.2	17.4
49.5	168	-249.8	3.8	-202.2	2.0	-146.6	9.4	-159.4	3.5	-159.0	0.4	-194.7	2.5	-166.3	1.7	-168.8	0.8
49.5	168	-241.6	3.7	-190.4	2.9	-207.0	3.6	-132.9	9.2	-151.5	2.0	-187.2	0.4	-162.7	0.5	-166.2	1.5
50.0	88	-241.3	2.7	-209.8	15.4	-171.3	16.0	-173.6	6.6	-173.9	4.6	-199.9	1.8	-171.6	2.0	-170.5	1.5
51.0	89	-254.3	1.3	-217.3	2.1	-175.6	1.1	-182.6	2.4	-178.7	4.8	-186.8	1.0	-171.0	3.3	-174.7	0.6
53.5	172	-285.1	0.7	-239.1	5.9	-178.3	4.5	-158.7	3.6	-162.4	2.5	-191.2	1.1	-193.8	1.0	-193.0	1.4
53.5	172	-284.1	1.9	-237.8	3.4			-150.8	7.6	-158.0	2.2	-184.2	0.9	-193.5	1.9	-182.2	1.0
54.5	173	-293.5	2.9	-243.5	5.7	-174.0	3.8	-170.6	1.1	-171.9	3.0	-189.6	4.7	-205.6	1.5	-193.4	3.1
55.0	93	-288.3	1.6	-227.0	2.3	-257.2	0.3	-159.3	4.3	-169.0	6.4	-193.3	0.7	-200.9	0.9	-199.0	0.2
60.0	98	-258.4	0.6	-231.8	3.2	-151.8	5.7	-166.8	1.3	-165.8	1.8	-185.6	3.2	-158.2	2.0	-152.1	0.4
60.5	179	-269.6	3.4	-228.6	0.4	-178.6	4.7	-161.6	4.0	-156.8	0.3	-177.7	2.7	-155.8	0.0	-154.9	0.9
63.0	101	-259.1	1.3	-220.9	4.5	-169.0	2.0	-149.3	1.8	-158.5	3.1	-179.7	4.0	-179.6	2.1	-176.3	3.3
64.0	102	-275.7	3.3	-233.7	4.7	-194.1	1.2	-177.5	2.6	-180.5	2.0	-202.8	2.4	-213.9	2.9	-206.4	3.1
65.0	103	-287.0	2.2	-236.7	1.8	-178.8	0.9	-165.1	2.8	-167.0	2.2	-191.4	0.6	-194.7	1.5	-188.3	0.4
68.0	106	-277.8	1.7	-231.9	0.1	-226.5	4.3	-160.9	2.1	-167.5	0.7	-190.4	3.2	-183.8	0.6	-185.0	2.2
69.0	107	-292.4	2.2	-250.7	0.6	-191.7	1.1	-183.7	1.7	-178.7	1.1	-196.0	2.5	-204.2	0.3	-198.4	1.3
70.0	108	-291.8	1.4	-235.6	0.9	-223.0	1.5	-165.2	2.1	-168.3	1.9	-193.9	1.3	-205.5	0.9	-196.5	2.1
79.0	117	-270.3	2.6	-212.6	3.9	-165.3	2.4	-150.9	1.4	-148.7	2.2	-169.0	2.2	-159.7	1.9	-126.8	4.8
79.0	117	-286.4	2.0	-217.3	2.0	-199.1	2.0	-143.8	1.4	-153.8	1.7	-167.0	1.3	-156.0	0.7	-159.8	1.3
83.0	121	-277.7	6.8	-212.6	1.0	-234.0	3.4	-143.0	3.6	-139.8	3.9	-175.5	3.1	-139.2	2.5	-146.9	4.6
83.0	121	-276.6	3.1	-225.8	1.0	-235.2	3.5	-129.3	1.5	-136.6	1.4	-171.9	1.5	-137.7	1.7	-137.9	0.4
85.0	123	-269.4	1.8	-218.6	3.1	-165.0	3.1	-137.1	2.8	-136.6	1.3	-167.5	4.6	-135.9	0.3	-145.5	0.5
87.0	125	-227.6	2.5	-187.1	3.1	-189.5	7.1	-123.5	3.5	-133.8	9.9	-163.6	3.1	-138.6	1.3	-141.6	2.2
88.0	126	-286.6	6.6	-224.6	1.1	-186.6	2.8	-152.6	2.9	-151.1	0.9	-175.2	2.1	-156.7	1.1	-153.8	3.7
89.0	127	-239.8	9.5	-187.9	3.2	-179.9	4.1	-141.6	2.5	-144.7	4.4	-171.5	5.6	-146.1	1.8	-147.2	0.8
90.0	128	-165.7	1.2	-165.4	2.7	-157.8	1.1	-129.7	4.1	-133.9	5.1	-158.5	1.8	-137.6	0.4	-140.7	1.9
100.0	138	-237.4	2.4	-126.0	6.9	-190.4	1.7	-153.9	2.5	-160.1	2.1	-190.6	3.1	-163.3	1.3	-158.4	1.7
101.0	139	-182.3	8.5	-249.8	2.3			-190.7	2.3	-165.7	1.7	-169.2	2.0	-195.5	2.6	-163.5	2.1
102.0	140	-184.3	13.8	-246.3	3.0			-189.8	1.7	-158.5	3.0	-163.2	1.2	-190.7	1.5	-157.7	1.2
103.0	141	-180.0	5.7	-254.8	1.4			-195.3	2.1	-165.2	0.4	-168.7	1.1	-196.3	4.7	-192.8	1.4
104.0	142	-164.2	14.4	-258.5	0.8			-196.5	1.9	-167.8	2.3	-166.1	1.5	-193.3	5.1	-205.3	2.2
105.0	143	-204.0	6.9	-211.9	2.9	-207.7	4.8	-156.0	3.0	-154.4	1.5	-162.4	3.1	-149.9	0.8	-149.4	2.5
109.0	147	-214.3	7.4	-222.3	1.7	-172.2	7.6	-150.1	1.0	-164.2	0.3	-178.0	1.6	-165.7	1.3	-163.5	2.8

Depth (cm)	ID	C14	σ	C16	σ	C18	σ	C20	σ	C22	σ	C24	σ	C26	σ	C28	σ
114.0	152	-234.3	1.7	-263.9	5.8	-174.6	5.5	-177.9	6.2	-181.0	1.9	-180.0	2.4	-174.5	0.6	-167.7	0.7
115.0	153	-227.6	2.1	-262.8	1.6	-154.2	3.9	-164.5	1.5	-167.2	0.7	-181.4	0.8	-178.9	2.3	-168.7	2.5
116.0	154	-227.3	2.2	-264.3	1.9	-193.8	3.1	-196.7	2.7	-185.7	0.8	-177.5	1.0	-179.5	0.7	-175.5	1.4
120.0	242	-238.1	5.5	-275.9	1.9	-172.3	2.7	-175.1	1.2	-177.6	1.7	-172.2	1.3	-180.1	2.4	-173.2	1.8
125.0	252	-257.4	1.4	-280.8	4.1	-185.0	1.9	-203.4	2.4	-195.4	0.6	-199.1	1.6	-195.9	1.0	-193.6	1.2
130.0	262	-215.1	2.4	-233.6	4.7	-208.5	1.7	-179.5	6.7	-177.7	2.2	-174.7	6.8	-175.6	4.6	-155.2	6.8
134.0	270	-207.3	5.2	-238.4	0.9	-215.2	1.7	-186.2	8.4	-178.4	0.9	-191.5	1.6	-175.6	3.1	-172.8	3.8

APPENDIX H

ELEMENTAL ANALYSIS DATA: LAKE E

Depth (cm)	Organic C (%)	N (%)	C:N
0.0	5.6	1.1	5.2
0.5	5.9	0.9	6.9
1.0	5.8	1.0	5.6
1.5	5.5	1.0	5.6
2.0	4.9	0.9	5.5
2.5	4.0	0.9	4.4
3.0	4.0	0.9	4.3
3.5	4.5	0.9	5.1
5.0	4.7	1.1	4.5
5.5	5.7	1.1	5.1
6.0	5.5	1.0	5.3
6.5	5.5	1.0	5.8
7.0	6.5	1.2	5.5
7.5	8.7	1.6	5.6
8.0	6.9	1.3	5.4
8.5	5.8	0.9	6.2
9.0	6.0	1.2	5.2
9.5	6.5	1.1	6.0
10.0	6.6	1.1	6.2
10.5	6.4	1.1	5.9
11.0	6.7	1.0	6.7
11.5	6.7	1.1	5.9
12.0	6.3	1.0	6.1
12.5	6.8	1.1	6.3
13.0	8.0	1.5	5.4
13.5	8.1	1.5	5.4
14.5	6.9	1.2	5.7
15.0	9.8	1.3	7.4
15.5	7.7	1.1	7.1
16.0	7.3	1.2	6.0
16.5	10.6	1.1	9.7
17.0	12.4	1.3	9.5
17.5	16.4	1.7	9.9
18.0	16.1	1.5	10.7
18.5	16.9	1.5	11.4
19.0	14.9	1.2	12.0
19.5	13.0	1.1	11.5
20.0	13.7	1.2	11.3
20.5	14.4	1.3	11.0
21.0	10.5	1.0	10.7
21.5	9.9	0.9	11.0
22.0	10.0	0.9	10.8
22.5	11.5	1.1	10.6
23.0	14.4	1.3	11.2
23.5	15.0	1.3	11.6
24.0	14.5	1.4	10.7
24.5	15.6	1.4	11.1
25.0	17.7	1.6	11.2
25.5	19.5	1.8	10.7
27.0	15.2	1.4	10.5
28.5	13.6	1.3	10.1
29.0	14.3	1.4	9.9
29.5	13.7	1.5	9.4
30.0	15.4	1.6	9.7
30.5	15.0	1.6	9.7
31.0	15.6	1.6	9.8
31.5	16.5	1.5	10.7
32.0	16.1	1.6	10.2
32.5	16.3	2.0	8.1
33.0	14.5	1.4	10.4
33.5	12.7	1.7	7.4
34.0	14.4	2.0	7.3
34.5	15.1	2.0	7.5
35.0	15.4	1.5	10.1
35.5	14.8	1.3	11.1
36.0	15.7	1.3	12.1
36.5	17.8	1.5	12.0
37.0	18.2	1.6	11.3
37.5	17.6	1.5	11.4
38.0	18.0	1.6	11.3
38.5	19.2	1.6	11.7
39.0	20.3	1.7	12.2
39.5	20.6	1.7	12.4
40.5	18.7	1.9	9.9
41.0	19.2	2.0	9.6
41.5	20.0	2.1	9.6
42.0	18.1	2.0	9.1
42.5	19.2	2.2	8.8
43.0	18.3	2.1	8.7
43.5	17.4	1.9	9.3
44.0	21.5	2.1	10.1
44.5	22.6	2.1	10.9
45.0	19.4	1.9	10.0
45.5	14.6	1.7	8.5
46.0	16.3	2.1	7.9
46.5	14.9	1.9	8.0
47.0	13.8	1.8	7.7
47.5	16.5	1.7	9.9
48.0	14.5	2.0	7.5
48.5	13.2	1.6	8.3
49.0	12.2	1.4	9.0
49.5	13.4	1.5	9.2
50.0	13.5	1.5	8.9
51.0	14.5	1.8	8.2
51.5	14.7	1.9	7.9
52.0	15.4	2.0	7.9
52.5	14.1	1.7	8.5
53.0	15.5	1.8	8.7
53.5	15.7	2.0	8.0
54.0	15.8	1.9	8.3

Depth (cm)	Organic C (%)	N (%)	C:N	Depth (cm)	Organic C (%)	N (%)	C:N
54.5	17.5	2.0	8.6	80.0	11.9	1.0	12.1
55.0	18.5	2.3	8.1	80.5	11.5	1.0	11.6
55.5	17.0	1.7	10.1	81.0	12.9	1.1	11.4
56.0	16.2	2.2	7.3	81.5	12.1	1.0	12.0
57.0	14.8	1.9	7.7	82.0	11.4	1.0	11.3
57.5	15.4	2.0	7.9	82.5	12.9	1.2	10.8
58.0	17.4	2.1	8.3	83.0	13.9	1.4	10.2
58.5	17.7	2.2	7.9	83.5	13.5	1.3	10.2
59.0	17.1	2.2	7.8	84.0	10.4	1.0	10.3
59.5	17.1	2.1	8.0	84.5	12.0	1.1	10.8
60.0	17.0	2.2	7.9	85.0	13.5	1.2	10.9
60.5	15.6	2.0	8.0	85.5	12.7	1.2	11.0
61.0	18.1	2.2	8.1	86.0	12.8	1.3	10.3
61.5	20.2	2.3	8.8	86.5	12.5	1.3	9.8
62.0	21.8	2.4	9.2	87.0	13.6	1.4	9.8
62.5	20.8	2.5	8.2	87.5	15.4	1.6	9.5
63.0	17.7	2.3	7.6	88.0	16.1	1.7	9.7
63.5	12.3	1.7	7.1	88.5	16.1	1.6	9.9
64.0	12.6	1.7	7.6	89.0	16.6	1.7	9.9
64.5	14.3	1.7	8.4	89.5	16.3	1.7	9.8
65.0	14.4	1.8	8.2	90.0	14.1	1.3	10.5
65.5	13.3	1.3	10.5	90.5	14.7	1.4	10.8
66.0	13.3	1.4	9.8	91.0	14.5	1.3	10.9
66.5	12.6	1.3	9.9	91.5	14.7	1.3	11.0
67.0	11.7	1.2	9.5	92.0	13.5	1.2	10.8
67.5	12.3	1.3	9.7	92.5	15.8	1.5	10.3
68.0	13.4	1.4	9.9	93.0	17.8	1.7	10.4
68.5	14.8	1.5	9.8	93.5	18.8	1.8	10.6
69.0	16.8	1.8	9.5	94.0	18.8	1.8	10.4
69.5	16.3	1.7	9.8	94.5	18.8	1.7	10.9
70.0	14.8	1.4	10.4	95.0	17.8	1.7	10.6
70.5	14.6	1.4	10.5	95.5	15.6	1.5	10.3
71.0	13.5	1.3	10.4	96.0	16.4	1.5	10.7
71.5	15.1	1.5	10.4	96.5	19.2	1.8	10.6
72.0	13.7	1.3	10.3	97.0	19.5	1.9	10.4
72.5	14.6	1.4	10.2	97.5	21.3	2.0	10.4
73.0	13.1	1.2	10.6	98.0	21.1	1.9	11.0
73.5	14.3	1.3	11.0	98.5	22.4	2.0	11.1
74.0	13.2	1.2	11.1	99.0	21.2	2.0	10.6
74.5	11.4	1.1	10.3	99.5	16.2	1.6	10.2
75.0	10.0	1.0	10.5	100.0	15.8	1.5	10.5
75.5	11.3	1.1	10.0	100.5	14.3	1.4	10.1
76.0	12.3	1.3	9.7	101.0	14.6	1.5	10.0
76.5	13.5	1.4	9.7	101.5	16.9	1.7	10.2
77.0	13.9	1.4	9.9	102.0	18.0	1.8	10.1
77.5	14.4	1.4	10.1	102.5	17.8	1.7	10.7
78.0	14.7	1.5	10.2	103.0	16.4	1.5	11.1
78.5	12.2	1.1	10.8	103.5	14.3	1.3	11.0
79.0	10.5	0.9	11.6	104.0	15.1	1.5	10.1
79.5	11.3	0.9	12.0	104.5	17.3	1.7	10.5

Depth (cm)	Organic C (%)	N (%)	C:N
105.0	18.2	1.7	10.8
105.5	18.5	1.7	11.2
106.0	19.2	1.6	11.9
106.5	17.6	1.5	11.6
107.0	18.5	1.7	11.0
107.5	17.9	1.7	10.7
108.0	15.1	1.4	11.0
108.5	15.2	1.3	11.3
109.0	12.5	1.1	11.5
109.5	12.3	1.1	11.2
110.0	11.8	1.0	11.6
110.5	12.7	1.1	11.5
111.5	13.4	1.2	11.2
112.0	13.0	1.2	11.2
112.5	13.7	1.2	11.9
113.0	14.2	1.1	12.6
113.5	14.3	1.2	12.0
114.0	14.9	1.3	11.8
114.5	12.2	1.0	12.0
115.0	12.5	1.1	11.4
115.5	13.7	1.2	11.5
116.0	13.4	1.2	11.3
116.5	12.1	1.1	11.4
117.0	14.6	1.3	11.4
117.5	12.7	1.1	11.3
118.0	12.4	1.1	11.4
118.5	14.6	1.3	11.6
119.0	14.7	1.2	12.1
119.5	14.2	1.3	10.9
120.0	12.0	1.0	11.5
120.5	11.8	0.9	12.6
121.0	12.3	1.0	12.6
121.5	12.3	0.9	13.1
122.0	12.7	1.1	11.7
122.5	13.2	1.1	12.0
123.0	12.4	1.0	11.9
123.5	12.6	1.1	11.9
124.0	12.4	1.1	11.5
124.5	11.1	0.9	11.8
125.0	12.3	1.0	12.1
125.5	13.6	1.1	12.4
126.0	12.8	1.1	12.2
126.5	13.5	1.2	11.6
127.0	11.4	1.0	11.9
127.5	13.1	1.1	11.8
128.0	18.1	1.5	12.3
128.5	15.8	1.3	11.8
129.0	15.0	1.3	11.6
129.5	16.3	1.6	10.4
130.0	13.8	1.4	9.9

Depth (cm)	Organic C (%)	N (%)	C:N
130.5	12.3	1.2	10.2
131.0	14.1	1.3	11.0
131.5	16.6	1.5	10.9
132.0	12.6	1.2	10.2
132.5	11.8	1.1	10.5
133.0	11.0	1.1	9.8
133.5	12.4	1.2	10.8
134.0	15.1	1.4	10.8
134.5	11.3	1.1	10.7
135.0	11.9	1.1	11.0
135.5	10.8	1.0	11.1
136.0	13.0	1.2	11.0
136.5	9.3	0.9	11.0
137.0	11.1	1.0	10.8
137.5	10.9	1.0	11.3
138.0	12.0	1.1	11.3
138.5	11.4	1.0	11.3
139.0	9.6	0.9	10.9
139.5	8.9	0.9	10.4
140.0	10.5	1.0	10.8
140.5	11.2	1.0	11.6
141.0	10.8	0.9	11.4
141.5	7.9	0.7	11.6
142.0	7.2	0.7	10.9
142.5	8.2	0.8	10.2
143.0	10.2	0.9	11.7
143.5	10.5	1.0	10.5
144.0	7.7	0.7	10.4
144.5	4.9	0.6	8.2
145.0	5.0	0.5	9.3
145.5	5.9	0.6	9.9
146.0	6.7	0.6	10.6
146.5	6.9	0.7	10.2
147.0	7.4	0.8	9.7
147.5	6.0	0.6	9.8
148.0	4.0	0.4	9.2
148.5	3.7	0.5	7.3
149.0	4.4	0.6	6.9
149.5	5.6	0.7	8.4
150.0	5.4	0.6	9.4
150.5	4.7	0.5	8.7
151.0	2.8	0.5	5.7
151.5	4.9	0.5	9.2
152.0	5.2	0.5	9.6
152.5	6.4	0.6	11.0
153.0	5.8	0.7	8.6
153.5	5.4	0.6	8.9
154.0	4.3	0.6	7.6
154.5	3.4	0.4	8.2
155.0	3.6	0.5	7.9

Depth (cm)	Organic C (%)	N (%)	C:N
155.5	4.0	0.4	9.8
156.0	3.8	0.5	8.4
156.5	3.7	0.4	8.5
157.0	3.5	0.5	7.8
157.5	2.9	0.4	7.6
158.0	3.8	0.5	8.0
158.5	3.2	0.4	8.2
159.0	3.9	0.5	8.1
159.5	1.1	0.3	3.8
160.0	3.8	0.5	7.9
160.5	3.8	0.5	7.7
161.0	4.3	0.6	7.8
162.5	4.0	0.4	9.8
163.0	4.4	0.4	10.4

Depth (cm)	Organic C (%)	N (%)	C:N
163.5	4.8	0.5	9.5
164.0	5.1	0.5	10.0
164.5	4.7	0.5	9.5
165.0	4.7	0.5	10.1
165.5	4.1	0.5	7.8
166.0	4.6	0.6	7.8
166.5	4.0	0.4	9.3
167.0	2.9	0.4	7.9
167.5	2.6	0.4	6.5
168.0	2.0	0.5	4.3
168.5	1.4	0.3	5.5
169.0	1.4	0.3	4.3
169.5	1.8	0.4	4.7
170.0	2.0	0.3	6.1
170.5	2.3	0.5	4.8

Note: Elemental analyses on Lake E sediment core E-01 were conducted by William J. D'Andrea as part of a M.S. project with Dr. Sherilyn C. Fritz at the University of Nebraska – Lincoln.

APPENDIX I

ELEMENTAL ANALYSIS DATA: BRAYA SØ

Depth (cm)	Organic C (%)	$\delta^{13}C$	N (%)	$\delta^{15}N$	C/N
0.0	13.8	-30.5	1.6	2.5	8.4
0.5	13.4	-30.6	1.6	3.4	8.2
1.0	8.1	-29.4	0.9	3.2	8.7
1.5	9.2	-29.2	1.1	3.8	8.2
2.0	8.8	-29.0	1.1	3.5	8.2
2.5	7.2	-28.2	0.9	3.2	7.6
3.0	6.7	-28.3	0.8	2.6	8.2
3.5	7.7	-27.9	1.0	2.4	8.1
4.0	6.2	-27.6	0.8	2.1	7.6
4.5	7.7	-27.8	1.2	2.3	6.5
5.0	9.8	-28.3	1.4	1.9	7.2
5.5	8.5	-28.1	1.1	2.1	7.6
6.0	11.9	-27.7	1.1	2.6	10.8
6.5	6.2	-29.2	0.7	3.1	9.3
7.0	6.8	-29.4	0.7	4.0	9.8
7.5	6.7	-29.8	0.7	4.3	9.2
8.0	8.3	-28.2	1.1	3.3	7.9
8.5	4.3	-28.2	0.5	2.3	8.9
9.0	7.2	-28.8	0.8	1.8	9.0
9.5	11.4	-28.0	1.3	1.9	8.7
10.0	9.8	-28.2	1.2	2.4	8.4
10.8	14.4		1.9		7.8
11.0	10.7	-27.8	1.2	1.6	8.9
11.5	7.0	-28.3	0.7	1.9	9.4
12.0	6.3	-28.5	0.6	2.5	10.3
12.3	10.8	-29.2	1.2	4.0	9.1
12.5	8.7	-28.7	0.9	3.3	9.3
13.0	10.4	-28.2	1.0	2.1	10.9
13.5	8.0	-27.8	0.9	1.9	8.8
14.0	10.4	-27.7	1.4	1.9	7.4
14.5	10.5	-28.0	1.1	1.3	9.4
15.0	12.1	-29.5	1.0	2.7	12.4
15.5	10.4	-28.1	1.0	2.0	10.8
16.0	12.9	-27.9	1.2	1.3	11.2
16.5	10.2	-27.3	1.1	2.0	8.9
17.0	8.1	-28.3	0.9	3.8	9.5
17.5	11.8	-27.9	1.1	3.3	10.4
18.0	10.5	-27.6	1.0	2.8	10.1
19.0	10.5	-28.2	1.0	4.2	10.1
19.5	11.1	-30.4	1.1	3.3	10.3
20.0	19.4	-31.9	1.7	3.5	11.4
20.3	12.8	-31.2	1.3	4.2	9.6
20.5	18.3	-27.9	2.5	2.6	7.4
21.0	18.3	-27.7	2.1	1.6	8.5
21.5	18.0	-26.8	2.0	2.3	8.9
22.0	21.1	-27.2	2.1	1.7	9.9
22.5	20.4	-27.1	2.8	1.7	7.4
23.0	19.9	-27.4	2.4	1.6	8.3
23.5	18.4	-27.4	2.4	1.6	7.7

Depth (cm)	Organic C (%)	$\delta^{13}C$	N (%)	$\delta^{15}N$	C/N
24.0	10.8	-28.1	1.2	2.7	8.9
24.5	12.8	-28.2	1.6	2.8	8.0
25.0	13.0	-29.5	1.5	3.3	8.5
25.5	13.5	-30.3	1.7	3.7	7.8
26.0	9.7	-29.3	1.0	3.7	9.9
26.5	14.6	-28.0	1.9	3.3	7.5
27.0	15.5	-28.4	1.6	3.1	9.4
27.5	12.6	-29.4	1.6	1.9	8.1
28.0	17.5	-31.1	2.2	3.3	8.1
28.5	9.9	-30.7	1.3	3.5	7.9
29.0	11.9	-30.7	1.4	3.5	8.6
29.5	12.8	-31.0	1.6	3.5	8.0
30.0	11.4	-29.6	1.3	3.9	8.9
30.5	12.0	-30.3	1.5	3.7	8.2
31.5	11.3	-31.0	1.4	4.3	8.2
32.0	13.7	-30.8	1.4	4.4	10.0
32.5	14.3	-30.1	1.8	4.2	8.0
33.0	13.7	-28.6	1.5	2.4	9.2
33.5	15.3	-28.4	1.5	2.3	10.0
34.0	17.6	-27.7	2.1	2.5	8.3
34.5	13.5	-29.7	1.8	3.4	7.7
35.0	11.0	-30.9	1.3	4.1	8.5
36.0	14.2	-31.8	1.4	4.4	10.1
36.5	13.2	-29.6	1.7	3.3	7.9
37.0	11.1	-27.6	1.2	2.1	9.3
37.5	11.7	-27.8	1.6	1.7	7.3
38.0	13.9	-28.2	1.9	1.9	7.4
38.5	15.7	-28.1	1.9	1.8	8.2
39.0	16.8	-28.4	1.8	1.6	9.3
39.5	11.9	-27.3	1.4	2.1	8.5
40.0	12.0	-28.5	1.2	3.2	10.0
40.5	13.6	-27.1	1.7	1.7	8.2
41.0	10.1	-28.4	1.1	2.6	9.4
41.5	8.5	-29.4	0.9	4.3	9.1
42.0	12.8	-29.2	1.2	3.7	11.0
42.5	9.2	-28.4	1.0	3.7	9.6
43.0	8.6	-28.5	0.8	3.0	10.5
43.5	10.0	-29.6	1.1	4.5	9.5
44.0	16.4	-28.6	1.7	3.2	9.5
44.5	16.0	-26.7	2.5	1.3	6.4
45.0	13.6	-27.6	1.6	2.1	8.6
45.5	12.8	-26.8	1.6	1.0	7.8
46.0	11.0	-27.3	1.0	1.4	10.8
46.5	8.9	-27.9	1.0	3.2	8.7
47.0	10.8	-28.3	1.1	4.0	10.2
47.5	6.5	-28.4	0.8	3.5	8.4
48.0	10.6	-29.4	1.2	3.4	8.7
48.5	8.8	-28.6	1.0	3.5	8.5
49.0	11.4	-29.0	1.2	3.7	9.6

Depth (cm)	Organic C (%)	$\delta^{13}C$	N (%)	$\delta^{15}N$	C/N
49.5	9.6	-28.1	1.1	3.3	8.6
50.0	13.4	-28.2	1.4	3.3	9.9
50.5	10.5	-28.5	1.2	3.3	8.8
51.0	10.5	-27.6	1.2	2.5	8.6
51.5	11.4	-27.0	1.5	2.0	7.7
52.0	8.6	-27.8	0.9	3.1	9.1
52.5	9.4	-27.6	1.2	3.5	7.8
53.0	12.1	-28.2	1.3	3.3	9.2
53.5	14.4	-28.7	2.0	3.1	7.3
54.0	19.0	-30.2	2.5	2.9	7.7
54.5	16.3	-31.3	2.3	3.5	7.2
55.0	22.0	-32.1	3.0	3.6	7.3
55.5	16.8	-31.8	2.0	3.0	8.3
56.0	19.1	-31.3	2.1	3.4	9.1
56.5	15.5	-30.5	1.7	3.0	9.1
57.0	19.5	-28.5	1.9	2.5	10.3
57.5	23.1	-26.7	3.5	1.7	6.6
58.0	20.3	-26.5	2.6	1.7	7.9
58.5	13.2	-26.4	1.7	2.0	7.7
59.0	17.7	-26.6	2.8	1.5	6.4
59.5	12.1	-25.8	1.6	1.1	7.6
60.0	12.2	-27.5	1.4	2.8	8.5
60.5	15.3	-27.3	2.0	3.1	7.7
61.0	15.7	-27.3	1.9	2.8	8.3
61.5	15.2	-27.7	2.2	2.3	7.0
62.0	15.3	-28.5	1.8	2.8	8.6
62.5	14.2	-27.8	1.9	2.7	7.4
63.0	11.4	-29.5	1.4	2.6	8.1
63.5	12.7	-30.6	1.6	2.3	7.9
64.0	10.5	-30.7	1.2	2.5	8.6
64.5	14.0	-30.7	1.8	3.2	7.9
65.0	13.6	-31.1	1.7	3.3	7.8
65.5	14.6	-30.3	1.7	2.2	8.4
66.0	12.2	-30.6	1.2	3.0	10.2
66.5	14.0	-29.8	1.6	2.3	8.5
67.0	11.2	-29.0	1.0	2.2	11.0
67.5	15.1	-29.3	1.8	2.2	8.3
68.0	13.5	-30.4	1.5	2.4	9.0
68.5	12.8	-30.4	1.5	2.1	8.5
69.0	15.4	-31.5	1.8	2.5	8.5
69.5	15.3	-30.1	1.9	2.0	8.2
70.0	15.1	-31.4	1.7	2.3	9.0
70.5	14.0	-30.7	1.8	2.5	7.6
71.0	12.5	-31.0	1.5	2.5	8.4
71.5	10.7	-31.0	1.5	2.7	7.3
72.0	14.2	-31.4	1.6	2.5	8.7
72.5	11.0	-31.3	1.4	2.3	8.1
73.0	11.9	-31.8	1.3	2.2	9.1
73.5	11.4	-31.7	1.3	2.3	8.7

Depth (cm)	Organic C (%)	$\delta^{13}C$	N (%)	$\delta^{15}N$	C/N
74.5	10.3	-32.1	1.4	2.0	7.6
75.0	9.6	-32.1	1.1	1.6	9.1
75.5	8.1	-31.5	0.9	2.4	8.8
76.0	9.4	-32.0	0.9	2.2	10.7
76.5	11.2	-30.9	1.2	1.9	9.6
77.0	10.5	-30.3	0.9	2.0	11.6
77.5	8.2	-30.8	0.8	1.5	9.7
78.0	7.8	-32.0	0.9	2.1	9.0
78.5	7.2	-31.2	0.8	2.3	9.2
79.0	5.2	-29.7	0.5	2.0	10.0
79.5	5.2	-30.2	0.6	1.7	9.5
80.0	7.7	-30.5	0.8	2.0	10.1
80.5	10.6	-30.3	1.2	2.2	9.0
81.0	6.9	-30.3	0.7	1.5	9.6
81.5	5.3	-31.5	0.7	2.4	7.7
82.0	6.9	-31.0	0.7	2.0	10.3
82.5	5.9	-31.7	0.7	2.2	8.7
83.0	6.4	-30.6	0.6	1.9	10.6
83.5	6.6	-30.9	0.8	2.0	8.9
84.0	6.2	-31.1	0.7	1.8	9.1
84.5	6.7	-30.5	0.8	1.9	8.3
85.0	7.5	-31.4	0.8	1.7	10.0
85.5	6.7	-31.4	0.8	1.8	8.9
86.0	4.3	-30.8	0.4	1.1	9.8
86.5	5.4	-31.0	0.6	1.7	8.6
87.0	4.8	-31.2	0.5	1.8	10.5
87.5	5.5	-32.0	0.6	1.8	9.3
88.0	5.5	-32.7	0.6	1.8	9.9
88.5	4.0	-33.6	0.4	2.6	9.5
89.0	3.5	-32.0	0.3	2.8	10.5
89.5	2.8	-31.5	0.3	2.7	9.2
90.0	3.9	-32.1	0.4	1.9	10.0
90.5	2.9	-31.4	0.3	2.2	8.9
91.0	2.3	-32.1	0.2	2.8	10.9
91.5	2.1	-31.1	0.2	2.2	10.2
92.0	3.1	-31.8	0.3	2.1	9.9
92.5	3.6	-32.0	0.4	1.8	9.1
93.0	3.2	-33.5	0.3	2.5	10.5
93.5	2.4	-32.8	0.3	2.2	9.4
94.0	1.8	-33.5	0.2	3.2	10.6
94.5	1.1	-31.5	0.1	2.2	9.3
95.0	1.1	-31.9	0.1	3.2	10.4
95.5	0.8	-29.2	0.1	2.8	10.1
96.0	1.0	-26.6	0.1	2.5	8.7
96.5	0.9	-27.0	0.1	3.0	9.3
97.5	0.8	-27.6	0.1	3.2	11.0
98.0	0.7	-25.6	0.1	2.3	8.7
98.5	0.8	-24.6	0.1	2.1	8.3
99.0	0.7	-28.1	0.1	3.0	10.0

Depth (cm)	Organic C (%)	$\delta^{13}C$	N (%)	$\delta^{15}N$	C/N
99.5	0.7	-27.6	0.1	3.8	9.1
100.0	0.7	-27.3	0.1	3.4	9.1
100.5	0.9	-27.1	0.1	3.4	9.0
101.0	1.0	-28.3	0.1	2.2	10.2
101.5	0.8	-29.7	0.1	2.8	9.1
102.0	0.8	-28.1	0.1	2.6	9.1
102.5	1.0	-28.7	0.1	2.9	9.2
103.0	0.8	-28.8	0.1	3.1	10.7
103.5	1.1	-28.7	0.1	2.3	8.9
104.0	2.0	-23.5	0.3	0.8	6.7
104.5	2.5	-23.8	0.4	0.8	5.8
105.0	1.2	-28.1	0.1	2.3	9.2
105.5	1.0	-28.5	0.1	3.1	9.6
106.0	1.5	-24.9	0.2	1.0	9.6
106.5	3.1	-23.8	0.4	0.7	7.2
107.0	3.4	-24.2	0.4	0.8	8.5
107.5	3.6	-24.2	0.5	0.7	6.9
108.0	4.4	-24.1	0.7	0.8	6.7
108.5	4.0	-25.1	0.6	1.3	6.8
109.0	3.3	-26.3	0.4	1.2	8.0
109.5	3.2	-25.6	0.4	1.9	8.1
110.0	3.7	-25.6	0.5	0.9	8.1
110.5	2.8	-25.0	0.4	1.1	8.0
111.0	3.0	-24.2	0.4	0.3	8.0
111.5	2.7	-24.8	0.4	0.9	7.6
112.0	2.7	-23.4	0.3	-0.2	8.7
112.5	3.3	-23.1	0.4	-1.1	8.1
113.0	5.0	-23.1	0.6	-1.0	7.9
113.5	5.6	-23.2	0.8	-0.4	6.7
114.0	6.1	-23.7	0.9	0.4	7.2
114.5	4.1	-24.2	0.6	-0.3	7.2
115.0	5.0	-24.1	0.7	0.7	6.9
115.5	4.9	-24.4	0.7	0.4	6.7
116.0	4.0	-22.6	0.5	-0.8	8.6

Depth (cm)	Organic C (%)	$\delta^{13}C$	N (%)	$\delta^{15}N$	C/N
116.5	5.7	-22.3	1.0	-0.5	5.8
117.5	5.2	-23.3	0.9	-0.3	5.9
118.0	5.5	-23.7	0.8	-0.1	7.2
118.5	5.0	-23.1	0.7	-0.8	7.3
119.0	6.0	-23.8	0.8	-0.9	7.4
119.5	5.1	-23.2	0.7	-0.8	7.3
120.0	6.3	-23.9	0.8	-0.4	7.6
120.5	5.0	-23.1	0.7	-1.0	7.6
121.0	5.6	-22.9	0.7	0.0	7.8
121.5	3.5	-24.1	0.5	-0.1	7.4
122.0	4.0	-23.9	0.5	-0.5	8.0
122.5	4.0	-23.7	0.6	-0.7	7.2
123.5	3.3	-23.8	0.4	-0.8	7.4
124.0	3.9	-23.7	0.5	-0.3	7.4
124.5	4.2	-24.1	0.6	-1.1	7.3
124.5	4.0	-23.9	0.6	-1.6	7.3
125.0	4.0	-24.4	0.5	-0.8	7.9
125.5	4.0	-24.9	0.6	-0.8	7.0
126.0	3.9	-25.9	0.4	-0.5	9.9
126.5	4.0	-26.2	0.6	-0.4	6.8
127.5	2.9	-26.8	0.4	1.0	6.8
128.0	2.5	-27.4	0.4	1.3	7.1
128.5	1.6	-27.2	0.2	1.2	6.7
129.0	0.8	-28.7	0.1	1.4	8.8
129.5	0.2	-27.7	0.0	-0.6	7.5
130.0	0.6	-27.1	0.1	1.0	8.1
130.5	0.6	-27.5	0.1	1.3	8.0
131.0	0.4	-27.1	0.0	-1.0	9.3
131.5	0.3	-27.1	0.0	0.9	9.7
132.0	0.3	-26.7			
132.5	0.5	-27.0	0.1	1.2	8.7
133.5	0.7	-26.3	0.1	1.6	7.8
134.0	0.9	-25.9	0.1	1.1	8.1

APPENDIX J

ELEMENTAL ANALYSIS DATA: SS6

SS6-3

Depth (cm)	N (%)	$\delta^{15}N$	Organic C (%)	$\delta^{13}C$	C/N
0.50	0.5	3.7	4.4	-33.2	8.2
1.50	0.5	3.7	4.0	-33.7	7.8
2.50	0.6	2.6	4.3	-33.0	7.3
3.50	0.5	3.8	3.2	-33.4	6.8
4.50	0.4	2.3	3.3	-33.0	7.6
5.25	0.4	3.1	3.1	-32.9	8.1
6.25	0.4	3.9	2.9	-32.1	7.4
7.25	0.4	1.7	2.7	-30.8	7.6
8.25	0.3	4.7	2.0	-27.9	7.5
9.25	0.4	1.5	2.3	-27.0	6.5
10.25	0.3	1.8	2.3	-28.1	7.5
11.25	0.3	3.4	2.0	-28.5	7.5
12.25	0.4	1.1	2.5	-28.0	7.1
13.25	0.5	2.6	3.6	-28.6	6.8
14.25	0.7	2.0	4.3	-29.6	6.3
15.25	0.9	2.6	6.5	-28.9	7.5
16.25	0.5	3.7	3.4	-28.8	7.4
16.50	0.5	2.7	3.3	-28.1	7.2
17.25	0.7	2.5	4.9	-28.7	7.5
18.00	0.9	5.4	6.6	-28.5	7.2
19.00	0.7	0.9	5.5	-28.3	7.7
19.75	1.0	2.0	7.5	-28.6	7.6
21.00	0.9	2.1	6.9	-28.4	7.5
22.00	1.2	1.9	8.8	-28.7	7.3
23.00	1.4	1.3	9.9	-28.3	7.1
24.00	0.9	1.7	6.5	-28.2	7.2
25.00	1.0	2.1	7.5	-29.1	7.7
26.00	1.2	1.7	7.7	-28.8	6.5
27.00	0.9	1.5	6.2	-28.6	6.7
28.00	0.5	1.6	4.1	-28.8	7.5
29.00	0.9	2.7	5.7	-28.3	6.7
30.50	0.6	2.3	5.0	-29.1	8.2
31.50	0.4	1.8	3.3	-28.6	7.9
33.50	0.6	2.3	5.8	-28.6	10.4
34.50	0.7	1.7	8.9	-29.3	12.5
35.00	0.7	1.9	9.2	-29.1	12.8
36.50	0.5	2.1	4.2	-28.3	9.0
37.75	0.7	3.2	5.8	-29.5	8.7
38.50	1.0	2.7	7.1	-28.1	7.3
39.75	0.6	2.8	5.5	-29.1	8.9
41.00	0.8	2.8	6.4	-30.3	8.2
41.75	1.1	3.1	8.3	-29.6	7.8
43.00	1.9	1.6	10.3	-28.1	5.5
44.00	1.5	3.0	11.3	-28.6	7.4
45.00	2.1	1.2	14.0	-28.4	6.6
46.00	1.8	1.2	10.8	-28.0	5.9

Depth (cm)	N (%)	$\delta^{15}N$	Organic C (%)	$\delta^{13}C$	C/N
47.25	1.5	1.0	9.8	-27.8	6.4
48.00	2.5	1.1	14.2	-27.6	5.7
49.00	0.7	0.0	5.2	-27.9	7.6
50.50	0.9	3.2	7.5	-30.2	8.0
51.25	1.1	3.2	8.0	-32.0	7.4
52.25	2.1	3.4	13.4	-28.5	6.3
53.50	2.0	2.4	12.2	-30.5	6.0
54.50	1.5	2.3	11.4	-30.7	7.5
55.00	0.6	1.8	6.2	-30.1	10.9
56.00	1.3	2.8	9.0	-31.7	7.0
57.00	2.2	2.8	13.2	-30.8	6.1
58.00	0.8	3.4	5.8	-30.7	7.2
58.50	2.1	1.8	15.1	-30.4	7.2
59.00	1.3	2.4	10.4	-29.6	7.9
60.25	1.3	3.6	10.9	-31.4	8.3
61.25	1.4	2.2	10.0	-28.8	7.3
62.25	2.3	2.0	15.2	-28.6	6.5
63.00	1.3	2.7	10.7	-31.2	8.2
63.20	0.6	1.8	4.7	-30.1	7.9
64.00	0.6	2.6	5.3	-31.3	8.8
66.00	1.9	3.3	17.2	-30.3	9.0
66.25	1.2	2.6	8.4	-31.2	7.3
67.00	1.6	1.3	11.3	-28.4	7.3
68.00	1.8	2.7	12.6	-29.0	6.9
68.25	0.8	1.9	6.2	-31.7	7.6
69.00	2.4	1.4	12.6	-28.4	5.2
70.00	0.8	0.9	5.9	-27.4	7.3
71.00	1.1	1.6	8.1	-27.7	7.5
71.25	2.3	1.8	20.0	-32.3	8.6
72.00	1.1	2.0	8.8	-30.6	8.3
73.10	0.7	1.7	6.2	-29.0	8.3
73.25	2.2	0.9	17.2	-30.9	7.7
74.20	1.1	1.3	8.4	-28.6	7.7
75.00	1.9	1.2	13.1	-28.0	7.0
76.00	2.2	1.0	13.4	-26.7	6.2
78.25	0.9	2.5	7.0	-28.6	7.4
79.25	1.8	2.7	12.2	-28.9	6.6
80.25	0.9	3.0	7.6	-29.4	8.8
81.50	1.2	2.6	8.4	-28.9	7.0
82.25	0.6	1.8	4.6	-28.4	8.4
82.50	1.1	2.2	8.6	-29.4	8.1
83.50	1.4	1.8	9.2	-27.4	6.8
84.50	1.6	2.5	11.6	-27.8	7.2
85.50	1.6	2.4	13.9	-30.9	8.8
86.75	1.8	2.9	11.9	-31.5	6.8
87.50	1.4	2.7	11.1	-31.0	8.2
88.50	2.0	0.6	13.7	-27.3	6.7
89.50	1.6	0.7	12.7	-27.9	7.9
90.20	1.6	1.1	11.8	-26.5	7.3
91.00	1.3	1.2	9.4	-27.2	7.4

Depth (cm)	N (%)	δ15N	Organic C (%)	δ13C	C/N
92.25	1.1	2.5	9.5	-29.0	8.4
93.50	1.8	1.7	14.7	-30.1	8.3

SS6-4

Depth (cm)	N (%)	δ15N	Organic C (%)	δ13C	C/N
39.75	1.3	2.8	11.6	-28.9	8.6
41.00	0.8	2.5	7.2	-29.5	8.6
42.00	1.2	2.4	9.1	-29.5	7.3
43.00	1.1	2.5	9.2	-30.3	8.5
43.75	1.4	0.3	10.4	-27.8	7.5
45.00	1.3	2.4	10.6	-28.5	8.5
46.00	1.0	2.7	8.6	-29.2	8.5
47.00	1.8	2.4	14.0	-30.8	7.6
48.00	2.0	2.8	13.7	-31.6	7.0
49.00	1.4	2.4	11.7	-30.5	8.4
50.50	1.7	1.0	11.4	-26.7	6.7
51.50	1.7	1.5	11.5	-28.4	6.9
52.50	2.3	0.7	16.3	-26.5	7.1
53.50	2.1	2.3	13.9	-28.1	6.6
54.50	1.5	2.8	11.3	-28.4	7.5
54.50	1.4	2.5	10.8	-28.4	7.5
55.50	2.0	2.1	16.3	-29.5	8.2
56.50	1.8	1.8	11.9	-31.3	6.7
56.50	1.9	0.4	14.2	-29.5	7.6
57.50	1.4	2.4	11.8	-30.4	8.2
58.50	2.3	2.0	14.6	-30.7	6.5
58.50	2.3	2.2	14.3	-30.7	6.1
59.50	1.4	2.0	11.7	-30.2	8.2
60.25	1.5	1.6	11.4	-28.6	7.8
61.25	1.8	2.1	12.7	-30.8	7.0
63.20	0.8		7.0	-29.8	8.4
65.25	1.2	2.0	9.3	-30.7	7.9
66.25	0.9	3.4	7.2	-30.6	8.1
67.25	1.2	1.6	9.3	-31.1	7.5
68.25	1.0	1.4	8.0	-31.4	8.3
69.25	2.0	2.4	12.7	-30.3	6.5
70.25	0.9	1.4	8.7	-31.3	9.2
71.25	0.9	1.7	8.7	-32.4	9.2
73.25	0.7	0.9	6.6	-30.6	9.0
74.75	0.6	1.5	6.5	-31.8	11.5

APPENDIX K

RADIOCARBON DATA TABLE: SS6

SS6 Radiocarbon Dates

Core ID	Material	Depth in core (cm)	14C Age (yrs BP)	1 σ
SS6-III	bulk sediment	8.25	1900	30
SS6-III	bulk sediment	15	1570	30
SS6-III	bulk sediment	25.25	1420	45
SS6-III	wood fragment	36.5	650	70
SS6-III	bulk sediment	37	935	35
SS6-III	gastropod shell	44	1050	30
SS6-III	bulk sediment	44	1450	30
SS6-III	bulk sediment	58.25	1950	30
SS6-III	bulk sediment	70	3320	35
SS6-III	bulk sediment	78.5	2920	45
SS6-III	bulk sediment	92.5	3870	35
SS6 IV	leaf	57	3760	150
SS6 IV	bulk sediment	73	5130	35

* AMS 14C analyses performed at NOSAMS, WHOI

APPENDIX L

ALKENONE UNSATURATION DATA: SS6

SS6-3

Depth (cm)	ID	UK37	UK ' 37
0.00	SS6-1d	-0.626	0.079
0.25	SS6-2	-0.617	0.083
0.50	SS6-3	-0.611	0.084
1.00	SS6-5	-0.625	0.079
1.50	SS6-7a	-0.627	0.073
1.75	SS6-8	-0.628	0.074
2.00	SS6-9	-0.621	0.079
2.25	SS6-10	-0.615	0.081
2.50	SS6-11	-0.617	0.075
2.75	SS6-12	-0.602	0.081
3.00	SS6-13	-0.608	0.079
3.25	SS6-14	-0.629	0.071
3.50	SS6-15	-0.643	0.070
3.75	SS6-16	-0.639	0.069
5.00	SS6-21	-0.633	0.070
5.25	SS6-22	-0.637	0.068
5.50	SS6-23	-0.636	0.069
5.75	SS6-24	-0.631	0.068
6.00	SS6-49	-0.623	0.074
6.25	SS6-50	-0.622	0.077
8.25	SS6-58b	-0.604	0.081
8.50	SS6-59	-0.604	0.078
8.75	SS6-60	-0.614	0.080
9.00	SS6-61b	-0.634	0.072
9.25	SS6-62	-0.631	0.081
10.00	SS6-65	-0.642	0.077
10.25	SS6-66	-0.648	0.075
10.50	SS6-67	-0.657	0.071
10.75	SS6-68	-0.660	0.075
11.00	SS6-69	-0.663	0.072
11.25	SS6-70	-0.660	0.074
11.50	SS6-71	-0.662	0.074
11.75	SS6-72	-0.659	0.075
12.00	SS6-73	-0.665	0.075
12.25	SS6-74z	-0.661	0.073
12.50	SS6-75	-0.665	0.072
12.75	SS6-76	-0.659	0.073
13.00	SS6-77	-0.659	0.073
13.25	SS8-78	-0.655	0.074
13.50	SS6-79	-0.654	0.072
13.75	SS6-80	-0.650	0.073
14.00	SS6-81a	-0.633	0.082
14.25	SS6-82	-0.637	0.079
14.50	SS6-83	-0.634	0.079
14.75	SS6-84	-0.633	0.077
15.00	SS6-85	-0.631	0.078
15.25	SS6-86z	-0.641	0.070
15.50	SS6-87	-0.636	0.076

Depth (cm)	ID	UK37	UK ' 37
15.75	SS6-88	-0.637	0.074
16.00	SS6-89	-0.643	0.076
16.25	SS6-90	-0.643	0.076
16.50	SS6-91	-0.637	0.085
16.75	SS6-92	-0.648	0.076
17.00	SS6-93	-0.646	0.075
17.25	SS6-94	-0.647	0.078
17.50	SS6-95	-0.642	0.078
17.75	SS6-96	-0.636	0.081
18.00	SS6-97	-0.638	0.079
18.25	SS6-98	-0.621	0.076
18.50	SS6-99	-0.613	0.081
19.00	SS6-100	-0.626	0.079
19.25	SS6-101	-0.630	0.078
19.50	SS6-102	-0.634	0.078
19.75	SS6-103	-0.640	0.077
20.00	SS6-104	-0.647	0.078
20.25	SS6-105	-0.660	0.072
20.50	SS6-106	-0.659	0.068
21.00	SS6-107	-0.660	0.069
21.25	SS6-108	-0.653	0.078
21.50	SS6-109	-0.646	0.079
21.75	SS6-110	-0.634	0.080
22.00	SS6-111	-0.633	0.082
22.75	SS6-112	-0.637	0.081
23.00	SS6-113	-0.636	0.079
23.25	SS6-25	-0.648	0.071
23.50	SS6-26	-0.652	0.070
23.75	SS6-27	-0.648	0.076
24.00	SS6-28	-0.654	0.071
24.25	SS6-29	-0.650	0.070
24.50	SS6-30	-0.650	0.075
24.75	SS6-31	-0.644	0.074
25.00	SS6-32	-0.643	0.076
25.25	SS6-33	-0.636	0.077
25.50	SS6-34	-0.647	0.075
25.75	SS6-35	-0.658	0.071
26.00	SS6-36	-0.660	0.072
26.50	SS6-37	-0.663	0.072
26.75	SS6-38	-0.653	0.075
27.00	SS6-39	-0.656	0.072
27.25	SS6-40	-0.655	0.075
27.50	SS6-41	-0.649	0.076
27.75	SS6-42	-0.640	0.076
28.00	SS6-43	-0.645	0.078
28.25	SS6-44	-0.651	0.074
28.50	SS6-45	-0.648	0.075
28.75	SS6-46	-0.646	0.075
29.00	SS6-47	-0.646	0.075

Depth (cm)	ID	UK37	UK ' 37
29.25	SS6-48	-0.644	0.074
29.50	SS6-114	-0.639	0.072
29.75	SS6-115	-0.639	0.072
30.00	SS6-116	-0.644	0.073
30.25	SS6-117	-0.653	0.072
30.50	SS6-118	-0.651	0.073
30.75	SS6-119	-0.646	0.074
31.00	SS6-191	-0.652	0.065
31.25	SS6-192	-0.652	0.061
31.50	SS6-193	-0.650	0.064
31.75	SS6-194	-0.651	0.064
32.00	SS6-195	-0.651	0.061
32.25	SS6-196	-0.617	0.075
32.50	SS6-197	-0.625	0.076
33.00	SS6-198	-0.627	0.076
33.50	SS6-199	-0.633	0.073
34.00	SS6-200	-0.633	0.067
34.50	SS6-201	-0.635	0.068
35.00	SS6-202	-0.635	0.075
36.00	SS6-203	-0.631	0.077
36.50	SS6-204	-0.626	0.074
37.00	SS6-205	-0.630	0.073
37.25	SS6-206	-0.629	0.076
37.50	SS6-207	-0.634	0.075
37.75	SS6-208	-0.634	0.077
38.00	SS6-209	-0.633	0.074
38.25	SS6-210	-0.628	0.075
38.50	SS6-211	-0.627	0.075
38.75	SS6-212	-0.625	0.075
39.00	SS6-213	-0.632	0.075
39.50	SS6-215	-0.652	0.071
39.75	SS6-143	-0.662	0.063
40.00	SS6-216	-0.654	0.072
42.00	SS6-127	-0.662	0.073
42.25	SS6-128	-0.659	0.075
42.50	SS6-129d	-0.658	0.075
42.75	SS6-130	-0.663	0.066
43.00	SS6-131	-0.655	0.071
43.25	SS6-132	-0.657	0.064
43.50	SS6-133	-0.653	0.064
43.75	SS6-134	-0.655	0.066
44.00	SS6-135	-0.646	0.067
44.25	SS6-136	-0.661	0.066
44.50	SS6-137	-0.659	0.065
44.75	SS6-138	-0.656	0.071
45.00	SS6-139	-0.660	0.068
45.25	SS6-140	-0.668	0.067
45.50	SS6-141	-0.669	0.066
45.75	SS6-142	-0.669	0.068

Depth (cm)	ID	UK37	UK ' 37
46.00	SS6-144	-0.669	0.067
46.25	SS6-145	-0.669	0.069
46.50	SS6-146	-0.668	0.068
47.25	SS6-147	-0.656	0.065
47.50	SS6-148	-0.657	0.065
48.00	SS6-149	-0.655	0.066
48.25	SS6-150	-0.658	0.063
48.50	SS6-151	-0.680	0.060
48.75	SS6-152	-0.672	0.064
49.75	SS6-156	-0.638	0.070
50.00	SS6-157	-0.653	0.070
50.25	SS6-158	-0.657	0.067
50.50	SS6-159	-0.687	0.065
50.75	SS6-160	-0.686	0.065
51.00	SS6-161a	-0.693	0.064
51.25	SS6-162	-0.691	0.065
51.50	SS6-163	-0.688	0.067
51.75	SS6-164	-0.694	0.065
52.00	SS6-165	-0.679	0.067
52.25	SS6-166	-0.671	0.067
52.50	SS6-167	-0.673	0.064
52.75	SS6-168	-0.673	0.070
53.00	SS6-169	-0.674	0.068
53.25	SS6-170	-0.681	0.071
53.50	SS6-171	-0.688	0.069
55.50	SS6-179	-0.684	0.069
55.75	SS6-180	-0.682	0.070
56.00	SS6-181	-0.681	0.071
56.25	SS6-182	-0.683	0.070
56.50	SS6-183	-0.688	0.067
56.75	SS6-184	-0.682	0.067
57.25	SS6-186	-0.659	0.073
57.50	SS6-187	-0.668	0.071
57.75	SS6-188	-0.654	0.074
58.00	SS6-189	-0.662	0.068
58.25	SS6-190	-0.644	0.072
58.50	SS6-217	-0.650	0.074
58.75	SS6-218	-0.668	0.064
59.00	SS6-219	-0.673	0.070
59.25	SS6-220	-0.671	0.068
59.75	SS6-222	-0.683	0.068
60.00	SS6-223	-0.672	0.072
60.25	SS6-224	-0.660	0.073
60.50	SS6-225	-0.670	0.072
60.75	SS6-226	-0.679	0.066
61.00	SS6-227	-0.671	0.069
61.25	SS6-228	-0.660	0.071
61.40	SS6-229	-0.657	0.070
61.60	SS6-230	-0.658	0.064

Depth (cm)	ID	UK37	UK ' 37
61.75	SS6-231	-0.655	0.070
62.00	SS6-232	-0.655	0.071
62.25	SS6-233	-0.657	0.073
62.40	SS6-234	-0.677	0.069
62.75	SS6-235	-0.683	0.067
63.00	SS6-236	-0.675	0.069
63.25	SS6-237	-0.681	0.068
63.50	SS6-238	-0.681	0.069
63.75	SS6-239	-0.679	0.068
64.00	SS6-240	-0.676	0.066
64.25	SS6-241	-0.677	0.067
64.50	SS6-242	-0.647	0.075
64.75	SS6-243	-0.636	0.077
66.00	SS6-244	-0.644	0.075
66.25	SS6-245	-0.624	0.079
66.50	SS6-246	-0.628	0.080
66.75	SS6-247	-0.638	0.078
67.00	SS6-248	-0.641	0.070
67.25	SS6-249	-0.648	0.071
67.50	SS6-250	-0.645	0.074
67.75	SS6-251a	-0.648	0.073
67.75	SS6-251b	-0.651	0.068
67.75	SS6-251	-0.650	0.071
68.00	SS6-252	-0.646	0.074
68.25	SS6-253	-0.637	0.076
68.50	SS6-254	-0.640	0.072
70.75	SS6-263	-0.682	0.068
71.00	SS6-264	-0.631	0.093
71.25	SS6-265	-0.639	0.073
71.50	SS6-266	-0.651	0.072
71.75	SS6-267	-0.650	0.064
72.25	SS6-269	-0.674	0.070
72.75	SS6-271	-0.658	0.071
72.90	SS6-272	-0.639	0.074
73.10	SS6-273	-0.654	0.071
73.25	SS6-274	-0.661	0.072
73.50	SS6-275	-0.635	0.076
73.70	SS6-276	-0.643	0.072
73.90	SS6-277	-0.640	0.075
74.20	SS6-278	-0.624	0.080
75.00	SS6-279	-0.631	0.075
75.25	SS6-280	-0.638	0.074
75.50	SS6-281	-0.611	0.081
75.75	SS6-282	-0.638	0.069
76.00	SS6-283	-0.623	0.072
76.25	SS6-284	-0.622	0.079
76.50	SS6-285	-0.639	0.067
76.75	SS6-286	-0.630	0.078
77.00	SS6-287	-0.634	0.078

Depth (cm)	ID	UK37	UK ' 37
77.50	SS6-289	-0.648	0.070
78.25	SS6-292	-0.621	0.073
78.50	SS6-293	-0.605	0.095
78.75	SS6-294	-0.625	0.076
79.00	SS6-295	-0.661	0.071
79.25	SS6-296	-0.675	0.069
79.50	SS6-297	-0.685	0.068
79.75	SS6-298	-0.668	0.067
80.00	SS6-299	-0.686	0.047
80.25	SS6-300	-0.686	0.049
81.50	SS6-301	-0.684	0.048
81.75	SS6-302	-0.646	0.059
82.00	SS6-303	-0.680	0.053
82.25	SS6-304	-0.682	0.054
82.50	SS6-305	-0.689	0.050
82.75	SS6-306	-0.665	0.050
83.25	SS6-307	-0.662	0.049
83.50	SS6-308	-0.673	0.048
83.75	SS6-309	-0.688	0.052
84.00	SS6-310	-0.692	0.047
84.25	SS6-311	-0.693	0.047
84.50	SS6-312	-0.689	0.043
84.75	SS6-313	-0.681	0.050
85.00	SS6-314	-0.677	0.055
85.25	SS6-315	-0.680	0.054
85.50	SS6-316	-0.667	0.057
85.75	SS6-317	-0.669	0.057
86.75	SS6-318	-0.648	0.060
87.00	SS6-319	-0.645	0.061
87.25	SS6-320	-0.651	0.060
87.50	SS6-321	-0.658	0.059
87.75	SS6-322	-0.667	0.059
88.00	SS6-323	-0.668	0.063
88.25	SS6-324	-0.674	0.061
88.50	SS6-325	-0.679	0.061
88.75	SS6-326	-0.673	0.060
89.00	SS6-327	-0.667	0.061
89.25	SS6-328	-0.675	0.058
89.50	SS6-329	-0.671	0.065
89.75	SS6-330	-0.657	0.068
90.20	SS6-331	-0.643	0.070
90.50	SS6-332	-0.639	0.066
90.75	SS6-333	-0.651	0.064
91.00	SS6-334	-0.652	0.064
91.50	SS6-335	-0.648	0.069
91.75	SS6-336	-0.653	0.064
92.00	SS6-337	-0.646	0.072
92.25	SS6-338	-0.650	0.069
92.50	SS6-339	-0.649	0.071

Depth (cm)	ID	UK37	UK ' 37
92.75	SS6-340	-0.659	0.067
93.00	SS6-341	-0.666	0.066
93.00	SS6-341b	-0.666	0.066

Depth (cm)	ID	UK37	UK ' 37
93.00	SS6-341	-0.666	0.066
93.25	SS6-342	-0.657	0.069
93.50	SS6-343	-0.644	0.070

SS6-4

Depth (cm)	ID	UK37	UK ' 37
39.75	SS6-344	-0.678	0.059
40.25	SS6-345	-0.684	0.063
40.50	SS6-346	-0.689	0.063
40.75	SS6-347a	-0.686	0.063
41.00	SS6-348	-0.670	0.064
41.25	SS6-349	-0.673	0.063
41.50	SS6-350	-0.661	0.063
41.75	SS6-351	-0.668	0.064
42.00	SS6-352	-0.674	0.066
42.25	SS6-353	-0.654	0.063
42.50	SS6-354	-0.646	0.063
42.75	SS6-355	-0.667	0.065
43.00	SS6-356	-0.666	0.065
43.25	SS6-357	-0.667	0.068
43.50	SS6-358	-0.661	0.068
43.75	SS6-359	-0.666	0.048
44.00	SS6-360	-0.661	0.048
44.25	SS6-361	-0.666	0.047
44.50	SS6-362	-0.689	0.043
44.75	SS6-363a	-0.691	0.045
45.00	SS6-364	-0.687	0.054
45.25	SS6-365	-0.688	0.054
45.50	SS6-366	-0.683	0.055
45.75	SS6-367	-0.643	0.090
46.00	SS6-368	-0.667	0.058
46.25	SS6-369	-0.671	0.060
46.50	SS6-370	-0.665	0.061
46.75	SS6-371	-0.661	0.060
47.00	SS6-372	-0.661	0.061
47.25	SS6-373	-0.660	0.063
47.50	SS6-374	-0.652	0.065
47.75	SS6-375	-0.633	0.066
48.00	SS6-376a	-0.639	0.067
48.25	SS6-377	-0.644	0.065
48.50	SS6-378	-0.642	0.067
48.75	SS6-379	-0.655	0.064

Depth (cm)	ID	UK37	UK ' 37
49.00	SS6-380	-0.662	0.065
49.25	SS6-381	-0.662	0.065
49.50	SS6-382	-0.663	0.067
49.75	SS6-383	-0.671	0.067
50.00	SS6-406	-0.660	0.073
50.25	SS6-385	-0.669	0.064
50.50	SS6-386	-0.663	0.064
50.75	SS6-387	-0.660	0.065
51.00	SS6-388	-0.669	0.061
51.25	SS6-389	-0.668	0.067
51.50	SS6-390	-0.665	0.070
51.75	SS6-391b	-0.657	0.070
52.00	SS6-392	-0.644	0.073
52.25	SS6-393	-0.633	0.074
52.50	SS6-394	-0.629	0.074
52.75	SS6-395	-0.647	0.071
53.00	SS6-396	-0.645	0.072
53.25	SS6-397	-0.646	0.072
53.50	SS6-398	-0.646	0.072
53.75	SS6-399	-0.645	0.073
54.00	SS6-400	-0.643	0.074
54.25	SS6-401	-0.646	0.075
54.50	SS6-402	-0.646	0.076
54.75	SS6-403	-0.654	0.072
55.00	SS6-404	-0.655	0.073
55.25	SS6-405	-0.663	0.071
55.50	SS6-384	-0.665	0.066
55.75	SS6-407	-0.652	0.070
56.00	SS6-408	-0.641	0.074
56.25	SS6-409	-0.644	0.074
56.50	SS6-410	-0.642	0.074
56.75	SS6-411	-0.637	0.071
58.00	SS6-412	-0.650	0.071
59.00	SS6-413	-0.642	0.073
60.00	SS6-414	-0.647	0.072
61.00	SS6-415	-0.651	0.073
62.00	SS6-416	-0.628	0.080
63.20	SS6-417	-0.615	0.080
64.00	SS6-418	-0.611	0.082

APPENDIX M

WATER COLUMN DISSOLVED INORGANIC CARBON $\delta^{13}C$:

BRAYA SØ, SS6, LIMNÆA SØ

Lake	Depth (m)	DIC $\delta^{13}C$	1σ*
Braya Sø	0.1	1.1	0.15
Braya Sø	5	0.9	0.15
Braya Sø	10	1	0.15
Braya Sø	15	0.5	0.15
Braya Sø	20	0.3	0.15
SS6	0.1	2	0.15
SS6	4	2.1	0.15
SS6	8	2	0.15
SS6	12.5	2.3	0.3
Limnæa Sø	5	2.7	0.3
Limnæa Sø	10	2.9	0.3
Limnæa Sø	15	2.6	0.3
Limnæa Sø	20	2.8	0.3

* Analytical precision

Note: Samples collected June 2007

APPENDIX N

WATER COLUMN DISSOLVED INORGANIC CARBON $\delta^{13}C$ AND DISSOLVED ORGANIC CARBON $\delta^{13}C$: BRAYA SØ

Braya Sø

Depth (m)	**DIC (mg/L)**	**1 σ***	**DIC $\delta^{13}C$**	**1 σ***	**DOC (mg/L)**	**DOC $\delta^{13}C$**
0.4	80.4	0.4	0.5	0.5	34.3	-21.8
1.2	78.5	0.4	0.8	0.5	35.3	-21.8
2.4	129.3	0.4	-0.1	0.5	51.3	-24.6
3.6	196.4	0.4	-0.1	0.5	72.8	-24.3
4.8	165.9	0.4	0.6	0.5	63.9	-23.2
6	216.15	0.4	-0.1	0.5	78.7	-24.4
12	239.2	0.4	-0.6	0.5	83.9	-24.7
20	175.8	0.4	-0.9	0.5	105.2	-23.9

* Indicates analytical precision

Water samples collected 15 June 2005

Analyzed by Chris Osburn, National Research Lab

APPENDIX O

WATER COLUMN METALS DATA: BRAYA SØ

Braya Sø — **Concentrations mg/L**

Depth (m)	B	U	Al	Ba	Ca	Cr	Cu	Fe	Mg	Mn	Ni	K	Na	Sr	V	Zn
2	0.09	0.0011	0.012	0.033	18	0.0014	0.0033	ND	200	0.0011	0.002	160	490	0.39	0.0024	0.005
5	0.13	0.0016	0.0047	0.067	23	0.0022	0.0074	ND	180	0.0022	0.002	140	450	0.35	0.002	0.0068
10	0.12	0.0014	0.0044	0.069	24	0.0024	0.0031	ND	190	0.0034	0.0021	150	470	0.37	0.0024	0.0054
14	0.12	0.0015	0.0032	0.049	25	0.0023	0.0024	ND	200	0.0011	0.002	160	490	0.39	0.0024	0.005
17	0.12	0.0015	0.004	0.051	24	0.002	0.0017	ND	190	0.0014	0.0021	160	470	0.37	0.0015	0.005
20	0.12	0.0014	0.003	0.05	23	0.0025	0.0012	ND	200	0.024	0.0017	160	490	0.38	0.0027	0.0037
10*	0.12	0.0016	0.0035	0.054	25	0.0038	0.0099	0	200	0.0044	0.0021	170	490	0.4	0.0012	0.0048

Upper Braya

Depth (m)	B	U	Al	Ba	Ca	Cr	Cu	Fe	Mg	Mn	Ni	K	Na	Sr	V	Zn
2	0.059	0	0.0081	0.058	30	0.0013	0.0019	0.15	31	0.0031	0.0012	21	50	0.14	0.0027	0.0078
6	0.05	0	0.0084	0.054	41	0.0012	0.0019	0.22	37	0.0035	0.0024	23	57	0.17	0.0023	0.0065

* Western basin in Braya Sø
Samples collected June 28, 2007

APPENDIX P

WATER COLUMN PROFILES FOR CORED LAKES: APRIL 2006

Lake	Date	Depth (m)	Temp (degC)	Cond (µS)	DO (%)	pH	Chl (µg/L)
Braya Sø	21-Apr-06	0.5	1.28	3367	48.1	8.84	4
Braya Sø	21-Apr-06	1	1.39	3371	48.4	8.84	4
Braya Sø	21-Apr-06	1.5	1.39	3372	48.4	8.84	4
Braya Sø	21-Apr-06	2	1.39	3373	48.3	8.83	4
Braya Sø	21-Apr-06	2.5	1.4	3374	48.4	8.84	4
Braya Sø	21-Apr-06	3	1.4	3374	48.4	8.83	4.5
Braya Sø	21-Apr-06	4	1.4	3372	48.3	8.83	4.5
Braya Sø	21-Apr-06	5	1.4	3371	48.2	8.84	4.1
Braya Sø	21-Apr-06	6	1.4	3369	48.3	8.83	4.1
Braya Sø	21-Apr-06	7	1.42	3368	48.1	8.83	4
Braya Sø	21-Apr-06	8	1.46	3364	47.8	8.83	4.2
Braya Sø	21-Apr-06	9	1.53	3363	46.4	8.83	3.9
Braya Sø	21-Apr-06	10	1.55	3360	44.2	8.84	4
Braya Sø	21-Apr-06	11	2.3	3354	26.9	8.81	5
Braya Sø	21-Apr-06	12	3.24	3416	1.7	8.76	14.9
Braya Sø	21-Apr-06	13	3.61	3447	1.7	8.74	23
Braya Sø	21-Apr-06	14	3.81	3461	1.8	8.73	25.9
Braya Sø	21-Apr-06	15	3.83	3458	2	8.73	25.4
Braya Sø	21-Apr-06	16	3.82	3451	2.3	8.71	27.8
Braya Sø	21-Apr-06	17	3.8	3448	2.5	8.69	31
Braya Sø	21-Apr-06	18	3.78	3443	2.9	8.7	31.9
Braya Sø	21-Apr-06	19	3.77	3440	3.2	8.68	34.1
Braya Sø	21-Apr-06	20	3.43	3430	4	8.68	34.1
Braya Sø	21-Apr-06	21	3.77	3422	4.8	8.65	36.9

Lake	Date	Depth (m)	Temp (degC)	Sal (ppt)	Cond (µS)	DO (mg/L)	pH	Chl (µg/l)	Flourescence (%)
Limnæa Sø	22-Apr-06	0.5	0.79	2.64	5010	10.29	9	4.5	0.9
Limnæa Sø	22-Apr-06	1	0.84	2.63	5000	10.28	9	4.1	0.8
Limnæa Sø	22-Apr-06	1.5	0.84	2.63	5000	10.28	9	4.3	0.9
Limnæa Sø	22-Apr-06	2	0.84	2.63	5000	10.28	9	4.6	1
Limnæa Sø	22-Apr-06	2.5	0.84	2.63	5000	10.29	9	4.7	1.1
Limnæa Sø	22-Apr-06	3	0.84	2.63	5000	10.27	9	5.2	1.1
Limnæa Sø	22-Apr-06	3.5	0.84	2.63	5000	10.27	9	5.4	1.2
Limnæa Sø	22-Apr-06	4	0.84	2.63	5000	10.25	9	5.1	1.1
Limnæa Sø	22-Apr-06	4.5	0.84	2.63	5000	10.24	9	5	1.1
Limnæa Sø	22-Apr-06	5	0.84	2.63	4990	10.25	9	5	1.1
Limnæa Sø	22-Apr-06	5.5	0.84	2.63	4990	10.24	9	5	1.1
Limnæa Sø	22-Apr-06	6	0.84	2.63	4990	10.22	9	5	1.2
Limnæa Sø	22-Apr-06	6.5	0.84	2.63	4990	10.22	9	4.6	1.1
Limnæa Sø	22-Apr-06	7	0.84	2.63	4990	10.22	9.01	4.8	1.1
Limnæa Sø	22-Apr-06	7.5	0.85	2.63	4990	10.2	9	4.1	1.1
Limnæa Sø	22-Apr-06	8	0.85	2.63	4990	10.2	9	4.4	1
Limnæa Sø	22-Apr-06	8.5	0.89	2.63	4990	10.21	9	4.9	1.1
Limnæa Sø	22-Apr-06	9.5	0.92	2.63	4990	10.16	9	4.8	1.1
Limnæa Sø	22-Apr-06	10	0.94	2.63	4990	10.2	9.01	4.5	1
Limnæa Sø	22-Apr-06	10.5	0.98	2.63	4990	9.97	9.01	4.8	1.1
Limnæa Sø	22-Apr-06	11	1.25	2.63	4990	9.65	9.01	4.2	1.1
Limnæa Sø	22-Apr-06	11.5	1.32	2.64	5000	8.82	9.02	4.6	1.1
Limnæa Sø	22-Apr-06	12	1.85	2.03	4990	7.81	9.01	4.5	1.1
Limnæa Sø	22-Apr-06	12.5	2.25	2.64	5000	6.7	9.01	4.4	1
Limnæa Sø	22-Apr-06	13	2.84	2.64	4980	5.19	9	4.3	1
Limnæa Sø	22-Apr-06	13.5	3.14	2.66	5000	4.86	9	4	0.9
Limnæa Sø	22-Apr-06	14	3.75	2.68	5020	4.98	9	3.6	0.9
Limnæa Sø	22-Apr-06	14.5	3.89	2.69	5040	4.91	9	3.3	0.9
Limnæa Sø	22-Apr-06	15	3.93	2.69	5040	4.8	9	3.6	0.8
Limnæa Sø	22-Apr-06	15.5	3.93	2.69	5040	4.75	9	3.4	0.8
Limnæa Sø	22-Apr-06	16	3.93	2.69	5040	4.72	9	3.6	0.8
Limnæa Sø	22-Apr-06	16.5	3.91	2.69	5040	4.65	9	3.3	0.8
Limnæa Sø	22-Apr-06	17	3.9	2.69	5040	4.54	9	3	0.8

Lake	Date	Depth (m)	Temp (degC)	Sal (ppt)	Cond (µS)	DO (mg/L)	pH	Chl (µg/l)	Flourescence (%)
Limnæa Sø	22-Apr-06	17.5	3.87	2.63	5040	4.33	9	3.6	0.8
Limnæa Sø	22-Apr-06	18	3.83	2.63	5040	3.98	9	3.5	0.8
Limnæa Sø	22-Apr-06	18.5	3.82	2.63	5040	3.8	9	3.2	0.8
Limnæa Sø	22-Apr-06	19	3.79	2.69	5040	3.49	9	3.5	0.8
Limnæa Sø	22-Apr-06	19.5	3.77	2.69	5040	3.43	9	3.3	0.7
Limnæa Sø	22-Apr-06	21	3.74	2.69	5040	3.45	9	3.4	0.8
Limnæa Sø	22-Apr-06	21.5	3.74	2.68	5030	3.38	9	3.8	0.8
Limnæa Sø	22-Apr-06	22	3.74	2.68	5030	3.38	9	3.8	0.7
Limnæa Sø	22-Apr-06	22.5	3.74	2.68	5030	3.19	9	3.2	0.7
Limnæa Sø	22-Apr-06	23	3.74	2.68	5030	3.04	9	3.1	0.7
Limnæa Sø	22-Apr-06	23.5	3.74	2.68	5030	2.89	9	3.2	0.7
Limnæa Sø	22-Apr-06	24	3.75	2.68	5020	2.71	9	3.4	0.8
Limnæa Sø	22-Apr-06	24.5	3.76	2.68	5020	2.39	9	3.7	0.8
Limnæa Sø	22-Apr-06	25	3.81	2.67	5020	1.43	8.99	2.8	0.8
Limnæa Sø	22-Apr-06	25.5	3.83	2.67	5010	0.64	8.98	3	0.6
Limnæa Sø	22-Apr-06	26	3.84	2.67	5000	0.16	8.98	4	0.8
Limnæa Sø	22-Apr-06	26.5	3.84	2.66	5000	0.16	8.98	3.5	0.8
Limnæa Sø	22-Apr-06	27	3.85	2.66	4990	0.18	8.97	3.7	0.9
Limnæa Sø	22-Apr-06	27.5	3.85	2.64	4970	0.28	8.97	3.7	0.8
Limnæa Sø	22-Apr-06	28	3.85	2.64	4950	0.37	8.97	3.6	0.9
Limnæa Sø	22-Apr-06	28.5	3.84	2.63	4950	0.6	8.96	7.7	1.8

Lake	Date	Depth (m)	Temp (degC)	Sal (ppt)	DO (mg/L)	pH	Chl (µg/L)	Cond (µS)	Flourescence (%)
SS7	27-Apr-06	0.4	1.24	0.1	11.46	7.29	28.1	204	6.3
SS7	27-Apr-06	1	3.5	0.12	8.02	7	22.3	257	4.9
SS7	27-Apr-06	1.6	3.51	0.12	7.65	7	20.3	257	4.5
SS7	27-Apr-06	2.5	3.51	0.12	6.88	6.99	19.6	257	4.3
SS7	27-Apr-06	3	3.52	0.12	5.01	6.97	17.6	260	4.1
SS7	27-Apr-06	4	3.66	0.13	1.5	6.99	14.8	272	3.4
SS7	27-Apr-06	5	3.92	0.14	1.48	7.02	13.8	291	3.1
SS7	27-Apr-06	5.3	3.92	0.13	2.86	7.1	13.9	282	3.2

Lake	Date	Depth (m)	Temp (degC)	Sal (ppt)	DO (mg/L)	pH	Chl (µg/L)	Cond (mS)	Flourescence (%)
SS42	24-Apr-06	0.2	0.38	1	8.42	8.28	4.3	1.998	1
SS42	24-Apr-06	1	1.29	0.99	8.1	8.27	4.5	1.979	1
SS42	24-Apr-06	2	1.29	0.99	8.03	8.26	4.7	1.979	1.1
SS42	24-Apr-06	3	1.3	0.99	7.95	8.26	4.7	1.978	1.1
SS42	24-Apr-06	4	1.31	0.99	7.79	8.25	4.3	1.978	1
SS42	24-Apr-06	5	1.33	0.99	7.63	8.24	4.5	1.976	1
SS42	24-Apr-06	6	1.4	0.99	6.74	8.21	4.2	1.976	1
SS42	24-Apr-06	7	1.48	0.99	5.54	8.18	4.5	1.974	1
SS42	24-Apr-06	8	1.68	0.99	4.35	8.08	4.4	1.974	1
SS42	24-Apr-06	9	1.85	1	2.97	8	4.9	1.978	1.1
SS42	24-Apr-06	10	2.06	1	2.26	7.96	6.1	1.983	1.5
SS42	24-Apr-06	10.5	2.12	1	1	7.88	9.4	1.98	2.2
SS42	24-Apr-06	11	2.58	1.04	0.63	7.9	78.2	2.055	15.3
SS42	24-Apr-06	11.5	2.7	1.06	0.37	7.69	16.3	2.072	3.9
SS42	24-Apr-06	12	2.78	1.05	0.85	7.6	8.3	2.075	1.8

Lake	Date	Depth (m)	Temp (degC)	Sal (ppt)	DO (mg/L)	pH	Chl (µg/L)	Cond (mS)	Flourescence (%)
SS71	26-Apr-06	0.6	0.31	1.13	7.81	7.7	5.4	2.252	1.2
SS71	26-Apr-06	1	2.77	1.11	7.79	7.72	5.3	2.194	1.2
SS71	26-Apr-06	2	2.78	1.11	7.68	7.72	5.6	2.192	1.3
SS71	26-Apr-06	3	2.78	1.11	7.69	7.72	5.1	2.189	1.2
SS71	26-Apr-06	4	2.79	1.11	7.61	7.73	5.2	2.186	1.2
SS71	26-Apr-06	5	2.79	1.11	7.47	7.72	5.4	2.182	1.3
SS71	26-Apr-06	6	2.8	1.1	7.21	7.72	5.2	2.17	1.3
SS71	26-Apr-06	7	2.75	1.1	6.72	7.66	5.2	2.179	1.2

Lake	Date	Depth (m)	Temp (degC)	Sal (ppt)		pH	Chl (µg/L)	Cond (mS)	Flourescence (%)
SS1122	25-Apr-06	0.4	0.4	2.24		8.51	6	4.286	1.4
SS1122	25-Apr-06	1	2.27	3.01		8.42	10.1	5.638	2.2
SS1122	25-Apr-06	2	2.27	3.01		8.4	10.3	5.638	2.3
SS1122	25-Apr-06	3	2.29	3		8.37	8	5.63	1.8
SS1122	25-Apr-06	4	2.14	3.02		8.33	9.3	5.658	2.2
SS1122	25-Apr-06	5	2.29	3.21		8.3	79.8	5.996	18
SS1122	25-Apr-06	6	2.81	3.93		7.9	98.8	7.228	22.5
SS1122	25-Apr-06	7	3.06	5.02		7.17	52.2	9.08	11.9
SS1122	25-Apr-06	8	3	5.61		7.05	56.9	10.05	12.9
SS1122	25-Apr-06	9	2.82	5.99		6.99	62.2	10.75	14.1
SS1122	25-Apr-06	10	2.7	6.11		6.98	65.2	10.96	14.8
SS1122	25-Apr-06	11	2.59	6.16		7	70.1	11.05	15.9
SS1122	25-Apr-06	12	2.55	6.14		7.05	63.2	11.01	14.3
SS1122	25-Apr-06	13	2.51	6.1		7.12	47.9	10.94	10.8
SS1122	25-Apr-06	14	2.49	5.97		7.18	50.3	10.74	13

Lake	Date	Depth (m)	Temp (degC)	Sal (ppt)	DO (mg/L)	pH	Chl (μg/L)	Cond (mS)	Flourescence (%)
SS1164	25-Apr-06	0.1	0.32	0.82	3.43	7.42	3.3	1.663	0.7
SS1164	25-Apr-06	0.5	0.94	0.87	3.8	7.45	3.2	1.745	0.7
SS1164	25-Apr-06	0.75	2.76	1.09	4.03	7.42	4.1	2.118	0.9
SS1164	25-Apr-06	1.1	3.63	1.2	4.83	7.46	4.5	2.346	1
SS1164	25-Apr-06	2	3.66	1.2	4.72	7.46	4.1	2.347	1
SS1164	25-Apr-06	3	3.67	1.2	4.57	7.46	5.1	2.35	1.1
SS1164	25-Apr-06	4	3.68	1.2	4.6	7.45	4.1	2.351	0.9
SS1164	25-Apr-06	5	3.62	1.2	3.9	7.43	4.3	2.355	1.9
SS1164	25-Apr-06	6	2.97	1.22	1.25	7.32	11.4	2.407	2.7
SS1164	25-Apr-06	7	2.84	1.27	0	7.33	71	2.487	16.8
SS1164	25-Apr-06	8	3.17	1.31	0	7.29	138.5	2.559	31.2
SS1164	25-Apr-06	9	3.31	1.37	0.06	7.2	43.6	2.671	9.8
SS1164	25-Apr-06	10	3.26	1.4	0.1	7.18	38.4	2.732	7.6
SS1164	25-Apr-06	11	3.17	1.45	0.23	7.16	28.3	2.814	6.4
SS1164	25-Apr-06	12	3.07	1.47	0.32	7.14	26.7	2.854	5.9
SS1164	25-Apr-06	13	3.02	1.48	0.36	7.15	27.9	2.869	6.3
SS1164	25-Apr-06	14	2.95	1.48	0.5	7.14	28.5	2.884	6.5
SS1164	25-Apr-06	15	2.93	1.49	0.63	7.15	30.8	2.89	7
SS1164	25-Apr-06	16	2.98	1.49	0.77	7.15	29.9	2.887	6.8

Lake	Date	Depth (m)	Temp (degC)	Sal (ppt)	DO (mg/L)	pH	Chl (µg/L)	Cond (mS)	Flourescence (%)
SS1371	25-Apr-06	0.2	0.23	2.52	4.5	8.99	33	4.821	7.4
SS1371	25-Apr-06	1	1.04	2.69	4.26	8.68	16.9	5.1	4
SS1371	25-Apr-06	2	1.04	2.69	4.2	8.68	17.7	5.094	3.9
SS1371	25-Apr-06	3	1.04	2.68	4.2	8.67	16.9	5.09	3.9
SS1371	25-Apr-06	4	1.04	2.68	3.66	8.68	17.1	5.092	3.9
SS1371	25-Apr-06	5	1.18	2.69	3.8	8.67	24.6	5.107	5.5
SS1371	25-Apr-06	6	1.4	2.83	0	8.65	65.8	5.34	15
SS1371	25-Apr-06	7	1.91	2.91	0	8.5	66	5.485	19.6
SS1371	25-Apr-06	8	2.15	2.96	0	8.39	65.8	5.564	15
SS1371	25-Apr-06	9	2.27	3.03	0	8.26	63.1	5.666	14.1
SS1371	25-Apr-06	10	2.25	3.09	0.01	8.11	62.4	5.789	14.1
SS1371	25-Apr-06	11	2.21	3.13	0.03	8.04	63.2	5.853	14.4
SS1371	25-Apr-06	12.25	2.2	3.15	0.06	8	66	5.902	15
SS1371	25-Apr-06	13.5	2.19	3.16	0.11	7.99	69.6	5.917	15.6
SS1371	25-Apr-06	14.5	2.19	3.18	0.19	7.95	66.1	5.943	14.9
SS1371	25-Apr-06	15.5	2.19	3.19	0.2	7.92	67.2	5.963	14.7
SS1371	25-Apr-06	16.5	2.2	3.2	0.27	7.91	65.7	5.967	14.9
SS1371	25-Apr-06	17.5	2.2	3.2	0.3	7.91	67.8	5.973	15.1
SS1371	25-Apr-06	18.5	2.2	3.2	0.36	7.89	65.4	5.977	14.8
SS1371	25-Apr-06	19.5	2.21	3.2	0.42	7.87	65.1	5.99	14.9
SS1371	25-Apr-06	20.5	2.24	3.21	0.35	7.85	65.6	6.011	15

Lake	Date	Depth (m)	Temp (degC)	Sal (ppt)	DO (mg/L)	pH	Chl (µg/L)	Cond (mS)	Flourescence (%)
SS1381	23-Apr-06	0.2	0.38	0.33	8.82	7.85	3.8	0.689	0.9
SS1381	23-Apr-06	1	2.17	0.33	8.46	7.85	3.7	0.691	0.9
SS1381	23-Apr-06	2	3.09	0.34	8.32	7.84	3.7	0.695	0.8
SS1381	23-Apr-06	3	3.1	0.34	8.32	7.84	3.7	0.691	0.9
SS1381	23-Apr-06	4	3.11	0.34	8.28	7.83	5.4	0.696	0.9
SS1381	23-Apr-06	5	3.11	0.34	8.28	7.83	4.3	0.697	0.9
SS1381	23-Apr-06	6	3.11	0.34	8.28	7.83	4.2	0.697	1
SS1381	23-Apr-06	7	3.11	0.34	8.26	7.83	4	0.697	0.9
SS1381	23-Apr-06	8	3.11	0.34	8.2	7.82	3.9	0.697	0.8
SS1381	23-Apr-06	9	3.11	0.34	8.08	7.81	3.8	0.698	0.8
SS1381	23-Apr-06	10	3.11	0.34	7.83	7.8	3.7	0.7	0.8
SS1381	23-Apr-06	11	3.11	0.34	7.32	7.75	3.8	0.701	0.8
SS1381	23-Apr-06	12	2.93	0.34	5.26	7.58	3.7	0.708	0.8
SS1381	23-Apr-06	13	2.81	0.35	2.77	7.51	4.3	0.712	0.9
SS1381	23-Apr-06	14	2.76	0.35	2.1	7.52	4	0.73	0.8
SS1381	23-Apr-06	15	2.78	0.35	2.1	7.52	4	0.73	0.8
SS1381	23-Apr-06	16	2.83	0.35	1.43	7.57	4.9	0.72	0.9
SS1381	23-Apr-06	17	2.93	0.36	1.49	7.69	3.7	0.74	0.8
SS1381	23-Apr-06	18	3.01	0.36	2.8	7.81	4.6	0.74	1

Lake	Date	Depth (m)	Temp (degC)	Sal (ppt)	DO (mg/L)	pH	Chl (µg/L)	Cond (µS)	Flourescence (%)
SS1421	23-Apr-06	0.3	0.41	2.5	8.76	8.93	6.1	4772	1.4
SS1421	23-Apr-06	0.75	0.61	2.49	8.72	8.94	7.1	4763	1.6
SS1421	23-Apr-06	1.5	0.82	2.49	8.64	8.93	6.7	4743	1.5
SS1421	23-Apr-06	2	0.83	2.49	8.64	8.93	6.8	4750	1.6
SS1421	23-Apr-06	2.5	0.83	2.49	8.58	8.93	6.6	4750	1.5
SS1421	23-Apr-06	3	0.82	2.49	8.58	8.93	6.6	4750	1.5
SS1421	23-Apr-06	3.5	0.82	2.49	8.47	8.93	6.8	4742	1.7
SS1421	23-Apr-06	4	0.82	2.49	8.29	8.92	6.4	4747	1.5
SS1421	23-Apr-06	4.5	0.85	2.49	7.92	8.92	6.4	4744	1.4
SS1421	23-Apr-06	5	1.11	2.49	6.31	8.92	6.2	4749	1.4
SS1421	23-Apr-06	5.5	1.48	2.5	3.3	8.93	8.4	4752	1.9
SS1421	23-Apr-06	6	2.26	2.58	0.16	8.91	64.2	4877	14.9
SS1421	23-Apr-06	6.5	2.72	2.62	0.16	8.9	196	4936	46.8
SS1421	23-Apr-06	7	3.21	2.63	0.16	8.91	55.9	4989	12.7
SS1421	23-Apr-06	7.5	3.57	2.73	0.17	8.9	34.2	5126	7.8
SS1421	23-Apr-06	8.5	3.87	2.82	0.18	8.84	28	5271	6.3
SS1421	23-Apr-06	9.5	3.94	2.82	0.19	8.77	25.6	5398	5.8
SS1421	23-Apr-06	10.5	3.87	2.92	0.2	8.73	24.5	5446	5.5
SS1421	23-Apr-06	11.5	3.84	2.92	0.21	8.72	24.3	5460	5.4
SS1421	23-Apr-06	12.5	3.8	2.93	0.23	8.7	22.8	5468	5.2
SS1421	23-Apr-06	13.5	3.77	2.93	0.23	8.69	22.9	5475	5.1
SS1421	23-Apr-06	14.5	3.75	2.93	0.24	8.69	22.2	5469	5.1
SS1421	23-Apr-06	15.5	3.75	2.92	0.26	8.68	22.7	5461	5.3
SS1421	23-Apr-06	16.5	3.75	2.92	0.27	8.67	23.1	5455	5.2
SS1421	23-Apr-06	17.5	3.76	2.91	0.29	8.67	23.3	5448	5.2
SS1421	23-Apr-06	18.5	3.75	2.91	0.32	8.67	22.4	5438	5
SS1421	23-Apr-06	19.5	3.74	2.9	0.37	8.67	21.8	5425	5.1
SS1421	23-Apr-06	20.5	3.73	2.89	0.42	8.66	22.2	5406	5.9
SS1421	23-Apr-06	21.5	3.72	2.88	0.5	8.65	21.7	5390	4.9
SS1421	23-Apr-06	22.5	3.7	2.85	0.72	8.63	21.6	5360	4.9

Lake	Date	Depth (m)	Temp (degC)	Sal (ppt)	DO (mg/L)	pH	Chl (µg/L)	Cond (mS)	Flourescence (%)
SS2006	27-Apr-06	0.5	3.86	0.03	13.73	6.96	3.2	0.065	0.8
SS2006	27-Apr-06	1.5	4.14	0.03	13.61	6.92	3.7	0.066	0.9
SS2006	27-Apr-06	2.4	4.15	0.03	13.33	6.9	3.2	0.066	0.7
SS2006	27-Apr-06	3.5	4.17	0.03	12.63	6.85	3.7	0.066	0.8
SS2006	27-Apr-06	4.5	4.2	0.03	9.62	6.81	3.1	0.068	0.7
SS2006	27-Apr-06	5.5	4.21	0.03	7.26	6.76	3	0.077	0.8
SS2006	27-Apr-06	6.5	4.17	0.03	5.59	6.77	3.2	0.076	0.7
SS2006	27-Apr-06	7.4	4.14	0.04	4.23	6.8	3.2	0.077	0.7
SS2006	27-Apr-06	8.3	4.14	0.04	3.55	6.84	3.1	0.078	0.8
SS2006	27-Apr-06	9.2	4.1	0.04	2.65	6.9	3.3	0.08	0.8
SS2006	27-Apr-06	10.35	4.19	0.04	2.27	7.02	3.2	0.083	0.7
SS2006	27-Apr-06	11.6	4.26	0.04	3.3	7.21	3.1	0.087	0.8

Lake	Date	Depth (m)	Temp (degC)	Sal (ppt)	DO (mg/L)	pH	Chl (µg/L)	Cond (mS)	Flourescence (%)
SS2007	28-Apr-06	0.5	1.65	0.02	11.36	7.3	3.5	0.054	0.9
SS2007	28-Apr-06	1.6	4.83	0.04	14.48	7.11	4.3	0.094	1
SS2007	28-Apr-06	2.7	4.59	0.05	14.34	7.06	4.6	0.098	1
SS2007	28-Apr-06	3.6	4.08	0.05	14.2	7.04	7.1	0.098	1.5
SS2007	28-Apr-06	4.7	4.06	0.05	14.22	7.03	8.2	0.098	1.8
SS2007	28-Apr-06	5.3	4.06	0.05	14.16	7.02	7.1	0.098	1.6
SS2007	28-Apr-06	6.5	4.05	0.05	14.03	6.99	7.5	0.098	1.7
SS2007	28-Apr-06	7.6	4.05	0.05	13.93	7.63	7.8	0.098	1.8
SS2007	28-Apr-06	8.3	4.05	0.05	13.21	6.9	7.9	0.098	1.8
SS2007	28-Apr-06	9.5	3.89	0.05	11.42	6.84	6.1	0.101	1.4
SS2007	28-Apr-06	10.3	3.59	0.05	8.75	6.74	6.3	0.109	1.3
SS2007	28-Apr-06	11.5	3.52	0.05	7.5	6.79	5.2	0.114	1.2
SS2007	28-Apr-06	12.4	3.63	0.05	6.7	6.93	6.5	0.116	1.5

APPENDIX Q

Pb-210 CHRONOLOGIES FOR SHORT CORES: BRAYA SØ AND SS6

Sample ID	Upper Depth (cm)	Lower Depth (cm)	Pb-210 Total Activity (DPM/g)	Error Pb-210 +/- 1 S.D. (DPM/g)	Pb-210 Unsup-ported Activity (DPM/g)	Age at Bottom of Extrapolated Section in Years (CRS Model Estimate)	Depth of bottom edge of current section (cm)	DPM/cm^2 in Section	CRS Sediment Accumu-lation Rate (g/cm^2/yr)	Age at Bottom of Extrapolated Section in Years (Linear Regression Model Estimate)
BS (0.25-0.5)	0.25	0.50	27.95	1.65	27.86	3.5	0.6	0.589	0.0060	2.5
BS (0.75-1.0)	0.75	1.00	26.55	0.76	26.45	8.6	1.1	0.739	0.0055	5.9
BS (1.25-1.5)	1.25	1.50	20.05	0.62	19.95	14.2	1.6	0.698	0.0062	10.0
BS (1.75-2.0)	1.75	2.00	13.71	0.42	13.62	21.5	2.1	0.742	0.0075	16.5
BS (2.25-2.5)	2.25	2.50	10.52	0.31	10.43	29.8	2.6	0.662	0.0076	24.1
BS (2.75-3.0)	2.75	3.00	9.04	0.31	8.95	38.3	3.1	0.523	0.0069	31.1
BS (3.25-3.5)	3.25	3.50	6.04	0.28	5.94	46.5	3.6	0.386	0.0080	38.9
BS (3.75-4.0)	3.75	4.00	4.25	0.20	4.16	55.6	4.1	0.331	0.0087	48.4
BS (4.25-4.5)	4.25	4.50	2.09	0.15	2.00	64.1	4.6	0.233	0.0138	62.3
BS (4.75-5.0)	4.75	5.00	1.97	0.14	1.87	76.2	5.1	0.244	0.0107	77.9
BS (5.25-5.5)	5.25	5.50	1.34	0.13	1.25	88.4	5.6	0.168	0.0110	93.9
BS (5.75-6.0)	5.75	6.00	0.93	0.12	0.83	95.5	6.0	0.072	0.0122	104.3
BS (6.0-6.5)	6.00	6.50	0.75	0.09	0.66	105.6	6.5	0.078		118.4
BS (6.5-7.0)	6.50	7.00	0.58	0.09	0.48	122.3	7.3	0.086		139.8
BS (7.5-8.0)	7.50	8.00	0.55	0.09	0.45	158.3	8.3	0.085		162.2
BS (8.5-9.0)	8.50	9.00	0.22	0.07	0.12	181.7	9.3	0.021		183.3
BS (9.5-10.0)	9.50	10.00	0.14	0.07	0.04	197.8	10.0	0.008		206.1

Sample ID	Upper Depth (cm)	Lower Depth (cm)	Po-210 Total Activity (DPM/g)	Error Po-210 +/- 1 S.D. (DPM/g)	Po-210 Unsup-ported Activity (DPM/g)	Age at Bottom of Extrapolated Section in Years (CRS Model Estimate)	Depth of bottom edge of current section (cm)	DPM/cm2 in Section	CRS Sediment Accumu-lation Rate (g/cm2/yr)	Age at Bottom of Extrapolated Section in Years (Linear Regression Model Estimate)
SS6 (0.25-0.5)	0.25	0.50	13.72	0.46	13.20	6.7	0.6	0.742	0.0083	7.3
SS6 (0.75-1.0)	0.75	1.00	12.12	0.34	11.61	16.3	1.1	0.818	0.0074	16.5
SS6 (1.25-1.5)	1.25	1.50	8.52	0.28	8.01	24.8	1.6	0.549	0.0081	25.4
SS6 (1.75-2.0)	1.75	2.00	6.01	0.24	5.50	38.2	2.1	0.621	0.0084	40.1
SS6 (2.25-2.5)	2.25	2.50	3.73	0.18	3.21	51.8	2.6	0.411	0.0094	56.7
SS6 (2.75-3.0)	2.75	3.00	3.38	0.18	2.87	73.0	3.1	0.379	0.0062	73.9
SS6 (3.25-3.5)	3.25	3.50	1.90	0.16	1.39	99.6	3.6	0.229	0.0062	95.4
SS6 (3.75-4.0)	3.75	4.00	0.94	0.10	0.43	119.3	4.1	0.081	0.0096	119.8
SS6 (4.25-4.5)	4.25	4.50	0.78	0.10	0.26	144.3	4.6	0.052	0.0079	145.5
SS6 (4.75-5.0)	4.75	5.00	0.64	0.10	0.13	168.1	5.1	0.023	0.0073	168.2
SS6 (5.25-5.5)	5.25	5.50	0.33	0.08	-0.18		5.6	-0.027		
SS6 (5.75-6.0)	5.75	6.00	0.17	0.07	-0.34		6.0	-0.034		
SS6 (6.0-6.5)	6.00	6.50	0.44	0.08	-0.07		6.5	-0.010		
SS6 (6.5-7.0)	6.50	7.00	0.38	0.08	-0.13		7.3	-0.020		
SS6 (7.5-8.0)	7.50	8.00	0.64	0.10	0.13		8.0	0.020		

APPENDIX R

THERMISTER DATA SUMMER 2006: LIMNÆA SØ AND BRAYA SØ

		Thermistor ID and Water Depth				
		0704	0701	0712	0695	0706
		0m	3m	5m	7m	15m
Lake	**Date**	**Temperature (°C)**				
Limnæa So	4/23/2006	-0.10	0.69	0.70	0.90	3.70
Limnæa So	4/24/2006	-1.20	0.69	0.70	0.88	3.70
Limnæa So	4/25/2006	-4.00	0.70	0.76	0.90	3.70
Limnæa So	4/26/2006	-4.10	0.70	0.78	0.90	3.70
Limnæa So	4/27/2006	-3.98	0.70	0.79	0.90	3.70
Limnæa So	4/28/2006	-2.85	0.70	0.74	0.89	3.70
Limnæa So	4/29/2006	-2.13	0.70	0.75	0.90	3.70
Limnæa So	4/30/2006	-1.71	0.70	0.76	0.90	3.70
Limnæa So	5/1/2006	-1.67	0.71	0.78	0.90	3.70
Limnæa So	5/2/2006	-1.93	0.70	0.77	0.90	3.70
Limnæa So	5/3/2006	-1.69	0.79	0.80	0.93	3.70
Limnæa So	5/4/2006	-2.11	0.74	0.80	0.98	3.70
Limnæa So	5/5/2006	-2.11	0.74	0.79	0.95	3.70
Limnæa So	5/6/2006	-1.28	0.79	0.80	0.98	3.70
Limnæa So	5/7/2006	-0.30	0.80	0.83	0.98	3.69
Limnæa So	5/8/2006	0.20	0.88	0.96	1.07	3.68
Limnæa So	5/9/2006	0.88	1.03	1.05	1.20	3.68
Limnæa So	5/10/2006	0.82	1.22	1.20	1.39	3.65
Limnæa So	5/11/2006	0.50	1.35	1.35	1.54	3.67
Limnæa So	5/12/2006	0.25	1.47	1.54	1.61	3.65
Limnæa So	5/13/2006	0.16	1.60	1.60	1.66	3.68
Limnæa So	5/14/2006	0.13	1.60	1.60	1.73	3.68
Limnæa So	5/15/2006	0.18	1.60	1.60	1.83	3.70
Limnæa So	5/16/2006	0.28	1.70	1.70	1.89	3.70
Limnæa So	5/17/2006	0.40	1.85	1.85	2.03	3.70
Limnæa So	5/18/2006	0.38	1.96	1.97	2.15	3.71
Limnæa So	5/19/2006	0.35	2.07	2.09	2.21	3.70
Limnæa So	5/20/2006	0.27	2.10	2.18	2.28	3.71
Limnæa So	5/21/2006	0.23	2.19	2.20	2.30	3.70
Limnæa So	5/22/2006	0.28	2.20	2.22	2.37	3.64
Limnæa So	5/23/2006	0.36	2.26	2.35	2.48	3.53
Limnæa So	5/24/2006	0.35	2.32	2.36	2.50	3.57
Limnæa So	5/25/2006	0.32	2.31	2.37	2.55	3.59
Limnæa So	5/26/2006	0.35	2.43	2.49	2.65	3.60
Limnæa So	5/27/2006	0.46	2.55	2.58	2.69	3.59
Limnæa So	5/28/2006	0.64	2.63	2.64	2.83	3.60
Limnæa So	5/29/2006	0.68	2.68	2.76	2.90	3.60
Limnæa So	5/30/2006	0.64	2.80	2.87	3.00	3.55
Limnæa So	5/31/2006	0.68	2.96	2.95	3.12	3.50
Limnæa So	6/1/2006	1.41	3.00	3.00	3.18	3.50
Limnæa So	6/2/2006	2.65	3.03	3.06	3.20	3.33
Limnæa So	6/3/2006	3.44	3.28	3.14	3.31	3.48
Limnæa So	6/4/2006	3.08	3.57	3.26	3.39	3.43
Limnæa So	6/5/2006	3.58	3.79	3.30	3.38	3.51
Limnæa So	6/6/2006	4.75	4.08	3.44	3.48	3.50
Limnæa So	6/7/2006	5.98	4.18	3.53	3.53	3.48
Limnæa So	6/8/2006	6.70	4.65	3.64	3.55	3.48

Limnæa So	6/9/2006	6.64	4.43	3.64	3.58	3.53
Limnæa So	6/10/2006	6.51	5.62	3.82	3.73	3.49
Limnæa So	6/11/2006	7.39	5.58	3.84	3.71	3.52
Limnæa So	6/12/2006	8.20	5.36	4.00	3.79	3.48
Limnæa So	6/13/2006	8.68	6.21	3.95	3.83	3.48
Limnæa So	6/14/2006	7.76	5.90	4.26	3.92	3.53
Limnæa So	6/15/2006	7.58	6.81	4.31	3.95	3.55
Limnæa So	6/16/2006	7.55	7.02	4.33	3.98	3.53
Limnæa So	6/17/2006	7.58	7.04	4.95	4.07	3.56
Limnæa So	6/18/2006	7.33	7.14	5.05	4.20	3.53
Limnæa So	6/19/2006	7.47	7.33	5.71	4.28	3.54
Limnæa So	6/20/2006	7.95	7.63	6.26	4.33	3.53
Limnæa So	6/21/2006	8.52	8.21	6.17	4.30	3.55
Limnæa So	6/22/2006	8.27	8.07	6.43	4.42	3.53
Limnæa So	6/23/2006	8.93	8.63	7.90	4.31	3.52
Limnæa So	6/24/2006	9.75	9.40	7.14	4.58	3.53
Limnæa So	6/25/2006	10.15	9.79	8.93	4.49	3.50
Limnæa So	6/26/2006	11.14	10.93	9.04	4.59	3.53
Limnæa So	6/27/2006	10.73	10.35	8.88	4.77	3.57
Limnæa So	6/28/2006	11.16	10.73	10.18	5.00	3.55
Limnæa So	6/29/2006	11.98	11.21	9.64	5.11	3.57
Limnæa So	6/30/2006	11.28	11.01	9.43	5.14	3.58
Limnæa So	7/1/2006	11.23	10.77	10.53	5.11	3.59
Limnæa So	7/2/2006	10.98	10.89	10.08	5.38	3.59
Limnæa So	7/3/2006	11.10	10.97	10.87	5.33	3.60
Limnæa So	7/4/2006	11.99	11.43	11.08	5.43	3.59
Limnæa So	7/5/2006	12.73	11.98	10.93	5.47	3.59
Limnæa So	7/6/2006	12.31	11.97	10.58	5.37	3.60
Limnæa So	7/7/2006	12.32	12.07	11.90	5.83	3.60
Limnæa So	7/8/2006	13.43	12.68	12.12	5.83	3.60
Limnæa So	7/9/2006	13.82	13.15	11.93	6.16	3.61
Limnæa So	7/10/2006	13.02	12.83	12.71	6.47	3.60
Limnæa So	7/11/2006	12.83	12.64	11.74	6.12	3.62
Limnæa So	7/12/2006	12.20	11.93	11.60	8.67	3.65
Limnæa So	7/13/2006	12.53	12.37	12.25	8.37	3.67
Limnæa So	7/14/2006	12.96	12.72	12.25	8.99	3.69
Limnæa So	7/15/2006	13.04	12.90	11.89	8.87	3.70
Limnæa So	7/16/2006	12.98	12.78	12.46	9.66	3.70
Limnæa So	7/17/2006	13.80	13.38	12.64	9.64	3.70
Limnæa So	7/18/2006	13.33	13.12	11.46	9.14	3.70
Limnæa So	7/19/2006	12.90	12.80	12.74	10.06	3.73
Limnæa So	7/20/2006	12.35	12.16	11.68	9.81	3.79
Limnæa So	7/21/2006	12.63	12.41	12.13	11.09	3.95
Limnæa So	7/22/2006	13.03	12.95	12.72	11.28	3.88
Limnæa So	7/23/2006	13.28	13.00	12.30	11.27	3.88
Limnæa So	7/24/2006	13.92	13.40	12.51	11.18	3.85
Limnæa So	7/25/2006	14.15	13.98	13.06	11.02	3.87
Limnæa So	7/26/2006	14.40	13.90	12.93	11.26	3.88
Limnæa So	7/27/2006	14.84	14.09	12.70	11.27	3.88
Limnæa So	7/28/2006	14.68	14.18	13.66	11.27	3.89
Limnæa So	7/29/2006	15.18	14.98	13.22	11.34	3.89
Limnæa So	7/30/2006	15.43	15.05	13.38	11.33	3.91

Limnæa So	7/31/2006	15.38	15.21	13.77	11.43	3.90
Limnæa So	8/1/2006	15.44	15.38	13.60	11.48	3.91
Limnæa So	8/2/2006	15.21	15.13	14.41	11.95	3.98
Limnæa So	8/3/2006	15.08	14.68	14.19	11.67	3.94
Limnæa So	8/4/2006	14.71	14.58	14.19	11.62	3.94
Limnæa So	8/5/2006	14.44	14.28	14.14	12.46	3.96
Limnæa So	8/6/2006	14.38	14.34	14.32	12.08	4.01
Limnæa So	8/7/2006	14.37	14.27	14.16	12.39	3.98
Limnæa So	8/8/2006	14.28	14.20	14.11	13.42	3.98
Limnæa So	8/9/2006	14.18	14.16	14.17	12.88	4.01
Limnæa So	8/10/2006	14.04	13.91	13.91	13.13	4.02
Limnæa So	8/11/2006	13.94	13.83	13.77	13.59	4.01
Limnæa So	8/12/2006	14.01	13.92	13.89	12.83	4.03
Limnæa So	8/13/2006	13.83	13.72	13.67	13.44	4.03
Limnæa So	8/14/2006	14.14	14.01	13.87	13.25	4.03
Limnæa So	8/15/2006	14.19	14.09	13.86	12.97	4.04
Limnæa So	8/16/2006	13.75	13.72	13.74	13.59	4.09
Limnæa So	8/17/2006	13.67	13.60	13.68	13.55	4.07
Limnæa So	8/18/2006	13.53	13.44	13.51	13.56	4.08
Limnæa So	8/19/2006	13.33	13.28	13.35	13.45	4.08
Limnæa So	8/20/2006	13.27	13.21	13.21	13.23	4.08
Limnæa So	8/21/2006	13.13	13.08	13.13	13.17	4.08
Limnæa So	8/22/2006	12.94	12.88	12.89	12.92	4.08
Limnæa So	8/23/2006	12.76	12.68	12.71	12.76	4.09

		Thermisor ID and Depth			
		0696	0694	1336	0693
		1m	3m	5m	7m
Lake	**Date**	**Temperature (°C)**			
Braya Sø	4/23/2006	-0.10	1.30	1.40	1.28
Braya Sø	4/24/2006	-0.08	1.33	1.40	1.28
Braya Sø	4/25/2006	-0.08	1.40	1.40	1.30
Braya Sø	4/26/2006	-0.12	1.40	1.47	1.37
Braya Sø	4/27/2006	-0.70	1.39	1.45	1.35
Braya Sø	4/28/2006	-1.56	1.39	1.45	1.31
Braya Sø	4/29/2006	-1.42	1.40	1.48	1.40
Braya Sø	4/30/2006	-1.27	1.40	1.48	1.38
Braya Sø	5/1/2006	-1.21	1.40	1.50	1.40
Braya Sø	5/2/2006	-1.26	1.40	1.50	1.40
Braya Sø	5/3/2006	-1.25	1.43	1.50	1.40
Braya Sø	5/4/2006	-1.33	1.45	1.50	1.40
Braya Sø	5/5/2006	-1.48	1.48	1.50	1.40
Braya Sø	5/6/2006	-1.10	1.50	1.50	1.40
Braya Sø	5/7/2006	-0.48	1.53	1.55	1.46
Braya Sø	5/8/2006	-0.15	1.60	1.60	1.54
Braya Sø	5/9/2006	0.05	1.67	1.68	1.61
Braya Sø	5/10/2006	0.19	1.82	1.86	1.73
Braya Sø	5/11/2006	0.36	1.96	1.97	1.91
Braya Sø	5/12/2006	0.44	2.09	2.15	2.04
Braya Sø	5/13/2006	0.23	2.17	2.24	2.13
Braya Sø	5/14/2006	0.16	2.21	2.30	2.20
Braya Sø	5/15/2006	0.13	2.27	2.35	2.23
Braya Sø	5/16/2006	0.39	2.35	2.39	2.32
Braya Sø	5/17/2006	0.58	2.48	2.53	2.44
Braya Sø	5/18/2006	0.53	2.57	2.64	2.50
Braya Sø	5/19/2006	0.54	2.71	2.79	2.64
Braya Sø	5/20/2006	0.37	2.85	2.92	2.78
Braya Sø	5/21/2006	0.25	2.93	3.00	2.89
Braya Sø	5/22/2006	0.34	2.98	3.04	2.94
Braya Sø	5/23/2006	0.45	3.06	3.14	3.03
Braya Sø	5/24/2006	0.41	3.16	3.22	3.05
Braya Sø	5/25/2006	0.38	3.25	3.31	3.16
Braya Sø	5/26/2006	0.23	3.33	3.36	3.20
Braya Sø	5/27/2006	0.27	3.40	3.43	3.28
Braya Sø	5/28/2006	0.38	3.59	3.51	3.43
Braya Sø	5/29/2006	0.38	3.90	3.53	3.42
Braya Sø	5/30/2006	0.44	4.25	3.59	3.50
Braya Sø	5/31/2006	0.47	4.80	3.67	3.50
Braya Sø	6/1/2006	0.58	5.13	3.73	3.50
Braya Sø	6/2/2006	2.23	5.23	3.73	3.48
Braya Sø	6/3/2006	3.77	4.67	3.82	3.61
Braya Sø	6/4/2006	4.48	5.03	4.03	3.58
Braya Sø	6/5/2006	5.16	5.31	4.07	3.64
Braya Sø	6/6/2006	6.11	5.71	4.04	3.67
Braya Sø	6/7/2006	7.33	6.04	4.15	3.68

Braya Sø	6/8/2006	7.80	6.55	4.18	3.73
Braya Sø	6/9/2006	7.65	7.55	4.52	3.73
Braya Sø	6/10/2006	7.48	7.35	4.51	3.78
Braya Sø	6/11/2006	8.11	7.93	4.38	3.83
Braya Sø	6/12/2006	9.03	8.80	4.54	3.83
Braya Sø	6/13/2006	9.45	9.32	4.71	3.89
Braya Sø	6/14/2006	9.16	9.12	4.94	3.98
Braya Sø	6/15/2006	8.36	8.35	5.10	4.03
Braya Sø	6/16/2006	8.34	8.33	5.23	4.09
Braya Sø	6/17/2006	8.26	8.26	5.50	4.13
Braya Sø	6/18/2006	7.98	7.96	6.60	4.09
Braya Sø	6/19/2006	8.23	8.13	6.86	4.13
Braya Sø	6/20/2006	8.54	8.50	7.65	4.15
Braya Sø	6/21/2006	9.23	9.15	8.48	4.21
Braya Sø	6/22/2006	9.22	9.23	8.40	4.19
Braya Sø	6/23/2006	9.62	9.56	9.15	4.15
Braya Sø	6/24/2006	10.44	10.33	9.53	4.18
Braya Sø	6/25/2006	10.89	10.74	9.88	4.25
Braya Sø	6/26/2006	11.57	11.45	10.43	4.20
Braya Sø	6/27/2006	11.62	11.37	10.88	4.27
Braya Sø	6/28/2006	12.04	11.77	10.58	4.37
Braya Sø	6/29/2006	12.78	12.38	10.74	4.43
Braya Sø	6/30/2006	12.34	12.32	11.03	4.67
Braya Sø	7/1/2006	12.25	12.06	11.12	4.68
Braya Sø	7/2/2006	11.88	11.88	11.40	4.83
Braya Sø	7/3/2006	11.83	11.78	11.63	4.89
Braya Sø	7/4/2006	12.13	12.04	11.87	5.06
Braya Sø	7/5/2006	12.99	12.80	12.00	4.96
Braya Sø	7/6/2006	13.13	13.13	11.94	5.22
Braya Sø	7/7/2006	12.98	12.96	12.75	5.22
Braya Sø	7/8/2006	13.67	13.49	12.87	5.30
Braya Sø	7/9/2006	14.15	14.01	12.86	5.42
Braya Sø	7/10/2006	13.73	13.70	13.12	5.76
Braya Sø	7/11/2006	13.68	13.58	13.18	5.73
Braya Sø	7/12/2006	13.25	13.08	13.03	6.07
Braya Sø	7/13/2006	13.20	13.18	13.08	6.23
Braya Sø	7/14/2006	13.64	13.53	13.33	6.21
Braya Sø	7/15/2006	13.83	13.74	13.53	6.73
Braya Sø	7/16/2006	13.93	13.88	13.70	6.77
Braya Sø	7/17/2006	14.16	14.18	14.07	7.11
Braya Sø	7/18/2006	14.17	14.19	14.13	6.97
Braya Sø	7/19/2006	13.77	13.78	13.82	7.83
Braya Sø	7/20/2006	13.33	13.37	13.30	10.46
Braya Sø	7/21/2006	13.43	13.40	13.24	11.83
Braya Sø	7/22/2006	13.83	13.83	13.59	11.68
Braya Sø	7/23/2006	14.03	13.83	13.70	11.47
Braya Sø	7/24/2006	14.46	14.06	13.58	11.61
Braya Sø	7/25/2006	14.56	14.44	13.70	11.54
Braya Sø	7/26/2006	14.70	14.57	13.77	11.50
Braya Sø	7/27/2006	15.50	15.23	14.03	11.42

Braya Sø	7/28/2006	15.78	15.49	14.14	11.52
Braya Sø	7/29/2006	16.03	15.96	14.26	11.29
Braya Sø	7/30/2006	15.99	15.92	14.36	11.41
Braya Sø	7/31/2006	15.91	15.83	14.87	11.32
Braya Sø	8/1/2006	15.85	15.84	15.11	11.41
Braya Sø	8/2/2006	15.61	15.63	15.09	11.50
Braya Sø	8/3/2006	15.53	15.32	14.81	11.58
Braya Sø	8/4/2006	15.19	15.14	14.78	12.33
Braya Sø	8/5/2006	14.93	14.79	14.68	12.82
Braya Sø	8/6/2006	14.83	14.84	14.78	12.60
Braya Sø	8/7/2006	14.90	14.80	14.75	12.53
Braya Sø	8/8/2006	14.84	14.83	14.78	12.89
Braya Sø	8/9/2006	14.64	14.66	14.68	12.85
Braya Sø	8/10/2006	14.50	14.41	14.36	13.14
Braya Sø	8/11/2006	14.37	14.35	14.33	13.11
Braya Sø	8/12/2006	14.40	14.35	14.28	13.18
Braya Sø	8/13/2006	14.29	14.26	14.23	13.18
Braya Sø	8/14/2006	14.47	14.41	14.31	13.37
Braya Sø	8/15/2006	14.40	14.42	14.39	13.31
Braya Sø	8/16/2006	14.17	14.16	14.17	13.68
Braya Sø	8/17/2006	13.82	13.83	13.85	13.39
Braya Sø	8/18/2006	13.65	13.67	13.67	13.35

APPENDIX S

ALKENONE CONCENTRATION DATA FROM LONG CORES: BRAYA SØ, LAKE E AND SS6

Braya Sø Depth (cm)	C37 extracted (mg)	[C37] mg/g Sediment
0.0	0.43	1.24
0.5	0.95	2.11
1.0	0.31	0.69
1.5	0.2	0.45
2.0	0.26	0.57
2.5	0.07	0.15
3.0	0.05	0.11
3.5	0.05	0.11
4.0	0.01	0.03
5.0	0.05	0.1
5.5	0.03	0.07
6.0	0.07	0.16
6.5	0.05	0.11
7.0	0.18	0.39
7.5	0.29	0.64
8.0	0.08	0.18
8.5	0.02	0.05
9.0	0.03	0.08
9.5	0.03	0.06
10.0	0.05	0.1
10.5	0.06	0.14
10.8	0.08	0.26
11.0	0.06	0.14
11.5	0.05	0.1
12.0	0.1	0.29
12.3	0.68	1.49
12.5	0.32	0.72
13.0	0.05	0.1
13.5	0.02	0.04
14.0	0.02	0.05
14.5	0.03	0.06
15.0	0.03	0.08
15.5	0.02	0.04
16.0	0.02	0.04
16.5	0.03	0.07
17.0	0.02	0.04
17.5	0.07	0.16
18.0	0.02	0.04
18.5	0.04	0.1
19.0	0.14	0.3
19.5	0.93	2.59
20.0	1.2	2.67
20.3	1.46	3.24

Braya Sø Depth (cm)	C37 extracted (mg)	[C37] mg/g Sediment
20.5	0.18	0.39
21.0	0.15	0.32
21.0	0.12	0.25
21.5	0.07	0.16
22.0	0.05	0.11
22.5	0.06	0.13
23.0	0.1	0.23
23.5	0.15	0.32
24.0	0.15	0.33
24.5	0.06	0.14
25.0	0.14	0.31
25.5	0.27	0.59
26.0	0.17	0.39
26.5	0.05	0.11
27.0	0.19	0.41
27.5	0.65	1.48
28.0	0.67	1.51
28.5	0.54	1.17
29.0	0.47	1.06
29.5	0.35	0.77
30.0	0.05	0.12
30.5	0.34	0.74
31.5	0.39	1.05
32.0	0.38	0.8
32.5	0.34	0.76
33.0	0.03	0.08
33.5	0.01	0.03
34.0	0.04	0.09
34.0	0.04	0.09
34.5	0.39	0.85
34.5	0.32	0.71
35.0	0.32	0.7
36.0	0.6	1.31
36.5	2.1	4.67
37.0	0.04	0.09
37.5	0.01	0.03
38.0	0.05	0.1
38.5	0.16	0.35
39.0	0.04	0.09
39.5	0.02	0.04
40.0	0.06	0.14
40.5	0.06	0.12
41.0	0.04	0.08

Braya Sø Depth (cm)	C37 extracted (mg)	[C37] mg/g Sediment
41.5	0.48	1.07
42.0	0.05	0.12
43.0	0.08	0.18
44.0	0.01	0.03
44.5	0.12	0.26
45.0	0.01	0.03
45.5	0.06	0.12
46.0	0.02	0.04
46.5	0.04	0.09
47.0	0.02	0.04
47.5	0.03	0.07
48.0	0.03	0.08
48.5	0.02	0.05
49.0	0.04	0.1
49.5	0.02	0.05
50.0	0.03	0.06
50.5	0.04	0.09
51.0	0.03	0.06
51.5	0.01	0.02
52.0	0.02	0.03
52.5	0.01	0.01
53.0	0.07	0.14
53.5	0.1	0.22
54.0	0.32	0.7
54.5	0.3	0.65
55.0	0.3	0.65
56.0	0.28	0.62
57.0	0.2	0.43
58.0	0.09	0.21
59.0	0.06	0.14
60.5	0.03	0.07
61.0	0.58	1.29
61.5	0.81	1.8
62.0	0	0
62.5	0.64	1.42
63.0	0.97	2.16
63.5	0.76	1.7
64.0	0.75	1.66
64.0	0.74	1.64
64.5	0.57	1.27
65.0	1.11	2.48
65.0	1.11	2.46
66.0	1.28	2.85

Braya Sø Depth (cm)	C37 extracted (mg)	[C37] mg/g Sediment
66.5	1	2.22
67.5	0.6	1.33
68.0	1.09	2.42
68.5	1.12	2.48
69.5	1.18	2.61
70.0	1.06	2.35
70.5	1.06	2.34
71.0	0.98	2.18
71.5	0.58	1.29
72.0	0.8	1.79
72.5	0.71	1.59
73.0	1.14	2.53
73.5	1.38	3.06
74.0	1.24	2.75
74.5	1.9	4.22
75.0	1.48	3.29
75.5	1.81	4.03
76.5	1.96	4.35
77.0	2.42	5.37
77.5	0.79	1.75
78.0	1.16	2.57
78.5	1.41	3.14
79.0	0.74	1.64
79.5	1.69	3.76
80.0	1.81	4.01
80.5	1.12	2.49
81.0	1.56	3.47
81.0	1.58	3.51
81.5	0.71	1.59
82.0	0.86	1.9
82.5	0.89	1.97
83.0	0.23	0.51
84.0	0.81	1.8
85.0	0.14	0.29
86.0	0.08	0.17
87.0	0.05	0.1
88.0	0.07	0.15
89.0	0.03	0.06
90.0	0.01	0.02
91.0	0.01	0.02
92.5	0.38	0.84
93.0	0.04	0.09
93.5	0.01	0.03

Braya Sø Depth (cm)	C37 extracted (mg)	[C37] mg/g Sediment
94.0	0.19	0.43
95.0	0.02	0.05

Lake E Depth (cm)	**C37 extracted (mg)**	**[C37] mg/g Sediment**
2.0	0.11	0.25
3.0	0.08	0.23
3.5	0.15	0.21
5.0	0.05	0.06
5.5	0.05	0.05
6.0	0.05	0.05
6.5	0.08	0.06
7.0	0.20	0.26
7.5	0.36	0.42
8.0	0.16	0.59
8.5	1.16	0.89
9.0	0.76	1.15
9.5	2.09	1.30
10.0	0.14	0.79
10.5	0.48	0.82
11.0	0.68	0.62
11.5	1.03	0.86
12.0	0.15	0.37
12.5	0.11	0.08
13.0	0.10	0.15
13.5	0.26	0.26
14.0	0.22	0.34
14.5	0.72	0.54
15.0	0.25	0.70
15.5	0.50	0.44
16.0	0.79	1.03
16.5	0.69	1.06
17.0	1.60	2.87
17.5	0.45	0.63
18.5	0.31	0.56
19.5	1.31	2.17
20.0	1.05	2.64

Lake E Depth (cm)	**C37 extracted (mg)**	**[C37] mg/g Sediment**
20.5	1.14	2.00
21.0	1.48	1.95
21.5	1.42	2.08
22.0	1.30	2.68
22.5	2.28	2.25
23.5	2.56	3.20
24.5	1.36	2.50
25.0	0.71	3.51
25.5	0.64	1.15
27.0	0.37	1.09
28.5	0.50	0.77
29.5	0.28	0.75
30.0	0.17	1.00
31.5	0.69	1.19
32.5	0.57	0.97
33.5	0.41	0.52
34.5	0.28	0.60
35.0	0.12	0.61
36.5	0.90	1.01
37.5	0.63	2.18
38.5	1.77	2.50
39.5	1.10	3.34
40.5	0.18	2.60
41.5	1.77	2.69
42.5	1.61	2.90
43.5	0.22	0.22
45.5	0.10	0.13
46.5	0.14	0.17
47.5	0.12	0.27
48.5	0.20	0.31
49.5	0.30	0.41
50.0	0.42	0.63

Lake E Depth (cm)	C37 extracted (mg)	[C37] mg/g Sediment
51.0	0.46	1.01
51.5	0.93	1.23
52.5	1.22	1.55
53.5	1.42	1.99
55.5	1.34	1.63
56.0	1.27	2.45
57.0	0.72	1.77
58.0	0.38	2.57
58.5	0.48	0.89
59.5	0.51	0.89
60.5	0.40	1.02
61.5	0.22	1.47
62.5	0.38	1.50
63.5	1.12	1.52
64.5	0.11	1.69
65.5	1.86	1.78
66.5	0.53	0.66
67.5	1.01	1.05
68.5	1.18	1.87
69.5	0.85	1.19
70.5	1.45	2.10
71.5	1.38	2.35
72.5	0.83	1.10
73.5	0.54	1.06
74.5	0.46	0.60
75.5	0.17	0.29
76.5	0.26	0.41
77.5	0.19	0.30
78.5	0.09	0.14
84.5	0.54	0.69
86.0	0.71	0.83
87.0	1.24	0.72
88.0	0.32	0.77
89.0	0.35	1.02
90.0	1.02	1.83
91.0	1.09	1.54
92.0	0.64	0.94
93.0	0.61	1.02

Lake E Depth (cm)	C37 extracted (mg)	[C37] mg/g Sediment
94.0	0.67	1.42
95.0	1.34	1.59
96.0	1.13	1.57
97.0	1.29	2.58
98.0	1.77	2.33
98.5	0.63	2.61
99.5	1.17	1.30
100.5	0.36	1.08
101.5	0.46	0.57
102.5	0.32	0.64
103.5	0.48	0.71
104.5	0.69	0.92
105.5	0.35	0.49
106.5	0.94	0.86
107.5	0.63	1.18
108.5	1.44	1.90
109.5	0.28	0.45
110.5	0.03	0.09
111.5	0.07	0.09
112.5	0.34	0.72
113.5	0.52	0.51
114.5	0.21	0.30
115.5	0.45	0.74
116.5	0.35	0.32
117.5	0.74	0.55
118.5	0.57	0.61
120.5	0.19	0.14
121.5	0.09	0.14
122.5	0.48	0.58
123.5	0.42	0.27
124.5	0.52	0.41
125.5	1.32	1.44
126.5	1.28	1.15
127.5	1.46	1.09
128.5	0.28	1.19
129.5	0.96	1.58
130.5	1.63	1.46
131.0	1.93	2.43

Lake E Depth (cm)	C37 extracted (mg)	[C37] mg/g Sediment
132.0	0.86	0.91
133.0	1.89	1.71
134.0	0.97	1.05
135.0	1.85	1.33
136.0	2.70	2.08
137.0	0.71	0.55

Lake E Depth (cm)	C37 extracted (mg)	[C37] mg/g Sediment
138.0	0.86	0.50
139.0	0.12	0.17
140.0	0.43	0.64
141.0	0.37	0.67
141.5	0.68	0.77
142.0	1.50	1.65
143.0	2.14	2.13

SS6 Depth (cm)	C37 extracted (mg)	[C37] (mg/g Sediment)
6.25	0.01	1.9
8.25	0.02	2.5
9.25	0.01	1.2
10.25	0.03	20.1
11.25	0.02	3.5
12.25	0.04	6.4
13.25	0.05	8.9
13.25	0.05	15.7
14.25	0.06	9.9
15.25	0.07	56.9
16.25	0.04	12
16.50	0.08	24.2
17.25	0.07	20.2
18.00	0.06	32
19.00	0.07	25.4
19.75	0.10	85
21.00	0.04	16.9
22.00	0.18	62.4
23.00	0.15	94
24.00	0.05	19.9
25.00	0.08	48.3
26.00	0.17	41.5
27.00	0.07	13.9
28.00	0.04	11.1

SS6 Depth (cm)	C37 extracted (mg)	[C37] (mg/g Sediment)
29.00	0.05	10.5
30.50	0.19	69.5
30.50	0.19	182.8
31.50	0.04	16.6
33.50	0.04	14.4
34.50	0.03	11.5
35.00	0.02	21.4
36.50	0.03	7.8
37.75	0.08	23.4
38.50	0.06	20.4
39.75	0.14	104.3
41.00	0.43	125.7
41.75	0.35	94.8
43.00	0.14	47.8
44.00	0.23	109.9
45.00	0.16	160.8
46.00	0.07	34.2
47.25	0.09	47.5
48.00	0.10	49.7
50.50	0.21	176.4
51.25	0.54	216.1
52.25	0.21	102.5
53.50	0.39	136.5
54.50	0.56	246.2

SS6 Depth (cm)	C37 extracted (mg)	[C37] (mg/g Sediment)
55.00	0.18	147
56.00	0.71	263.3
57.00	0.41	132.2
58.00	0.28	66.7
58.50	0.08	55.7
59.00	0.27	148.1
60.25	0.56	443.1
61.25	0.20	115.4
62.25	0.16	76.9
63.00	0.42	178.1
63.20	0.40	201.5
64.00	0.20	73.9
66.00	0.82	742.7
66.25	0.21	129.1
67.00	0.17	117.1
68.00	0.30	115.2
68.25	0.21	89.7
69.00	0.07	26.8
71.00	0.08	27.3
71.25	0.10	85.9
72.00	0.27	165.5
73.10	0.25	81.9
73.25	0.67	523.6
74.20	0.26	270.9
75.00	0.13	120
76.00	0.11	58.5

SS6 Depth (cm)	C37 extracted (mg)	[C37] (mg/g Sediment)
78.25	0.03	8.9
79.25	0.33	89.5
80.25	0.40	185.4
81.50	0.36	117.5
82.25	1.02	344.1
82.50	0.54	195.2
83.50	0.07	23.1
84.50	0.14	43.5
85.50	1.37	1134.6
86.75	0.90	435
87.50	1.09	615.7
88.50	0.65	327.6
89.50	0.62	429.6
90.20	0.17	109.5
91.00	0.25	131.8
92.25	0.43	314.9
93.50	0.47	398.6
94.90	0.44	224.1
95.70	0.97	638.4
96.20	0.52	365.6
96.90	0.79	421
98.40	0.33	202.3

*data only available from core SS6-III